TURKISH JOURNAL OF AGRICULTURAL ENGINEERING RESEARCH

TURKAGER

e-ISSN: 2717-8420

https://dergipark.org.tr/en/pub/turkager

VOLUME : 2
ISSUE : 2
YEAR : 2021

Turkish Journal of Agricultural Engineering Research (TURKAGER)

Volume 2,
Issue 2,
Year 2021

Indexing

Turkish Journal of Agricultural Engineering Research (TURKAGER)

Turkish Journal of Agricultural Engineering Research (TURKAGER)

Volume 2,
Issue 2,
December 31, 2021

SECTION EDITORS & REFEREES (*)

Turkish Journal of Agricultural Engineering Research (TURKAGER)

Volume 2, Issue 2, December 31, 2021

Turkish Journal of Agricultural Engineering Research

https://dergipark.org.tr/en/pub/turkager
https://doi.org/10.46592/turkager.2021.v02i02.001

Turk J Agr Eng Res (TURKAGER)
e-ISSN: 2717-8420
2021, 2(2): 260-275

Research Article

Evaluating the Effects of Milling Speed and Screen Size on Power Consumed During Milling Operation

Ademola Adebukola ADENIGBA[ID][a] **Samuel Dare OLUWAGBAYIDE**[ID][a*]

[a]*Department of Agricultural and Bio- Environmental Engineering, Federal Polytechnic, Ilaro, Ogun State, NIGERIA,*

(*): Corresponding author, *samuel.oluwagbayide@federalpolyilaro.edu.ng*

ABSTRACT

This study was conducted to evaluate the effect of rotor speed and screen size on power consumed during milling operation. The milling system was tested using three fish feed ingredients; bone meal, groundnut cake and maize. The moisture contents of the ingredients bought from the market are 13.1%, 14.7% and 17.5% dry basis, respectively. The milling machine was evaluated with the 3 kg of each feed ingredient and was replicated three times for each of the experimental parameters. The machine parameters varied during the experiment includes four screen sizes (1.5 mm, 2.0 mm, 2.5 mm and 3.0 mm) and five rotor speeds (1500 rpm, 1800 rpm, 2100 rpm, 2400 rpm and 2700 rpm). Regression analysis was carried out on the data collated. The analysis was used to develop a model which is capable of predicting the electrical energy (kJ) consumed. There was no significant effect of screen size on the average power consumed during milling since there is no linear relationship between power consumed and screen size. However, there is a significant effect of speed on average power consumed, the power consumed increases as speed decreases therefore making milling operation at higher speed to be cost effective since it doesn't require much power to achieve the required output. The P-Value depicts that screen size has no significant effect on the electrical energy consumed during the milling operation while speed has a significant effect on the electrical energy used at 95% confidence level.

RESEARCH ARTICLE

Received: 04.12.2020
Accepted: 29.01.2021

Keywords:

- Electrical energy,
- Milling,
- Power,
- Screen size,
- Fish feed and rotor speed,
- Kernel size

To cite: Adenigba AA, Oluwagbayide SD (2021). Evaluating the Effects of Milling Speed and Screen Size on Power Consumed During Milling Operation. Turkish Journal of Agricultural Engineering Research (TURKAGER), 2(2): 260-275. *https://doi.org/10.46592/turkager.2021.v02i02.001*

INTRODUCTION

In ancient times, cereal grains were crushed between two stones and made into crude cake. The advent of modern automated systems employing steel material such as hammer mills has revolutionized the processing of cereals and their availability as human foods and for other purposes (Donnel, 1983). Most of the existing hammer mill machines are designed for very large-scale production by the multinational companies such as breweries, feed mills and flour mills. But due to the recent sensitization of the public on the need for self-employment, there is an increase in small-scale companies. Thus, there is a very high demand for small-scale hammer mill machines (Adeomaya and Samuel, 2014). Nowadays there are increasing attempts to develop standard practical diets for farmed fish in Nigeria. A wide range of feed stuffs are produced as by-products from animal processing industries. Some of this feed stuffs are currently used in rations for both terrestrial animals and fish (Udo and Umoren, 2011). Since fish feeds are generally the largest single cost item of most fish farm operations, it follows that the selection of meal ingredients for use within diets will play a major role in dictating its ultimate nutritional and economic success (Ovie and Eze, 2013).

This project aims to alleviate the problems of peasant farmers in rural settlements and animal feed production companies, whose wish is to process their grain/cereal into animal feed at the minimum energy cost. Due to the exorbitant fee being levied as energy (power) tariff, some millers don't do adequate milling in order to cut down the energy consumed during the milling process, this recurrent behavior has led to production of feed with inappropriate particle size. The primary aim of this work is to evaluate the effect of milling (rotor) speed and screen size on the energy consumed during milling operation.

MATERIALS AND METHODS

Materials

The fish feed ingredients used for the performance evaluation were sourced from commercial feed milling centers (freedom feed mill and K2 feed mill) within Akure, Ondo State, Nigeria. The ingredients used are bone meal, groundnut cake and maize grain.

The Milling Machine

An existing milling machine was used to carryout the research. The milling system consists of the following components, the electric motor, transmission system, pneumatic system, hammering unit, screen, pressure relief unit, cyclone and the support frame.

Power unit: The system is driven by an electric motor of 10 hp which has a revolution of 2900 rpm.

Transmission system: It consists of shafts, pulleys and belts. The electric motor is the prime mover of the machine, as the pulley which is connected to the shaft of the electric motor is being propelled into action by the rotation of the electric motor; power is being transmitted from this pulley via a belt to another pulley which is connected to the shaft of the hammering unit.

Hammering unit: The hammering unit consists of four sets of hammers; each set is positioned on a role and each role has six hammers thereby making a total of 24 hammers. Individual hammers are of 5.1 by 7.2 cm.

Screen: The screens used for this research work are of varying aperture sizes; 1.5 mm, 2 mm, 2.5 mm and 3 mm.

Pneumatic system: The pneumatic system has a blower which positioned above the screen in the hammering unit. This blower consists of blades which are of 1.5 by 7.8 cm in dimension. The blower sucks the milled products which drops from the screen and subsequently transports the milled product pneumatically via the duct down into the cyclone.

Pressure relief unit: The air pressure in the pneumatically conveyed material is separated with the aid of the pressure relief fabric. The air pressure is able to escape through the fabric material while the milled particle dust gradually settles in the cyclone.

Bone meal Groundnut cake Maize

Figure 1. Fish feed ingredients.

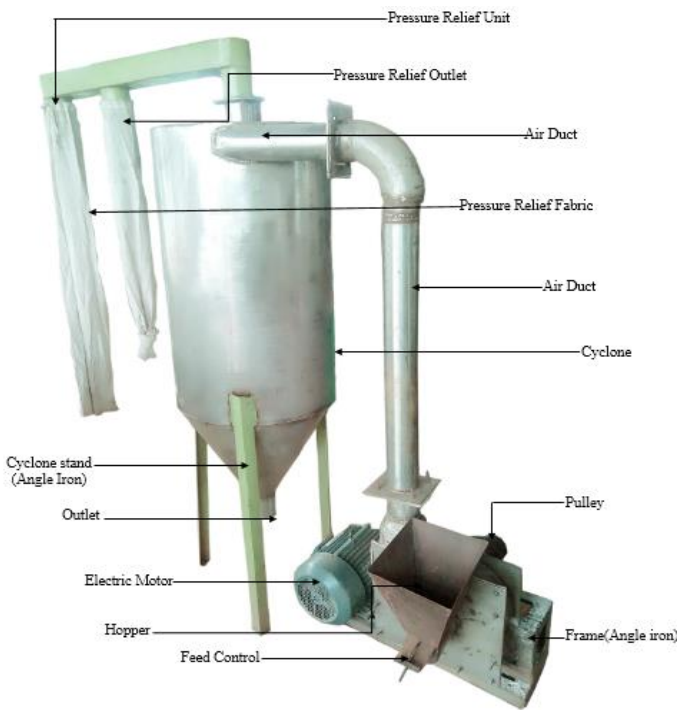

Figure 2. A milling system with pneumatic conveyor and cyclone.

Determination of average power consumed

A digital volt meter was used to measure the voltage consumed by the milling and mixing system during the period of operation of the machines, the voltmeter has accuracy specification of +/- 0.5% rdg and maximum input of 1000 VDC, 750 VAC for direct and alternating current, respectively. The ammeter used during the performance evaluation is a 3 phase, 4 wire, 10 (100) amps (whole current) electronic credit meter (Figure 3).

Figure 3. Measuring instrument (Ammeter & Digital volt meter).

Moisture content determination

An oven (Searchtech instrument DHG-9053A) was used to determine the ingredients moisture content.

Description of the dry oven

The drying chamber: This is the upper part of the mechanical dryer. It has a door, which is keyed to the top of the dryer, where the specimens are being loaded and off loaded. It allows contains four suspended sample baskets which are made of stainless steel. This is where the drying takes place. The base of the drying chamber is made up of perforated steel.

The heating chamber: This contains the heating element which is located at the lower part of the oven.

The centrifugal fan: This is attached to one side of the oven. It is operated by an electric motor. The fan sucks fresh air from the surrounding and blows it across the drying element which is located at the lower part of the dryer. The speed of the fan was regulated by electric voltage regulator.

The heating element: This serves as a source of heat for the dryer located at the lower part of the dryer. Heat is circulated into the drying chamber when the fan is blown across the heating element.

The exhaust: Also called the chimney, a square shaped hole on the top of upper part of the oven to allow moist air to leave, and regulate the airflow and temperature within the oven.

The drying layers: The drying layers are located inside the oven, they are made of stainless steel, and they are suspended inside the oven to ensure uniform drying.

Control panel: This is where the dryer is switched on and off. The heating element of the oven is trigged on from the switch on the control panel to pre-heat the oven to a certain air temperature before the agricultural product is introduced into the oven on the sleeve (Figure 4).

Figure 4. Laboratory oven (search tech instrument DHG-9053A).

Methods

Determination of machine speed

The milling and mixing machine was evaluated at five different speeds, in order to achieve the required speeds, the revolution per minute of the electric motor on the milling and mixing system needs to be reduced with the aid of pulleys. The pulley size required was determined with the equation bellow.

$$N_1 D_1 = N_2 D_2 \qquad (1)$$

Where: N_1 is speed of the driving pulley in rpm (speed of the electric motor)
D_1 is diameter of the driving pulley (mm), N_2 is speed of the driven pulley in rpm (speed of the hammering unit) and D_2 is diameter of the driven pulley (Pyarelal *et al.*, 2017) and (Aderemi *et al.*, 2020). The pulleys' diameters were measured with a venire caliper and the speed (2900 rpm, 10 HP) of the electric motor was specified on the electric motor by the manufacturer.

Pulley diameter

In order to achieve the required speed for the evaluation of the milling machine, it is imperative to vary the pulley diameters on the driven shaft. Below are the calculated pulley diameters and the corresponding speeds.

Table1. Required pulley diameter and the corresponding speed on the milling machine.

Pulley diameter (mm)	Speed (rpm)
145	1500
120	1800
105	2100
90	2400
80	2700

Determination of the ingredient's moisture content

The percentage moisture content of the ingredients was determined on dry basis.

$$MC = \frac{Ww - Wd}{Wd} \times 100 \qquad (2)$$

Where:
W_w is weight of wet material
W_d is weight of dry material (Chambliss, 2002).

Table 2. Ingredients moisture content.

Ingredients	Moisture content (db)
Bone meal (BM)	13.1%
Groundnut cake (GNC)	14.7%
Maize (M)	17.5%

Evaluation of the milling machine

Masses of 3 kg of bone mill, ground nut cake and corn grain were measured using a mass balance and each of the samples measured was replicated three times. These measured samples in three replicates were milled respectively at five different speeds (1500 rpm, 1800 rpm, 2100 rpm, 2400 rpm and 2700 rpm) and four different screen sizes (1.5 mm, 2 mm, 2.5 mm, 3 mm). The time taken to mill the ingredients was recorded using a stop watch while the average milling time and machine output for the three replicates of each ingredient at various speeds and its corresponding screen size was calculated. The electrical power consumed during each milling operation was recorded with an electric meter and the corresponding average voltage was measured with a digital volt meter.

Determination of machine power consumption

i) To measure power requirement an ammeter was connected between the electric motor of the grinding mill and the electrical supply.
ii) The current taken up by the machine when there is no input of grain i.e. the idle current before commencement of milling process was measured using an ammeter.
iii) The feed was emptied into the milling machine at a constant feed rate. Meter readings were taken at every 5 seconds intervals until all the grains were milled. This was indicated by the meter reading when it goes back to the idle power.
iv) Voltage readings were taken using a voltmeter across the power supplies.

v) Power was obtained by using

$$p = (A \times V \times PF)/100 \quad (3)$$

Where:

P is the power (kW),

A is the current (ampere),

V is the voltage and

PF is the dimensionless power factor between (-1) and +1 generated respectively with grinding time read from the clamp meter.

The power factor of an electrical power system is defined as the ratio of the real power flowing to the load with the apparent power in the circuit (Norazatul *et al.*, 2015).

Electrical energy consumption during milling

The electrical energy consumption during milling was calculated using Eqaution (3).

$$E = P \times t \quad (4)$$

Where E is the energy (kWs with conversion of 1 kWh = 3600 kJ) and t is grinding time.

The specific energy consumption during milling operation was calculated using Equation (4).

$$Esc = \frac{input\ electrical\ energy; E(kj)}{weight\ of\ milled\ product\ (kg)} \quad (5)$$

Where: E_{sc} is the specific energy input (kJ kg^{-1}) (Norazatul *et al.*, 2015).

Statistical analysis

Milling performances parameters' values (average power consumed and electrical energy used during milling) were subjected to statistical analysis to determine the mean, standard deviation, coefficient of variation, linear and nonlinear regressions. One-way ANOVA was used to test for significance among the treatments and post hoc comparison using Tukey test to separate significantly differing treatment means after main effects were found significant at $p < 0.05$. The significance tests of the milling performances parameters' (average power consumed and electrical energy used during milling) of the main treatment effects (speed and screen size) and their interactions were performed using the Analysis of Variance (ANOVA) within the General Linear Model (GLM) procedure using Minitab 17 statistical software. Multiple Range Test (DMRT) was used to compare the mean at 95% confidence level.

RESULTS AND DISCUSSION

The Tables (3-7) below show the relatioship between varying milling speeds, mass of product (BM, GNCand MAIZE), screen sizes, milling time and pulley size and their corresponding effect on power consummmed during milling.

Table 3. Evaluation of the hammer mill at 1500 rpm.

Speed (rpm)	Mass of feed 3 kg (Mf)	Mass of product (kg) (Mp)			Milling time (minutes)	Power (kW)	Pulley size (mm)	Screen size (mm)
		GNC	BM	Maize				
1500	3	1.6			18	0.3	145	2
1500	3			1	12	0.25	145	2
1500	3		1.8		14.1	0.26	145	2
1500	3			1.8	18.01	0.28	145	1.5
1500	3	1.5			17.13	0.3	145	1.5
1500	3		2		15.2	0.27	145	1.5
1500	3		2.9		9.5	0.2	145	2.5
1500	3			2.3	19	0.4	145	2.5
1500	3	2.1			18.31	0.3	145	3
1500	3			2.1	17.1	0.3	145	3
1500	3		2.6		10	0.1	145	3
1500	3	2.4			17.03	0.3	145	2.5

Table 4. Evaluation of the hammer mill at 1800 rpm.

Speed (rpm)	Mass of feed 3 kg (Mf)	Mass of product (kg) (Mp)			Milling time (minutes)	Power (KW)	Pulley size (mm)	Screen size (mm)
		GNC	BM	Maize				
1800	3	2.9			9.3	0.23	120	2
1800	3			1.6	11.18	0.35	120	2
1800	3		2.9		5.01	0.1	120	2
1800	3	2.1			8.15	0.2	120	1.5
1800	3			2.3	6.01	0.1	120	1.5
1800	3		2.85		4.12	0.07	120	1.5
1800	3			1.7	12.17	0.2	120	3
1800	3	2.5			10.02	0.3	120	3
1800	3			2.2	4.3	0.1	120	2.5
1800	3		2.85		5	0.1	120	3
1800	3	2.5			4.45	0.1	120	2.5
1800	3		2.5		3.25	0.1	120	2.5

Table 5. Evaluation of the hammer mill at 2100 rpm.

Speed (rpm)	Mass of feed 3 kg (Mf)	Mass of product (kg) (Mp)			Milling time (minutes)	Power (kW)	Pulley size (mm)	Screen size (mm)
		GNC	BM	Maize				
2100	3		2.8		1.16	0.1	105	2
2100	3			2.7	2.15	0.1	105	2
2100	3	2.9			2.1	0.07	105	2
2100	3	2.7			4.4	0.1	105	1.5
2100	3			2.85	7.49	0.2	105	1.5
2100	3		3		4.03	0.1	105	1.5
2100	3			2.6	11.1	0.3	105	3
2100	3	2.1			8	0.1	105	3
2100	3		3		3.55	0.1	105	3
2100	3		2.7		2.35	0.1	105	2.5
2100	3			2	4.1	0.1	105	2.5
2100	3	2.6			3.58	0.1	105	2.5

Table 6. Evaluation of the hammer mill at 2400 rpm.

Speed (rpm)	Mass of feed 3 kg (Mf)	Mass of product (kg) (Mp)			Milling time (minutes)	Power (kW)	Pulley size (mm)	Screen size (mm)
		GNC	BM	Maize				
2400	3			3	3.02	0.1	90	2
2400	3		3		4.16	0.05	90	1.5
2400	3			2.6	9.01	0.1	90	1.5
2400	3	2.6			6.15	0.1	90	1.5
2400	3	3			3.3	0.1	90	3
2400	3			2.3	7	0.2	90	3
2400	3		3		3.14	0.1	90	3
2400	3		2.7		2.4	0.1	90	2.5
2400	3			2.7	3	0.1	90	2
2400	3		3		2	0.05	90	2
2400	3	3			1.56	0.1	90	2
2400	3	2.9			1.5	0.1	90	2.5

Table 7. Evaluation of the hammer mill at 2700 rpm.

Speed (rpm)	Mass of feed 3 kg (Mf)	Mass of product (kg) (Mp)			Milling time (minutes)	Power (kW)	Pulley size (mm)	Screen size (mm)
		GNC	BM	Maize				
2700	3		2.9		1.46	0.05	80	2.5
2700	3	2.95			2.45	0.1	80	2
2700	3		2.95		2.25	0.1	80	2
2700	3			2.75	3.18	0.1	80	2.5
2700	3			2.9	3.41	0.1	80	2
2700	3			2.85	6.02	0.1	80	1.5
2700	3		3		4.01	0.2	80	1.5
2700	3	2.9			5	0.1	80	1.5
2700	3		3		1.45	0.05	80	3
2700	3	3			2.07	0.06	80	3
2700	3			2.6	4.15	0.1	80	3
2700	3	2.87			2.03	0.1	80	2.5

Power consumed during milling

The chart (Figure 5 and 6) shows that there is no significant effect of screen size on the average power consumed during milling, this can be seen in the chart as it shows no linear relationship between power consumed and screen size. From the data gathered during the research in the tables above, Table (3-7) shows that screen size does not have a significant effect on the power consumed during milling. In table 3, 0.1 kW of power was recorded at all the screen sizes during some of the milling operations, same thing was obtained in Table 3, where 0.3 kW power was also recorded to be consumed during some of the milling operations carried out with all the screen sizes. It is also shown in Table 3 that the highest power (0.4 kW) consumed occurred at 2.5 mm screen. However, there is a significant effect of speed on average power consumed as it is shown in Figure 6, the power consumed increases as speed decreases therefore making milling operation at higher speed to be cost effective since it doesn't require much power to achieve the required output. It was observed during the process of the research that lower milling speeds takes more time to mill the same quantity of product when compared with higher speeds, this observation shows that power consumption during milling is a factor of speed and the retention time (duration of milling).

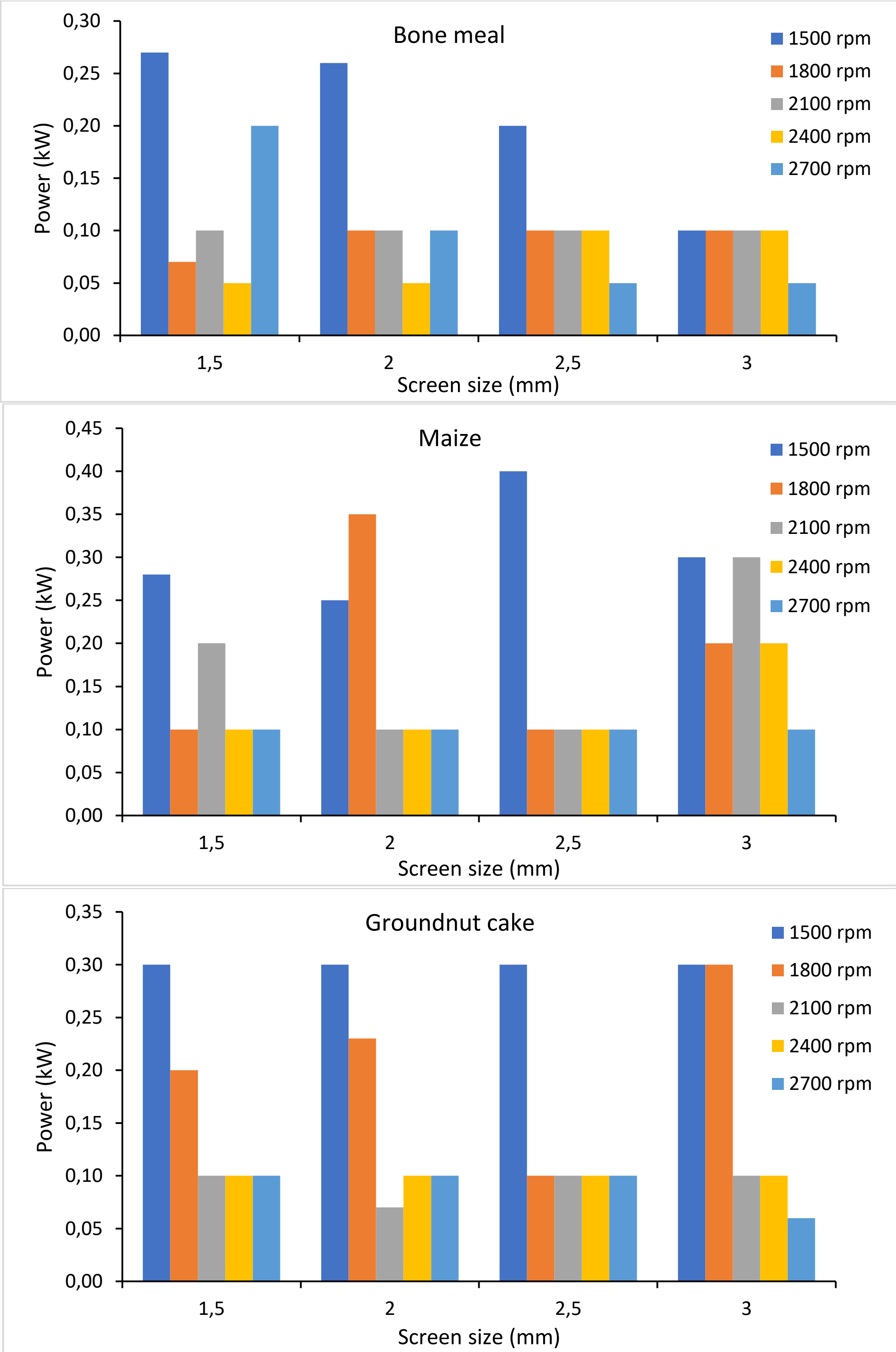

Figure 5. Effect of screen size on power consumed during milling.

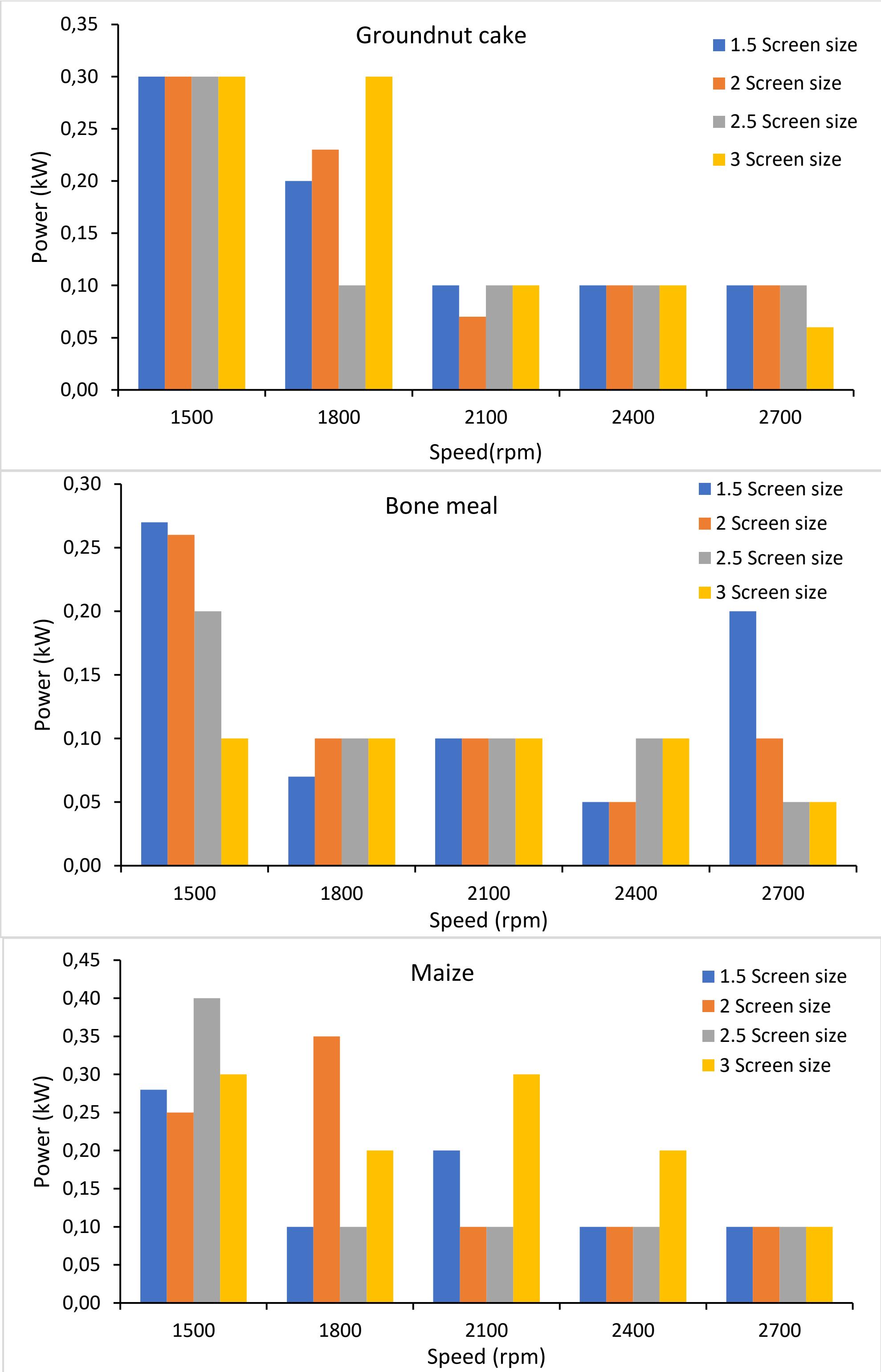

Figure 6. Effect of speed on power consumed during milling.

Effect of speed and screen size on electrical energy consumption

The effect of screen size and rotor (milling) speed was evaluated on the performance of a milling system, the tables below (Table 8) show the factors considered and Table 9 shows the level of significance of the factors. The P-Value depicts that screen size has no significant effect on the electrical energy consumed during the milling operation while speed has significant effect on the electrical energy used at 95% confidence level.

For more precise verification of the level of significance and the interaction differences between the various factors, the factors were subjected to Turkey and Bonferroni simultaneous test at 95% confidence level. Figure 8 shows the difference of means for electrical energy, there is a slight difference in the electrical energy consumed between (2400-1800 rpm) and (2400-1500 rpm) while there is significant difference between (2700-1500 rpm) and (2700-1800 rpm). Nonetheless, there is no significant difference when the effect of screen size was compared in Figure 9.

Table 8. Factor information (electrical energy).

Factor	Type	Levels	Values
Speed (rpm)	Fixed	5	1500, 1800, 2100, 2400, 2700
Screen size (mm)	Fixed	4	1.5, 2.0, 2.5, 3.0

Table 9. Analysis of variance (electrical energy).

Source	DF	Adj SS	Adj MS	F-Value	P-Value
Speed (rpm)	4	42549	10637	4.19	0.006
Screen size (mm)	3	5416	1805	0.71	0.551
Speed (rpm)*Screen size (mm)	12	56264	4689	1.85	0.073
Error	40	101573	2539		
Total	59	205803			

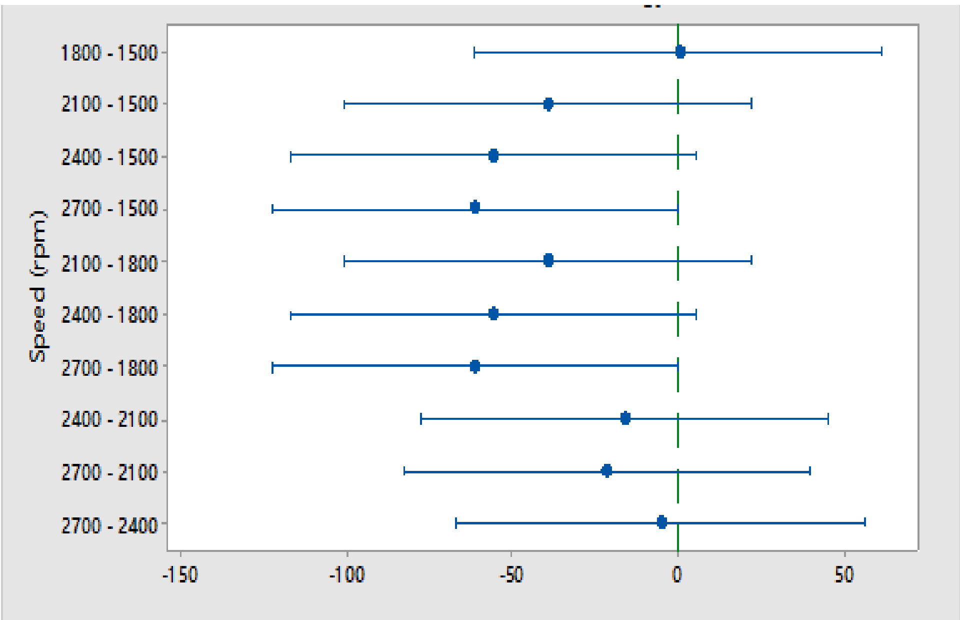

Figure 7. Differences of means for electrical energy (milling speed, rpm).

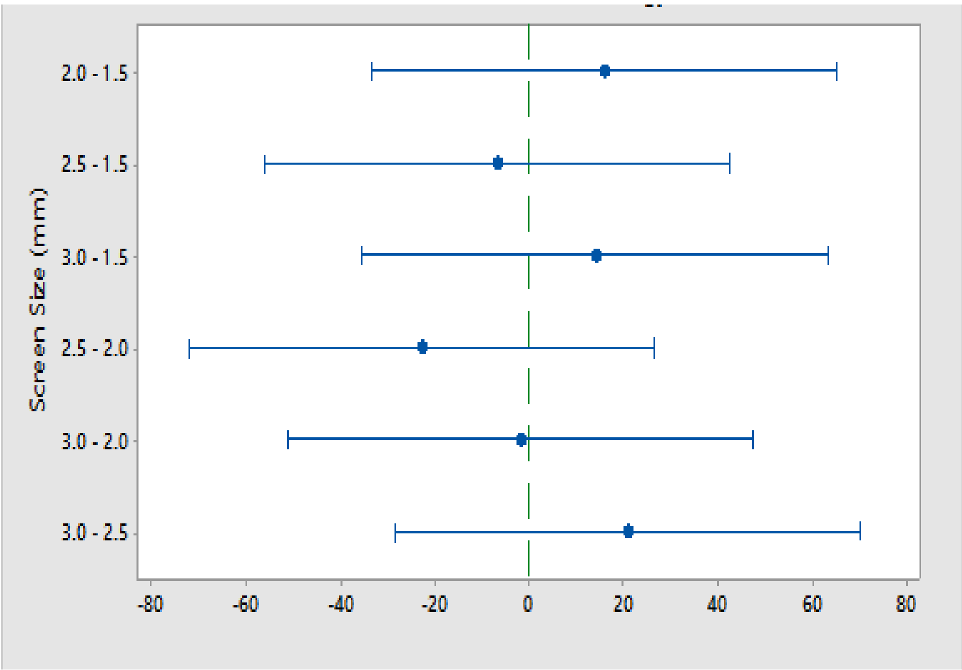

Figure 8. Differences of means for electrical energy (milling screen size, mm).

The electrical energy main effect plot in Figure 7 shows there is no significant difference in the electrical energy consumed between 1500 rpm and 1800 rpm and there is a subsequent decrease in the electrical energy used as the speed increase further. Figure 9 and 10 shows that screen size does not have a significant effect on the energy used.

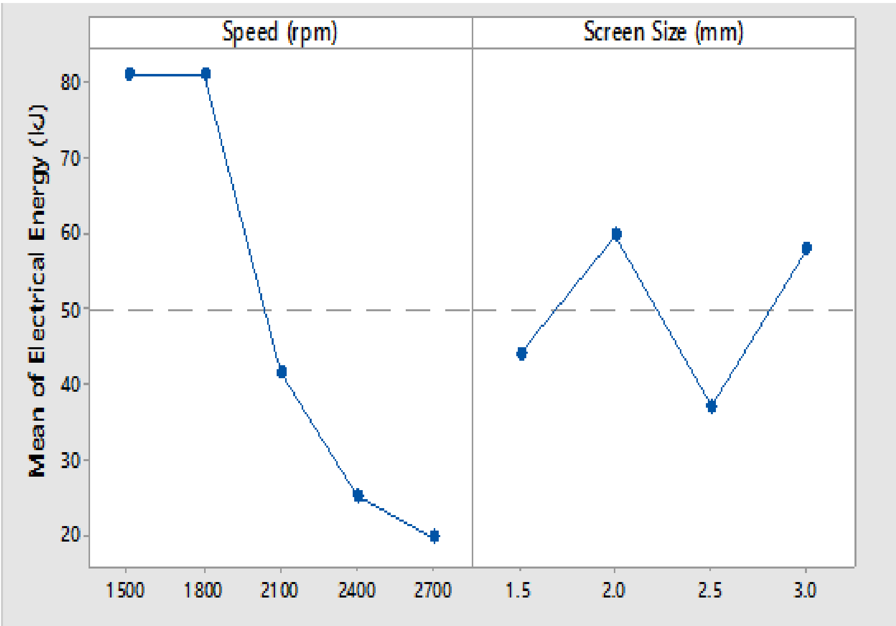

Figure 9. Electrical energy versus speed and screen size.

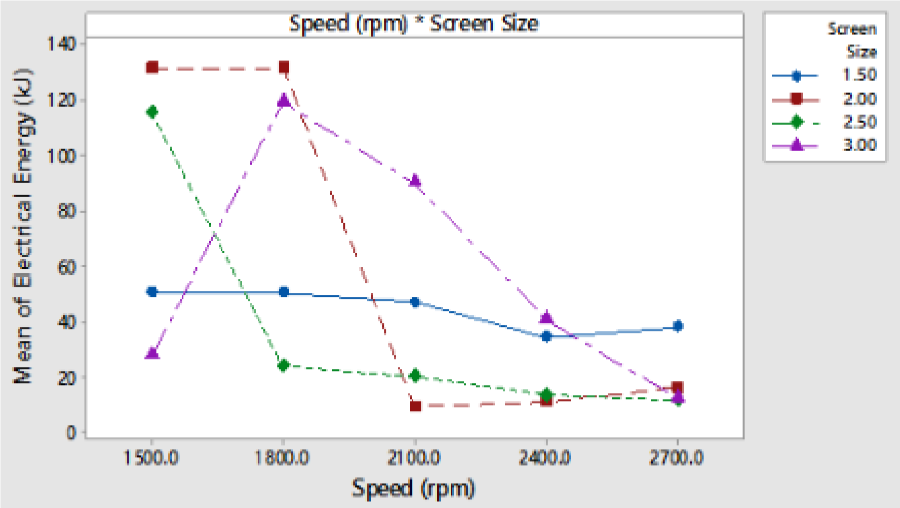

Figure 10. Effect of speed on electrical energy consumption (milling).

In Figure 9 above, it is shown that the electrical energy consumed reduces as speed increases, at lower speed more electrical energy is consumed because the ingredient spends longer time in the milling chamber before adequate milling is achieved.

Statistical model

Regression Analysis: Electrical Energy (milling) (kJ)

Table 10. Regression analysis: Electrical energy (milling, kJ).

Model No	Model Equation	R^2
I	$16.9 - 0.0078Sp + 4.9Ss + 5.61Mt$	0.296
II	$-510 + 0.467Sp + 5.5Ss + 8.44Mt - 0.000107Sp^2$	0.344
III	$-96 - 0.0033Sp + 100Ss + 6.09Mt - 21.1Ss^2$	0.304
IV	$-79.2 + 0.0045Sp + 8.8Ss + 25.65Mt - 1.015Mt^2$	0.460
V	$546 + 0.18Sp + 248Ss + 24.9Mt - 0.00006Sp^2 - 80.7Ss\ 1.22Mt^2 + 0.05Sp*Ss + 0.0018Sp*Mt + 2.44Ss*Mt$	0.569
VI	$-590 + 0.20Sp + 278Ss + 42.2Mt - 0.00005Sp^2 - 77.3Ss^2 - 1.19Mt^2 + 0.03Sp*Ss - 0.009Sp*Mt - 5.7Ss*Mt + 0.005Sp*Ss*Mt$	0.573

Evaluation of the statistical models

Energy used during milling (kJ)

The model that best described data characteristic is the one that gives the highest R^2 as shown in Table 11 below with the lowest χ^2 and RMSE values. Based on these criteria, Model 6 is the best fit for the data with R^2, χ^2 and RMSE values of 0.57, 1504.03 and 38.45 respectively.

Table 11. Model of lowest χ^2 and RMSE values.

Models	R^2	MSE	RMSE	X^2
1	0.296	2413.650	49.129	2454.560
2	0.344	2249.820	47.432	2287.950
3	0.304	2388.450	48.872	2428.930
4	0.460	1852.440	43.040	1883.840
5	0.569	1480.910	38.483	1506.010
6	0.573	1478.960	38.457	1504.030

CONCLUSION

There is no significant effect of screen size on the average power consumed during milling since there is no linear relationship between power consumed and screen size. However, there is a significant effect of speed on average power consumed, the power consumed increases as speed decreases thereby making milling operation at higher speed to be cost effective since it doesn't require much power to achieve the required output. It was observed during the process of the research that lower milling (rotor) speeds takes more time to mill the same quantity of product when compared with higher speeds. This observation shows that power consumption during milling is a factor of speed and the retention time. The P-Value depicts that screen size has no significant effect on the electrical energy consumed during the milling operation while speed has a significant effect on the electrical energy used at 95% confidence level.

DECLARATION OF COMPETING INTEREST

The authors declare that there are no conflict of interest

CREDIT AUTHORSHIP CONTRIBUTION STATEMENT

Ademola Adebukola Adenigba: Conceptualization, methodology, investigation and writing of the original draft.
Samuel Dare Oluwagbayide: Data analysis and edting of drafted copy.

REFERENCES

Adeomaya SO and Samuel OD (2014). Design and development of a petrol-powered hammer mill for rural Nigerian farmers. *Journal of Energy Technologies and Policy, 4(4): 65-74.*

Aderemi AM, Adedipe JO, Aluko KA, Odetoyinbo AP and Raji AA (2020). Development of a multi seed pneumatic cleaner. *Journal of Multidisciplinary Engineering Science and Technology, 7(9): 12617-12624.*

Chambliss CG (2002). Forage moisture content testing. AG-181. University of Florida cooperative extension service, *University of Florida*, Gainesville.

Donnel H (1983). Farm power and machinery. McGraw Hill, New Delhi, India. Anon. 1980. Encyclopedia Britanica, Vol. 21, pp.1157-72. *William Benton*, Chicago, IL, USA.

Norazatul HM, Nyuk LC and Yusof YA (2015). Grinding characteristics of Asian originated peanuts (*Arachis hypogaea* L.) and specific energy consumption during ultra-high-speed grinding for natural peanut butter production. *Journal of Food Engineering, 152: 1-7.*

Ovie SO and Eze SS (2013). Lysine requirement and its effect on the body composition of Oreochromis Niloticus fingerlings. *Journal of Fisheries and Aquatic Science, 8: 94-100.*

Pyarelal SP, Swapnil CW, Gaurav RD, Akash GC, Vogita DK and Shradh HB (2017). Deshelling of "*Semecarpus anacardium*" (Bibba Seed): A review study. *International Journal of Advance Research and Innovative Ideas in Education, 3(2): 1432-1439.*

Udo IU and Umoren UE (2011). Nutritional evaluation of some locally available ingredients uses for least-cost ration formulation for African Catfish (*Claris gariepinus*) in Nigeria. *Asian Journal of Agricultural Research, 5: 164-175.*

Turkish Journal of Agricultural Engineering Research

https://dergipark.org.tr/en/pub/turkager
https://doi.org/10.46592/turkager.2021.v02i02.002

Turk J Agr Eng Res (TURKAGER)
e-ISSN: 2717-8420
2021, 2(2): 276-288

Research Article (Araştırma Makalesi)

Influence of Irrigation Water pH on Biomass, Rooting, Root and Shoot Growth of Grapevine Rootstocks

Selda DALER[ID][a]* **Rüstem CANGİ**[ID][b]

[a]*Bahçe Bitkileri Bölümü, Ziraat Fakültesi, Yozgat Bozok Üniversitesi, 66900, Erdoğan Akdağ Kampüsü, Yozgat, TÜRKİYE*

[b]*Bahçe Bitkileri Bölümü, Ziraat Fakültesi, Tokat Gaziosmanpaşa Üniversitesi, 60240, Taşlıçiftlik Yerleşkesi, Tokat, TÜRKİYE*

(*): Corresponding author, selda.daler@yobu.edu.tr

ABSTRACT

In this study, the effects of irrigation water pH on root and shoot developments in grapevine rootstocks were investigated. Cuttings of Kober 5 BB and 41 B rootstocks were planted in plastic pots containing perlite and irrigated with 6 different pH values (5.5, 6.0, 6.5, 7.0, 7.5 and 8.0). At the end of the 90-day growing period, root and shoot characteristics of rootstocks were examined and determined that the highest rooting rates occurred at neutral and about neutral pH levels. In both rootstocks, it was recorded that the value of fresh and dry root weight reached the highest level at pH: 6.0. In addition, the highest dry matter ratios were obtained from pH: 6.0 (6.15%) in 41 B rootstocks, and from pH: 6.0 and 6.5 (respectively, 4.46% and 4.20) in 5 BB rootstocks. It was determined that the highest values of mean shoot weight and mean shoot length of rootstocks were obtained from pH: 6.5. chlorophyll measurement in SPAD, it was seen that there was no statistically significant difference between irrigation solutions with pH 5.5-7.5 on both rootstocks. As a result of the research, it was determined that irrigation solutions with different pH levels played an important role on the morphological and physiological characteristics of grapevine rootstocks.

RESEARCH ARTICLE

Received: 11.06.2021
Accepted: 03.08.2021

Keywords:

- Irrigation water quality,
- 41 B,
- 5 BB,
- Root and shoot growth,
- Chlorophyll content

To cite: Daler S, Cangi R (2021). Influence of Irrigation Water pH on Biomass, Rooting, Root and Shoot Growth of Grapevine Rootstocks. Turkish Journal of Agricultural Engineering Research (TURKAGER), 2(2): 276-288. *https://doi.org/10.46592/turkager.2021.v02i02.002*

Sulama suyu pH'sının Asma Anaçlarının Biyokütle, Köklenme, Kök ve Sürgün Gelişimi Üzerine Etkisi

ÖZET

Bu çalışmada, sulama suyu pH'sının asma anaçlarında kök ve sürgün gelişimi üzerine etkileri incelenmiştir. Kober 5 BB ve 41 B anaçlarına ait çelikler perlit içeren plastik potlara dikilerek, 6 farklı pH değerine sahip (5.5, 6.0, 6.5, 7.0, 7.5 ve 8.0) sulama çözeltisi ile sulanmışlardır. 90 günlük yetiştirme periyodunun sonucunda, anaçlara ait kök ve sürgün özellikleri incelenmiş ve en yüksek köklenme oranının nötr ve nötre yakın pH derecelerinde meydana geldiği belirlenmiştir. Her iki anaçta da yaş ve kuru kök ağırlığı değerlerinin pH: 6.0'da en yüksek seviyeye ulaştığı kaydedilmiştir. Ayrıca, en yüksek kuru madde oranının 41 B anacında pH: 6.0'dan (%6.15), 5 BB anacında ise pH: 6.0 ve 6.5 derecelerinden (sırasıyla, %4.46 ve %4.20) alındığı belirlenmiştir. Anaçların ortalama sürgün ağırlığı ve ortalama sürgün uzunluğu değerlerinin en yüksek pH: 6.5 derecesinden elde edildiği belirlenirken; SPAD cinsinden gerçekleştirilen klorofil ölçümleri sonucunda her iki anaçta da pH'sı 5.5-7.5 olan sulama solüsyonları arasında istatistiksel olarak önemli bir farklılığın bulunmadığı saptanmıştır. Araştırma sonucunda, farklı pH derecelerine sahip sulama çözeltilerinin asma anaçlarının morfolojik ve fizyolojik özellikleri üzerinde önemli rol oynadığı belirlenmiştir.

ARAŞTIRMA MAKALESİ

Alınış tarihi: 11.06.2021
Kabul tarihi: 03.08.2021

Anahtar Kelimeler:

- Sulama suyu kalitesi,
- 41 B,
- 5 BB,
- Kök ve sürgün gelişimi,
- Klorofil içeriği

Alıntı için: Daler S, Cangi R (2021). Sulama suyu pH'sının Asma Anaçlarının Biyokütle, Köklenme, Kök ve Sürgün Gelişimi Üzerine Etkisi. Turkish Journal of Agricultural Engineering Research (TURKAGER), 2(2): 276-288. *https://doi.org/10.46592/turkager.2021.v02i02.002*

GİRİŞ

Bitki gelişimini sınırlandıran faktörlerin başında kök bölgesinde bulunan yarayışlı suyun eksikliği gelmektedir (Lal, 1991; Falkenmark ve Rockström, 1993). Sulama suyu kalitesinin toprağa ve bitkiye olan etkileri; toprağın fiziksel ve kimyasal özelliklerine, yetiştirilen bitkinin adaptasyon derecesine, bölgenin iklim koşullarına, uygulanan sulama yöntemine, sulama aralığına ve sulama suyu miktarına bağlı olarak değişiklik göstermektedir (Rhoades, 1972). Bununla birlikte sulama suyunun en önemli kalite göstergelerinden biri olan pH değeri, ortamın fiziksel, kimyasal ve mikrobiyolojik özellikleri üzerine etkilidir (Şinik, 2011).

pH değeri, hidrojen iyonu konsantrasyonunun 10 tabanına göre negatif logaritmasıdır. Suların pH değerleri 0-14 arasında değişmekte ve pH'sı 7 olan sular nötr olarak ifade edilmektedir. Nötr pH'da hidrojen ve hidroksit iyonları denge halinde olup, asit ve alkali reaksiyonlar bulunmamaktadır. Sulama suyunun hidrojen iyonu konsantrasyonunun artması asit ($pH<7$); hidroksit iyonu konsantrasyonunun artması ise bazik ($pH>7$) karakter almasına neden olmaktadır. Genel olarak yeraltı suları, pH'sı 7'nin altında asidik özellik taşıyan sular olarak bilinirken; yüzeysel sular pH'sı genellikle 8'in üstünde bazik özellikteki sular olarak tanımlanmaktadır (Tuncay, 1994; Güler, 1997; Şimşek ve ark., 2017). Alkali koşullarda bazı bitki besin elementlerinin, özellikle de N, P, K, Ca, Mg ve Mo minerallerinin bitkiler tarafından alınabilirliği artmakta ve ortamın mikrobiyal aktivitesi yükselmektedir. Alkaliliğin fazla yüksek olması, başta K olmak üzere bazı besin elementlerinin yarayışlılığını azaltmaktadır. Asidik koşullarda ise H, Al, Mn ve Cu iyonlarının bitkilere toksik etki yapabilecek düzeyde çözünürlüklerinin arttığı ifade edilmektedir (Zhao, 2003; Rosas ve ark., 2007; Zhao ve ark., 2013).

Sulama sularında pH'nın sınır değerleri aşması, bitkilerde dengesiz beslenmeye veya toksik maddelerin birikimine neden olmaktadır (Anonim, 1994).

Sulama sularının optimum pH aralığı, bitki türlerine göre değişiklik göstermektedir ve her bitki türü yalnızca uygun pH aralığında ihtiyacı olan tüm besin maddelerini absorbe ederek normal gelişimini sürdürebilmektedir (Zhao, 2003).

Kanber ve ark. (1992), tarımsal amaçlı kullanılan sulama sularında pH değerlerinin 6.5-8.0 aralığında olması gerektiğini ifade ederken; Iyengar ve ark. (2011), ideal toprak pH'sının 5.5 ile 6.5 aralığında ve sulama suyu pH'sının ise 5.5 ile 7.0 aralığında olması gerektiğini bildirmektedir.

Dünya bağcılığında on yedinci yüzyılın sonlarından itibaren, filoksera *(Daktulosphaira vitifoliae)* salgını, tüm Avrupa'da *Vitis vinifera* L. ile yapılan eski bağcılığın bitmesine neden olmuştur (Riley, 1891). Amerikan asma anaçları kullanılarak aşılama metoduyla yeni bağcılığa geçilmiştir (Spoerr, 1902). Seleksiyon yardımıyla asma anaçlarının ıslahı ise son yüzyılda hız kazanmış olup, bunlar içerisinde *Vitis vinifera* L. türüne giren çeşitlerle iyi bir uyuşma gösteren, üzerine aşılanan çeşitlerin verim ve kalite özellikleri üzerine olumlu etkilerde bulunan, çoğaltımları kolay ve filokseraya dayanıklı *Vitis riparia*, *Vitis rupestris* ve *Vitis berlandieri* Amerikan asma türleri tespit edilmiştir (Ruckenbauer ve Traxler, 1974). Ardından, türler arası melezlemelerle (Amerikan × Amerikan; Vinifera × Amerikan) hibrit anaçlar elde edilerek günümüzde aşı randımanı, afinitesi, ekolojik koşullara adaptasyon yeteneği, köklenme kabiliyeti, beslenme, büyüme ve gelişme kuvveti gibi verim ve kalite özellikleri bakımından farklılık gösteren pek çok anaç geliştirilmiştir (Mullins ve ark., 1992; Çelik, 1996). Asmaların kök sistemini oluşturan anaçların asıl görevi, bitki-su ilişkilerini kontrol ederek, besin maddelerinin alımı, taşınması ve depolanmasını sağlamak ve bununla birlikte büyümeyi düzenleyici maddelerin sentezlenmesinde rol alarak bitki metabolizmasını yönetmektir (Richards, 1983; Çelik, 1996).

Bağcılıkta kullanılan anaçların iklim ve toprak şartlarına adaptasyonları ile üzerlerine aşılanan çeşitlerle uyuşma kabiliyetleri farklı olduğundan gelişme ve verim düzeyleri de değişiklik göstermektedir. Bununla birlikte, yapılan araştırmalar farklı anaçların bünyelerinde depolayabilecekleri besin maddesi içeriği bakımından geniş bir varyasyon gösterdiklerini ve toprakta mevcut besin maddesi miktarına göre en uygun anacın seçilmesinin mümkün olabileceğini ortaya koymuştur (Cirami ve ark., 1985; Scienze ve ark., 1986; Hayes ve Mannini, 1988; Tangolar ve Ergenoğlu, 1989; Loué, 1990; Volpe ve Boselli, 1990; Fardossi ve ark., 1991; Rühl, 1991; Williams ve Smith, 1991; Boselli ve Volpe, 1993; Çelik, 1996).

Bitki besin elementlerinin farklı pH koşullarında alınım miktarları da farklı olmaktadır. Bitkiler için mutlak gerekli olan besin elementleri özellikle bitkilerin bulundukları ortamların pH değerlerine göre ele alınmalı ve eğer toprak reaksiyonu için bir düzenleme yapılacaksa, elementlerin uygun olmayan pH derecelerinde toksisite ya da noksanlıklarının ortaya çıkabileceği göz ardı edilmemelidir (Şinik, 2011). Topraktaki pH, bitki gelişimi üzerinde önemli bir rol oynamaktadır (Zhao ve ark., 2013).

Bu araştırmada farklı pH derecelerine (pH: 5.5, 6.0, 6.5, 7.0, 7.5 ve 8.0) sahip sulama solüsyonlarının, 41 B ve 5 BB anaçlarında morfolojik (köklenme oranı, yaş kök ağırlığı, kuru kök ağırlığı, kuru madde oranı, sürgün sayısı, ortalama sürgün ağırlığı ve ortalama sürgün uzunluğu) ve fizyolojik özellikler (klorofil miktarı) üzerindeki etkilerinin belirlenmesi amaçlanmıştır.

MATERYAL ve YÖNTEM

Materyal

Bu araştırma, Yozgat Bozok Üniversitesi Ziraat Fakültesi Bahçe Bitkileri Bölümü'ne ait sıcaklık ve nem kontrollü iklim odasında yürütülmüştür. Araştırmada bitkisel materyal olarak kullanılan 41 B ve 5 BB Amerikan asma anacı çelikleri, Tokat Gaziosmanpaşa Üniversitesi Ziraat Fakültesi'nden temin edilmiştir.

41 B Millardet et de Grasset (41 B MGt): *V. vinifera* × *V. berlandieri* melezidir. Vejetasyon periyodu kısa olan, erkencilik ve yüksek verim sağlayan anaç, kirece karşı çok yüksek bir dayanım gösterirken, filokseraya orta derecede toleranslı, ilkbahar yağışlarına, nematodlara, mildiyöye ve tuza karşı hassastır. Çelikleri zor köklenir, masa başı aşılamadaki başarı oranı düşükken, bağda aşılamada daha yüksektir Çelik (1996).

Kober 5 BB: *V. berlandieri* × *V. riparia* melezidir. Kuvvetli gelişen, vejetasyon süresi kısa, kök-ur nematodlarına ve kirece dayanımı orta derece, nemli ve kumlu topraklara iyi uyum sağlayabilen, kurak koşullara hassas bir anaçtır. Çelikleri kolay köklenir, bağda aşılamada kalemden kök oluşturma eğilimi yüksektir Çelik (1996).

Yöntem

Dinlenme döneminde alınan çelikler, 5 gözlü ve 35-40 cm uzunluğunda hazırlanarak, içerisinde perlit bulunan plastik potlara (15×15×18 cm) dikilmişlerdir. pH ayarlama çözeltileri olarak 0.1 N sodyum hidroksit (NaOH, Merck-Germany) ve 0.1 N hidroklorik asit (HCl, Merck-Germany) kullanılmış olup, pH dereceleri 5.5, 6.0, 6.5, 7.0, 7.5 ve 8.0 olan 6 farklı sulama suyu stok çözeltisi hazırlanmıştır. Nötr pH uygulaması (pH: 7.0) kontrol olarak kabul edilmiştir. Çalışmanın yürütüldüğü iklim odası; 25 ± 2°C sıcaklık, %70 nem ve 16/8 (gündüz/gece) fotoperiyot koşullarına sahiptir. Kontrollü koşullarda yetiştirilen çelikler 90 günlük yetiştirme periyodu süresince haftada 2 kez farklı pH derecelerine sahip sulama çözeltileriyle sulanmışlardır. Her sulama uygulamasına, solüsyon drenaj deliklerinden çıkıncaya kadar devam edilmiştir. Besin çözeltisi ise Hoagland ve Arnon (1950) tarafından önerilen prosedüre göre hazırlanmış olup, HCI ve NaOH ile sulama suyu pH değerlerine uyumlu olacak şekilde ayarlanarak 10'ar gün aralıklarla bitki kök bölgesine verilmiştir. 90 günlük gelişme süresini takiben anaçlarda morfolojik ve fizyolojik analizler gerçekleştirilmiştir.

Morfolojik incelemeler

Köklenme oranı (%): Kök oluşturan çeliklerin sayısının, toplam anaç sayısına oranlanması ile % olarak belirlenmiştir.

Yaş kök ağırlığı (mg): Köklerin yaş ağırlıkları 0.0001 g hassasiyetindeki analitik terazi ile tartılmıştır.

Kuru kök ağırlığı (mg): Kökler, 72 saat süreyle, 65°C sıcaklıktaki hava sirkülasyonlu etüvde kurutularak, tartılmıştır.

Kuru madde oranı (%): Kuru kök ağırlıklarının, yaş kök ağırlıklarına oranlanması ile % olarak hesaplanmıştır.

Sürgün sayısı (adet): Her uygulamaya ait çeliklerden süren sürgünler sayılarak kaydedilmiştir.

Ortalama sürgün ağırlığı (mg): 0.0001 g hassas analitik terazi ile tartılmıştır.

Ortalama sürgün uzunluğu (cm): Sürgünün uç kısmından itibaren dip noktasına kadar olan mesafe bir cetvel yardımıyla ölçülerek ortalamaları cm olarak kaydedilmiştir.

Fizyolojik incelemeler
Klorofil miktarı (SPAD): Yaprakların klorofil içerikleri Konica Minolta SPAD-502 Plus Klorofilmetre cihazı kullanılarak SPAD cinsinden hesaplanmıştır.

İstatistiksel analizler
Deneme; tesadüf parselleri deneme desenine göre 3 tekerrürlü ve her tekerrürde 50 adet olmak üzere toplam 900 bitki üzerinde yürütülmüştür. Çalışmadan elde edilen sayısal verilerin değerlendirilmesinde SPSS (20.0) istatistiki analiz programından yararlanılmıştır ($p<0.05$). Uygulamalar arasındaki farklılıklar Duncan çoklu ortalama karşılaştırma metodu ile belirlenmiştir.

BULGULAR ve TARTIŞMA

Sulama suyunun farklı pH değerleri, anaçlara göre değişmekle birlikte morfolojik ve fizyolojik özellikler üzerinde önemli istatistiksel farklılıklara neden olmuştur (Çizelge 1 ve 2). Çalışmadan elde edilen bulgular, 5 BB anacının köklenme oranının, 41 B'ye göre daha yüksek olduğunu göstermektedir (Çizelge 1; Şekil 1 ve 2).

Şekil 1. Farklı pH derecelerinin 41 B anacının kök gelişimi üzerine etkisi.
Figure 1. *The effect of different pH degrees on root development of 41 B rootstock.*

Şekil 2. Farklı pH derecelerinin 5 BB anacının kök gelişimi üzerine etkisi.
Figure 2. *The effect of different pH degrees on root development of 5 BB rootstock.*

Çizelge 1. Sulama suyu pH'sının 5 BB ve 41 B çeliklerinin kök özellikleri üzerine etkileri.
Table 1. *Effects of irrigation water pH on root properties of 5 BB and 41 B cuttings.*

Anaç	pH: 5.5	pH: 6.0	pH: 6.5	pH: 7.0	pH: 7.5	pH: 8.0
			Köklenme oranı (%)			
5 BB	93.75 ± 4.45 Ab*	87.50 ± 1.83 Ac	93.75 ± 2.76 Ab	97.50 ± 1.04 Aa	93.75 ± 1.36 Ab	87.50 ± 3.62 Ac
41 B	90.00 ± 2.75 Ab	87.50 ± 1.64 Ab	93.75 ± 3.51 Aa	93.75 ± 3.87 Ba	81.25 ± 2.02 Bc	81.25 ± 2.34 Bc
			Yaş kök ağırlığı (mg)			
5 BB	827.69 ± 138.54 Bc	1342.11 ± 211.93 Ba	1120.85 ± 246.72 Bb	1187.48 ± 324.66 Bb	1194.02 ± 199.41 Bb	803.72 ± 281.05 Bc
41 B	1451.16 ± 373.09 Ad	1953.44 ± 401.60 Aa	1762.39 ± 226.65 Ab	1415.02 ± 114.82 Ad	1539.75 ± 360.44 Acd	1601.64 ± 291.70 Ac
			Kuru kök ağırlığı (mg)			
5 BB	21.32 ± 1.35 Be	58.16 ± 4.52 Ba	49.77 ± 3.27 Bb	39.53 ± 1.78 Bc	37.85 ± 2.64 Bc	31.55 ± 2.91 Bd
41 B	79.95 ± 4.68 Ab	120.04 ± 2.07 Aa	92.71 ± 3.43 Ab	58.32 ± 2.79 Ac	69.13 ± 1.34 Ab	61.68 ± 5.25 Ac
			Kuru madde oranı (%)			
5 BB	2.40 ± 0.03 Be	4.46 ± 0.17 Ba	4.20 ± 0.09 Bab	3.58 ± 0.05 Bc	3.37 ± 0.06 Bd	3.75 ± 0.02 Ab
41 B	5.51 ± 0.02 Ab	6.15 ± 0.14 Aa	5.13 ± 0.07 Ac	4.25 ± 0.03 Ae	4.53 ± 0.06 Ad	3.75 ± 0.06 Af

*:Aynı sütunda farklı büyük harfler taşıyan ortalamalar arasında farklılık bulunmaktadır, aynı satırda farklı küçük harfler taşıyan ortalamalar arasında farklılık bulunmaktadır ($p<0.05$)

Çizelge 2. Sulama suyu pH'sının 5 BB ve 41 B çeliklerinin sürgün özellikleri üzerine etkileri.
Table 2. *Effects of irrigation water pH on shoot properties of 5 BB and 41 B cuttings.*

Anaç	pH: 5.5	pH: 6.0	pH: 6.5	pH: 7.0	pH: 7.5	pH: 8.0
			Sürgün sayısı (adet)			
5 BB	1.94 ± 0.093 Aab*	1.56 ± 0.062 Ad	1.75 ± 0.077 Ac	2.06 ± 0.118 Aa	1.81 ± 0.054 Ab	1.81 ± 0.015 Ab
41 B	1.63 ± 0.0074 Aa	1.50 ± 0.0041 Ab	1.69 ± 0.0125 Aa	1.50 ± 0.0089 Bb	1.50 ± 0.0051 Ab	1.38 ± 0.0062 Bc
			Ort. sürgün ağırlığı (mg)			
5 BB	4372.82 ± 381.65 Bb	3681.75 ± 320.08 Bd	4737.01 ± 273.41 Ba	4449.62 ± 255.52 Ab	4319.17 ± 416.19 Bb	3895.42 ± 248.24 Bc
41 B	6274.92 ± 563.14 Aa	5941.55 ± 423.92 Ab	6282.41 ± 208.39 Aa	5819.23 ± 636.75 Abc	6076.64 ± 194.88 Ab	5478.08 ± 301.25 Ac
			Ort. sürgün uzunluğu (cm)			
5 BB	29.73 ± 1.45 b	28.40 ± 0.94 bc	32.17 ± 2.21 a	27.75 ± 1.87 c	29.94 ± 1.59 b	25.33 ± 1.68 d
41 B	41.58 ± 2.67 c	43.39 ± 2.09 b	45.88 ± 3.15 a	41.48 ± 2.53 c	41.40 ± 4.48 c	33.72 ± 3.76 d
			Klorofil miktarı (SPAD)			
5 BB	17.03 ± 0.64 Aab	17.66 ± 0.81 Aab	19.79 ± 1.17 Aa	19.32 ± 0.55 Aa	19.37 ± 1.06 Aa	16.11 ± 1.28 Ab
41 B	15.04 ± 0.14 Aab	16.25 ± 0.65 Aa	15.82 ± 0.98 Ba	16.06 ± 1.02 Ba	15.51 ± 0.39 Bab	14.28 ± 1.37 Bb

*: Aynı sütunda farklı büyük harfler taşıyan ortalamalar arasında farklılık bulunmaktadır, aynı satırda farklı küçük harfler taşıyan ortalamalar arasında farklılık bulunmaktadır ($p<0.05$)

İncelenen anaçlarda en yüksek köklenme oranının 41 B anacında %93.75 ile pH: 6.5 ve 7.0'den; 5 BB anacında ise %97.50 ile pH: 7.0 derecesinden alındığı belirlenmiştir (Şekil 3). Bulgularla uyumlu olarak Bates ve ark. (2002), Concord üzüm çeşidinde pH derecesinin 4.5'in altına düştüğünde kök ve sürgün biyokütlesinde önemli oranda azalma olduğunu; 7.5 pH seviyesinde sürgün biyokütlesinde düşüşlerin meydana geldiğini ve 5.0-7.5 aralığındaki değerlerde ise vejetatif büyümede önemli bir fark bulunmadığını kaydetmişlerdir.

Araştırmada her iki anaçta da yaş (41 B, 1 953.44 mg; 5 BB, 1 342.11 mg) ve kuru (41 B, 120.04 mg; 5 BB, 58.16 mg) kök ağırlıklarına ait en yüksek değerlerin pH: 6.0 derecesinden elde edildiği belirlenmiştir (Şekil 4 ve 5). Sonuçlara paralel olarak Çakır ve Atalay (2020) tarafından Sultani Çekirdeksiz / 5 BB ve Sultani Çekirdeksiz / 41 B aşı kombinasyonunda farklı pH derecelerinin (4.5, 7.0 ve 8.5) yaş kök ağırlığı üzerine etkili olduğu; artan pH ile yaş kök ağırlığının önemli ölçüde azaldığı ifade edilmiştir. Valdez-Aguilar ve ark. (2009)'de alkali pH'ya sahip sulama suyunun düğünçiçeği bitkisinin kök ağırlığında önemli oranda azalmaya neden olduğunu ve alkaliliğin bitki büyümesi üzerinde stres yarattığını ifade etmektedirler. Vršič ve ark. (2016), 6 farklı asma anacını içerisinde farklı tabakalar halinde çakıl, yüksek kireçli Rendzina toprağı (pH: 8.54) ve turba-toprak karışımı (pH: 4.94) bulunan saksılarda yetiştirmişler ve sonuçta yüksek pH koşullarına daha iyi uyum sağlayabilen Fercal anacının kuru kök ağırlığı bakımından daha yüksek değerlere sahip olduğunu ifade etmişlerdir.

Kuru kök ağırlığının, yaş kök ağırlığına oranlanması ile elde edilen kuru madde oranı; 41 B anacında en yüksek pH: 6.0 derecesinde %6.15 olarak belirlenirken; 5 BB anacında pH: 6.0 ve 6.5 derecelerinde sırasıyla, %4.46 ve 4.20 olarak tespit edilmiştir (Şekil 6). Çakır ve Atalay (2020), yüksek pH'nın asma çeşit ve anaçları üzerindeki olumsuz etkisinin kök gelişimine kıyasla sürgün gelişimi üzerinde daha belirgin olduğunu ifade etmişlerdir. Araştırmadan elde edilen bulgulara göre 41 B anacında en fazla sürgünün pH: 5.5 ve 6.5 derecelerinden sırasıyla, 1.63 ve 1.69 adet olduğu belirlenirken; 5 BB anacında pH: 5.5 ve 7.0 derecelerinden sırasıyla, 1.94 ve 2.06 adet olduğu kaydedilmiştir (Şekil 7). Bulgulara benzer şekilde Fischer ve ark. (2016), Briteblue ve Delite yaban mersini çeşitlerinde 4.5, 5.5, 6.0 ve 6.9 (kontrol) pH derecelerine sahip sulama suyu ile Indol Bütirik Asidin (IBA) etkilerini araştırmışlar ve çelik başına ortalama sürgün sayısının sulama suyunun asitlenmesi ile arttığını tespit etmişlerdir. Zhao ve ark. (2013), şakayık (*Paeonia lactiflora* Pall.) bitkisinde pH'sı 4.0 ve 10.0 olan ortamların kontrolle (pH 7.0) karşılaştırıldığında yaprak sayısı hariç bitkinin tüm morfolojik parametrelerinde azalmaya neden olduğunu bildirmişlerdir.

Ortalama sürgün ağırlıklarına ait en yüksek değerlerin 41 B anacında 6 282.41 mg ve 5 BB anacında 4 737.01 mg olarak; pH: 6.5 derecesinden elde edildiği belirlenmiştir (Şekil 8). Bavaresco ve ark. (2003) tarafından da benzer sonuçlar kaydedilmiş, topraktaki yüksek karbonat içeriği, yaprak ve sürgün gelişimi ile toplam kuru madde üretimini azaltmıştır. Vršič ve ark. (2016), yüksek pH koşullarına daha iyi uyum sağlayabilen Fercal dahil üç anacın biyokütle üretimi bakımından daha yüksek değerlere sahip olduğunu ifade etmişlerdir. Valdez-Aguilar ve ark. (2009) ise kum kültürlerinde yetiştirilen düğünçiçeği bitkisinde (*Ranunculus asiaticus*) elektriki iletkenliği (EC) 2, 3, 4 ve 6 dS m−1 ve pH kontrolü olan (pH: 6.4) ve olmayan (pH: 7.8) sulama suyunda; pH: 7.8'in, pH: 6.4 ile karşılaştırıldığında sürgün kuru ağırlığında önemli oranda azalmaya neden olduğunu bildirmektedirler.

Çalışmadan elde edilen bulgulara göre, anaçların ortalama sürgün uzunluklarına ait en yüksek değerlerin 41 B'de 45.88 cm ve 5 BB'de 32.17 cm olmak üzere sulama suyu pH'sı 6.5 olan ortamdan alındığı kaydedilmiştir (Şekil 9). Bulgularla benzer olarak Çakır ve Atalay (2020), farklı pH derecelerinin Sultani Çekirdeksiz / 5 BB aşı kombinasyonunda sürgün uzunluğu ve yaprak alanı değerlerini önemli ölçüde etkilediğini; pH değeri arttıkça sürgün uzunluğu ve yaprak alanının azaldığını belirlemişlerdir. Valdez-Aguilar ve ark. (2009), tuzluluğun, alkali pH ile kombinasyonu sonucunda düğünçiçeği bitkisinin gövde uzunluğunda önemli derecede azalmaya neden olduğunu bildirmişlerdir. Zhao ve ark. (2013) ise şakayık bitkisinde büyümenin, sulama suyundaki aşırı pH'dan önemli ölçüde etkilendiğini ve en ciddi stresin pH: 10.0'da gerçekleştiğini bildirmektedir.

SPAD cinsinden gerçekleştirilen klorofil ölçümleri sonucunda her iki anaçta da pH'sı 5.5-7.5 olan sulama çözeltileri arasında istatistiksel olarak önemli bir farklılık bulunmadığı; bununla birlikte en düşük değerlerin pH derecesi 8.0 olan çözeltiden elde edildiği kaydedilmiştir (Şekil 10). Zhao ve ark. (2013), pH derecesi 4.0 ve 10.0 olan çözeltilerle sulanan şakayık bitkisinde pH: 7.0 ile sulananlarla karşılaştırıldığında, klorofil a, klorofil b, klorofil a + b gibi fizyolojik indekslerin arttığını kaydederek, şakayık bitkisinin klorofil miktarı açısından asit ve alkali ortam direnci gösterdiğini ifade etmişlerdir.

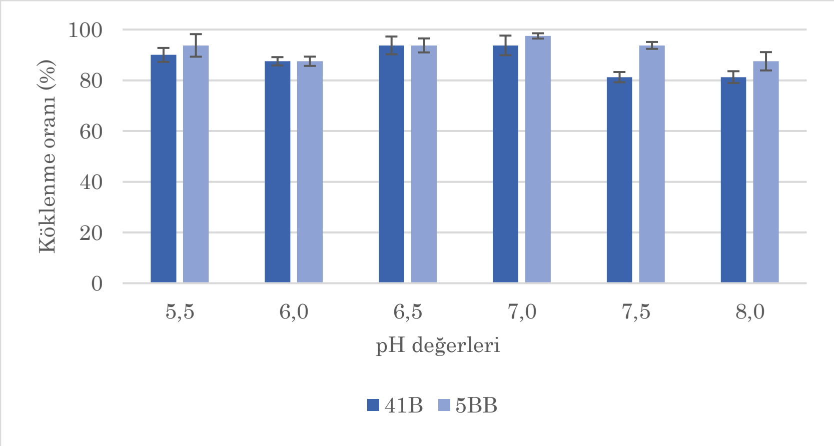

Şekil 3. Anaçlara ait köklenme oranları.
Figure 3. *Rooting ratio of the rootstocks.*

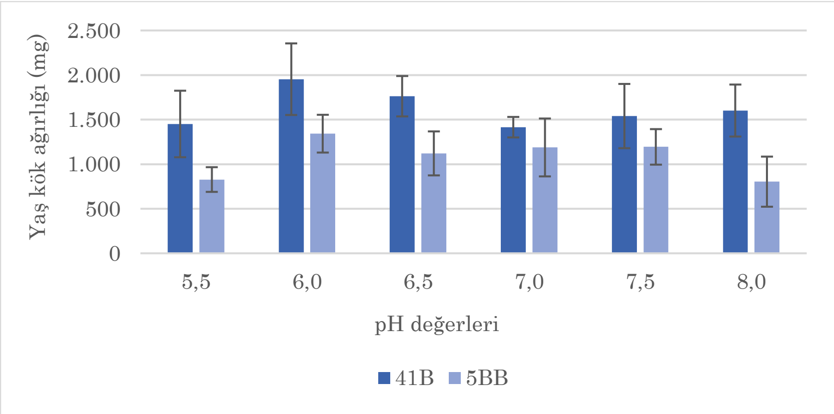

Şekil 4. Anaçlara ait yaş kök ağırlıkları.
Figure 4. *Fresh root weight of the rootstocks.*

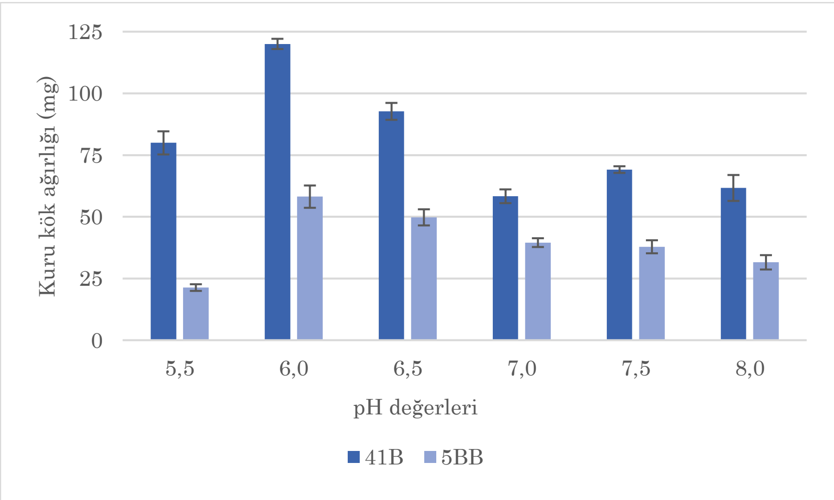

Şekil 5. Anaçlara ait kuru kök ağırlıkları.
Figure 5. *Dry root weight of the rootstocks.*

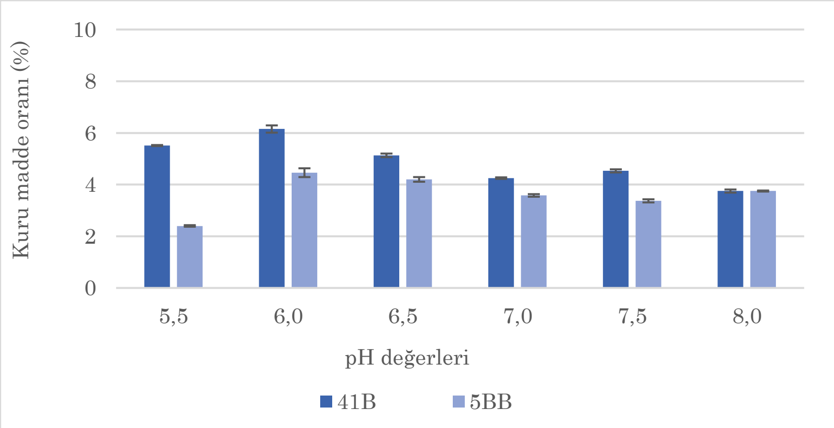

Şekil 6. Anaçlara ait kuru madde oranları.
Figure 6. *Dry matter ratio of the rootstocks.*

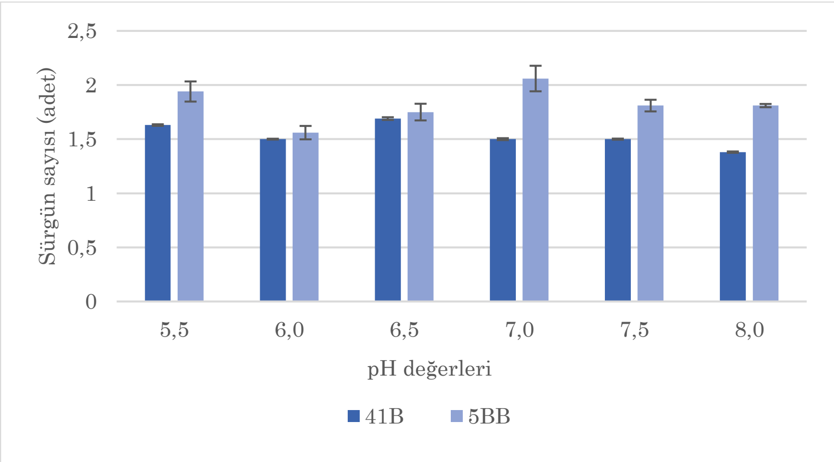

Şekil 7. Anaçlara ait sürgün sayıları.
Figure 7. *Shoot number of the rootstocks.*

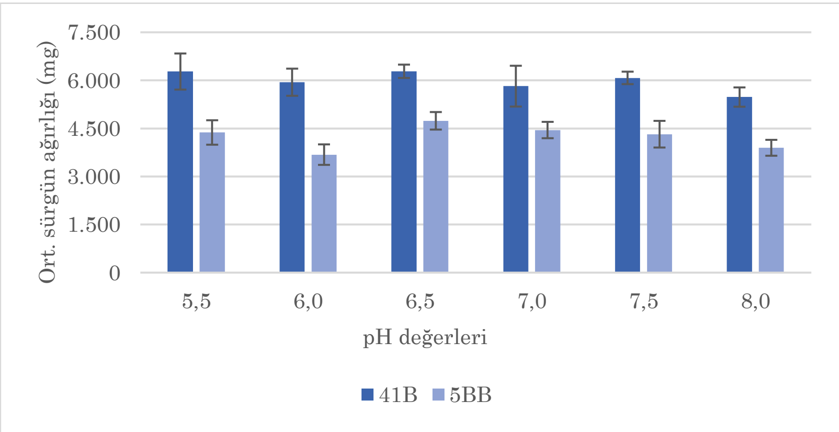

Şekil 8. Anaçlara ait ortalama sürgün ağırlıkları.
Figure 8. *Mean shoot weight of the rootstocks.*

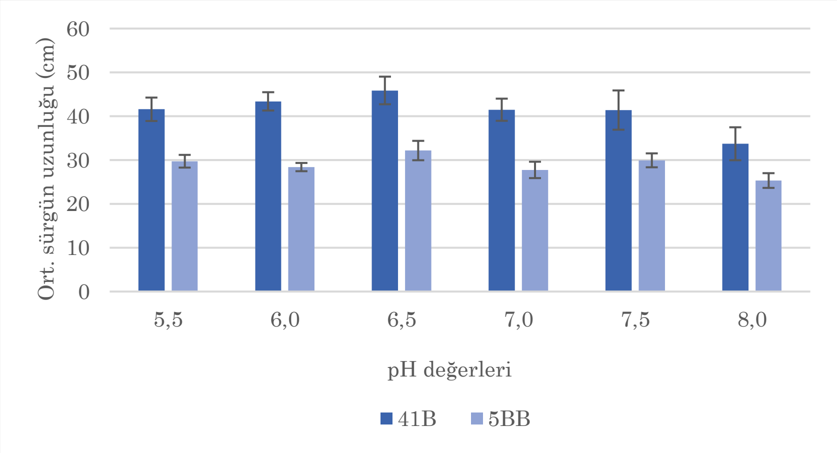

Şekil 9. Anaçlara ait ortalama sürgün uzunlukları.
Figure 9. *Mean shoot length of the rootstocks.*

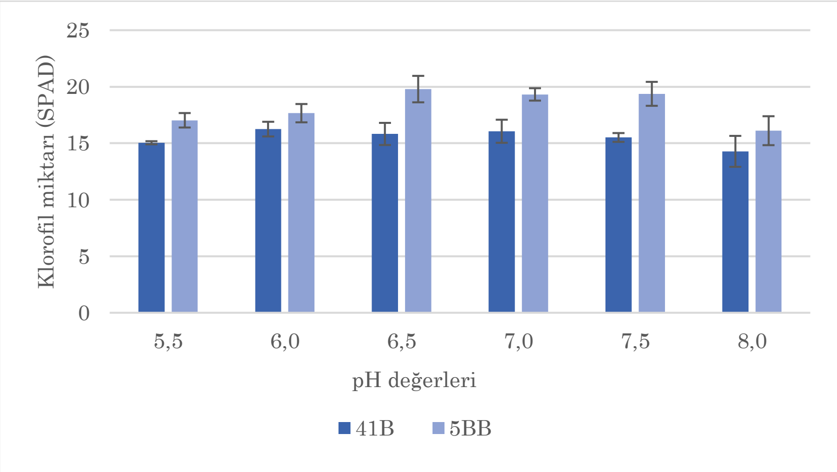

Şekil 10. Çeşitlere ait klorofil miktarları.
Figure 10. *Chlorophyll content of the rootstocks.*

SONUÇ

Sulama suyu pH'sının asma anaçlarının biyokütle, köklenme, kök ve sürgün gelişimi üzerine etkisinin incelendiği bu çalışmada, köklenme oranı bakımından en yüksek değerlerin nötr ve nötre yakın pH derecelerinden elde edildiği tespit edilmiştir. Yaş ve kuru kök ağırlıklarına ait en yüksek değerlerin her iki çeşitte de 6.0 pH derecesinden; en yüksek kuru madde oranlarının ise pH: 6.0 ve 6.5 derecelerinden elde edildiği kaydedilmiştir. Sürgün sayısı bakımından en yüksek değerlerin pH'sı 5.5, 6.5 ve 7.0 olan sulama solüsyonlarından alındığı belirlenirken; çeşitlerin ortalama sürgün ağırlığı ve ortalama sürgün uzunluklarına ait en yüksek değerlerin pH: 6.5 derecesinden elde edildiği saptanmıştır. Her iki çeşitte de 5.5-7.5 pH aralığındaki sulama çözeltileri arasında klorofil içeriği bakımından önemli bir farklılık bulunmazken, pH'sı 8.0 olan sulama solüsyonlarında yapraklardaki klorofil miktarının azaldığı belirlenmiştir. Araştırma sonuçları düşük pH derecelerinden ziyade alkali pH'ya sahip sulama solüsyonlarının her iki asma anacı için de hem morfolojik hem de fizyolojik kriterler bakımından sınırlayıcı etki gösterdiğini kanıtlamıştır. Elde edilen bulgular sulama suyu pH değerlerinin asmanın büyüme ve gelişmesi üzerindeki rolünün göz ardı edilemeyeceğini göstermiştir.

ÇIKAR ÇATIŞMASI

Yazarlar olarak, çalışmanın planlanması, yürütülmesi ve makalenin hazırlanması aşamalarında herhangi bir çıkar çatışması içerisinde olmadığımızı beyan ederiz.

YAZAR KATKISI

Yazarlar, makalenin altta belirtilen iş planına göre yürütüldüğünü beyan ederler.

Rüstem Cangi: Çalışmanın planlanması, bitkisel materyallerin temin edilmesi, istatistiksel analizlerin gerçekleştirilmesi ve makaleye son şeklinin verilmesinde katkı sağlamıştır.
Selda Daler: Denemenin kurulması, morfolojik ve fizyolojik analizlerin yürütülmesi, verilerin yorumlanması ve makalenin yazılmasında katkı sağlamıştır.

KAYNAKLAR

Anonim (1994). FAO, water quality for agriculture. *Irrigation and Drainage Paper,* Rome.

Bates TR, Dunst RM, Taft T and Vercant M (2002). The vegetative response of 'Concord' grapevines to soil pH. *The American Society for Horticultural Science, 37(6): 890-893.*

Bavaresco L, Giachino E and Pezutto S (2003). Grapevine rootstocks effects on lime-induced chlorosis, nutrient uptake, and source-sink relationships. *Journal of Plant Nutrition, 26: 1451-1465.*

Boselli M and Volpe B (1993). Influence of rootstock on potassium content, the pH and concentration of organic acids of the must of cv "Chardonnay". *Papers of the School of Viticulture and Enology, University of Turin (Italy), 16: 37-40.*

Cirami RM, McCarthy MG and Furkaliev DG (1985). Minimum pruning of Shiraz vines - effects on yield and wine colour. *Australian & New Zealand Grapegrower & Winemaker, 263: 26-27.*

Çakır B and Atalay YI (2020). *pH, 'Sultani Çekirdeksiz', Kober 5 BB, 41 B, plant growth, mineral content.* 30. International Horticultural Congress IHC2018: International Symposium on Viticulture: Primary Production and Processing, 12-16 August 2018. Istanbul-Turkey (in English).

Çelik H (1996). Bağcılıkta anaç kullanımı ve yetiştiricilikteki önemi. *Anadolu Ege Tarımsal Araştırma Enstitüsü Dergisi, 6(2): 127-148.*

Falkenmark M and Rockstrom J (1993). Curbing rural exodus from tropical drylands. Food fiber need sand to enhance water use efficiency. *USDA-ARS Water Management User Unit Bushland,* Texas.

Fardossi A, Hepp E, Mayer C and Kalchgruber R (1991). *Untersuchungen über den Einfluß verschiedener Unterlasgssorten auf die Nährstoffgehalte bei Grümer Veltliner im Gefaßversuch. Mitteilungen Klosterneuburg, 41: 137-142.*

Fischer DLO, Fernandes GW, Borges EA, Piana CFB and Pasa MS (2016). Rooting of blueberry hardwood cuttings as affected by irrigation water pH and IBA. *Acta Horticulturae, 1130: 431-436.*

Güler Ç (1997). Su kalitesi kitabı. *Çevre Sağlığı Temel Kaynak Dizisi,* Ankara.

Hayes PF and Mannini F (1988). *Nutrient levels in Sauvignon Blanc garafted to different rootstocks.* In 'Second international seminar cool climate viticulture and oenology' pp. 43-44. 11-15 January 1988. Auckland, New Zealand.

Hoagland DR and Arnon DI (1950). The water culture method for growing plants without soil. *Circular - California Agricultural Experiment Station, 347: 32.*

Iyengar K, Gahrotra S, Mishra A, Kaushal A, Kumar K and Dutt M (2011). Greenhouse a reference manual. *National Committee on Plasticulture Applications in Horticulture, Ministry of Agriculture,* India.

Kanber R, Kırda C ve Tekinel O (1992). Sulama suyu niteliği ve sulamada tuzluluk sorunları. *Çukurova Üniversitesi Ziraat Fakültesi Yayınları: 6.*

Lal D (1991). Cosmic ray labeling of erosion surfaces: in situ nuclide production rates and erosion models. *Earth and Planetary Science Letters, 104(2-4): 424-439.*

Loue A (1990). Le diagnostic foliaire (ou pétiolaire) dans les enquêtes de nutrition minérale des vignes. *Progrès agricole et viticole (Montpellier), 107: 439-453.*

Mullins MG, Bouquet A and Williams LE (1992). Biology of the grapevine. *Cambridge University Press, 239p.*

Rhoades JD (1972). Quality of water for irrigation. *Soil Science, 113: 227-284.*

Richards D (1983). The grape root system. Horticultural reviews, *AVI Publishing* Company, Westport, Connecticut.

Riley CV (1891). The Phylloxera and American resistant stocks. *Scientific American, 31(788): 12596-12597.*

Rosas A, Rengel Z and de la Luz Mora M (2007). Manganese supply and pH influence growth, carboxylate exudation and peroxidase activity of ryegrass and white clover. *Journal of Plant Nutrition, 30: 253-270.*

Ruckenbauer W and Traxler H (1974). Weinbau heute. Handbuch für Beratung, *Schule und Praxis*, Stutgard.

Rühl EH (1991). Effect of potassium supply on cation uptake and distribution in grafted *Vitis campinii* and *Vitis berlandieri* × *Vitis rupestris* rootstocks. *Australian Journal of Experimental Agriculture, 31: 687-691.*

Scienze A, Failla O and Romano F (1986). Untersuchungen zur sortenspezifischen Mineralstoffaufnahme bei Reben. *Vitis, 25: 160-168.*

Spoerr R (1902). Nurseries for grapevine grafts. *American Scientific, 53: 21904-21906.*

Şimşek G, Çanlı M, Karadavut U, Yazıcı ME ve Soğancı K (2017). Sulama yapılan alanların bazı su parametreleri açısından ayırma (discriminant) analizi kullanılarak incelenmesi. *Türk Tarım ve Doğa Bilimleri Dergisi 4(3): 339–346.*

Şinik E (2011). *Edirne ilinde bulunan asit karakterli toprakların bitki besin elementleri ve bazı ağır metal içeriklerinin belirlenmesi üzerine bir araştırma.* Yüksek Lisans Tezi, Namık Kemal Üniversitesi, Fen Bilimleri Enstitüsü, Toprak Bilimi ve Bitki Besleme Anabilim Dalı, 48 s., Tekirdağ.

Tangolar S ve Ergenoğlu F (1989). Değişik anaçların erkenci bazı üzüm çeşitlerinde yaprakların mineral besin maddesi ve çubukların karbonhidrat içerikleri üzerine etkisi. *Doğa, 13(3B): 1267-1283.*

Tuncay H (1994). Su kalitesi (I. Basım). *Ege Üniversitesi Ziraat Fakültesi Yayınları,* İzmir.

Valdez-Aguilar LA, Grieve CM and Poss J (2009). Hypersensitivity of *Ranunculus asiaticus* to salinity and alkaline pH in irrigation water in sand cultures. *Hortscience, 44(1): 138-144.*

Volpe B and Boselli M (1990). The effect of the rootstock on the mineral nutrition and on certain qualitative and quantitative parameters of the grapevine cultivar Croatina. *Vignevini,17(4): 51-55.*

Vršič S, Kocsis L and Pulko B (2016). Influence of substrate pH on root growth, biomass and leaf mineral contents of grapevine rootstocks grown in pots. *Journal of Agricultural Science and Technology, 18: 483-490.*

Williams LE and Smith RJ (1991). The effect of rootstock on the partitioning of dry weight, nitrogen and potassium and root distribution of Cabernet Sauvignon grapevines. *American Journal of Enology and Viticulture 42(2): 118-122.*

Zhao D, Hao Z, Wang J and Tao J (2013). Effects of pH in irrigation water on plant growth and flower quality in herbaceous peony (*Paeonia lactiflora* Pall.). *Scientia Horticulturae, 154: 45-53.*

Zhao JX (2003). Studies on the soil pH and plant growth. *Inner Mongolia Agricultural Science and Technology, 6: 33-42.*

Turkish Journal of Agricultural Engineering Research

https://dergipark.org.tr/en/pub/turkager
https://doi.org/10.46592/turkager.2021.v02i02.003

Turk J Agr Eng Res
(TURKAGER)
e-ISSN: 2717-8420
2021, 2(2): 289-297

Research Article

Modelling Kinetics of Extruded Fish Feeds in a Continuous Belt Dryer

Funmilayo OGUNNAIKE[a*] **Ayoola Patrick OLALUSI**[b]

[a]*Department of Agricultural and Bio-Environmental Engineering, The Federal Polytechnic, Ado, Ekiti State, NIGERIA*

[b]*Department of Agricultural Engineering, Federal University of Technology, Akure, Ondo State, NIGERIA*

(*): Corresponding author, *ogunnaikeaderoju@gmail.com*

ABSTRACT

Feed is the major inputs in aquaculture production which affects the development growth of aquaculture in the African continent. Extruded fish feeds are dried to desire moisture content to increase the shelf life. Conventional method of drying fish feeds had gained attention recently in Nigeria in order to reduce high cost of producing fish feeds. However, this method is still grossly underutilized. Extrude floating fish feed was dried using continuous belt dryer at drying air temperature from 60°C to 100°C at an interval of 10°C, velocity of air using for drying from 0.8 m s^{-1} to 1.0 m s^{-1} at an interval of 0.1 m s^{-1} using a constant linear belt speed of 50 m s^{-1}. Various moisture contents gotten at different conditions were changed to ratio of the dried extrudates moisture so as to obtain curves of drying by plotting the ratio of moisture against time. The dried extrudates behaviour was determined by fixing the drying curves with five well known models. Model with high determination coefficient and low reduced chi-square, low standard error, low value of least square and low standard deviation error (SEE) was used as best model. Midilli et al model was found suitable in describing the behaviour of extruded fish feed during drying. The temperature of air used for drying was discovered to have a major influence on the drying kinetics of the extruded fish feeds based on the conditions of this experiment.

RESEARCH ARTICLE

Received: 29.05.2021
Accepted: 22.08.2021

Keywords:

- Kinetic of drying,
- Extruded fish feed,
- Drying curves,
- Belt dryer,
- Drying model

To cite: Ogunnaike F, Olalusi P (2021). Modelling Kinetics of Extruded Fish Feeds in a Continuous Belt Dryer. Turkish Journal of Agricultural Engineering Research (TURKAGER), 2(2): 289-297. *https://doi.org/10.46592/turkager.2021.v02i02.003*

INTRODUCTION

Extruded feed is the most typical form of animal feed produced in the western world. Fish feed which contributes a global demand of 50 - 75 million tons per year; has shown an annual growth rate of more than 6% in the last few decades. According to FAO (2020) the global fish production in 2018 is estimated as 179 million tones and this is expected to increase to 204 million by 2030 as a result of increase in production of extruded fish feeds. Although, either floating or sinking feed can produce satisfactory growth, but most fish species prefer floating than sinking. This is due to the fact that extruded feed have superior water stability, better floating properties, ease in digestion, zero water pollution, optimized labour usage, zero wastage of raw materials (Amalraaj, 2010) and a higher energy than sinking pelleted feed (Hilton *et al.*, 1981; Johnson and Wanderwick, 1991; Momo *et al.*, 2016). Drying according to Kallia and Patankar (2001) can be defined has the universal method of conditioning the material by removing moisture to such a level that it is in equilibrium with the normal atmospheric air in order to preserve the quality and nutritive value of the food product. According to Misha *et al.* (2013), to obtain the best conditions of drying and for energy saving during procedure for drying, it is imperative to know the solid temperature and effects of the drying variables (temperature of air use for drying, velocity of air use for drying etc) in moisture removal. Drying of temperature sensitive materials such as food and agricultural products, particularly at temperatures sensitive enough to cells, lead to probable cell damage and gelatinization (Fernando *et al.*, 2008). Pacheco *et al.* (2011) stated that low temperature between 30°C to 70°C is the sorption isotherms required for an extruded fish feed and that the energy equilibrium of thermal system is delineated by heat and mass transfer in a continuous convective dryer. In estimating the coefficient of heat and mass transfer, the heat transfer coefficient is often used because of its reliability than the mass transfer coefficient (Sander *et al.*, 2001). Haubjerg *et al.* (2014) opined that this is true since surface temperature can more easily be measured over the course of drying. Barati and Esfahani (2011) also reported that the center and surface temperature are almost same especially when drying with for Biot numbers less than one especially for small fish feed pellets convectively exposed hot air use for drying (Haubjerg *et al.*, 2014). For the best management of operation parameters and prediction of process involved in drying, mathematical models are used. According to Brooker *et al.* (1992), semi–empirical and empirical models are used to estimate how moisture varies in feed materials. The condition of drying, dryer type and the characterization of the feeds (Ozdemir and Devres, 1999) to be dried are factors that affect drying kinetics of the feeds. Most aquatic and pet feeds are dry mostly in belt dryer, this is due to the fact that it has high efficiency and simple design (FAO, 2020). Although, there had been studies on kinetic modeling of fish feeds, but few literatures on kinetic modeling of extruded fish feeds in a continuous belt dryer. Investigating the influence of drying variables on the drying kinetics of fish feed extrudates using continuous flow belt dryer and using seven known models with the objectives of selecting the most well adopted model were objectives of the research.

MATERIALS AND METHODS

Feed ingredients were procured from a retail outlet at Akure, Ondo State. The feedwas formulated using ingredients used for catfish feed production in Nigeria according to Fagbenro and Adebayo (2005). The materials were extruded byusing a single screw extruder, developed at The Federal University of Technology, Akure. The extruded fish feed preliminary moisture content was evaluated by drying the sample in an oven at 102°C until the weights remain steady. A continuous flow belt dryer (Figure 1) was used in drying the extruded feeds.

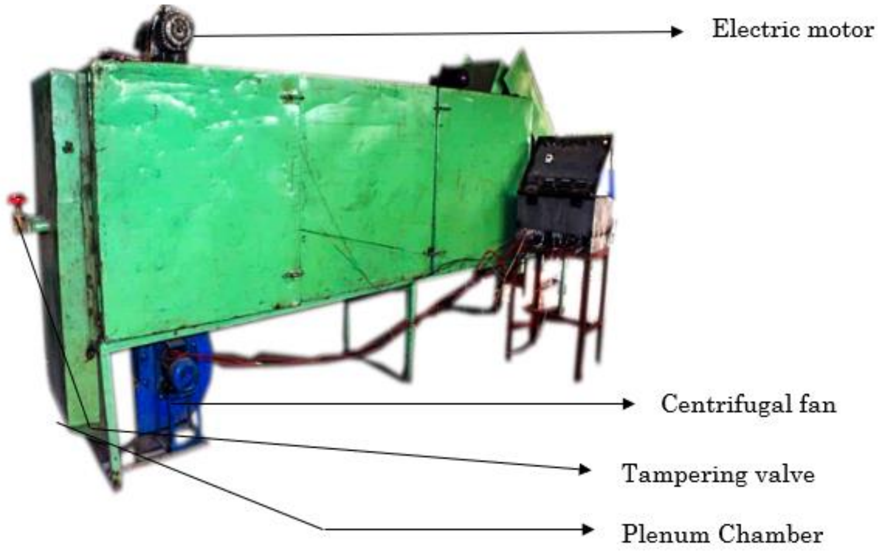

Figure 1. Side view of continuous flow belt dryer.

A digital balance was used to weigh the samples every 30 minutes. Five temperatures (60 to 100°C) of air used for drying and three velocitie of air for drying (0.7 to 0.9 m s^{-1}) were chosen to investigate the influence of temperature of air use for drying and velocity of air use for drying on the feeds. A constant value of 50 m s^{-1} was used as the linear belt speed. 2000 g of wet extruded fish feeds as thin layer were loaded inside the dryer. The procedure for drying continues until the weight of the feed was steady for ten successive readings.

Table 1 shows the drying models. The ratio of the moisture by using the models is given has

$$M_i = \frac{M_t - M_s}{M_o - M_s} \tag{1}$$

Where; M_i is amount of moisture in the extruded fish feed (dry basis) at any time; M_0 is initial amount of moisture in the extruded fish feed; M_s is amount of stable moisture in the extruded fish feed. In contrast to M_t and M_0, the amount of extrudate stable in water is small, thus Equation 1 is simplified to

$$M_i = \frac{M_t}{M_o} \tag{2}$$

The thin layer models which describe the drying dynamic of the extruded fish feeds were fitted to Table 1 in order to ascertain the most acceptable model that can represent the extruded fish feeds drying curves. In validating the model that best describes the drying dynamic of the feed, R squared *(R^2)*, reduced chi – square *(x^2)*, standard deviation error *(SEE)*, least square error *(SSE)* standard error *(RMSE)* statistical methods were used. The goodness of fitness of the selected model to the experimental data was determined using these statistical methods. These methods were calculated has follows

$$X^2 = \sum_{i=1}^{N} \left(MR_{prei} - MR_{exp,i} \right)^2 \tag{3}$$

$$\text{RMSE} = r\left[\frac{1}{N}\sum_{i=1}^{N}\left(MR_{pre,i} - nMR_{expi}\right)^2\right]^{1r^2} \quad (4)$$

$$R^2 = 1 - \frac{\sum_{s=1}^{W}\left(AR_{exps} - AR_{pre\,s}\right)^2}{\sum_{s=1}^{W}\left(\overline{AR_{\exp s}} - AR_{pre\,s}\right)^2} \quad (5)$$

where $AR_{pre,i}$ is ratio of the moisture in nth predictions, AR_{expi} is ratio of observed experment in nth predictions, $AR_{exp\,s}$ is mean value of experimental dimensionless ratio of the moisture, N is amount of observations and n is the amount of constant in a model. A plot of curve drying model was used to determine the value of each model coefficient. MATLAB 2014R software was used to find the best model fit and the mathematical model coefficients.

Table 1. Mathematical model to predict the procedure of drying.

Model	Type	Reference
Newton	*MR = exp (-kt)*	Mujumdar (1987)
Page	*MR = exp* $(-kt)^n$	Diamante and Munro (1993)
Modified Page 1	*MR = exp* $[-(kt)^n]$	Whith et al. (1978)
Midilli, Kucuk and Yapar	*MR = a exp (-ktn) + bt*	Midilli et al. (2002)
Tow term	$MR = a\exp(k_0t) + b\exp(-k_1t)$	Henderson (1974)
Tow- term exponential	$MR = a\exp(-kt) + (1-a)\exp(-k_at)$	Sharaf-eldeen *et al.* (1980)
Wang and Singh	*MR = a exp (-kt) + (1 – a) exp (kbt)*	Yaldız *et al.* (2001)

RESULTS AND DISCUSSION

Figures 2 to 4 show the drying curve of extruded fish feeds dried in continuous flow belt dryer. It was observed that as the drying time increase, there is progressive reduction in the moisture ratio of the extrudate. The increase in the drying temperature of 60°C to 100°C leads to an increase in the amount moisture loss by the extrudate over the drying time considered in this study. This explains the fact that moisture at the surface of the extrudates evaporated at a faster rate when the temperature is high. This shows that the moisture on the outer surface layer of the sample evaporated very fast at higher temperatures. A similar trend has been reported by many researchers such as Arumuganathan *et al.* (2009) when drying mushroom; Meziane (2011) in drying pomace made from olive, Gorjian *et al.* (2011) when drying barberry. Also, similar result was reported by Haujerg *et al.* (2014) when drying extruded fish feed in a hot air convective dryer using temperature between 50°C and 80°C, Aghbashlo *et al.* (2012) in carrot drying, Ruiz-Celma *et al.* (2012) when drying tomatoes and corn drying (Odjo *et al.*, 2012).

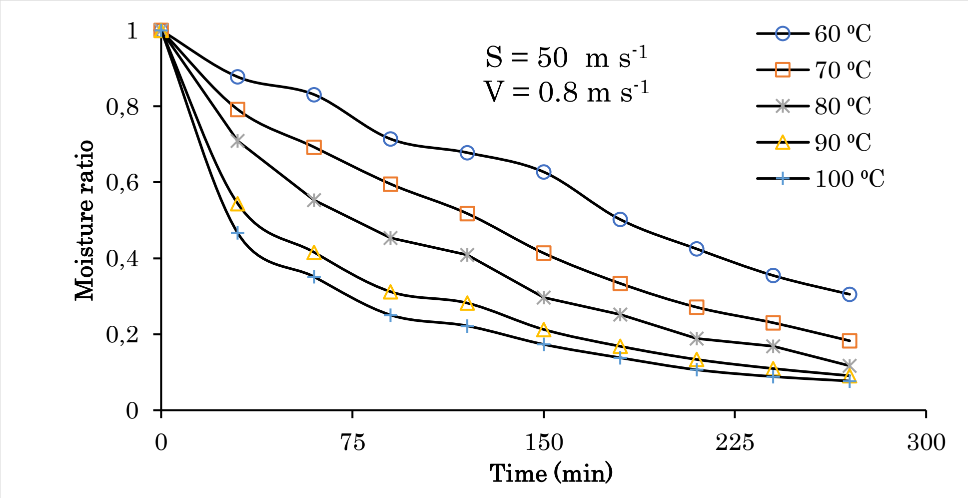

Figure 2. Influence of temperature on the moisture ratio vs time for drying for velocity of air for drying at 0.8 m s^{-1}.

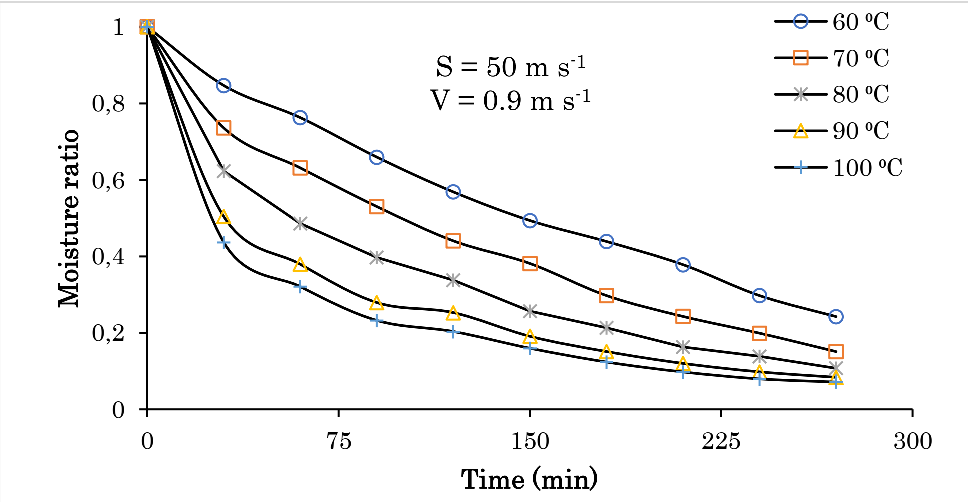

Figure 3. Influence of temperature on the moisture ratio vs time for drying for velocity of air for drying at 0.9 m s^{-1}.

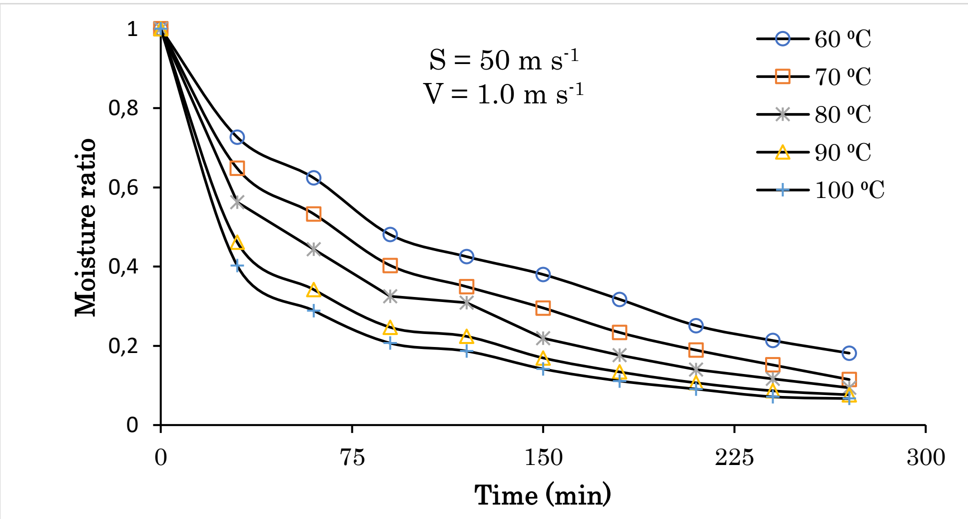

Figure 4. Influence of temperature on the moisture ratio vs time for drying for velocity of air for drying at 1.0 m s^{-1}.

Using non-linear regression approach on Microsoft Excel solver add, moisture ratio of the extruded fish feeds during the drying experiment was fitted with seven thin layer existing mathematic models as depicted in Table 1. The outcome of the goodness of fit variables for the best fitted mathematical model for different air temperatures and conveyor belt speed at 50 m s^{-1} is as shown in Table 2. The overall goodness of fit parameter showed that the *R* square *(R^2)*, standard error *(RMSE)*, standard deviation error *(SEE)*, reduced chi-square *(χ^2)*, least square error *(SSE)* values were obtained as $0.9923 \leq R^2 \leq 0.9995, 0.0071 \leq RMSE \leq 0.0193, 0.0091 \leq SEE \leq 0.2860, 0.0000 \leq \chi^2 \leq 0.0954, 0.0001 \leq SEE \leq 0.7632$ respectively. The highest values of coefficient of determination ($R^2 \geq 0.9995$) was given by Midilli et al model. Thus, this model may display the drying behaviuor of fish feed extrudates. The validation performance of the most suitable model selected shows that the predicted ratio of the moisture values and experiential moisture ratio (Figure 5a, 5b, 5c) data scattered adjacent to the 45° straight line. This implies that the Midilli et al model is used to forecast the drying characteristic of the extruded fish feeds.

Table 2. The goodness of fit parameters at different drying temperature and velocity of air for drying at conveyor speed of 50 m s^{-1}.

Velocity of air for drying (m s^{-1})	Drying air temperature (°C)	Model constant	R^2	RMSE	SEE	X^2	SSE
0.8	60	k = 0.0418, b = -0.1319, a = 0.9906, n = 0.6473	0.9923	0.0193	0.025	0.0001	0.0037
	70	k = 0.0844, b = 0.0377, a = 0.9843, n = 2.1488	0.9976	0.0124	0.016	0.0003	0.0015
	80	k = 0.4818, b = -0.0565, a = 1.0024, n = 0.5134	0.9961	0.0165	0.0213	0.0005	0.0027
	90	k = 0.8786, b = -0.0047, a = 0.9989, n = 0.5886	0.9983	0.0109	0.0154	0.0002	0.001
	100	k = 1.0585, b = -0.0047, a = 0.997, n = 0.5189	0.9992	0.0077	0.0099	0.0001	0.0006
0.9	60	k = 0.2323, b = -0.0448, a = 1.0014, n = 0.8232	0.9988	0.0082	0.0106	0.0001	0.0007
	70	k = 0.4207, b = -0.0321, a = 0.9966, n = 0.7006	0.9988	0.0088	0.0114	0.0001	0.0008
	80	k = 0.1266, b = 0.0016, a = 1.0457, n = 1.0047	0.9928	0.0221	0.0286	0.0008	0.0049
	90	k = 0.8309, b = -0.0424, a = 0.9831, n = 0.3685	0.998	0.014	0.0197	0.0004	0.002
	100	k = 0.1266, b = 0.0016, a = 1.0457, n = 1.0047	0.9995	0.0059	0.0076	0.0001	0.0003
1.0	60	k = 0.4719, b = -0.0219, a = 0.9999, n = 0.6659	0.9974	0.0125	0.0162	0.0001	0.0016
	70	k = 0.5775, b = -0.0461, a = 1.0024, n = 0.4736	0.9979	0.0118	0.0152	0.0002	0.0014
	80	k = 0.7961, b = -0.0182, a = 0.9997, n = 0.5329	0.9976	0.013	0.0167	0.0003	0.0017
	90	k = 1.0522, b = -0.0119, a = 1, n = 0.4685	0.9992	0.0077	0.011	0.0001	0.0005
	100	k = 1.2539, b = -0.0015, a = 0.9997, n = 0.4848	0.9993	0.0071	0.0091	0.0001	0.0005

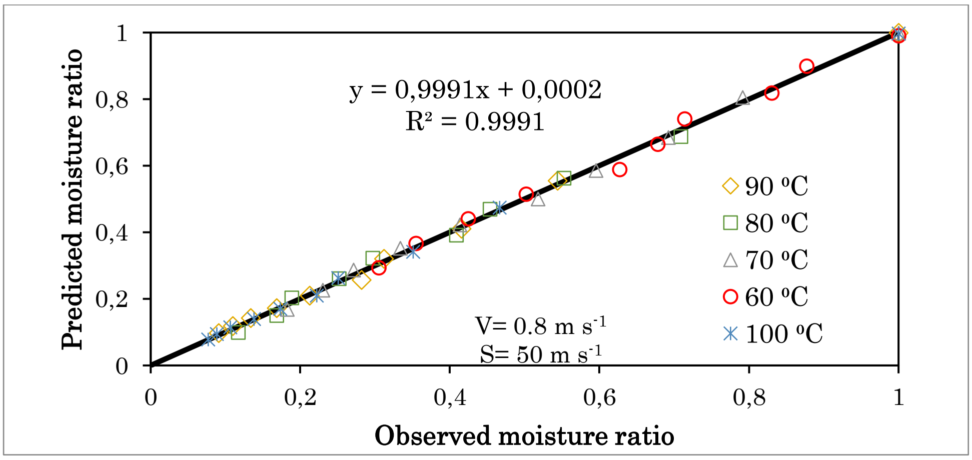

Figure 5a. The graph of predicted ratio versus observed moisture ratio at different temperature for drying, velocity of air for drying at 0.8 m s^{-1}.

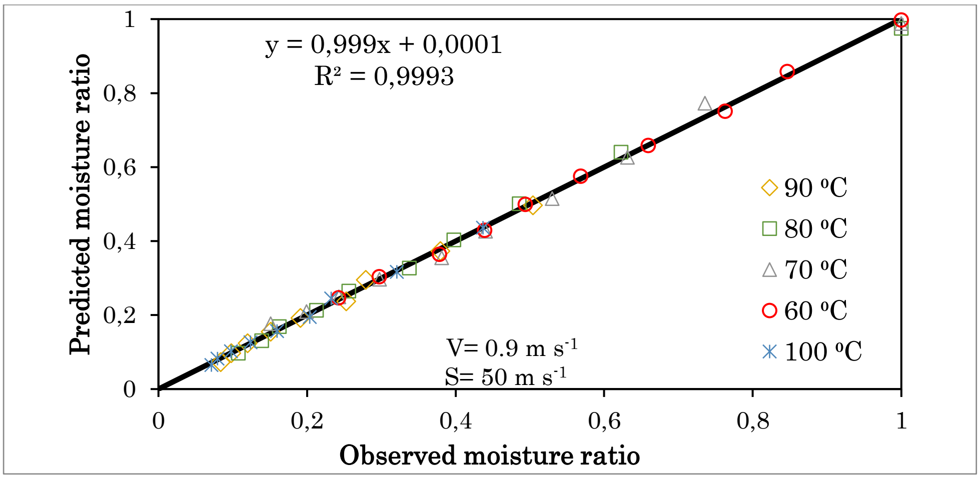

Figure 5b. The graph of predicted ratio versus observed moisture ratio at different temperature for drying, velocity of air for drying at 0.9 m s^{-1}.

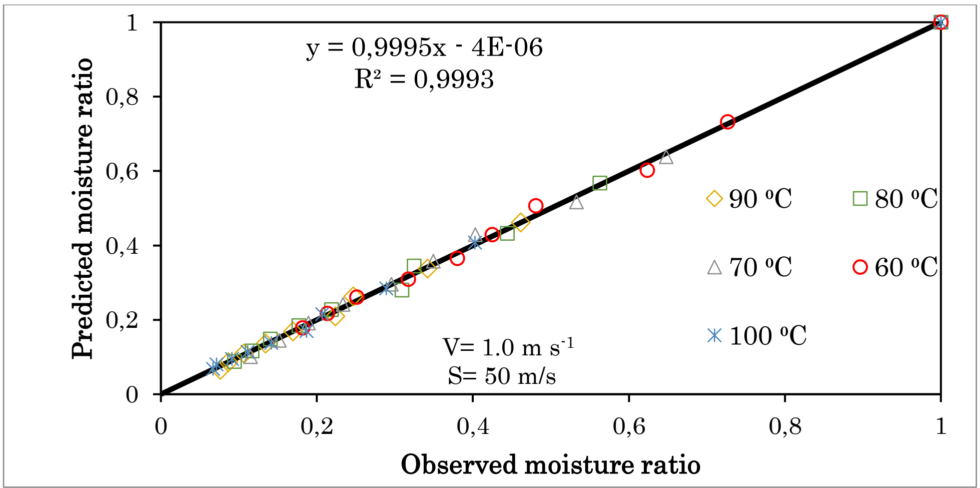

Figure 5c. The graph of predicted ratio versus observed moisture ratio at different temperature for drying, velocity of air for drying at 1.0 m s^{-1}.

CONCLUSION

The modeling kinetic of extruded floating fish feeds and influence of the temperature of air used for drying, velocity of air used for drying and a constant linear belt speed under different machine operational condition was investigated. A rise in the temperature of air for drying leads to reduction of time required to dry the fish feeds. Temperature of air for drying and velocity of air for drying were discovered to be the major influence on drying behavior of the fish feed with belt linear speed having the least effect. In predicting the drying kinetics of the extruded fish feeds, Midilli et al model was ascertained to be the most fitting model to use.

DECLARATION OF COMPETING INTEREST

The authors declare that there are no conflict of interest

CREDIT AUTHORSHIP CONTRIBUTION STATEMENT

Funmilayo Ogunnaike: Investigation of the manuscript, materials and methods used in the research, conceptualization, data analysis and validation and writing of the original draft of the manuscript.

Pius Olalusi: Investigation of the manuscript, materials and methods used in the research, conceptualization, edition of the manuscript and reviewing of the manuscript.

REFERENCES

Aghbashlo M, Mobli H, Rafiee S and Madadlou A (2012). Energy and exergy analyses of thespray drying process of fish oil microencapsulation. *Biosystems Engineering, 111(2): 229-241.*

Amalraaj S (2010). Extruded floating fish feed a boon for farmers. *Online Publication The Hindus Science Tech/Agriculture.*

Arumuganathan T, Manikantan MR, Rai RD, Anandakumar S and Khare V (2009). Mathematical modeling of drying kinetics of milky mushroom in a fluidized bed dryer. *International Agrophys. 23: 1-7.*

Barati E and Esfahani JA (2011). Mathematical modeling of convective drying: Lumpedtemperature and spatially distributed moisture in slab. *Energy, 36(4): 2294-2301.*

Brooker DB, Bakker-Arkema FW and Hall CW (1992). Drying and storage of grains and oilseeds. Westport: *International Journal of Engineering and Advancement Technology Studies, 23(2): 10-15.*

Diamente LM and Munro PA (1993). Mathematical modeling of the thin layer solar drying of sweet potato slices. *Solar Energy, 51(4): 271-276.*

FAO (2020). The state of World fisheries and aquaculture 2020. Sustainability in action. Rome.

Fagbenro OA and Adebayo OT (2005). A review of the animal and aqua feed industries in Nigeria. *A* synthesis of the formulated animal and aqua feed industry in sub-Saharan Africa, *CIFA* Occasion Paper No. 26: 66.

Fernando WJN, Ahmad LA, AbdShuko SR and Lok YK (2008). A model for constant temperature drying rates of case hardened slices of papaya and garlic. *Journal of Food Engineering,88: 229-238.*

Gorjian SH, Tavakoli Hashjin T, Khoshtaghaza MH and Nikbakht AM (2011). Drying kinetics and quality of barberry in a thin layer dryer. *Journal of Agricultural ScienceTechnology, 13, 303–314.*

Henderson SM (1974). Progress in developing the thin layer drying equation. *Transactions of the American Society of Agricultural Engineers, 17: 1167-1172.*

Haubjerg AF, Veje1 CT, Jørgensen BN, Simonsen B and Løvgreen S (2014). *Mathematical modelling of the drying of extruded fish feed and its experimental demonstration.* 19th International Drying Symposium, (IDS 2014), Lyon, France, August 24-27, 2014.

Hilton JW, Cho CY and Slingers SJ (1981). Effect of extrusion processing and steam pelleting diets on pellet durability and pellet water absorption and physiological response of rainbowtrout. *Aquaculture, 25: 185-194.*

Johnson TA and Wandsvick SK (1991). Fish nutrition and development in aquaculture. Published by C and H. 2-6 *Boundary Row*, London SEI 8HN 1-119.

Kallia KK and Patankar SV (2011). Performance analysis of a double-deck conveyor dryer computational approach. *Drying Technology, 17: 255-267.*

Meziane S (2011). Drying kinetics of olive pomace in a fluidized bed dryer. *Energy Conservation Management, 52: 1644-1649.*

Midilli A, Kucuk H and Yapar Z (2002). A new model for single layer drying. *Drying Technology, l20(7): 1503-1513.*

Misha S, Mat S, Rusian MH, Sopian K. and Salleh E (2013): The effect of drying air temperature and humidity on the drying kinetic of kenaf core. *Applied Mechanics and Material, 315: 710-714.*

Momo, AT, Abubakar, MY and Ipinjolu, JK (2016). Effect of ingredients substitution on binding, water stability and floatation of farm- made fish feed. *International Journal of Fisheries and Aquatic Studied, 4(3): 92- 97*

Mujumdar AS (1987). Handbook of industrial drying. New York: *Marcel Dekker.*

Odjo S, Malumba P, Dossou J, Janas S and Bera F (2012). Influence of drying and hydrothermal treatment of corn on the denaturation of salt-soluble proteins and color parameters. *Journal of Food Engineering, 109: 561–570.*

Ozdemir M and Devres YO (1999). The thin layer drying characteristics of hazelnuts during roasting, *Journal of Food Engineering, 42: 225-233.*

Pacheco ACW, Katekawa ME and Silva MA (2011). Modeling of drying and adsorption isotherms of the fish feed. *Brazilian Archives of Biology and Technology, 54: 577-588.*

Ruiz – Celma A, Cuadros F and Lopez-Rodriguez F (2012). Convective drying characteristics of sludge from treatment plants in tomato processing industries. *Food Biophysics Process, 90: 224-234.*

Sander A, Kardum JP and Skansi D (2001). Transport properties in drying of solids. *Chemical and Biochemical Engineering, 15(3): 131-137.*

Sharaf-eldeen YI, Blaisdell JL and Hamdy MY (1980). A model for ear corn drying. *Transaction of the ASAE, 23(5): 1261-1271.*

Whith G. MT, Brldges C, Loewer, OJ and Ross. I.J (1978). Seed coat damage in thin layer drying of soybeans as affected by drying conditions. ASAE paper no. 3052.

Yaldiz O, Ertekin C, and Uzun HI (2001). Mathematical modeling of thin layer solar drying of Sultana grapes, *Energy, 26: 457-465.*

Turkish Journal of Agricultural Engineering Research

https://dergipark.org.tr/en/pub/turkager
https://doi.org/10.46592/turkager.2021.v02i02.004

Turk J Agr Eng Res
(TURKAGER)
ISSN: 2717-8420
2021, 2(2): 298-307

Research Article

Effects of Different Carbonization Conditions on the Color Change of Biochar

Alperay ALTIKAT[ID][a]* **Mehmet Hakkı ALMA**[ID][b]

[a]*Department of Biosystem Engineering, Faculty of Agriculture, University of Iğdır, 76000, Iğdır -TURKEY*

[b] *Department of Biosystem Engineering, Faculty of Agriculture, University of Iğdır, 76000, Iğdır –TURKEY*

(*): Corresponding author, altikatalperay@gmail.com

ABSTRACT

The aim of this research was to determine the effects of different carbonization temperature, gas flow rate and heating rates on biochar's color change. Three different carbonization temperatures (400°C, 500°C, and 600°C), two different gas flow rates (0.2 l min^{-1} and 0.5 l min^{-1}) and two different heating temperature rates (30°C min^{-1} and 60°C min^{-1}) were used in the experiments. The color changes of biochar were examined utilizing the international approved *L*, a*, b** system. Atriplex nitens Schkuhr was used as a biomass source in the experiments. High carbonization temperature and high gas flow rate caused a decrease in the "*L*" value of biochar. It is an indication that the color is getting darker, when the *L* value approaches zero. In the study, only the effect of gas flow rate on the "*a*" value was found to be statistically significant (P≤0.05). The increase in gas flow rate caused the biochar to become darker by increasing the deep red tone. Heating rate and gas flow speed significantly influenced the "*b*" values of biochar. The slow heating rate and high gas flow rates made the biochar color darker. At end of the research, it can be said that the biochar produced at high carbonization temperature, low heating rate and high gas flow rates will have darker tones.

RESEARCH ARTICLE

Received: 09.05.2021
Accepted: 11.09.2021

Keywords :

- *Atriplex nitens Schkuhr*,
- Pyrolysis,
- Color Analysis,
- Biochar,
- Biomass

To cite: Altıkat A, Alma MH (2021). Effects of Different Carbonization Conditions on the Color Change of Biochar. Turkish Journal of Agricultural Engineering Research (TURKAGER), 2(2): 298-307. *https://doi.org/10.46592/turkager. 2021.v02i02.004*

INTRODUCTION

Biochar is a high carbon content combustion product formed by the combustion of organic material by thermochemical transformation processes in oxygen-free or limited oxygen conditions (Hardie *et al.*, 2014). Biochar contains between 60% and 80% C, depending on the production properties (Castellini and Ventrella, 2015). Due to this feature, it can be applied as a soil amendatory at the agricultural soils which have low carbon content (Genesio *et al.,* 2015). At the several studies have examined the effects of biochar on agricultural soils. According to the obtained results; biochar increases soil carbon content (Lal, 2015) and crop yield (Brassard *et al.,* 2016), reduces CO_2 emission from soil to atmosphere. In addition, the biochar improves soil physical bulk density, porosity, infiltration rate and water holding capacity, chemical pH, electrical conductivity, cation exchange capacity, organic matter content and biological (microbial mass, microbial mass, enzyme activity quality criteria (Ding *et al.,* 2016; Brassard *et al.,* 2016; Mukherjee and Lal, 2017; Lehmann *et al.,* 2011).

The thermal properties of the soil were affected by soil bulk density, (Abu-Hamdeh and Reeder, 2000; Usowicz *et al.,* 2013) soil moisture content, (Usowicz *et al.,* 2006) organic matter level, (Dec *et al.,* 2009) and application method into the soil (Paz-Ferreiro *et al.,* 2014). Addition of biochar into the soil changes soil temperature (Logsdon *et al.,* 2010; *Genesio et al.,* 2012; Meyer *et al.,* 2012). The dark color of biochar darkens the soil color and changes the albedo of the soil surface. Albedo is the ratio of solar radiation reflected from the soil to the atmosphere. Dark colored soils absorb more sunlight and have lower surface reflection than other soils.

Biochar added soils have lower reflectance than other soils. This situation reduces evaporation and increases soil moisture content. The studies (Zhang *et al.,* 2013; *Usowicz et al.,* 2016) have shown that when biochar was added into the soil at the rate of 4.5 to 30 Mg ha^{-1}, the albedo rate decreases. The effect of biochar application on soil temperature differs in daytime and nighttime measurements. From this point of view, it can be said that biochar application is an alternative method that can prevent fluctuations in soil temperature. In some studies, it has been concluded that the application of biochar into the soil increases soil temperature at night and reduces it during the day (Zhang *et al.,* 2013; Usowicz *et al.,* 2016; Ventura *et al.,* 2012). Oguntunde *et al.* (2008), stated that biochar application into the soil reduced soil albedo by 8%. In another study, when biochar at 30-60 t ha^{-1} norm was mixed into the soil, the albedo decreased more than 80% (Genesio *et al.,* 2012). In another study conducted in Germany, a 12% reduction in soil albedo was observed when the mixing biochar into the soil. (Meyer *et al.,* 2012).

The aim of this research is to determine how the carbonization temperature, heating rate and gas flow speed parameters used in the carbonization process cause a change in the color of biochar. In this research, biochar was produced in a laboratory type carbonization reactor at 3 different carbonization temperatures, 2 different heating rates and 2 different gas flow speeds.

MATERIALS and METHODS

Atriplex nitens S. plant was used as biomass material in the study (Figure 1a). After the plant was harvested, it was extracted from its branches, and the trunk part was ground in a laboratory type mill (Figure 1b) so that the aggregate diameter was less than 2 mm. The ground biomass was dried in the oven at 105°C for 24 hours (Suthar *et al.,* 2018).

A fixed bed laboratory type carbonization reactor (Figure 2) was used for the carbonization experiments. In the experiments three carbonization levels, two heating rates and two gas flow rates were used for biochar production. The experimental factors and levels were given in the Table 1.

a b

Figure 1. *Atriplex nitens Schkuhr* (a) and laboratory type mill (b).

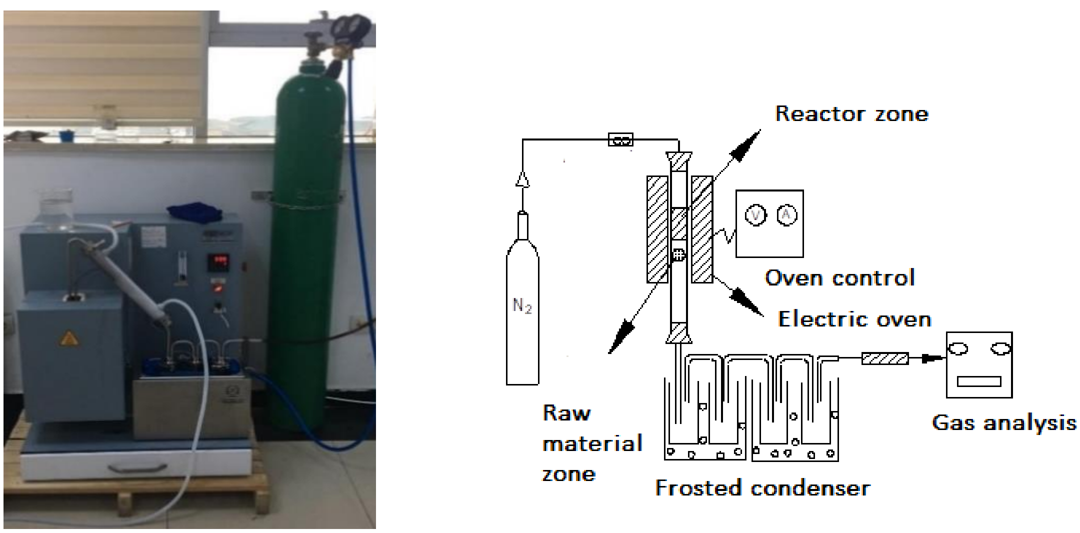

Figure 2. Fixed bed carbonization reactor and its schematic view.

Figure 3. Biochar obtained from the experiments.

Table 1. Experimental factors and factor levels.

Experimental factors	Factor levels
Carbonization temperature (°C)	400, 500, 600
Heating rate (°C min^{-1})	30, 60
Gas flow speed (l min^{-1})	0.2, 0.5

Before starting the experiments, the ground and oven dried biomass sample weighing 10 grams was placed in the carbonization reactor. Before the carbonization process, nitrogen gas was supplied to the system to eliminate the existing oxygen. In order to determine the color changes of biochar, color measurements were made after the carbonization process. Color measurement was carried out the international *L*, a*, b** system in the study (Figure 4). The "*L*" value represents brightness and ranges from 0 to 100 values. In the *L* value, zero (0) means blackness and hundred (100) means whiteness. In addition, "*a*" and "*b*" value is an indicator of redness - greenness, and blueness - yellowness, respectively. The "*a*" and "*b*" values vary between -90 - +90. A color measurement device (PCE-CSM 4) was used to determine the "*L*", "*a*" and "*b*" values (Figure 5).

The data received from each experiment with three replications were analyzed statistically to test for differences among treatments. An ANOVA procedure was used to perform the analysis of variance. Means were separated by Duncan when treatment effects were significant. IBM SPSS Statistic 25 program was used for statistical analyses.

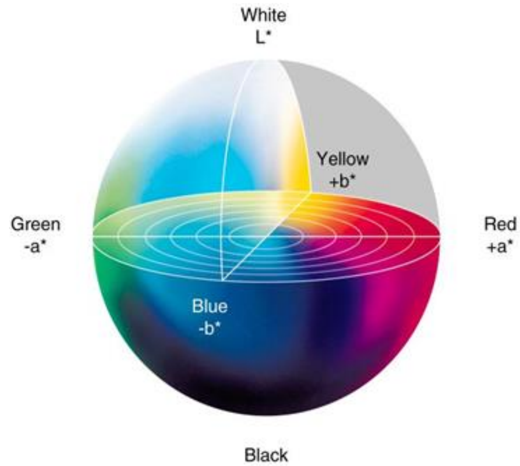

Figure 4. CIE *L*, a*, b** color space.

Figure 5. Color measurement device used in the experiments.

RESULTS and DISCUSSION

Variance analysis of the results regarding the *L* value of biochar produced under different conditions was given in Table 2. According to the results of the variance analysis, it can be said that the carbonization temperature and gas flow speed have statistically significant effects on the *L* parameter.

Table 2. Variance analysis results of *L* change in the biochar color.

Factors	*L*	
	F	**P**
Carbonization temperature (C.T)	19.72	0.000**
Heating rate (H.R)	2.99	0.097ns
Gas flow speed (G.S)	18.14	0.000**
C.T.* H.R	6.07	0.007**
C.T. * G.S	3.28	0.055ns
H.R. * G.S	0.054	0.818ns
C.T.* H.R. *G.S	2.2	0.133ns
Mean square error	46.004	

C.T: Carbonization temperature; H.R: Heating rate; G.S.: Gas flow speed; **: Statistically highly significant (P <0.01); *: Statistically significant (P <0.05), ns: Statistically non-significant

In the study, due to the increase in carbonization temperature, *a* decrease in the *L* value occurred. The lowest "*L*" value was obtained at a carbonization temperature of 600°C with 19.26 value. In addition, at the 400°C temperature "*L*" values were determined as 36.04. As a result of the experiments, an inverse relationship was determined between gas flow speed and the "*L*" value. It was observed that the "*L*" value decreased due to the increase in gas flow speed (Figure 6).

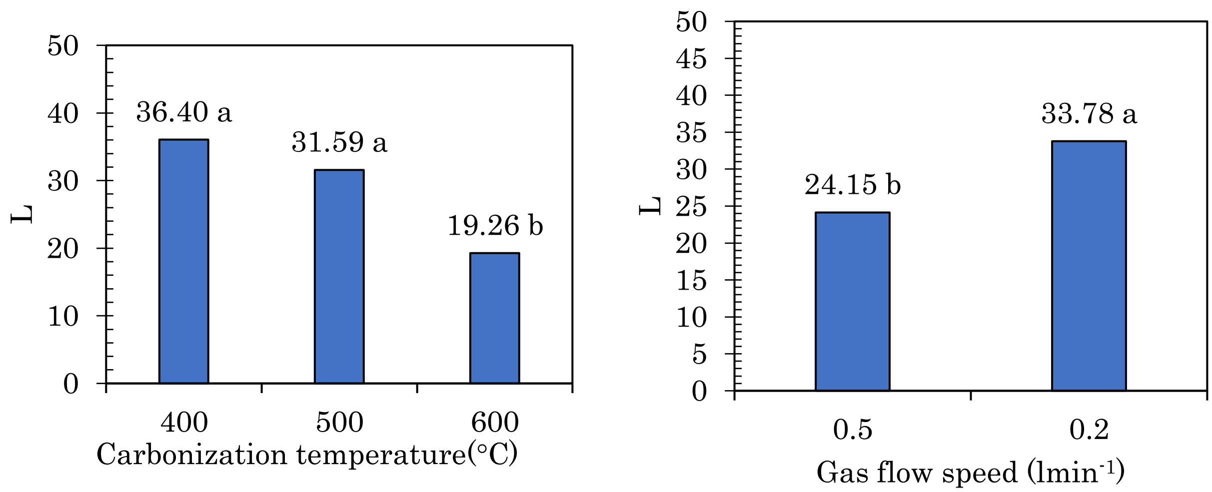

Figure 6. The change of "*L*" value according to carbonization temperature and gas flow speed.

The "*L*" value is considered a measure of black and whiteness. It means that the color gets darker as the "*L*" value approaches 0, and becomes white as it approaches 100. According to the results, it was concluded that the biochar produced at 600°C carbonization temperature and 0.5 l min^{-1} gas flow speed was darker color. The increase in gas flow speed caused an oxygen-free environment in the system at the time of carbonization, thus the raw material was completely carbonized without burning and turned darker.

Variance analysis results regarding the "*a*" value of biochar in the study are given in Table 3. According to the results, among the main factors, only the effect of gas flow speed on the "a" value was found to be statistically significant (P ≤0.05). The "*a*" values of biochar were determined as -8.76 and -1.67 for 0.2 and 0.5 l min^{-1} gas flow speed, respectively (Figure 7).

The "*a*" value denotes the red and greenness of the material color and takes a value between -90 and +90. Negative and positive values refer to red and green shades, respectively. As an expected result, the green shade of biochar was not observed.

Table 3. Variance analysis results of "*a*" change in the biochar color.

Factors	*a*	
	F	P
Carbonization temperature (C.T)	2.011	0.156ns
Heating rate (H.R)	1.280	0.269ns
Gas flow speed (G.S.)	6.096	0.021*
C.T.* H.R	7.478	0.003**
C.T. * G.S.	4.026	0.031*
H.R. * G.S.	0.034	0.856ns
C.T.* H.R. *G.S.	2.466	0.106ns
Mean square error	74,290	

C.T: Carbonization temperature; H.R: Heating rate; G.S.: Gas flow speed; **: Statistically highly significant (P<0.01); *: Statistically significant (P<0.05), ns: Statistically non-significant

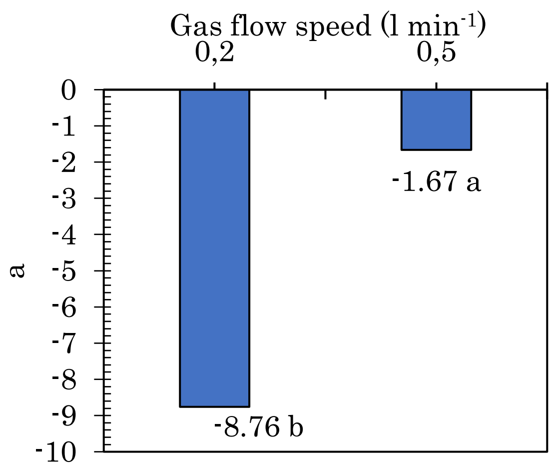

Figure 7. The change of "*a*" value according to gas flow speed.

The "*b*" value in the material color denotes tones of blue and yellow. The value of "*b*" takes a value between (-90) and +90. Negative and positive values refer to blue and yellow color tone, respectively.

Variance analysis results of the *b* value of biochar were given in Table 4. As a result of the variance analysis, it is seen that among the main factors, the heating rate and gas flow speed were statistically highly important (P ≤0.01) and important and (P ≤0.05), respectively.

Table 4. Variance analysis results of "b" change in the biochar color.

Factors	*b*	
	F	**P**
	1.80	0.187ns
Carbonization temperature (C.T)	12.90	0.001**
Heating rate (H.R)	4.88	0.037*
Gas flow speed (G.S)	9.35	0.001**
C.T.* H.R	1.99	0.158ns
C.T. * G.S.	0.13	0.712ns
H.R. * G.S.	3.08	0.064ns
C.T.* H.R. *G.S.	306.276	

C.T: Carbonization temperature; H.R: Heating rate; G.S.: Gas flow speed; **: Statistically highly significant (P<0.01); *: Statistically significant (P<0.05), ns: Statistically non-significant

The "*b*" values of biochar were determined to be negative. This result means that the biochar does not have a yellow tone and contains a tone close to navy blue. In the study, "*b*" values at 30°C min^{-1} and 60°C min^{-1} heating rates were determined as -43.63 and -22.68, respectively (Figure 8). Based on this result, it can be said that the color of biochar obtained at slow heating rates has a dark blue tone. In the study, the increase in gas flow rate caused the blue tone of biochar to darken. As a result of the experiments, the *b* value was determined as -26.71 at 0.5 l min^{-1} gas flow rate. Figure 8 illustrated that the change of *"b"* value according to heating rate and gas flow speed.

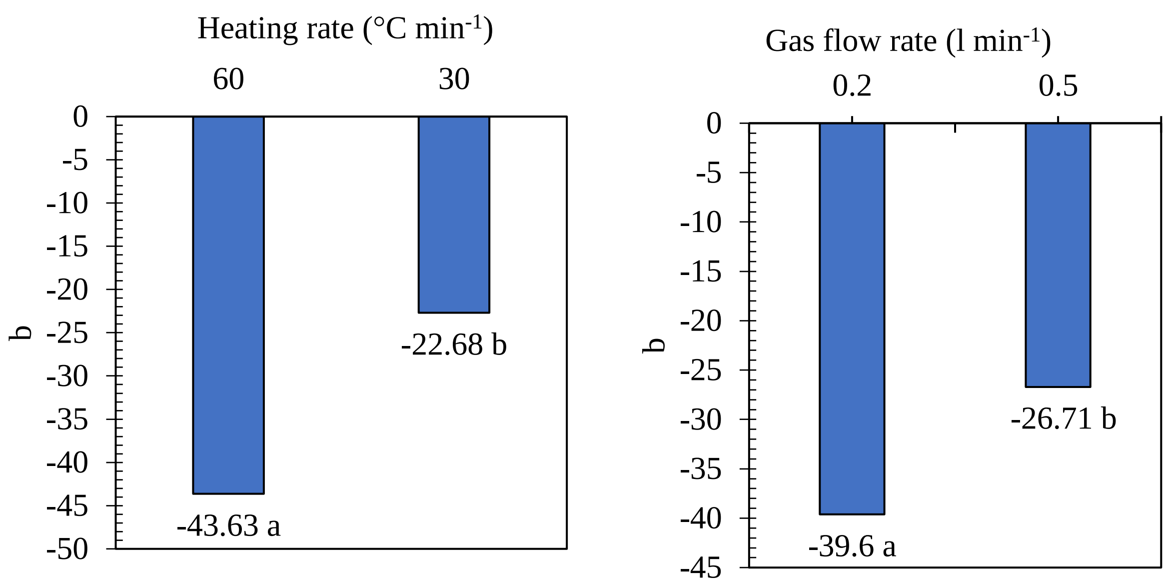

Figure 8. The change of "*b*" value according to heating rate and gas flow speed.

CONCLUSION

Due to its high carbon content and porous structure, biochar improves soil quality if mixed in to the soil with suitable methods. The biochar added soils have darker tones compared to other soils. This property of biochar affects soil albedo. The soils which were mixed with biochar have more darkness color compare to other soils. Therefore, this type of soil absorbs more sunlight than other soils thus the soil temperature rises. This effect changes accordance with day and night measurements.

In this study, the effects of different carbonization temperatures, gas flow rates and heating rates used in biochar production on changes in the color of biochar were investigated. As the carbonization temperature increased, the "*L*" value of biochar decreased. The fact that the *L* value approaches zero is an indication that black tones are more dominant. According to these results, high carbonization temperature leads to the formation of darker colored biochar. However, the issue to be considered here is the selection of gas flow rate and heating rates that are compatible with high carbonization temperature. If the carbonization temperature rises, an oxygen-free environment must be obtained in the system. In order to achieve such an environment, it may be suggested to increase the gas flow rate and decrease the heating rate. A similar trend was determined between gas flow rate and "*L*" values. In the study, due to the increase in the gas flow rate, a decrease in the "*L*" value occurred and darker biochar was obtained.

In the study, only the effect of gas flow rate on the "*a*" value was found to be statistically significant. The increase in gas flow rate caused the biochar to become darker by increasing the deep red tone. Heating rate and gas flow speed significantly influenced the "*b*" values of biochar. According to "*b*" values at the slow heating rate and high gas flow rates made the biochar color darker. Based on these data it can be said that the biochar produced at high carbonization temperature, low heating rate and high gas flow rates will have darker shades.

DECLARATION OF COMPETING INTEREST

The authors hereby declare that they have no conflict of interest whatsoever.

CREDIT AUTHORSHIP CONTRIBUTION STATEMENT

The authors hereby declare that the contributions given are correct.
Alperay Altıkat: Laboratory experiments, statistical analysis, writing the manuscript.
Mehmet Hakkı Alma: Examination, editing and formal analysis of manuscript.

REFERENCES

Abu-Hamdeh NH and Reeder RC (2000). Soil thermal conductivity: effects of density, moisture, salt concentration, and organic matter. *Soil Science Society of America Journal, 64: 1285-1290.*

Brassard P, Stephane G and Vijaya R (2016). Soil biochar amendment as a climate change mitigation tool: Key parameters and mechanisms involved. *Journal of Environmental Management, 181: 484-497.*

Castellini M and Ventrella D (2015). Impact of conventional and minimum tillage on soil hydraulic conductivity in typical cropping system in Southern Italy. *Soil & Tillage Research, 154: 1-13.*

Dec D, Dörner J and Horn R (2009). Effect of soil management on their thermal properties. *Journal of Plant Nutrition and Soil Science, 9: 26-39.*

Ding Y, Liu YG, Liu SB, Li, ZW, Tan XF and Huang XX (2016). Biochar to improve soil fertility: A review. *Agronomy for Sustainable Development,* 36: 36.

Genesio L, Miglietta F, Baronti S and Vaccari FP (2015). Biochar increases vineyard productivity without affecting grape quality: results from a four years field experiment in Tuscany. *Agriculture*, *Ecosystems* & Environment, *201: 20-25.*

Genesio L, Miglietta F, Lugato E, Baronti S, Pieri M and Vaccari FP (2012). Surface albedo following biochar application in durum wheat. *Environmental Research Letters, 7: 014025.*

Hardie M, Clothier B, Bound S, Oliver, G and Close, D (2014). Does biochar influence soil physical properties and soil water availability? *Plant Soil, 376: 347-361.*

Lal R (2015). Biochar and soil carbon sequestration. In: M. Guo, Z. He, and M. Uchimiya, editors, Agricultural and environmental applications of biochar: Advances and barriers. *SSSA Spec. Pub. 63. SSSA, Madison, WI.*

Lehmann J, Rillig MC, Thies J, Masiello CA, Hockaday WC and Crowley D (2011). Biochar effects on soil biota: A review. *Soil Biology* & *Biochemistry, 43: 1812-1836.*

Logsdon SD, Green TR, Bonta JV, Seyfried MS and Evett SR (2010). Comparison of electrical and thermal conductivities for soils from five states. *Soil Science, 175: 573-578.*

Meyer S, Bright RM, Fischer D, Schulz H and Glaser B (2012). Albedo impact on the suitability of biochar systems to mitigate global warming. *Environmental Science & Technology, 46: 12726-12734.*

Mukherjee A and Lal R (2017). Biochar and soil characteristics. In R. Lal, ed. Encyclopedia of soil science. 3rd ed. *Taylor & Francis*, Abingdon, UK. p. 183-188.

Oguntunde PG, Abiodun BJ, Ajayi AE and Van De Giesen N (2008). Effects of charcoal production on soil physical properties in Ghana. *Journal* of *Plant Nutrition* and *Soil Science, 171: 591-596.*

Paz-Ferreiro J, Méndez J, Tarquis AM, Cerdà and Gascó G (2014). Preface: environmental benefits of biochar. *Solid Earth, 5: 1301-1303.*

Suthar RG, Wang C, Nunes MCN, Chen J, Sargent SA, Bucklin RA, Gao B (2018). Bamboo biochar pyrolyzed at low temperature improves tomato plant growth and fruit quality. *Agriculture, 8(10): 153.*

Usowicz B, Lipiec J and Ferrero A (2006). Prediction of soil thermal conductivity based on penetration resistance and water content or air-filled porosity. *International Journal of Heat and Mass Transfer, 49: 5010-5017.*

Usowicz B, Lipiec J, Lukowski M, Marczewski W and Usowicz J (2016). The effect of biochar application on thermal properties and albedo of loess soil under grassland and fallow. *Soil & Tillage Research, 164: 45-51.*

Usowicz B, Lipiec J, Usowicz J and Marczewski W (2013). Effects of aggregate size on soil thermal conductivity: comparison of measured and model-predicted data. *International Journal of Heat and Mass Transfer, 57: 536-541.*

Ventura F, Salvatorelli F, Piana, S, Pieri L, and Pisa PR (2012). The effects of biochar on the physical properties of bare soil. Earth Environ. *Earth and Environmental Science Transactions of the Royal Society of Edinburgh, 103: 5-11.*

Verma M, Godbout S, Brar SK, Solomatnikova O, Lemay S P and Larouche JP (2012). Biofuels production from biomass by thermochemical conversion technologies. *International Journal of Chemical Engineering, 2012, 542426.*

Zhang Q, Wang X, Du Z, Liu X and Wang Y (2013). Impact of biochar on nitrate accumulation in an alkaline soil. *Soil Research, 51: 521-528.*

Turkish Journal of Agricultural Engineering Research

https://dergipark.org.tr/en/pub/turkager
https://doi.org/10.46592/turkager.2021.v02i02.005

Turk J Agr Eng Res (TURKAGER)
ISSN: 2717-8420
2021, 2(2): 308-320

Research Article

Effect of Moisture Content on the Mechanical Properties of Watermelon Seed Varieties

Paul Chukwuka EZE[a], Chikaodili Nkechi EZE[a], Patrick Ejike IDE[a*]

[a]*Department of Agricultural and Bioresource Engineering, Faculty of Engineering, Enugu State University of Science and Technology,Enugu State, NIGERIA*

(*): Corresponding author, patrick.ide@esut.edu.ng

ABSTRACT

The effect of moisture content on the mechanical properties of agricultural material is essential during design and adjustment of machines used during harvest, cleaning, separation, handling and storage. This study determined some mechanical properties of Black and Brown colored of watermelon seed grown in Nigeria under different moisture contents range of 6.5 to 27.8% (d.b). The results for the mechanical properties obtained ranged from 15.68-29.54 N for compressive force; 1.95-3.40 mm for compressive extension; 0.13-0.33 N mm^{-2} for compressive strength; and 0.17-1.93 kJ for deformation energy at vertical loading position while at horizontal loading position, results obtained ranged from 14.71-38.36 N for compressive force; 1.94-4.20 mm for compressive extension; 0.16-0.32 N mm^{-2} for compressive strength; and 1.47-76.39 kJ for deformation energy for Black colored watermelon seed. The compressive force, compressive extension, compressive strength, deformation energy ranged from 14.18-36.49 N, 1.85-5.20 mm, 0.19 0.76 N mm^{-2}, 26.23-189.75 kJ at vertical loading position and 16.47-41.82 N, 1.68-11.08 mm, 0.34- 0.57 N mm^{-2}, 27.67-319.99 kJ at horizontal loading position for Brown colored watermelon seed. The correlation between the mechanical properties and moisture content was statistically significant at ($p \leq 0.05$) level. It is also economical to load Black colored in vertical loading position at 27.8% moisture content and Brown colored in vertical loading position at 27.8% moisture content to reduce energy demand when necessary to crack or compress the seed. This research has generated data that are efficiently enough to design and fabricate processing and storage structures for Black and Brown water melon seeds.

RESEARCH ARTICLE

Received: 01.08.2021
Accepted: 27.09.2021

Keywords :

- Loading positions,
- Compressive force,
- Seeds varieties,
- Water content

To cite: Eze PC, Eze CN and Ide PE (2021). Effect of Moisture Content on the Mechanical Properties of Watermelon Seed Varieties. Turkish Journal of Agricultural Engineering Research (TURKAGER), 2(2): 308-320. *https://doi.org/10.46592/turkager.2021.v02i02.005*

INTRODUCTION

The effect of moisture content on the mechanical characteristics of agricultural material is essential during design and adjustment of machines used during harvest, cleaning, separation, handling and storage. This knowledge of mechanical properties of biomaterials is a prerequisite in the processing of agricultural products into different food products. Many researchers (Ide *et al.*, 2019; Eze and Eze 2017; Aviara *et al.*, 2012; Bart- Plange *et al.*, 2012; Sarpong and Earnest 2016; Altuntas *et al.*, 2005; Baumler *et al.*, 2006; Manuwa and Muhammad 2001; Guner *et al.*, 2003; Vursavus and Ozguven, 2004; Kibar *et al.*, 2010; Koya *et al.*, 2002; Oni and Olaoye, 2001; Sadeghi *et al.*, 2005; Aydın and Özcan 2002; Maduako *et al.*, 2001; Obi *et al.*, 2015; Paksoy *et al.*, 2010; Baumler *et al.*, 2006; Zareiforoush *et al.*, 2010) reported on the mechanical properties of different agricultural products under different treatments. Their results showed that under different treatments, the biomaterial displays different behavior (Ide *et al.*, 2019). Data on these properties are useful for application in designing equipment for milling, handling, storage, transportation, food processing (Aviara *et al.*, 2013; Agu and Oluka, 2013; Singh and Goswani, 1998). The mechanical ruptures on grain and seed as a result of threshing and handling operations causes reduction in germination power and viability of seeds, increases the chances of insect and pest infestation and also affects the quality of the final product (Ide *et al.*, 2019). Therefore, there is a need to understand these damages and bring solutions to it (Ide *et al.*, 2019; Aviara *et al.*, 2013; Amoah *et al.*, 2016).

According to Seyed and Elnaz (2006), It is a drought-docile crop which belongs to the Cucurbitaceae family of flowering plants. It is known as Citrullus species and it is known as *Citrullus vulgaris* (Okey and Luky, 2015; Mustafa *et al.*, 2010). According to Mustafa *et al.* (2010), watermelon seed had average value of 31.9%, 4.4%, 57.1%, 8.2%, 6.2%, 130 mg, 456 mg, 7.5 mg for protein, carbohydrate, fat, fiber, ash, calcium, phosphorus and Iron, respectively. Watermelon seeds also contain the vital amino acids such as Leucine, Isoleucine, Tryptophan and Valine (Gladvin *et al.*, 2017). Its essential benefits attracted this research on the mechanical properties in order to develop a method to ensure the mass processing of the watermelon seeds to various food products and exploit the numerous benefits of this underutilized biomaterial. The objective of this research was to experimentally study mechanical properties of watermelon seed and correlation with moisture content. The properties studied were compressive strength, toughness, stiffness, compressive force, compressive extension, deformation energy and moisture content.

MATERIALS and METHODS

Source of sample

Watermelon seeds samples used in this experiment were obtained from a local farm in Enugu North Local Government Area of Enugu State, Nigeria at stable moisture content. The two varieties were local varieties dominant in the study area and they were identified by the color of the seeds. These samples were Black and Brown varieties as shown in the Figure 1 below.

Black-coloured Watermelon seeds Brown-coloured watermelon seeds

Figure 1. Watermelon seed samples used for the experiment.

Sample Preparation

The seeds were properly sorted and cleaned to select viable seeds. After that, the sample were wrapped with polythene bag and covered in plastic containers to avoid change in moisture contents. Then the samples were taken to the laboratory where the mechanical properties were carried out. The apparatus used include Mettler-Toledo Electric digital weighing balance with model number XP204 and 0.001 sensitive, for weighing the samples at intervals OEM Multi- Purpose Oven Dryer with model 0A12ES, drying the sample and 3345-INSTRON Universal Testing Machine (IUTM), of Blue Hill 3 software, and Dell computer system of windows 8 software, for force-deformation characteristics determination. The moisture content of the samples at which the experiments were conducted were varied using the method reported by (Ide *et al.*, 2019) see Equation 5.

Determination of the Mechanical Properties

Compression tests were determined the sample at five different moisture levels at two different loading orientations namely horizontal and vertical using INSTRON Universal Testing Machine (IUTM) Model RVA 4500 Newport Scientific Australia controlled by a computer system. The cross-head load of 5 kN s^{-1} was used to compress the samples at speed of 5 mins. As the compression continues, the automated load deformation curve was plotted in relation to the behavior of each sample under compressive test. Fifty (50) randomly selected samples were tested at each loading orientation and at five different moisture contents. The force-deformations curves and its parameters were obtained. The sample were compressed at two different loading positions (horizontal and vertical loading). The samples were placed in the compressive jaws device ensuring that the center of the tool is aligned with the peak of the curvature of the watermelon seed. Force load was applied by clicking start test bottom on the computer system after zeroing the load and extension from the IUTM to avoid errors on the machine and in results. The IUTM compressed the sample until its cracks in the compressing arm of the testing load are noted. At the end of the compression test maximum at load, compressive extension at maximum load, Energy at maximum load and slope at maximum load were tabulated as reported by Ide *et al.*, 2019.

Figure 2. 3345-INSTRON Universal Testing Machine (IUTM), of Blue Hill 3 software, and Dell computer system of windows 8 software.

Compressive force (N): This is the load or force needed to cause crack on the sample at different moisture content. At this point other properties were determined. Compressive force values were generated in relation to the behavior of each sample under compressive test (Ide, *et al.*, 2019).

Compressive extension (mm): This is the change in size or shape of a body in response to the applied force. This is known as deformation, which depends on many factors such as rate of applied force, loading position, moisture content and biomaterial composition. Compressive extension values were generated in relation to the behavior of each sample under compressive test (Ide *et al.*, 2019).

Energy at maximum load (J): This is the maximum energy at maximum load required to crack the sample under compressive test. Energy at maximum values and energy at which the sample ruptured were generated in relation to the behavior of each sample under compressive test (Ide *et al.*, 2019).

Compressive strength (N mm^{-1}): This measures the strength at which each sample under a compressive test will crack. Compressive strength was determined using Equation 1 as recommended by Eze and Eze (2017). It was calculated as the ratio of applied force to the area of the sample, it is denoted as δc.

$$\delta c = \frac{f_c}{A}\left(\frac{N}{mm^2}\right) \quad (1)$$

Where; δc is the compressive strength (N mm^{-2}); f_c is the maximum load at fracture (N); A is the crosssectional area of the sample (mm^2).

Stiffness (N mm^{-2}): Stiffness is rigidity of a material under compression and the extent at which it resists deformation in response to applied load. The stiffness, St, of a material is measure of the resistance offered by an elastic material to deformation. It is given as the ratio of the stress to strain. It was determined using the Equation 2 reported by Ide *et al*., (2019). ($\delta\, \varepsilon^{-1}$), it is given as

$$S_t = \frac{F}{\delta} \tag{2}$$

Where St is the stiffness (N mm^{-2}); F is the force on the material; δ is the deformation on the material.

Toughness (J m^{-3}): This is define as the amount of energy per unit volume that a material under compression can absorb before rupture occurs. It is also defined as a material's resistance to fracture when stressed. It is approximated under the stress–strain curve using the Equation 3 reported by Ide *et al*., (2019).

$$Toughness = \frac{Rupture\ Energ}{Volume\ of\ the\ material} \tag{3}$$

Deformation Energy (N mm^{-1}): This is the total spent energy of a sample under a compressive test at which deformation occurs. It is determined using the Equation 4 reported by Ide *et al*., (2019).

$$Deformation\ Enery = Rupture\ force\ \chi\ Deformation\ at\ rupture \tag{4}$$

Moisture content (MC) %:
This is the quality of water contains in the sample. The experiment was carried out under the influence of three (3) different moisture contents 6.5, 10.5, 15.4, 18.6 and 27.8% under dry basis. The oven dry method of moisture content determination using a multi-purpose drying oven (OKH – HX – IA) drying oven was used to determine the moisture content (MC) of the samples. The weight of the wet sample and the weight of the dry sample were determined and moisture content is calculated using the Equation 5 reported by Ide *et al*., (2019).

Analysis of variance
The results obtained were submitted to analysis of variance (ANOVA), with the means compared by Duncan's test at 5% of significance. All results were expressed as the mean value standard error (SE). Statistical analyses were performed using SPSS for Windows 8.0.

$$MC = \frac{W_w - W_D}{W_D} X\ 100\% \tag{5}$$

Where; MC is the moisture content (%); W_w is the weight of wet sample (g); W_D is the weight of dry sample (g).

RESULTS and DISCUSSION

Effect of moisture content the mechanical properties of watermelon seed

Maximum load (N) The Table 1 presented the effect of moisture content on mechanical properties of water melon seeds and Figure 3-7 presented the force-deformation curve of mechanical properties water melon seed as effected by moisture content. It was observed that the maximum force required to crack the sample at horizontal loading position for black and brown watermelon sample ranged from 14.71 – 38.36 N and 16.47 – 41.82 respectively. Black and Brown colored samples had compressive forces at vertical loading position ranging from 1.95 to 3.40 and 1.85 – 5.20 N respectively for moisture content range of 6.5 – 27.8%. It was observed that, as the moisture content of both samples varied, the maximum force required to crack the sample at both horizontal and vertical loading position. The trend of the variation in moisture content and cracking force of the sample were found to be parabolic. It was observed that the sample required higher force at the horizontal loading position than vertical loading position and this could be attributed to structural lining of the sample was at vertical position. This findings gave an insight the maximum load required to crack both samples varies. Therefore it would be implored during the design and fabrication of processing machine for both samples.

Compressive strength: The results in Table 1, the compressive strength of Black and Brown coloured samples were 0.16 to 0.32 N mm^{-2} and 0.34–0.57 N mm^{-2} under horizontal loading position while 0.17–1.93 N mm^{-2} and 26.23–189.75 N mm^{-2} for vertical loading position respectively at moisture content range of 6.5–27.8% (db). It implies that the strength of watermelon seeds was found to be higher at vertical loading position than that of horizontal loading position and this may be attributed to the smaller contact that occurred during loading of the sample at vertical loading position. This position has higher resistance of the seed to be cracked. This finding reveals the required strength to process the seed samples and also generated data for strength properties of water melon in the design of handling machine.

Compressive extension (mm): The results in Table 1, the compressive extension of Black and Brown samples were 1.94–4.20 mm and 1.68–11.08 mm under horizontal loading position while 0.01–0.07 mm and 0.01–0.03 mm for vertical loading position at moisture content range of 6.5–27.8% (db) respectively. It was observed that as the moisture content varied the compressive extension. The moisture content variation displays parabolic trends for both samples. The compressive extension of a biomaterial under compressive test tells the extent a particular load/force causes deformation at different applied load. This research therefore, reveals that, the Black water melon deforms faster than Brown water melon and this should be considered during the design and fabrication of handling machine.

Energy: The maximum energy required to crack the samples were presented in Table 1. The energy ranged from 0.03 to 0.70 J and 0.02–0.14, 0.29 J for Black and Brown coloured samples respectively at the moisture content range of 6.5–27.8% for horizontal loading position.

However, these values ranged from 0.2 to 1.54 J and 0.33–1.22 J respectively at the moisture content range of 6.5–27.8% for vertical loading position. The energy was found to be varied with increase in moisture content at horizontal and vertical loading position but the energy variation with moisture content was not linear but parabolic in nature. It implies that lesser energy is required to crack the sample at vertical loading position than horizontal loading position for both samples across the moisture content tested.

Toughness (J mm^{-2}): The toughness of the sample as shown in the Table 1 ranged from 0.60–14.81 J m^{-2} and 0.81–6.97 J m^{-2} at the horizontal loading position for Black and Brown colored sample respectively at 6.5–27.8% moisture range and 0.20–1.54 J m^{-2} and 0.34–1.22 J m^{-2} for Black colored samples and Brown coloured sample in the vertical loading position respectively at moisture range of 6.5–27.8%. It was observed that, as the moisture content increases the toughness of the material also varied at vertical loading position while the variation of moisture content with toughness at horizontal loading position displayed a parabolic trend. The toughness of the samples were found to be higher at horizontal loading position. It was observed that the Black coloured sample is tougher in terms of cracking at horizontal position than vertical loading position.

Stiffness (N mm^{-2}) Tthe stiffness of the samples at different loading position were presented in the Table 1. As seen the Table 1, at horizontal loading position was recorded as 3.56 to 15.66 N mm^{-1} and 2.61–11.98 N mm^{-1} for Black and Brown coloured samples respectively at 6.5–27.8% moisture content while at vertical loading, stiffness were found to range from 0.17–0.33 N mm^{-1} and 0.26–0.76 N mm^{-1} for Black and Brown coloured samples respectively at 6.5–27.8% moisture content range. This result is similar to what was reported by Eze and Eze (2017) on Mucuna Veracruz. The stiffness of the samples revealed would be helpful during the design and fabrication of its handling equipment.

Deformation Energy (J): The values were presented in Table 1 at 6.5–27.8% moisture content range. The results obtained at horizontal loading position ranged from 0.76–76.39 kJ and 27.67 to 319.9 kJ for Black and Brown colored samples respectively at 6.5–27.8% moisture content respectively while at vertical loading position 0.17–1.93 kJ and 26.23–189.75 kJ for Black and Brown colored samples respectively at 6.5–27.8% moisture content respectively. It was observed that the increase in moisture content of the samples varied the total energy that will cause rupture on the samples. It was noticed that the deformation energy of Brown colored samples on both loading positions was higher than Black colored samples. It implies that, Brown colored sample is stronger at each of the loading positions It was observed that, at different moisture content level the energy required to rupture on the samples varies. It was noticed that the deformation energy of Brown colored sample on both loading positions was higher than Black colored sample. It implies that, Brown colored sample is stronger at each of the loading positions. But for both samples, deformation energy was found to be higher at every vertical loading position.

Table.1. Mechanical properties of black and brown colored watermelon seed at different moisture contents and loading orientations.

Properties		**Moisture content (%)**				
Black Colour Species	**Loading position**	**27.8**	**18.6**	**15.4**	**10.5**	**6.5**
Compressive force (N)	Vertical	15.68	17.13	24.54	27.61	29.54
	Horizontal	38.36	25.45	22.81	18.19	14.71
Compressive extension (mm)	Vertical	1.95	2.61	3.40	3.25	2.19
	Horizontal	2.45	1.94	3.92	4.20	4.13
Energy at Maximum load (J)	Vertical	0.02	0.01	0.07	0.07	0.02
	Horizontal	0.06	0.03	0.70	0.20	0.10
Toughness (J m^{-2})	Vertical	0.39	0.20	1.48	1.54	0.47
	Horizontal	1.16	0.60	14.81	4.39	2.34
Stiffness (N mm)	Vertical	59.32	6.56	7.22	8.50	13.49
	Horizontal	15.66	13.19	5.82	4.33	3.56
Compressive Strength (N mm^{-2})	Vertical	0.13	0.17	0.25	0.29	0.33
	Horizontal	0.32	0.25	0.23	0.19	0.16
Deformation Energy (kJ)	Vertical	0.31	0.17	1.72	1.93	0.59
	Horizontal	2.30	0.76	15.97	76.39	1.47
Brown Colour Specie						
Compressive force (N)	Vertical	14.18	16.15	19.01	31.42	36.49
	Horizontal	41.82	35.43	28.88	24.68	16.47
Compressive extension (mm)	Vertical	1.85	2.93	2.15	2.34	5.20
	Horizontal	3.49	3.48	11.08	4.32	1.68
Energy at Maximum load (J)	Vertical	0.01	0.01	0.03	0.01	0.01
	Horizontal	0.03	0.04	0.02	0.02	0.14
Toughness (J m^{-2})	Vertical	0.34	0.37	1.22	0.44	0.50
	Horizontal	1.02	1.49	0.81	0.88	6.97
Stiffness (N mm)	Vertical	7.66	5.51	8.84	13.43	7.02
	Horizontal	11.98	10.18	2.61	5.71	9.80
	Vertical	0.19	0.26	0.30	0.55	0.76
Compressive Strength (N mm^{-2})	Horizontal	0.56	0.57	0.46	0.43	0.34
Deformation Energy (kJ)	Vertical	26.23	47.32	40.87	73.52	189.75
	Horizontal	145.95	123.29	319.99	106.62	

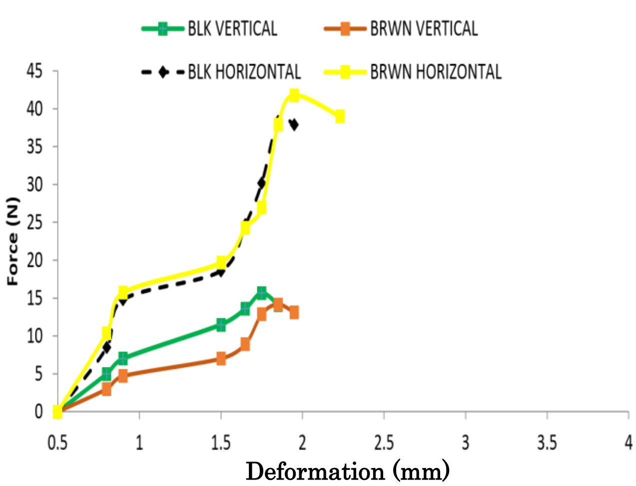

Figure 3. Force-Deformation curve of watermelon seed at 27.8% (d.b) under vertical and horizontal loading positions.

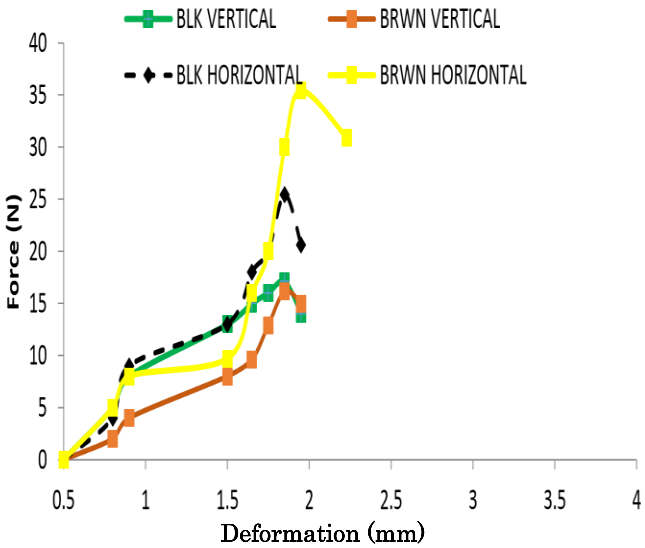

Figure 4. Force-Deformation curve of watermelon seed at 18.6% (d.b) under vertical and horizontal loading positions.

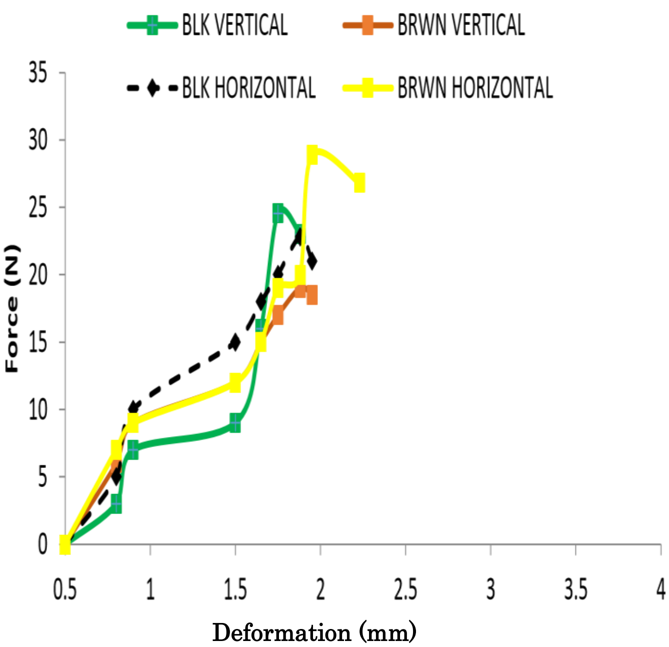

Figure 5. Force-Deformation curve of watermelon seed at 15.4% (d.b) under vertical and horizontal loading positions.

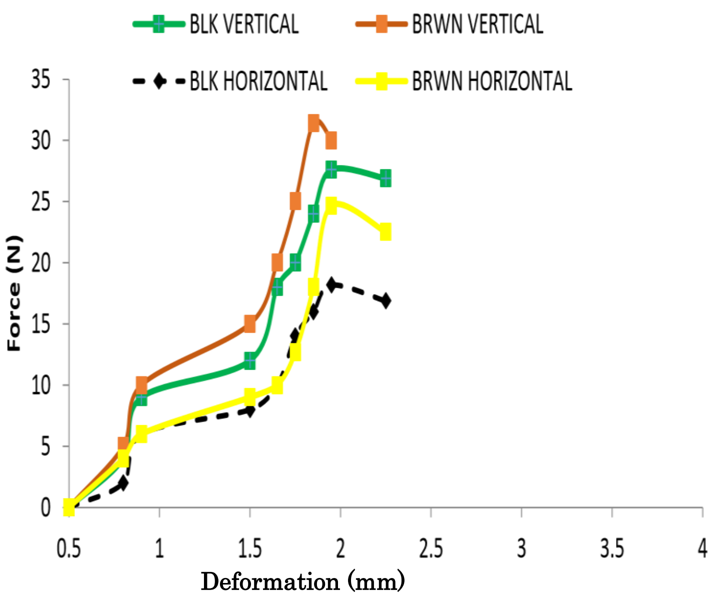

Figure 6. Force-Deformation curve of watermelon seed at 10.5% (d.b) under vertical and horizontal loading positions.

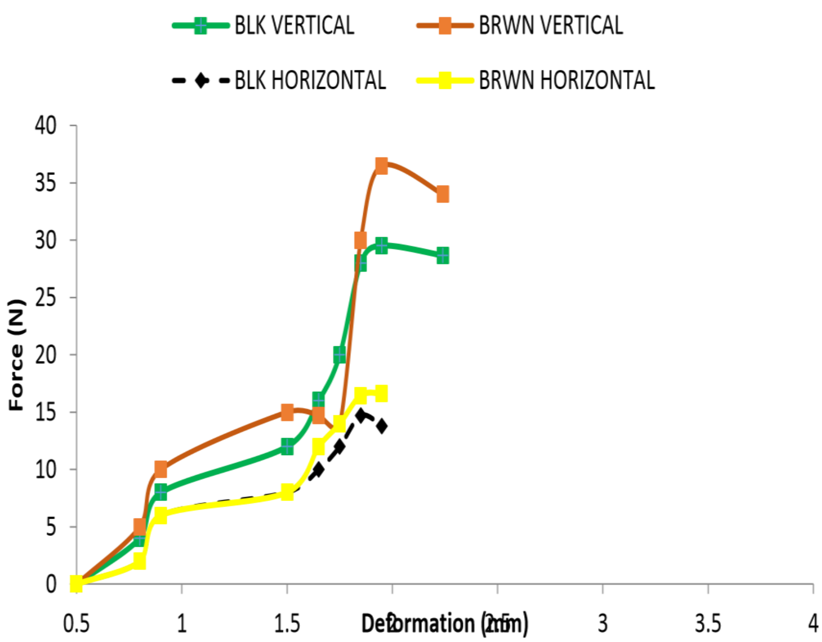

Figure 7. Force-Deformation curve of watermelon seed at 6.5% (d.b) under vertical and horizontal loading positions.

The effect of loading position, variety and moisture content on the force deformation characteristics were presented in Tables 2. It can be observed that they exhibited varying relationships with moisture content and loading positions. The R^2 values were found to range from 0.848-0.978. It was also observed that the relationship between species, moisture content and the vertical loading position was mainly quadratic in nature with the exception of seed samples at 15.4% (db). Here they exhibited linear (black) and logarithmic (brown) relationships. Similarly for moisture contents 10.5% db and lower the relationship between seed samples and loading position (horizontal) were also quadratic. However, as moisture content increased black seed samples exhibited linear relationship at horizontal loading while brown maintained its quadratic relationship. It can be inferred therefore that the force deformation characteristics of the samples tested showed that loading position, variety and moisture content had a significant effect on the mechanical properties.

Table 2. Relationships between mechanical properties of black and brown colored watermelon seeds at different moisture contents.

Sample	Effect of moisture content on force-deformation curves of watermelon seeds at 27.8% (db)			
	Horizontal		Vertical	
Black	$F= 24.04\,d_f - 11.12$	$R^2 = 0.921$	$F = -4.833\,d_f^2 + 22.07\,d_f - 9.579$	$R^2 = 0.978$
Brown	$F= -3.891\,d_f^2 + 32.08\,d_f - 13.68$	$R^2 = 0.886$	$F = 2.438\,d_f^2 + 3.083\,d_f - 1.399$	$R^2 = 0.933$
	Effect of moisture content on force-deformation curves of watermelon seeds at 18.6 % (db)			
	Horizontal		Vertical	
Black	$F = 15.55\,d_f - 7.442$	$R^2 = 0.931$	$F = -7.542\,d_f^2 + 29.31\,d_f - 12.93$	$R^2 = 0.97$
Brown	$F= 0.203\,d_f^2 + 17.60\,d_f - 9.414$	$R^2 =0.817$	$F = 4.798\,d_f^2 - 1.200\,d_f - 0.081$	$R^2 = 0.962$
	Effect of moisture content on force-deformation curves of watermelon Seeds at 15.4% (db)			
	Horizontal		Vertical	
Black	$F = -3.124\,d_f^2 + 22.40\,d_f - 9.966$	$R^2 = 0.972$	$F = 16.51\,d_f - 9.400$	$R^2 = 0.863$
Brown	$F = 14.01\,d_f - 5.530$	$R^2 = 0.884$	$F = 13.22\ln(d_f) + 9.182$	$R^2 = 0.964$
	Effect of moisture content on force-deformation curves of watermelon seeds at 10.5 % (db)			
	Horizontal		Vertical	
Black	$F = -1.868\,d_f^2 + 15.22\,d_f - 7.700$	$R^2 = 0.897$	$F = -2.367\,d_f^2 + 21.99\,d_f - 10.86$	$R^2 = 0.925$
Brown	$F = 1.123\,d_f^2 + 9.095\,d_f - 4.483$	$R^2 = 0.848$	$F = 8.005\,d_f^2 + 0.535\,d_f - 0.648$	$R^2 = 0.952$
	Effect of moisture content on force-deformation curves of watermelon seeds at 6.5 % (db)			
	Horizontal		Vertical	
Black	$F = 1.379d_f^2 + 6.057d_f - 2.867$	$R^2 = 0.942$	$F = -1.317\,d_f^2 + 20.38\,d_f - 10.62$	$R^2 = 0.891$
Brown	$F = 3.803d_f^2 + 1.877d_f - 1.238$	$R^2 = 0.953$	$F = 2.069\,d_f^2 + 12.49\,d_f - 6.127$	$R^2 = 0.803$

CONCLUSION

It was concluded that the data generated from mechanical properties of Black colored watermelon seed cannot be used in designing of food processing, handling and storage systems for Brown coloured watermelon seed as mechanical properties of both species tested varied with moisture content. This research work have solved a big problem as it revealed the variations existed between Black and Brown water melon seeds. It also generated data which aids the design and fabrication of handling equipment. The results of the force-performance properties of the Watermelon seed were observed to be moisture content dependent (6.5-27.8% db). The correlation that existed between moisture content and the force-deformation properties was statistically significant at ($p<0.05$) level. It is economical to crack the Black and Brown samples at vertical loading position and at 27.85% moisture content in order to reduce energy and strength demand when necessary to crack and compress the samples properly.

DECLARATION OF COMPETING INTEREST

The authors declare that they have no conflict of interest.

CREDIT AUTHORSHIP CONTRIBUTION STATEMENT

The authors declare the contributions to the manuscript such as the sections
Paul Chukwuka EZE decleared methodology, conceptualization and review.
Chikaodili Nkechi EZE decleared validation and visualization.
Patrick Ejike IDE decleared investigation, formal analysis, data curation, writing, original draft and editing.

REFERENCES

Agu O and Oluka I (2013). Selected physical and mechanical properties of Nerica paddy. *Journal of Experimental Research, 1: 49-62.*

Altuntas E and Yildiz M (2005). Effect of moisture content on some physical and mechanical properties of faba bean (*Vicia faba* L.) grains. *Journal of Food Engineering 78: 174-183.*

Amoah R, Abano EE and Anyidoho EK (2016). Effect of moisture and loading orientation on some physical and mechanical properties of 'Tafo Hybrid' and 'Amelonado' cocoa beans. *Journal of Food Process Engineering, 40(1): 1-9.*

Aviara NA, Onuh OA and Ehiabhi SE (2012). Influence of moisture content and loading orientation on some mechanical properties of *Mucuna flagellipes* nut. *Research in Agricultural Engineering, 58: 66-72.*

Aviara NA, Power PP and Abbas T (2013). Moisture-dependent on physical properties of *Moringa oleifera* seed relevant in bulk handling and mechanical processing. *Industrial Crop and Production, 42: 96-104.*

Aydın C and Özcan M (2002). Some physico-mechanical properties of terebinth (*Pistacia terebinthus* L.) fruits. *Journal of Food Engineering, 53: 97-101.*

Bart-Plange A, Mohammed-Kamil AP, Addo A and Teye E (2012). Some physical and mechanical properties of cashew nut and kernel growth. *International of Journal of Science and Nature (I.J.S.N), 3(2): 406-415.*

Baumler E, Cuniberti A, Nolasco SM and Riccobene IC (2006). Moisture dependent physical and compression properties of safflower seed. *Journal of Food Engineering. 72: 134-140.*

Eze PC and Eze CN (2017). Determination of some physical and mechanical properties of horse eye-bean (*Mucuna sloanei*) from South East Nigeria. *Journal of Experimental Research, 5(1): 33-41.*

Gladvin G, Sudhaakr G, Swathi V and Santhisri KV (2017) Mineral and Vitamin Gordon and Breach. Green healthy farmer 2019. Kenaf seeds. *Journal of Food Science and Technology, 52(6): 3254-3263.*

Guner M, Dursun E and Dursun IG (2003). Mechanical behaviour of hazelnut under compression loading. *Biosystem Engineering, 85(4): 485-491.*

Ide PE, Eze PC and Offor BC (2019) Effect of moisture content on the physico-mechanical properties of *Mucuna sloanei*. *International Journal of Scientific Engineering and Research (IJSER), 7(2): 91-96.*

Kibar H, Esen B and Ozturk T (2010). The effect of moisture content on physical and mechanical properties of rice. *Spanish Journal of Agricultural Research, 8(3): 741-748.*

Koya OA, Idowu A and Faborode MO (2002). Some properties of palm kernel and shell relevant in nut cracking and product seperation. *Journal of Agricultural Engineering, 12: 33-43.*

Maduako JN, Istifanus AB and Maunde FA (2001). *Determination of some mechanical properties of bambara nuts (Vigna subterranea Verds) relevant to shelling.* Department of Agricultural Engineering, Federal University of Technology, Yola. pp 1-10.

Manuwa SI and Muhammad HA (2011). Effects of moisture content and compression axis on mechanical properties of shea kernel. *Journal of Food Engineering, 105: 144-148.*

Mohsenin NN (1986). Physical properties of plant and animal material structure, physical characteristics and mechanical properties of 2 AUlf891, Seiten, Zahlr. ABB. Und Tab. *Gordon and Breach Science Publisher*, New York Press: 140.

Mustafa, RA, Abdul Hamid, Azizah and Mohamed, Suhaila (2010) Total phenolic compounds, flavonoids, and radical scavenging activity of 21 selected tropical plants. *Journal of Food Science, 75(1): 28-35.*

Paksoy M, Aydin C, Türkmen Ö and Seymen M (2010). Modeling of some physical properties of watermelon (*Citrullus lanatus* (Thunb.) Mansf.) seeds depending on moisture contents and mineral compositions. *Pakistan Journal of Botonic, 42(4):2775-2783.*

Obi OF, Offorha LC and Yıldız F (2015). Moisture-dependent physical properties of melon (*Citrullus colocynthis* L.) seed and kernel relevant in bulk handling. *Cogent Food & Agriculture, 1(1): 1020743.*

Okey Francis Obi and Lucky Chikadibia Offorha (2015). Moisture-dependent physical properties of melon (*Citrullus colocynthis* L.) seed and kernel relevantin bulk handling, *Cogent Food & Agriculture*, *1(1): 1-14.*

Oni KC and Olaoye JO (2001). Some physical and mechanical properties of selected grain crops. Department of Agricultural Engineering, University of Ilorin. *Proceedings of Nigerian Institution of Agricultural Engineers, 23: 315-318.*

Sadeghi M, Hemmat A and Ashtiani H (2005). Physico-mechanical properties of rough rice (*Oryza sativa* L.) grain as affected by variety and moisture content. *Agricultural Engineering International. CIGR E-journal. 12(3): 129-136.*

Sarpong RA and Ekow E (2016). Effect of moisture and loading orientation on some physical and mechanical properties of 'TafoHybrid' and "Amelonado" Cocoa Beans. *Journal of Food Process Engineering, 40(1):1-9.*

Seyed M. A. Razavi and Elnaz Milani (2006) Some physical properties of the watermelon seeds Seyed. *African Journal of Agricultural Research, 1(3): 65-69*.

Razavi SMA and Milani E (2006). Some physical properties of the watermelon seeds. *African Journal of Agricultural Research, 1(3): 65-69.*

Singh KK and Goswami TK (1998). Mechanical properties of cumin seed (*Cuminum cyminum linn.*) under compressive loading. *Journal of Food Engineering, 36: 311-321.*

Vursavus K and Ozguven F (2004). Mechanical behaviour of apricot pit under compression loading. *Journal of Food Engineering, 65: 255–261.*

Zareiforoush H, Mohtasebi SS, Tavakoli H and Alizadeh MR (2010). Effect of loading rate on mechanical properties of rice straw. *Australian Journal of Crop Science, 4(3): 190-194.*

Turkish Journal of Agricultural Engineering Research

https://dergipark.org.tr/en/pub/turkager
https://doi.org/10.46592/turkager.2021.v02i02.006

Turk J Agr Eng Res
(TURKAGER)
ISSN: 2717-8420
2021, 2(2): 321-329

Research Article

Multipurpose Fruit Juice Machine for Preventing Fruit Wastage in Nigeria Villages

Ayoola Olawole JONGBO[a*] ID

[a] *Department of Agricultural and Environmental Engineering, School of Engineering and Engineering Technology, Federal University of Technology, PMB 704, Akure, Ondo State, NIGERIA*

(*): Corresponding author, aojongbo@futa.edu.ng

ABSTRACT

Fruits are produced in large quantities in developing countries because of the favourable climatic conditions but the level of spoilage is high. It is essential to extract and preserve fruit juice to have a regular supply throughout the year. Therefore, it was necessary to develop a machine that could be used to extract juice from several fruits. Thus, the objective of the research work was to develop a multipurpose small scale fruit juice machine that could be adopted by an average farmer in the rural regions to increase their juice intake. A fruit juice extractor was designed, developed and tested. The machine utilised a serrated auger for crushing the fruits before squeezing out the juice. The performance evaluation showed that the machine has an extraction capacity of 88.4 kg h^{-1} and 84.5 kg h^{-1} for pineapple and sweet orange respectively. The efficiencies of the juice extractor for pineapple and sweet orange were 91.13% and 85.96% respectively. The average production cost of the machine was estimated as 390 US dollars.

RESEARCH ARTICLE

Received: 20.08.2021
Accepted: 01.10.2021

Keywords :

- Extraction capacity,
- Compressive force,
- Seeds varieties,
- Water content

To cite: Jongbo AO (2021). Multipurpose Fruit Juice Machine for Preventing Fruit Wastage in Nigeria Villages. Turkish Journal of Agricultural Engineering Research (TURKAGER), 2(2): 321-329. *https://doi.org/10.46592/turkager.2021.v02i02.006*

INTRODUCTION

The demand for agricultural produce was forecast to increase by about 40% between 2012 and 2050 and that it would exert more pressure on the global natural resources (FAO, 2019). Food production, "from an environmental perspective, is resource-intensive" and its wastage could negatively impact the environment (FAO, 2019). Globally, about 14% of the food produced is lost after harvesting (FAO, 2019). For farmers in low-income countries such as Nigeria, minimizing on-farm losses could allow them to improve their food availability, supply, and incomes. Furthermore, an additional reduction in food losses could be experienced with food processing, leading to higher food supply and security. Fruit processing, an arm of the food processing industry, involves the conversion of fruits into pulp and juice that could be preserved for consumption year-round (El-ramady *et al.,* 2015).

Even though the environment and climatic condition of the tropical region favour the production of fruits in large quantities, fruits are found to be scarce during off-seasons because of the wastage incurred due to inadequate storage and processing facilities. Fruits are one of the highly perishable agricultural products that require negligible processing steps to fulfill effective inactivation of pathogens (Ojha *et al.,* 2021). Fruit juices are popularly perceived to be natural and that for them to retain the nutritional, colour, taste, composition and organoleptic features of the initial fruits, it is expected that the fruits are suitably processed without containing preservatives, sugar, artificial flavours and other ingredients (Cendres *et al.,* 2011; Rajauria and Tiwali, 2018).

Fruit juice extraction involves crushing, squeezing, and pressing fruits to produce juice and pulp. It could also be described as a process of physically changing the nature of the fruits to liquid and pulp. A few decades ago, manual extraction of juice from the fruit was the most common method in use which could be very slow and tedious. However, with the introduction of various techniques of extracting juice, the limitations and problems of manual fruit extraction have been reduced or eliminated. With the advent of fruit juice extractors, fruit processors have been able to save time, improved their efficiency and produce a large quantity of juice at a particular period with ease. Various mechanical fruit juicers had been developed and well-reviewed (Mushtaq, 2018; Nnamdi *et al.*, 2020). In Nigeria, various fruit juicing machines had recently been developed. These varied from manually operated fruit juice machines (Eyeowa *et al.*, 2017) to mechanically operated fruit juicing machines (Adejumo *et al.,* 2014; Aviara *et al.*, 2013; Omoregie *et al.*, 2018; Suleiman *et al.*, 2020). Though the machines were reported to be very cheap, they could be time-consuming (manually operated machine) and also result in crushing the seeds during processing which could affect the sensory and quality of the fruit juice (Mphahlele *et al.*, 2018).

Over the year, the production rate of fruits has increased in some regions of the tropical humid climate at some months of the year and become scarce during the remaining months of the year due to lack of storage facilities and processing techniques in the villages in Nigeria. Most of the small-scale machines that were developed were inaccessible for most of the villagers. In addition, if the machines were available, they were time-consuming and could also crush the seeds in the fruit during processing. Therefore, developing a time-saving and highly efficient multipurpose fruit juicing machine that could carefully extract juice from the fruits without affecting the quality of the juice would improve the standard of living of the villagers in Nigeria and at the same time reduce food wastage and losses.

The specific objectives of this study were; (1) to design and fabricate a multipurpose fruit juice machine capable of extracting juice without affecting its quality and (2) to test and evaluate the performance of the machine.

MATERIALS and METHODS

Machine design and description

The fruit juice extractor was designed on a PC (Figure 1a) using computer-aided design and engineering software (i.e., SolidWorks) and constructed at the Department of Agricultural and Environmental Engineering, Federal University of Technology, Akure, Nigeria. The machine was designed and developed to extract juice from various tropical fruits. The fruit juice extractor comprised the feeding (hopper), crushing and extracting units. The extraction unit comprised a screen for sieving the juice before discharging it from the machine. The prismatic hopper, made of stainless steel and the sides slanted at an angle 60° to the horizontal, was constructed on a removable concave top cover that protected the serrated auger. The shaft (serrated auger) with a diameter of 0.18 m, made of stainless steel and operated at an average speed of 1400 rpm, cut and squeezed the fruits fed into the hopper to produce juice and pulp. The juices from the fruits were collected through the juice delivery chute under the crushing unit while the effluent was collected at the pulp delivery chute at one of the ends of the juice extractor. The power was transmitted from the electric motor to the crushing unit through the driving and driven pulleys (Figure 1b). The juice extractor was constructed with less expensive materials in which the engineering qualities and cost were considered. The total cost of production of the machine was estimated as three hundred and ninety dollars ($ 390.00).

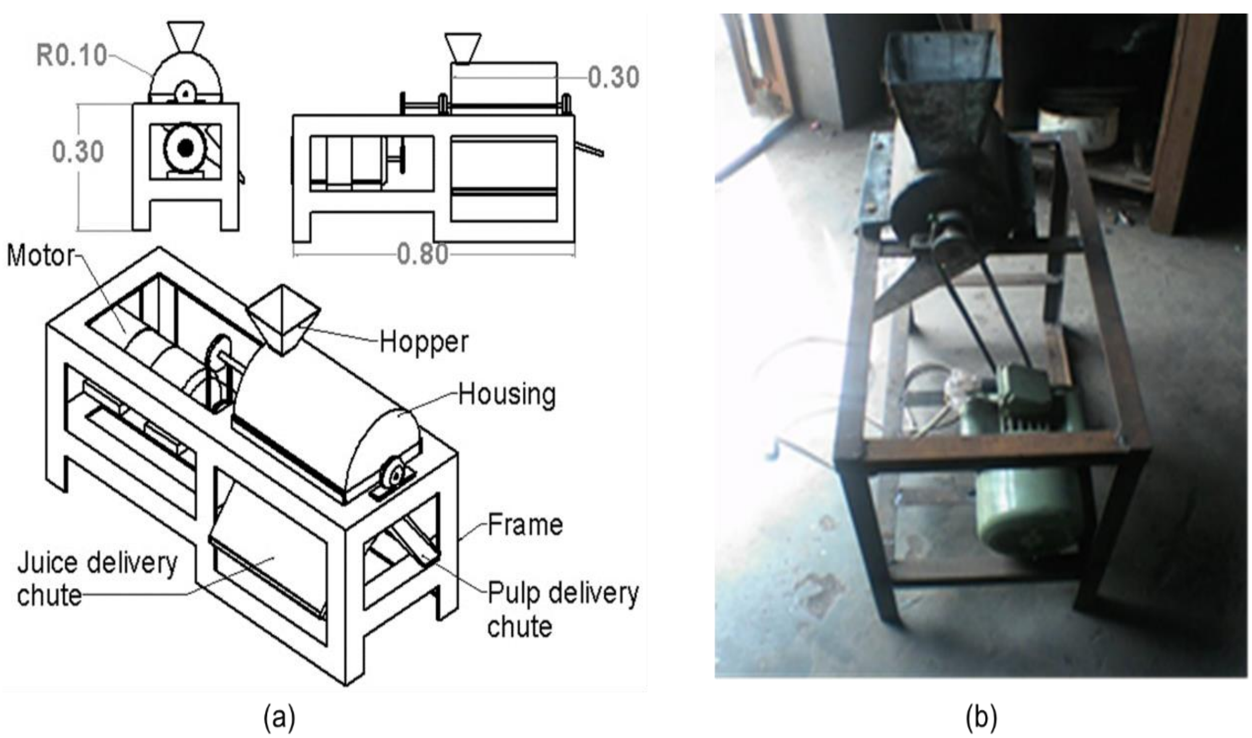

Figure 1. (a) Schematic and (b) pictorial view of the fruit juice machine (All dimensions in meters).

Shaft design

A shaft of a total length of 0.41 m has a uniformly distributed serrated auger of the length of 0.27 m. The machine has a strong frame that could absorb any possible stress and load. To determine the shear force and a bending moment of the shaft (beam) of the juicing machine, the weights of the shaft's component were mathematically determined. The weight of the pulley, made of mild steel, was estimated at 5.0 N. The weight of the serrated auger per unit length was estimated as 86.59 N m^{-1} and the machine was expected to be loaded with fruits of an average weight per unit length of 181.67 N m^{-1}.

The power required by the shaft

The linear velocity (V) of the shaft was estimated as 13.29 m s^{-1} using

$$V = rw \tag{1}$$

where r is the radius of the pulley and w is the angular velocity (revolution per second) of the pulley. The maximum bending moment (M_b) was estimated as 4.43 N m^{-1} using bending moment diagram (BMD) and the torsional moment (M_t) of 27.39 Nm was estimated using

$$M_t = \frac{P}{2\pi n} \tag{2}$$

Where; P is the estimated power required (4.044 kW or 5.4 HP) and n is the number of revolutions of the shaft per second. The diameter (d) of the shaft was estimated as 21.6 mm using

$$d^3 = \frac{16}{\pi S_s}\sqrt{(K_b M_b)^2 + (K_t M_t)^2} \tag{3}$$

where S_s is the allowable stress (34.6 MPa), K_b is the bending stress factor (1.5), K_t is the torsional stress factor (1.0), M_b is the maximum bending moment, and M_t is the torsional moment. The factor of safety considered suitable for the shaft diameter was 1.35. In this work, a standard shaft diameter of 25 mm was selected for the machine since a 21.6 mm diameter shaft was not readily available for the work.

Design of auger

The auger on the shaft (Figure 2) was designed to convey the pulps of the fruit to the pulp delivery chute. For the auger design, the theoretical capacity of the auger, which would convey materials of an average mass of materials of 5.0 kg, was estimated as 0.0222 m^3 min^{-1} using

$$Q = \frac{(D^2 - d^2) \times P_a \times n \times \emptyset}{36.6} \tag{4}$$

Where D is the pitch diameter of the auger (m), d is the diameter of the shaft (m), P_a is the pitch of the auger, n is the shaft speed (revolution per minute), $\varnothing$ is the filling factor (0.45). The torque T_c of the auger was estimated as 2.80 N m^{-1} using

$$T_c = \frac{975 \times P}{n} \quad (5)$$

Where; P and n are the power required and the speed of the auger respectively. The load propulsion speed V_c and load per unit length V_c of the auger of 0.94 m s^{-1} and 6.56×10^{-3} N m^{-1} were estimated using

$$V_c = \frac{P_a \times n}{60} \quad (6)$$

and

$$L_c = \frac{Q}{3.6V} \quad (7)$$

respectively. The axial thrust *(Th)* of the auger of 7.08×10^{-4} N was estimated using

$$Th = L_c \times L \times \mu \quad (8)$$

Where; L is the length of the auger and μ is the friction coefficient (0.4).

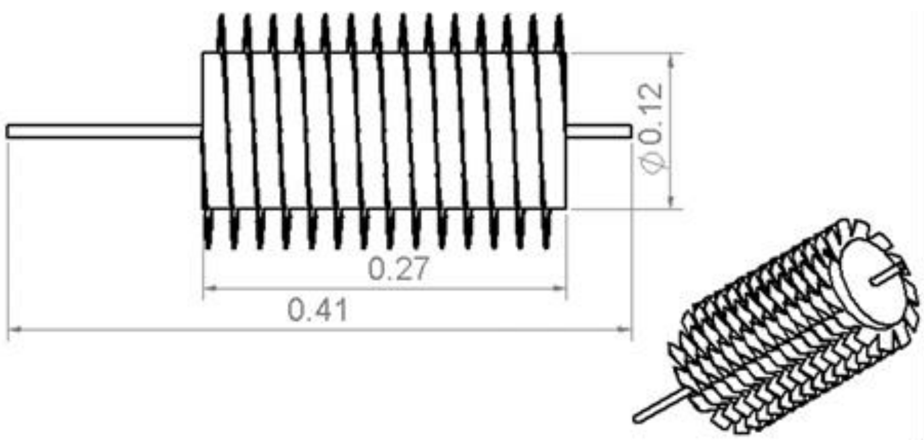

Figure 2. The serrated auger (all measurements in metres).

Belt and pulley design

The choice of the belt for the machine, over other power transmission devices such as chain, was based on its ability to prevent vibration transmission, less expensive, ability to transmit power between the axes of widely spaced shafts, and that its damage during operation would not negatively affect the machine. Therefore, the design details of the belt (Figure 3) of the machine are as follows. The wrap angle β of the belt was estimated as 180° using

$$\beta = 180° + 2sin^{-1}\frac{(R_1 - R_2)}{C} \quad (9)$$

Where; R_1 and R_2 are the radius of two pulleys (note that the pulleys have the same diameter), C is the distance between the centers of two pulleys. The length of the belt was estimated as 0.90 m using

$$L_b = 2C + \frac{\pi}{2}(D_1 + D_2) \quad (10)$$

Where; D_1 and D_2 are the diameters of the two pulleys. The tensions (T_1 and T_2) on the belt were estimated at 76.8 N and 24.97 N using

$$T_1 = Allowable\ stress\ (0.06\ MPa) \times Thichness\ of\ belt\ (0.02m) \times width\ of\ belt \quad (11)$$

and

$$\frac{T_1 - mV^2}{T_2 - mV^2} = e^{\mu\beta} \quad (12)$$

where m is the mass of the belt (kg), V is the estimated belt's speed (m s^{-1}), μ (0.25) is the friction coefficient between the belt and the pulley. The power capacity (P_b) of the belt was estimated as 0.25 kW using

$$P_b = (T_1 - T_2)V. \quad (13)$$

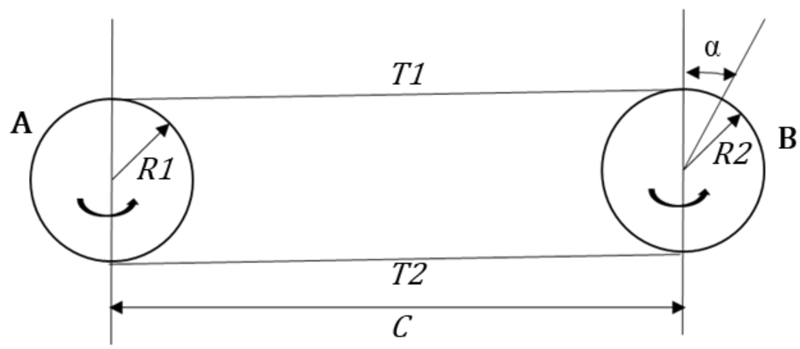

Figure 3. Belt design details

Experimental design and data analysis

The machine was tested with some fruits (sweet oranges and pineapple) based on their cultivation by most of the farmers. A total of 15 kg of each of the fruits was acquired from the local market during the study. The performance of the juice extractor was evaluated based on the machine speed (1400 rpm) and the two different types of fruits used (sweet oranges and pineapple). A motor with 1400 rpm was selected because of its price and availability in the local market. Most of the motors with variable speeds are expensive and farmers could find it difficult to replace if the need arises. The test was repeated three times with each containing 5 kg of the fruits. The time taken (minutes) by the machine to complete the extraction was noted. The extracted juice was collected and weighed as kg. The juice extraction capacity (kg h^{-1}) and the juice extraction efficiency (%) of the machine were determined using appropriate expressions.

$$\text{Juice extraction capacity (kg } hr^{-1}) = \frac{\text{mass of juice extracted}}{\text{Time spent for the extraction}} \quad (14)$$

$$\text{Juice extraction efficiency (\%)} = \frac{\text{mass of juice extracted}}{\text{mass of maximum extractable juice}} \times 100 \quad (15)$$

The data were processed using Microsoft Excel 2019 and analysed using JMP® Pro 13.0.0 (SAS Institute Inc., 2016). The data was subjected to statistical analysis (t-test) to determine the performance of the machine at a statistical significance of 5%.

RESULTS and DISCUSSION

The performance of the fruit juice machine was evaluated based on its extraction capacity and extraction efficiency. As shown in Figure 4, it could be observed that a higher mean extraction capacity per unit time (88.4 kg h^{-1}) of the machine was obtained from the pineapples. Since the fruits were ripe and peeled before being loaded into the machine, it could indicate that the machine was able to crutch and extract almost all the juice in the pineapple than it could with the sweet orange (84.50 kg h^{-1}). Eyeowa *et al.* (2017), reported that a manual juice extractor has an average extraction capacity of about 53% for both pineapple and orange while about 1.0 kg of the total orange (3.80 kg) loaded into a fruit juicing machine developed by Omoregie *et al.* (2018) was reported not be properly processed. Similarly, Aviara *et al.* (2013) reported that a multipurpose fruit juicer could produce about 79% and 77% of juice from the peeled pineapple and orange loaded into it respectively. The t-test analysis carried out showed that there was a significant difference ($p = 0.0047$) between the mean extraction capacity of the machine when tested with pineapple and sweet orange.

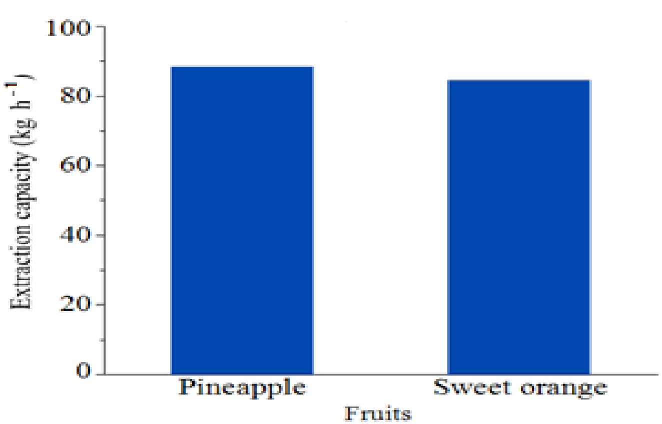

Figure 4. Juice extraction capacity of the fruit juicing machine.

The extraction efficiency of the fruit juice machine, as shown in Figure 5, indicated that the efficiency of the machine, when tested with pineapple (91.13%), was higher than that of sweet orange (85.96%). Higher efficiencies were reported by Aviara *et al.* (2013) who indicated that their multipurpose juice extractor achieved 97% and 94% extraction efficiencies when tested with peeled pineapple and orange respectively. However, the findings of Eyeowa *et al.* (2017) showed that the efficiency of a manually operated juicing machine when tested with orange (about 66%) was higher than that of pineapple (about 64%). The result of the statistical analysis (t-test) conducted showed that there was a significant difference ($p < 0.0001$) between the mean extraction efficiencies of the fruit juice machine when tested with pineapple and sweet orange.

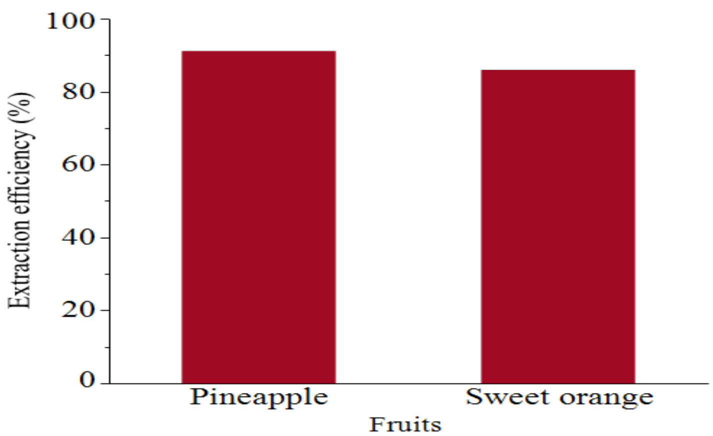

Figure 5. Juice extraction efficiency of the fruit juicing machine.

CONCLUSION

A multipurpose juicing machine with a serrated auger was developed and tested with peeled pineapples and sweet oranges. The results of this study have shown that replacing the smooth edge screw auger in the juicing machine with a serrated auger could increase the extraction capacity (kg h^{-1}) and efficiency (%) of the fruit juice machine. It has also been found out that using a serrated auger could increase the extraction of juice from pineapple which had been reported "to possess valuable bioactive compounds for medical purposes, increase appetite for food nourishment" and many other benefits (Mohd Ali *et al.*, 2020).

DECLARATION OF COMPETING INTEREST

The author would like to declare that there is no conflict of interest.

CREDIT AUTHORSHIP CONTRIBUTION STATEMENT

The author would like to declare that he solely developed all the sections in this manuscript.

REFERENCES

Adejumo OA, Adamade CA, Ayuba LO and Ozumba IC (2014). Performance evaluation of an improved NCAM multi-fruit juice extractor. *Journal of Agricultural Engineering and Technology (JAET), 22: 37-42.*

Aviara NA, Lawal AA, Nyam DS and Bamisaye J (2013). Development and performance evaluation of a multi-fruit juice extractor. *Global Journal of Engineering, Design and Technology, 2: 16-21.*

Cendres A, Chemat F, Maingonnat J and Renard CMGC (2011). An innovative process for extraction of fruit juice using microwave heating. *LWT - Food Science and Technology, 44: 1035-1041.*

El-ramady HR, Domokos-szabolcsy É, Abdalla NA, Taha HS and Fári M (2015). Postharvest management of fruits and vegetables storage postharvest management of fruits, in: Lichtfouse E. (Ed.), Sustainable Agriculture Reviews. *Springer International Publishing Switzerland*, pp. 65–152.

Eyeowa AD, Adesina BS, Diabana PD and Tanimola OA (2017). Design, fabrication and testing of a manual juice extractor for small scale applications. *Current Journal of Applied Science and Technology, 22: 1-7.*

FAO (2019). The state of food and agriculture 2019: Moving forward on food loss and waste reduction. Rome.

Mohd Ali M, Hashim N, Abd Aziz S and Lasekan O (2020). Pineapple (*Ananas comosus*): A comprehensive review of nutritional values, volatile compounds, health benefits, and potential food products. *Food Research International, 137: 109675.*

Mphahlele RR, Genis T, Fawole OA and Opara UL (2018). Sensory, quality and biochemical attributes of pomegranate juice as affected by method of extraction. *Acta Horticulturae, 1201: 115-121.*

Mushtaq M (2018). Extraction of fruit juice: an overview, in: Rajauria, G., Tiwari, B.K. (Eds.), Fruit Juices: Extraction, Composition Quality and Analysis. *Elsevier*, London, UK, pp. 131-159.

Nnamdi UB, Onyejiuwa CT and Ogbuke CR (2020). Review of orange juice extractor machines. *Advances in Science, Technology and Engineering Systems, 5: 485-492.*

Ojha S, Fröhling, A, Durek J, Ehlbeck J, Tiwari BK, Schlüter OK and Bußler S (2021). Principles and application of cold plasma in food processing, in: *Innovative Food Processing Technologies. Elsevier*, pp. 519-540.

Omoregie MJ, Francis-Akilaki TI and Okojie TO (2018). Design and fabrication of a juice extractor. *Journal of Applied Sciences and Environmental Management, 22: 207-212.*

Rajauria G and Tiwali BK (2018). Fruit juices: an overview, in: Rajauria, G., Tiwari, B.K. (Eds.), Fruit Juices: Extraction, Composition Quality and Analysis. *Academic Press, Elsevier*, London, UK, pp. 3-14.

SAS Institute Inc. (2016). Using JMP® 13. SAS Institute Inc., Cary, NC, USA.

Suleiman AI, Bello S, Eguoaje SO and Michael O (2020). Fabrication and testing of a motorized turmeric juice extracting machine. *International Journal of Scientific Research and Engineering Development, 3: 523-531.*

Turkish Journal of Agricultural Engineering Research

https://dergipark.org.tr/en/pub/turkager
https://doi.org/10.46592/turkager. 2021.v02i02.007

Turk J Agr Eng Res
(TURKAGER)
ISSN: 2717-8420
2021, 2(2): 330-338

Research Article

LabVIEW Based Real-time Color Measurement System

Abdullah BEYAZ[a*] ID

[a] *Department of Agricultural Machinery and Technologies Engineering, Faculty of Agriculture, Ankara University, 06130, Diskapi, Ankara, TURKEY*

(*): Corresponding author, abeyaz@ankara.edu.tr

ABSTRACT

Colorimetry is of paramount importance to the agricultural industry. Colorimetry refers to the processing of agricultural products for consumer needs from a marketing point of view, and therefore the agricultural industry spends a lot of money and time classifying each product. In the past, agricultural professionals had to use program codes that are difficult to learn, and even the most basic image analysis for agricultural product classification required mastering different program libraries. Today, the LabVIEW platform offers a flexible, fast, easy-to-learn, and complete image analysis infrastructure with various useful modules. For this reason, in this study, a method analysis for color perception with a simple USB webcam and software developed for real-time color analysis on the LabVIEW platform is presented and its success in the basic color analysis is tried to be revealed. The basic application developed for this purpose in LabVIEW v2019 using NI Vision Development Module v19 and NI IMAQ v19 modules. The basic fact that is the LabVIEW application is the idea that LabVIEW can only be analyzed with expensive IEEE 1394, but it should be known that these analyzes can be done with USB webcams. For this purpose, the application includes a USB webcam driver that can be stacked seamlessly. USB Webcam and colorimeter measurement-based results of ɣR factors for each of RGB color channels are 1.161232, 0.506287, 0.432229; ɣG factors for each of RGB color channels are 0.519619, 1.025383, 1.201444; at last ɣB factors for each of RGB color channels are 0.600362, 0.714016, 1.413406, respectively.

RESEARCH ARTICLE

Received: 15.08.2021
Accepted: 14.10.2021

Keywords :

- Color recognition,
- Colorimeter,
- Real-time measurement,
- Webcam,
- LabVIEW

To cite: Beyaz A (2021). LabVIEW Based Real-time Color Measurement System. Turkish Journal of Agricultural Engineering Research (TURKAGER), 2(2): 330-338.
https://doi.org/10.46592/turkager.2021.v02i02.007

INTRODUCTION

Agricultural production areas have a lot of industrial applications. The application of technology to agricultural processes has resulted in significant revenues. In addition, the use of technology provides for precision and speed in tasks that individuals are unable to perform. This situation leads to changes in agricultural output and processing. Different processes in agriculture benefit from the use of technology, such as robotic weed control systems, automatic harvesting systems, sorting machine systems, packing systems, grading and identification of agricultural products, and so on.

For all of these types of cases, we employ color measurements. As a result, the use of color sensors in agriculture is extremely important. Professional spectrometers, on the other hand, are useless in agricultural applications from the low-cost product perspective. In general, they are beneficial for data collection in laboratories. As a result, low-cost color sensors with repeatable errors are required for field measurements. There is also a lot of application in the literature about colormeter measurements.

The color of the fruit on the outside is an important factor for consumers when purchasing agricultural products (Leon *et al.*, 2006). The aesthetic quality standards of the items have an impact on the prices of fruits and vegetables. As a result, distinguishing the color change of fruits from the original fruits is difficult (Xing *et al.*, 2006). For the quality analysis of agricultural products, computer vision technology has advanced significantly (Brosnan and Wen Sun, 2004). Computer vision units are also commonly employed in industrial applications to identify fruit damage based on external color.

For evaluating faults on vegetables and fruits, Mendoza *et al.* (2006) investigated image analysis units that assess standard sRGB color, HSV, and *L*, a*, b** color spaces. Ratule *et al.* (2006) studied the effects of cold storage on the chilling injury of the ‘Berangan' banana (*Musa* cv. *berangan*).

Color measurement may be employed instead of chemical analysis, according to Fouda and Salah (2014). A link between the colored component and the chemical in the food may also exist. Color measurement is said to be easier and faster than chemical analysis.

Pawar and Dale (2016) used the Raspberry Pi 2 to detect flaws in 15 lemons and sort them into categories. They used the Python programming language with OpenCV to create algorithms for detecting and sorting lemons. They discovered that the faulty skin area may be recognized for one pixel up to 4.3677×10^{-6} cm^2. They further emphasize that their technology was discovered to be more cost-effective and clever.

Narendra and Hareesh (2010) discuss the current development and application of image analysis and computer vision systems in the agricultural and food industries for sorting and grading items. According to them, computer vision systems are rapidly being used in the business for inspection and evaluation. They also claim that the sorting and grading devices can deliver a quick, cost-effective, sanitary, uniform, and objective assessment. However, they point out that challenges remain, as seen by the comparatively delayed commercial adoption of computer vision technologies across all industries.

According to Mahendran *et al.* (2011), computer vision is a fast, consistent, and objective inspection tool that has spread across a wide range of industries. For completely automated processes, the approaches' speed and precision meet ever-increasing production and quality criteria.

The following factors influence the quality of agricultural products: size, color, shape, and type of skin defects according to the international marketing standard. The color of the food surface for customers is the first quality parameter. This is crucial in gaining market acceptance for the product. The goal of the study was to use color analysis to assess color change at RGB color samples.

MATERIALS and METHODS

The X-Rite Ci60 model colorimeter was used to determine the color of the primer (Figure 1). A white reflecting plate was used to calibrate an X-Rite Ci60 colorimeter.

Figure 1. Calibration plate and X-Rite Ci60 portable spectrometer.

The Ci6x line of portable spectrometers (Ci60, Ci62, Ci64, and Ci64UV) provide a quick and accurate way to determine the color at any point of the manufacturing process. The Ci6x Series allows us to manage color in a simple, portable, and cost-effective manner. It allows for all sizes of color measures due to the different alternatives of product family software. Repeatable performances are also possible with this robust measurement technology. As a result, the Ci6x series is a solid choice for a variety of agricultural tasks. Table 1 displays the spectrometer's technical parameters.

Table 1. Technical specifications of X-Rite Ci60 spectrometer (Anonymous, 2021).

Properties	Explanations
Measurement Geometrics	d/8°, DRS spectral engine, choice of optical aperture: 4 mm measurement area/6.5 mm target window 8 mm measurement area/14 mm target window 14 mm measurement area/20 mm target window
Receiver	Blue-enhanced silicon photodiodes
Light Source	Gas-filled tungsten lamp
Illuminant Type	A, C, D50, D55, D65, F2, F7, F11, and F12
Standard Observer	2° and 10°
Spectral Range	400nm – 700nm
Spectral Interval	10nm – measured, 10nm – output
Measurement Range	0 to 200% reflectance
Measuring Time	Approx. 2 seconds
Inter-Instrument Agreement (Ci60)	CIE L*a*b*: Avg. 0.40 ΔE*ab, based on avg. of 12 BCRA series II tiles (specular component included) Max. 0.60 ΔE*ab on any tile (specular component included)
Short-Term Repeatability (Ci60)	10 ΔE*ab on white ceramic (standard deviation)

RGB color plate webcam video was measured firstly with LabVIEW color measurement software to compare them with colorimeter measurements to get calibration factors. Measurements were done in the room light condition and it was 250 lux. The webcam was placed 25 cm far from the color plates for the measurements (Figure 2).

Figure 2. Webcam.

For graphical programming, LabVIEW software comprises two parts: a front panel and a block diagram. The front panel is an interactive software component that contains an interface area with several components and allows the user to insert data into the software (Figure 3).

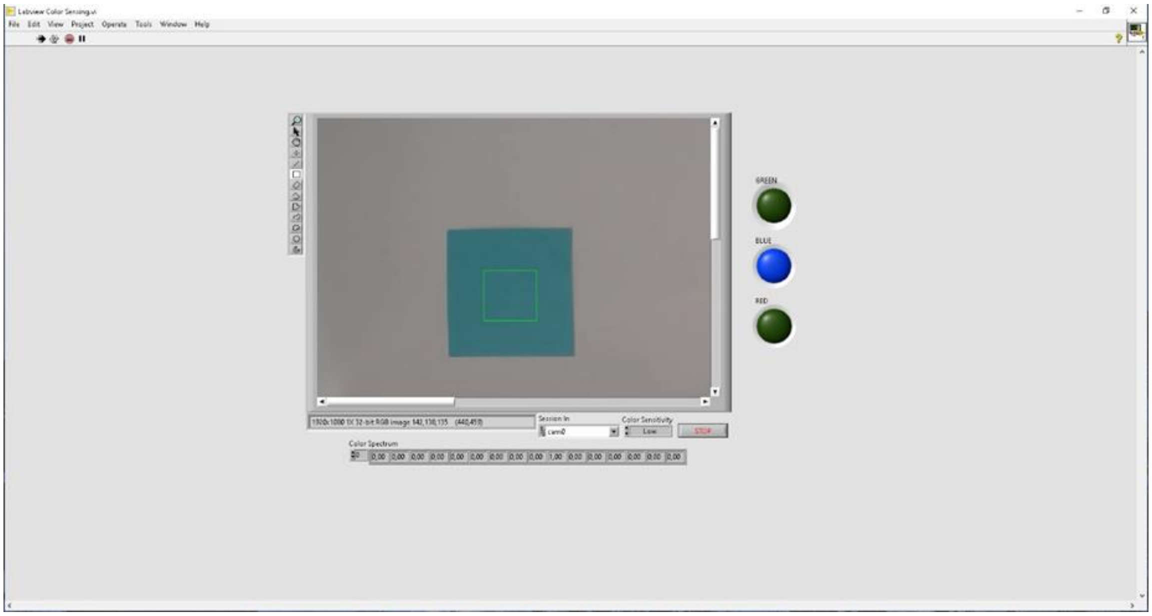

Figure 3. Color measurement application's front panel.

The actual programming procedure was carried out on the block diagram. The source codes run into this problem, which is caused by the use of virtual object linkages (Figure 4).

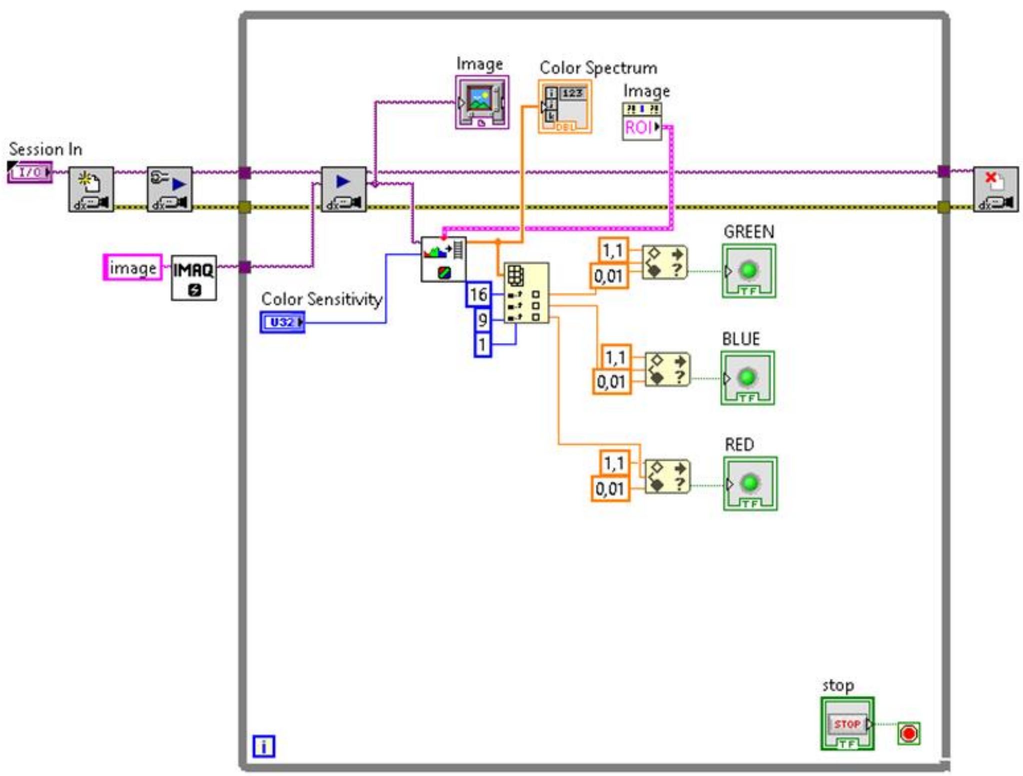

Figure 4. Application block diagram for color measurement.

In the block diagram of the color determination software, first, a session is opening with an image acquisition tool by this way video source is open for color sensitivity selection, after that color spectrum is determined by the software. In the end, colors are determined by the given ranges of the color spectrum.

RESULTS and DISCUSSION

According to test results, utilizing calibration factors, webcam-based LabVIEW software can deliver satisfactory accurate RGB data. As a result, a webcam can be used in agricultural and industrial applications. Table 2 displays the RGB color plate calibration factors. In the table, RRN, RGN, RBN values are red, green, blue values of red plate measured by using National Instruments LabVIEW software; RR, RG, RB values are red, green, blue values of red plate measured by using colorimeter; GRN, GGN, GBN values are red, green, blue values of green plate measured by using National Instruments LabVIEW software; GR, GG, GB values are red, green, blue values of green plate measured by using colorimeter; BRN, BGN, BBN values are red, green, blue values of plate measured by using National Instruments LabVIEW software; BR, BG, BB values are red, green, blue values of blue plate measured by using colorimeter.

Table 2. Calibration factors for the test materials.

	ɣR	**ɣG**	**ɣB**
Red plate	1,161232	0,519619	0,600362
Green plate	0,506287	1,025383	0,714016
Blue plate	0,432229	1,201444	1,413406

Red, green, and blue color plate measurements were taken at both devices to improve RGB color measuring efficiency (Figure 2).

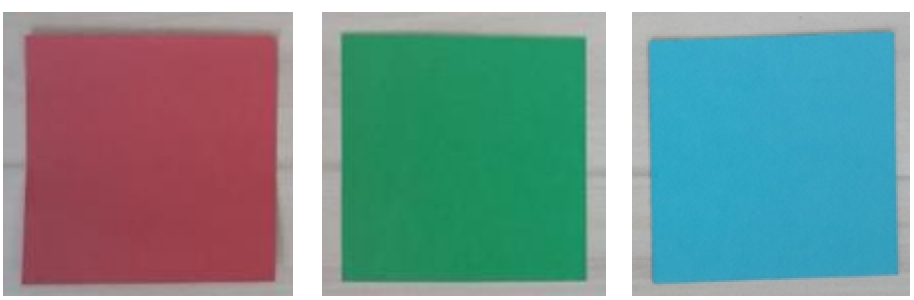

Figure 2. Plates in red, green, and blue color.

Table 3. Color measurements on red, green, and blue plates.

RRN	RGN	RBN	RR	RG	RB	GRN	GGN	GBN	GR	GG	GB	BRN	BGN	BBN	BR	BG	BB
160	72	81	161	68	81	68	138	94	59	138	93	59	149	180	62	159	183
160	72	80	161	68	81	68	136	92	72	139	97	56	154	175	52	156	181
159	71	80	159	71	83	69	138	94	72	139	96	56	155	178	61	160	184
160	71	80	161	72	84	69	138	95	60	139	94	57	157	182	62	159	183
158	70	79	161	72	84	69	138	95	62	141	96	58	160	185	60	159	183
163	69	79	160	72	83	68	136	94	70	138	95	57	156	182	60	159	183
160	70	80	160	71	83	67	135	93	72	139	97	56	155	180	63	160	183
158	70	79	160	71	83	68	136	94	67	135	93	56	155	180	59	159	183
158	70	79	160	71	83	68	136	95	70	136	94	56	154	175	60	159	183
158	70	80	160	71	83	68	136	94	68	136	93	57	155	181	60	159	183
159	70	79	160	71	83	68	136	95	70	137	94	56	155	181	61	160	184
158	70	80	160	70	82	69	138	96	68	135	93	56	157	181	62	160	184
159	71	80	161	72	83	69	138	95	70	137	94	56	157	180	61	160	184
159	70	79	161	72	84	68	136	94	67	135	92	57	157	182	53	156	181
161	71	79	160	69	82	68	136	95	70	137	94	57	157	181	52	156	181
163	71	80	160	71	83	70	139	98	68	135	93	59	162	185	52	156	181
160	71	80	160	72	83	69	138	96	70	136	94	60	166	189	51	156	181
164	72	80	160	71	83	68	136	95	69	137	95	61	166	191	52	156	181
164	73	80	160	71	83	68	136	94	72	138	96	61	167	191	53	156	181
164	73	80	160	71	83	71	139	96	73	140	97	60	166	189	52	156	181

There are a lot of applications for color analysis in the literature. For example, Yeni and Shaowei (2017) used LabVIEW and machine vision to develop a fault inspection system for the carbonized bamboo cane. According to the findings of the experiments, this system can classify five different types of bamboo canes with flaws at a speed of 70 mm s^{-1}, and the average recognition rate of defect bamboo canes can exceed 90.6%.

The creation of a flame detection system in LabVIEW is the focus of Riyadi and Aisyah's study. They imply that for the development of fire early warning systems, flame detection systems are useful. In general, traditional fire detection systems that rely on heat detectors to detect temperature changes are unable to detect the presence of fire. A camera acting as an image scanner sensor could be used to identify the shape or color of a flame. The goal of the research is to create an image processing flame detection system using image enhancement, color segmentation, and filtering techniques, all of which are implemented using LabVIEW's Vision Assistant. They stress that, the system runs at 30 frames per second with a resolution of 1024 x 768 pixels, with a 98 percent accuracy.

Rice clusters were separated at the rice harvest by Yu *et al.* (2021), who worked for high yield and grain quality. They created a system that utilized X-ray and RGB scanning as well as deep learning. They created a pipeline for analysis and came up with five distinct ways to count rice. As a result, good accuracy ($R^2 = 0.99$) and speed were achieved. The classification of indica and japonica yielded a 91 percent accuracy. It is worth noting that this is a positive outcome for rice breeding.

Given the literature results, the research findings appear to be more successful than those found in the literature.

CONCLUSION

It is required to meet the ever-increasing requirements of the agriculture business due to the development of color vision technology. As a result, imaging technology will see more use and popularity in the future years. After reviewing the literature and evaluating the results, we can conclude that a LabVIEW video processing-based color detection system is functional and may be used as part of a sorting machine for this purpose.

High quality and safety standards have begun to be sought as consumer expectations for agricultural products have risen. These product characteristics should be determined precisely, rapidly, and objectively. To achieve these objectives, the new vision offers an alternative to an automated, non-destructive, and cost-effective technique. Various image processing methods based on image analysis in the agriculture business have been developed in response to these requirements.

The image investigation in this study was conducted using a color detection system based on LabVIEW video processing. We can easily and inexpensively obtain data in the sector by utilizing computer vision frameworks. This article shows how these procedures, as well as further calibration, can help attain accuracy. On three color plates, the study is conducted for agricultural purposes. Automation of sorting applications for improving and classifying item quality is a significant advancement. This study shows how LabVIEW can be used in agriculture. This technique is adaptable and is being employed in a variety of agricultural products. More productive work can be done with the help of developed algorithms and efficient working methods. Snapshot analysis is based on picture analysis and is still in the early stages of development.

DECLARATION OF COMPETING INTEREST

The author would like to declare that there is no conflict of interest.

CREDIT AUTHORSHIP CONTRIBUTION STATEMENT

The author would like to declare that he solely developed all the sections in this manuscript.

REFERENCES

Anonymous (2021). Ci6X series spectrophotometer user manual. https://www.xrite.com/-/media/xrite/files/manuals_and_userguides/c/i/ci6x-500/ci6x-500_user_guide_en.pdf (29.08.2021)

Brosnan T and Wen Sun D (2004). Improving quality inspection of food products by computer vision-a review. *Journal of Food Engineering, 61: 3-16.*

Fouda T and Salah, S (2014). Using imaging analyses to predict chemical properties of orange fruits. Scientific Papers Series Management. *Economic Engineering in Agriculture and Rural Development, 14(3): 83-86.*

Leon K, Mery D and Leon J (2006). Colour measurment in L*a*b* units from RGB digital images. *Food Research International, 39: 1084-1091.*

Mahendran R and Jayashree GC and Alagusundaram K (2011). Application of computer vision technique on sorting and grading of fruits and vegetables. *Journal of Food Process Technology, S1-001.*

Mendoza F, Dejmek P and Aguilera JM (2006). Calibrated colour measurements of agricultural foods using image analysis. *Postharvest Biology and Technology*, *41: 285-295.*

Narendra VG and Hareesh KS (2010). Prospects of computer vision automated grading and sorting systems in agricultural and food products for quality evaluation. *International Journal of Computer Applications*, *(0975 – 8887), 1(4): 1-9.*

Pawar SS and Dale MP (2016). Lemon detection and sorting system based on computer vision. 3rd *International Conference on Electrical, Electronics, Engineering Trends, Communication, Optimization and Sciences (EEECOS) -2016, 376-379.*

Ratule MT, Osman A, Ahmad SH and Saari N (2006). Development of chilling injury of 'Berangan' banana (Musa cv. Berangan (AAA)) during storage at low temperature. *Journal of Food Agriculture & Environment, 4(1): 128-134.*

Riyadi DS and Aisyah S (2018). Vision based flame detection system for surveillance camera. In 2018 *International Conference on Applied Engineering (ICAE) (pp. 1-6). IEEE.*

Yu L, Shi J, Huang C, Duan L, Wu D, Fu D, Wu C, Xiong L, Yang W and Liu Q (2021). An integrated rice panicle phenotyping method based on X-ray and RGB scanning and deep learning. *The Crop Journal, 9(1): 42-56.*

Xing J, Bravo C, Moshou D, Roman H and Baerdemaeker JD (2006). Bruise detection on 'Golden Delicious' apples by vis/NIR spectroscopy. *Computers and Electronics in Agriculture, 52: 11-20.*

Yeni L and Shaowei Y (2017). Defect inspection system of carbonized bamboo cane based on LabView and Machine Vision. In 2017 *International Conference on Information, Communication and Engineering (ICICE) pp. 314-317. IEEE.*

Turkish Journal of Agricultural Engineering Research

https://dergipark.org.tr/en/pub/turkager
https://doi.org/10.46592/turkager.2021.v02i02.008

Turk J Agr Eng Res (TURKAGER)
e-ISSN: 2717-8420
2021, 2(2): 339-347

Research Article (Araştırma Makalesi)

Comparison of Yield and Yield Components of Different Anise (*Pimpinella anisum* L.) Populations Under Eskişehir Ecological Conditions

Nimet KATAR[a], Mustafa CAN[b]*, Duran KATAR[c]

[a] *İl Tarım ve Orman Müdürlüğü, Eskişehir, TÜRKİYE*

[b] *İl Tarım ve Orman Müdürlüğü, Uşak, TÜRKİYE*

[c] *Tarla Bitkileri Bölümü, Ziraat Fakültesi, Eskişehir Osmangazi Üniversitesi, Eskişehir, TÜRKİYE*

(*): Corresponding author, mustafican@gmail.com

ABSTRACT

In this study, it was aimed to reveal the effect of different genotypes (population) of anise (*Pimpinella anisum* L.) on yield and yield components. The experiment was carried out under Eskişehir ecological conditions in the growing season of 2017 and 2018. Four different anise population (Afyon, Bilecik, Çeşme and Burdur) obtained from different parts of Turkey was used in the study. Plant materials were cultivated in randomized complete block design with three replications. The results showed that the populations had a significant differences on other all parameters examined except 1000 seed weight (g). The highest seed yield (80.56 and 76.31 kg da^{-1}, respectively) and the highest essential oil yield (2.17 and 2.22 L da^{-1}, respectively) were obtained from Bilecik and Çeşme populations. On the other hand, the essential oil contents obtained from the populations varied between 2.67-2.92%, and it is seen that these values are above the 2% limit stated in the European pharmacopoeia. As a result, it was determined that Bilecik and Çeşme populations are superior populations among the populations examined in terms of high seed and essential oil yields.

RESEARCH ARTICLE

Received: 19.08.2021
Accepted: 24.10.2021

Keywords:
- *Pimpinella anisum*,
- Genotype,
- Yield,
- Essential oil content,
- Essential oil yield

To cite: Katar N, Can M, Katar D (2021). Comparison of Yield and Yield Components of Different Anise (*Pimpinella anisum* L.) Populations Under Eskişehir Ecological Conditions. Turkish Journal of Agricultural Engineering Research (TURKAGER), 2(2): 339-347. *https://doi.org/10.46592/turkager.2021.v02i02.008*

Eskişehir Ekolojik Koşullarında Farklı Anason (*Pimpinella anisum* L.) Populasyonlarının Verim ve Verim Öğelerinin Karşılaştırılması

ÖZET

Bu çalışmada, farklı genotiplerin (populasyon) anasonun (*Pimpinella anisum* L.*)* verim ve verim bileşenleri üzerindeki etkisini ortaya çıkarmak amaçlanmıştır. Deneme, Eskişehir ekolojik koşullarında 2017 ve 2018 yılları yetiştirme döneminde gerçekleştirilmiştir. Çalışmada Türkiye'nin farklı bölgelerinden temin edilen dört farklı anason populasyonu (Afyon, Bilecik, Çeşme ve Burdur) kullanılmıştır. Bitki materyalleri, tesadüf blokları deneme desenine göre üç tekerrürlü olarak yetiştirilmiştir. Sonuçlar, populasyonların 1000 tohum ağırlığı (g) hariç incelenen diğer tüm parametrelerde önemli farklılığa sahip olduğunu göstermiştir. Bilecik ve Çeşme populasyonlarından en yüksek tohum verimi (sırasıyla 80.56 ve 76.31 kg da^{-1}) ve en yüksek uçucu yağ verimi (sırasıyla 2.17 ve 2.22 L da^{-1}) elde edilmiştir. Diğer taraftan çalışmada elde edilen uçucu yağ oranı %2.67-2.92 arasında değişmiş, Avrupa farmakopesinde belirtilen % 2 sınırının üzerinde olduğu görülmüştür. Netice olarak; çalışmada yer alan populasyonlar arasında yüksek tohum ve uçucu yağ verimleri açısından Bilecik ve Çeşme populasyonlarının öne çıktığı belirlenmiştir.

ARAŞTIRMA MAKALESİ

Alınış tarihi: 19.08.2021
Kabul tarihi: 24.10.2021

Anahtar Kelimeler:

- *Pimpinella anisum*,
- Genotip,
- Verim,
- Uçucu yağ oranı,
- Uçucu yağ verimi

Alıntı için: Katar N, Can M, Katar D (2021). Eskişehir Ekolojik Koşullarında Farklı Anason *Pimpinella anisum* L.) Populasyonlarının Verim ve Verim Öğelerinin Karşılaştırılması. Turkish Journal of Agricultural Engineering Research (TURKAGER), 2(2): 339-347. https://doi.org/10.46592/turkager.2021.v02i02.008

GİRİŞ

Apiaceae familyası Dünya'da 300 cins ve yaklaşık 3000 türü ihtiva etmektedir. Bu familya içinde yer alan anason (*Pimpinella anisum*) bitkisi, Akdeniz havzasında ve Güney Batı Asya'da doğal yayılış gösteren tek yıllık aromatik bir bitkidir (Albulushi ve ark., 2014; Salim ve ark., 2016; Karac ve Efe, 2017). Yaklaşık 90 cm boyuna kadar büyüyen ve otsu bir bitki olan anason; şemsiye şeklinde, yaklaşık 3 mm çapında ve beyaz renkte çiçeklere sahip olup şizokarp meyveleri 3-5 mm uzunluğundadır (Albulushi ve ark., 2014; Hassan ve Elhassan, 2017). Ayrıca bitkinin meyveleri 1-3 mm genişlik ve 3-6 mm uzunlukta, kısa saplı, ters armut biçiminde, yeşilimsi-sarı veya gri-yeşil renkli olup üzeri tüylerle kaplıdır (Orav ve ark., 2008; Shojaii ve Abdollahi Fard, 2012). Son yıllarda yapılan birçok bilimsel çalışma, ilaç kaynağı olarak kullanılan birçok bitki türü olduğunu göstermiştir. Tıbbi amaçlı kullanılan önemli bitkilerden biri olan anason (*Pimpinella anisum* L.) bitkisinin özellikle meyveleri pek çok ülkenin halk hekimliğinde gaz giderici, mide koruyucu, aromatik ve dezenfektan olarak kullanılmıştır.

Bugüne kadar, anason tohumları üzerinde çok sayıda farklı bilimsel çalışma yapılmış, antimikrobiyal, antifungal, antiviral, antioksidan, kas gevşetici, ağrı kesici ve anti-spazmodik etkilerinin yanı sıra sindirim sistemi üzerinde farklı etkileri olduğu bildirilmiştir (Shojaii ve Abdollahi Fard, 2012; Salim ve ark., 2016). Günümüzde anason, eczane, parfümeri, gıda ve kozmetik endüstrilerinde kullanılan önemli bir hammaddedir (Albulushi ve ark., 2014). Ayrıca morfinizmi azaltıcı etkisinin yanı sıra kadınlarda adet ağrılarına ve menopozdaki kadınlarda yüksek ateşe karşı etkilidir. Şeker hastaları için, anason tohumları kandaki glikoz değerini ve lipid seviyesini düşürmekle birlikte aynı zamanda lipid peroksidasyonunu da azaltmaktadır (Shojaii ve Abdollahi Fard, 2012). Diğer taraftan anason, gıda endüstrisinde deniz ürünleri, dondurma, tatlılar ve sakız gibi farklı ürünlere lezzet ve aroma vermek için kullanılmaktadır (Salim ve ark., 2016).

Anason esansiyel yağı ve çayı aromaterapide nefes darlığını gidermek için kullanıldığı gibi doğal bir astım ilacı olarak da kullanılmaktadır. Ayrıca anason esansiyel yağı, bitler ve diğer böceklerin neden olduğu kaşıntı tedavisinde, baş ve vücut bitleri ile mücadelede etkili olmakla birlikte uçucu yağından elde edilen merhemlerin uyuz tedavisinde haricen kullanımı tavsiye edilmektedir (Albulushi ve ark., 2014). Anason tohumunun kalitesi, uçucu yağın oranı ve uçucu yağın bileşimi ile doğrudan ilgili olup, uçucu yağın bileşimi ise bitkinin genotipi ile yetiştirme yöntemine bağlı olarak önemli ölçüde değişmektedir (Albulushi ve ark., 2014).

Anason tohumunun, %9-13 nem, %18 protein, %8-23 yağ, %1.5-7.0 (ort. %2-3) uçucu yağ, %5 nişasta, %22-28 N-içermeyen özüt ve %12-25 ham lif ihtiva ettiği bildirilmiştir (Salim ve ark., 2016; Karac ve Efe, 2017). Avrupa farmakopesine göre ilaç olarak kullanılacak anason tohumlarının en az %2 uçucu yağ içermesi gerekmektedir (Albulushi ve ark., 2014). Anason tohumunun %1.5-7'sini oluşturan uçucu yağın en önemli bileşikleri trans-anethole, estragolle, γ-hymachalene, paraanisaldehyde ve methyl cavicol'dur (Shojaii ve Abdollahi Fard, 2012; Khalid, 2015; Hassan ve Elhassan, 2017). Bazı çalışmalar, anason uçucu yağının en önemli bileşiği olan trans-anetholün uçucu yağın %80-90'ını oluşturduğunu göstermiştir (Albulushi ve ark., 2014; Salim ve ark., 2016). Diğer taraftan yapılan farklı bir çalışmada ise anason uçucu yağının ana bileşeninin küminaldehit olarak belirlendiği rapor edilmiştir (Katar ve Katar, 2020).

Bitkilerin büyümesinde ve gelişmesinde etkili olan faktörler genellikle içsel ve dışsal faktörler olarak ikiye ayrılmaktadır. İçsel faktörler, bitkilerin genetik yapısı ile doğrudan ilgili olduğundan çeşitli kalıtsal özelliklere sahip bitkilerin büyüme ve gelişme performansları, genlerinin etkisine göre farklılık göstermektedir (Hussain ve ark., 2006). Tarımda daha yüksek verim ve kalite elde etmenin en önemli faktörlerinden biri, bölgeye adapte olmuş uygun genotip (tescilli çeşit/populasyon) seçimidir. Yerli bitki populasyonları genellikle bölgesel koşullara daha iyi uyum sağlamakla birlikte özellikle tescilli çeşit sayısı çok az olan ülkemiz tıbbi ve aromatik bitkilerin tarımında populasyonların tohumluk olarak kullanımı daha yaygındır. Nitekim yapılan bir araştırmada önemli tıbbi ve aromatik bitkilerden olan çörek otu tarımında çiftçilerin tescilli bir çeşit (Çameli) bulunmasına rağmen bu çeşidi sadece %1.37 oranında üretimde kullandığı, bir başka ifade ile %98.63 oranında çörek otu populasyonları tohumluğunu kullanarak üretim yaptığını ortaya koymuştur (Can, 2020). Bu nedenle çeşitli ekolojik koşullar altında bu popülasyon verim ve kalite potansiyelinin belirlenmesi gerekmektedir. Anason genotiplerinin verim, verim bileşenleri ve kalite karakterleri üzerindeki etkisi birçok araştırmacılar tarafından incelenmiştir (İpek ve ark., 2004; Nabizadeh ve ark., 2012; Faravani ve ark., 2013; Sönmez, 2018; Karık, 2020). Ancak bu çalışmaların her biri farklı ekolojik koşullar altında farklı anason genotipleri ile yapılmıştır.

Bu nedenle Eskişehir ekolojik koşullarında yürütülen bu çalışmada, farklı anason genotiplerinin (popülasyon) verim ve verim bileşenleri açısından performanslarının ortaya çıkarılması amaçlanmıştır.

MATERYAL ve YÖNTEM

Çalışma 2017 ve 2018 yıllarının ürün yetiştirme döneminde Eskişehir Osmangazi Üniversitesi Ziraat Fakültesi Tarla Bitkileri deneme tarlalarında gerçekleştirilmiştir. Denemede bitki materyali olarak Afyon, İzmir-Çeşme, Bilecik ve Burdur yörelerinde anason yetiştiriciliği yapan çiftçilerden temin edilen 4 farklı anason populasyonu kullanılmıştır. Çalışma alanı topraklarının özellikleri Çizelge 1'de verilmiştir. Buna göre toprağın tınlı tekstürde, hafif alkalin karakterde, orta kireçli, tuzluluk problemi olmayan, organik madde içeriğinin orta, faydalanılabilir fosfor oranının orta ve faydalanılabilir potasyum oranının yüksek olduğu belirlenmiştir.

Çizelge 1. Deneme alanı toprağının bazı fiziksel ve kimyasal özellikleri*.
Table 1. *Some physical and chemical characteristics of soils in experimental field.*

Tekstür	Toplam Kireç (%)	EC (ds m^{-1})	Faydalanılabilir P_2O_5 (kg da^{-1})	Faydalanılabilir K_2O (kg da^{-1})	pH	Organik Madde (%)
Tınlı (2017)	5.55	0.035	5.96	195.28	7.18	2.43
Tınlı (2018)	5.32	0.042	6.61	248.27	7.53	2.82

*Toprak analizleri Geçit Kuşağı Tarımsal Araştırma Enstitüsü Müdürlüğü Toprak-Su Laboratuvarında yapılmıştır.

Deneme alanının 2017, 2018 ve uzun dönem (1970-2011) ortalama sıcaklık ve toplam yağış verileri Çizelge 2'de sunulmuştur. 2017 (374.4 mm) ve 2018 (411.8 mm) yılları toplam yağış miktarı değerlerinin uzun dönem toplam yıllık yağış miktarı ortalamasından (338.8 mm) daha yüksek olduğu görülmüştür. Ayrıca, uzun dönemde gözlemlenen ortalama sıcaklık değerinin, hem 2017 hem de 2018 ortalama sıcaklık değerlerinden daha düşük olduğu görülmektedir. 2017 ve 2018'de ortalama sıcaklık sırasıyla 11.29°C ve 12.50°C olarak gerçekleşmiştir (Çizelge 2).

Çizelge 2. Deneme alanına ait bazı iklim verileri*.
Table 2. *Some climatic data of the experimental area.*

Aylar	Toplam yağış (mm)			Ortalama sıcaklık (°C)		
	2017	2018	UY	2017	2018	UY
Ocak	33.0	30.0	30.6	-2.0	1.4	-0.2
Şubat	9.2	28.8	26.1	1.9	5.6	0.9
Mart	16.2	49.8	27.6	7.6	8.9	4.9
Nisan	62.0	16.8	43.1	9.6	13.6	9.6
Mayıs	50.8	72.0	40.0	14.4	16.4	14.9
Haziran	44.8	60.6	23.7	19.1	19.3	19.1
Temmuz	13.4	42.0	13.1	23.1	21.9	22.1
Ağustos	31.4	19.3	9.2	22.0	22.7	21.8
Eylül	3.0	3.8	18.1	19.6	18.3	16.7
Ekim	46.6	30.1	32.8	10.8	13.0	11.7
Kasım	27.8	18.6	34.0	5.5	7.4	5.6
Aralık	36.2	40.0	40.5	3.9	1.7	1.7
Toplam	374.4	411.8	338.8	-	-	-
Ortalama	-	-	-	11.3	12.5	10.7

**Veriler Eskişehir Meteoroloji 3. Bölge Müdürlüğü'nden temin edilmiştir.* UY: Uzun Yıllar (1970-2011)

Tarla denemeleri tesadüf blokları deneme desenine göre 3 tekerrürlü olarak kurulmuştur. Tohumlar, dekara 2 kg hesabıyla, 2-3 cm derinliğe ve 20 cm sıra aralığında elle ekilmiştir. Ekim, birinci yıl 13 Nisan 2017 tarihinde, ikinci yıl 20 Nisan 2018 tarihinde gerçekleştirilmiştir. Her deneme parselinin uzunluğu 5 m olup 6 sıradan oluşmaktadır. Yabancı ot kontrolü gerektiğinde elle yapılmış, sulama uygulanmamıştır. Deneme parselleri, saf olarak dekara 5 kg N ve 4 kg P_2O_5 olacak şekilde gübrelenmiştir. 7 Temmuz 2017 ve 10 Temmuz 2018 tarihlerinde parsellerin her iki tarafından bir sıra kenar tesiri olarak bırakılmış ve ardından parsellerdeki bitkiler elle hasat edilmiştir. Uçucu yağ oranları su distilasyonu yöntemiyle belirlenmiştir. Uçucu yağların distilasyonu için 100 g tohum örnekleri 2000 ml'lik balonlara yerleştirildikten sonra 1 litre saf su eklenerek 3 saat boyunca distilasyon işlemi gerçekleştirilmiştir. Distilasyon işlemi tamamlandıktan sonra clevenger aparatının dereceli kısmından yağ miktarı okunarak % olarak belirlenmiştir (Anonim, 2010).

Çalışmadan elde edilen veriler SPSS paket programı kullanılarak tesadüf blokları deneme desenine göre varyans analizine tabi tutulmuş, incelenen özelliklerin önemlilik düzeyleri belirlenmiştir. Önemli çıkan ortalama değerler arasındaki farklar Tukey testi ($p \leq 0.05$) ile karşılaştırılmıştır.

BULGULAR ve TARTIŞMA

Çalışmada yer alan anason populasyonları, yıllar ve yıl x populasyon interaksiyonu bitki boyunda önemli ($p \leq 0.01$) farklılığa sebep olmuştur. Genotipler karşılaştırıldığında yıllar ortalamasında en yüksek bitki boyu Afyon (49.30 cm) ve Çeşme (48.23 cm) populasyonlarında belirlenirken, en düşük bitki boyu Burdur (43.14 cm) ve Bilecik (44.56 cm) populasyonlarında belirlenmiştir. 2017 yılında elde edilen ortalama bitki boyu değeri (45.85 cm) ile karşılaştırıldığında 2018 yılında daha yüksek bitki boyu değeri (46.77 cm) elde edilmiştir (Çizelge 3). Bu durum, yıllık toplam yağış değeri ile bitkinin ilk gelişim gösterdiği aylardaki (Nisan-Mayıs) ortalama sıcaklık değerlerinin 2018 yılında bir önceki yıla göre daha yüksek olmasından kaynaklandığı düşünülmektedir (Çizelge 2). Bitki boyu her ne kadar çevresel faktörlerden ve agronomik uygulamalardan etkilense de esas olarak bitki materyalinin genetik yapısı tarafından kontrol edilmektedir (Baloch ve ark., 2010). Bitki boyu değerleri yıl x populasyon interaksiyonu açısından incelendiğinde, 2017 yılında bitki boyu maksimum Afyon (48.80 cm), minimum Bilecik (42.79 cm) populasyonlarında, 2018 yılında ise bitki boyu maksimum Çeşme (49.90 cm), minimum Burdur (41.03 cm) populasyonlarında kaydedilmiştir. İpek ve ark. (2004) anasonda bitki boyunu 44.7-50.2 cm arasında, Yıldırım (2010), ise 33.73-39.73 cm arasında bulmuşlardır. Çalışmalarda elde edilen bitki boyu değerleri arasındaki farklılık, kullanılan bitki materyallerinin genetik yapısındaki değişim ve çalışma bölgelerinin farklı ekolojik koşulları ile açıklanabilir.

Yıllar ve populasyonlar bitki başına şemsiyeli dal sayısı üzerine $p \leq 0.01$ düzeyinde önemli bir farklılık göstermiştir. 2018 yılında (4.99 adet) 2017 yılına (3.78 adet) kıyasla daha yüksek bir bitki başına şemsiyeli dal sayısı değeri belirlenmiştir. Denemenin ikinci yılı (2018) toplam yağış ve ortalama sıcaklık değerlerinin ilk yıla (2017) kıyasla yüksek gerçekleşmesi bitkinin daha iyi gelişimini ve dallanmasını netice vermiş, bitki başına şemsiyeli dal sayısı daha fazla olmuştur. İki yıllık ortalama olarak bitki başına şemsiyeli dal sayısı 3.89-5.21 adet arasında değişmiş ve en yüksek değer Bilecik populasyonunda tespit edilmiştir (Çizelge 3). Benzer olarak Katar ve Katar (2020) anasonda bitki başına şemsiyeli dal sayısını 3.09-6.50 adet arasında bulmuşlardır.

Bin tohum ağırlığı açısından sadece yıllar arasında önemli bir fark bulunmuştur. Populasyonların ortalaması olarak 1000 tane ağırlığı 2017'de 3.46 g, 2018'de 4.29 g olarak kaydedilmiştir (Çizelge 3). Çalışmadan elde edilen 1000 tohum ağırlığı değerleri, incelenen anason populasyonlarının bu parametre üzerinde önemli bir etkisi olmadığını göstermiştir. Bununla birlikte, en yüksek bin tohum ağırlığı 2017 yılında Burdur (3.17 g) popülasyonundan, en düşük bin tohum ağırlığı ise 2018 yılında Çeşme (4.36 g) popülasyonundan alınmıştır. Yıllar ortalamasında ise Bilecik ve Burdur Afyon popülasyonlarından en düşük (3.77 g) ve Çeşme popülasyonundan en yüksek (4.02 g) değerler ölçülmüştür. Yapılan birçok araştırmada anasonda bin tohum ağırlığının 2.64-5.62 g arasında elde edildiği rapor edilmiştir (İpek ve ark., 2004; Faravani ve ark., 2013; Sönmez, 2018; Katar ve Katar, 2020).

Yılların ve populasyonların tohum verimi (kg da^{-1}) üzerindeki etkisi önemli olmuştur. Ortalama tohum verimi 2017'de 65.02 kg da^{-1} iken 2018'de 70.27 kg da^{-1} olarak belirlenmiştir. İki yıllık ortalamaya göre tohum verimi 56.66 ile 80.56 kg da^{-1} arasında değişmiş, en yüksek değer Bilecik populasyonunda tespit edilmiştir. Ancak tohum verimi açısından Bilecik (80.56 kg da^{-1}) ve Çeşme (76.31 kg da^{-1}) populasyonları arasında istatistiksel olarak anlamlı bir fark bulunmamıştır (Çizelge 3). Nabizadeh ve ark. (2012), anasonda tohum verimini 17.91-128.64 kg da^{-1} arasında, Faravani ve ark. (2013) ise 37.08-40.36 kg da^{-1} arasında aldıklarını rapor etmişlerdir. Bulgularımıza benzer sonuçlar sırasıyla 42.20-87.00 kg da^{-1} ve 62.16-86.20 kg da^{-1} olmak üzere İpek ve ark. (2004) ile Sönmez (2018) tarafından da elde edilmiştir.

Aromatik bitkilerden olan anason bitkisinin en önemli kalite kriterlerinden biri hiç şüphesiz uçucu yağ oranıdır. İki yıllık ortalamaya göre uçucu yağ oranı değerleri %2.67-2.92 arasında değişmiş olup, en yüksek değer Çeşme populasyonunda elde edilirken, bu populasyonu Burdur ve Bilecik populasyonları takip etmiştir. Her üç populasyon istatistiki olarak aynı grupta yer almıştır. 2017 ve 2018 yıllarında uçucu yağ oranları ise sırasıyla %2.68 ve %2.88 olarak belirlenmiştir (Çizelge 3). Bu çalışmada elde edilen tüm uçucu yağ oranı değerlerinin Avrupa farmakopesinde belirtilen eşik değerin (%2) üzerinde olduğu tespit edilmiştir. Aydın ekolojik koşullarında 4 anason genotipi (Gölhisar, Fethiye, Denizli ve Çeşme) ile yürütülen çalışmada uçucu yağ oranının %1.47-1.60 arasında bulunduğu rapor edilmiştir (Doğramacı ve Arabacı, 2015). Diğer taraftan Sönmez (2018), tarafından İzmir koşullarında Türkiye, İspanya ve Suriye orijinli anason genotiplerinin uçucu yağ oranının sırasıyla %2.95, %3.06 ve %2.84 olarak elde edildiği belirtilmiştir. Tıbbi ve aromatik bitkilerde uçucu yağ oranı ve veriminin bitkinin genotipine, bitkinin yaşına, yetiştirme lokasyonuna, hasat zamanlarına, gübreleme, sulama, kurutma, depolama ve damıtma işlemlerine bağlı olarak değiştiği bildirilmiştir (Mammadov, 2014; Sourestani ve ark., 2014; Kotyuk, 2015; Sönmez ve Bayram, 2017; Katar ve ark., 2020; Can ve Katar, 2020).

Yılların ve anason populasyonlarının uçucu yağ verimi üzerinde önemli etkileri (sırasıyla $p \leq 0.05$ ve $p \leq 0.01$) olmuştur. 2018 yılında elde edilen uçucu yağ verimi değeri (2.03 L da^{-1}) 2017 verilerinden (1.74 L da^{-1}) daha yüksek olmuştur. Tohum verimi ve uçucu yağ oranı değerlerinin ikinci yıl (2018) fazla olması, bu yılın uçucu yağ veriminin de yüksek çıkmasını netice vermiştir. İki yıllık ortalamaya göre populasyonların uçucu yağ verimi 1.52 ile 2.22 L da^{-1} arasında değişiklik göstermiş, en yüksek değer Bilecik populasyonu ile aynı istatistiki grupta yer alan Çeşme populasyonunda belirlenmiştir (Çizelge 3).

Çizelge 3. Farklı anason populasyonlarının verim ve verim komponentleri.
Table 3. *Yield and yield components of different anise populations.*

Populasyon	Bitki boyu (cm)			Semsiveli dal savısı (adet bitki^{-1})		
	2017	2018	Ortalama	2017	2018	Ortalama
Afyon	48.80 a	49.80 a	49.30 a	3.09 c	4.68 b	3.89 c
Çeşme	46.55 b	49.90 a	48.23 a	3.96 b	4.98 ab	4.47 b
Bilecik	42.79 d	46.33 a	44.56 b	4.67 a	5.74 a	5.21 a
Burdur	45.24 c	41.03 b	43.14 b	3.40 bc	4.57 b	3.99 c
Ortalama	45.85 B	46.77 A	46.31	3.78 B	4.99 A	4.39
Yıl (Y)	-	-	**	-	-	**
Populasyon (P)	**	**	**	**	*	**
Y x P	-	-	**	-	-	öd
VK (%)	5.03	8.46	6.91	17.53	11.26	19.66
Populasyon	**Bin tohum ağırlığı (gr)**			**Tohum verimi (kg da^{-1})**		
	2017	**2018**	**Ortalama**	**2017**	**2018**	**Ortalama**
Afyon	3.60	4.31	3.96	54.16 b	59.16 b	56.66 b
Çeşme	3.61	4.43	4.02	73.81 a	78.81 a	76.31 a
Bilecik	3.47	4.07	3.77	79.06 a	82.06 a	80.56 a
Burdur	3.17	4.36	3.77	53.03 b	61.03 b	57.03 b
Ortalama	3.46 B	4.29 A	3.88	65.02 B	70.27 A	67.64
Yıl (Y)	-	-	*	-	-	*
Populasyon (P)	öd	öd	öd	**	**	**
Y x P	-	-	öd	-	-	öd
VK (%)	11.11	8.04	14.28	19.99	16.68	18.33
Populasyon	**Uçucu Yağ Oranı (%)**			**Uçucu Yağ Verimi (L da^{-1})**		
	2017	**2018**	**Ortalama**	**2017**	**2018**	**Ortalama**
Afyon	2.57 ab	2.77	2.67 b	1.40 b	1.64 b	1.52 b
Çeşme	2.87 a	2.96	2.92 a	2.10 a	2.33 a	2.22 a
Bilecik	2.48 b	2.90	2.69 ab	1.96 a	2.38 a	2.17 a
Burdur	2.81 ab	2.90	2.86 ab	1.49 b	1.77 b	1.63 b
Ortalama	2.68	2.88	2.78	1.74 B	2.03 A	1.88
Yıl (Y)	-	-	öd	-	-	*
Populasyon (P)	*	öd	*	**	**	**
Y x P	-	-	öd	-	-	öd
VK (%)	7.64	5.48	7.41	19.49	18.56	20.23

*:p≤0.05; **:p≤0.01; öd: önemli değil. VK: Varyasyon katsayısı

Uçucu yağ verimine ilişkin bulgularımız Faravani ve ark. (2013) ile Doğan (2018)'ın değerlerinden (sırasıyla 0.68-2.01 ve 0.46-1.15 L da^{-1}) yüksek, Sönmez (2018)'in değerlerinden (1.67-2.93 L da^{-1}) düşük olmuştur.

Sonuçlar, bitki boyu (cm), bitki başına şemsiyeli dal sayısı, 1000 tohum ağırlığı (g), tohum verimi (kg da^{-1}) ve uçucu yağ verimi (L da^{-1}) üzerine yılların etkisinin önemli olduğunu göstermiştir. Bu durum, yağış, sıcaklık gibi gibi iklim faktörlerinin yıldan yıla değişmesi ile açıklanabilir. Nitekim değişen iklim koşulları bitki büyümesi ve gelişmesinde dolayısıyla ürünün verimi ve kalitesinde etkili olmaktadır (Turhan, 2006; Bieńkowski ve ark., 2016). Ayrıca populasyonların 1000 tohum ağırlığı (g) hariç incelenen diğer tüm parametreler üzerinde önemli etkiye sahip olduğu belirlenmiştir. Bu ise kullanılan materyalin genetik farklılığı ile izah edilebilir. Tıbbi ve aromatik bitkilerin verim ve kalitesi üzerine ekolojik koşullardan ziyade bitkinin genetik yapısının etkili olduğu bildirilmiştir (Mammadov, 2014). Özellikle varyasyon katsayıları (VK) incelendiğinde çalışmada yer alan anason populasyonları arasında en fazla değişim aralığının uçucu yağ veriminde (%20.23) olduğu gözlemlenmiştir. Diğer taraftan populasyonlar arasında bitki boyu ile uçucu yağ oranı değerleri bakımından düşük varyasyon katsayıları (VK) dikkate alındığında daha az değişim olduğu belirlenmiştir (Çizelge 3).

SONUÇ

Bu araştırmanın sonucuna göre; iki yılın ortalama değerleri incelendiğinde, tohum verimi ile uçucu yağ verimi en yüksek Bilecik ve Çeşme populasyonlarında tespit edilmiş olup her iki populasyon arasında istatistiki olarak önemli bir fark görülmemiştir. Bilecik ve Çeşme populasyonlarına kıyasla daha az tohum ve uçucu yağ verimi elde edilen Afyon ve Burdur populasyonları arasında da istatistiki açıdan önemli bir fark bulunmamıştır. Netice olarak; çalışmada yer alan populasyonlar arasında yüksek tohum ve uçucu yağ verimleri açısından Bilecik ve Çeşme populasyonlarının öne çıktığı belirlenmiştir.

ÇIKAR ÇATIŞMASI

Yazarlar herhangi bir çıkar çatışması olmadığını beyan ederler.

YAZAR KATKISI

Yazarlar olarak makaleye aşağıdaki katkıların sunulduğunu beyan ederiz.
Nimet Katar: Arazi ve laboratuvar çalışmaları, istatistik analizi, makalenin yazılması.
Mustafa Can: Arazi ve laboratuvar çalışmaları, istatistik analizi, makalenin yazılması.
Duran Katar: Arazi ve laboratuvar çalışmaları, istatistik analizi, makalenin yazılması.

KAYNAKLAR

Albulushi SMA, Al Saidi H, Amaresh N and Mullaicharam AR (2014). Study of physicochemical properties, antibacterial and gc-ms analysis of essential oil of the aniseed (*Pimpinella anisum* Linn.) in Oman. *Research and Reviews: Journal of Pharmacognosy and Phytochemistry, 2(4): 24-33.*

Anonim (2010). European pharmacopoeia (E.P.) 7th ed. European Directorate for the Quality of Medicines& Health Care (EDQM): *Strasbourg*, France, p.1231.

Baloch MS, Shah ITH, Nadim MA, Khan MI and Khakwani AA (2010). Effect of seeding density and planting time on growth and yield attributes of wheat. *The Journal of Animal & Plant Sciences, 20(4): 239-240.*

Bienkowski T, Zuk-Golaszewska K, Kurowski T and Golaszewski J (2016). Agrotechnical indicators for *Trigonella foenum-Gracum* L. production in the environmental conditions of Northeastern Europe. *Turkish Journal of Field Crops, 21(1): 16-28.*

Can M ve Katar D (2020). Yapraktan uygulanan farklı organik gübrelerin *Mentha x piperita* L. ve *Mentha spicata* L. türlerinin tarımsal ve kalite özelliklerine etkisi. *Anadolu Tarım Bilimleri Dergisi, 35(3): 361-373.*

Can M (2020). Çörek otu tarımında üretici davranışlarının belirlenmesi, sorunlar ve çözümler: Uşak ili örneği. *Ziraat Mühendisliği, 370: 18-33.*

Doğan Ö (2018). *Anason populasyonlarında verim ve kalite ile genetik ilişkilerin araştırılması*. Yüksek Lisans Tezi, Süleyman Demirel Üniversitesi, Fen Bilimleri Enstitüsü, Tarımsal Biyoteknoloji Ana Bilim Dalı, s. 47, Isparta.

Doğramacı S ve Arabacı O (2015). Anason (*Pimpinella anisum* L.) çeşit ve ekotiplerinin bazı teknolojik özellikleri üzerine organik ve inorganık gübre uygulamalarının etkisi. *Adnan Menderes Üniversitesi Ziraat Fakültesi Dergisi, 12(1): 41-47.*

Faravani M, Salari B, Heidari M, Kashki TM and Gholami BA (2013). Effects of fertilizer and plant density on yield and quality of anise (*Pimpinella anisum* L.). *Journal of Agricultural Sciences, 58(3): 209-215.*

Hassan OM and Elhassan IA (2017). Characterization of essential oils from fruits of umbelliferous crop cultivated in Sudan I. *Pimpinella anisum* L (Anise) and *Anethum graveolens* L. (Dill). *Journal of Pharmacognosy and Phytochemistry*, *6(1): 109-112*.

Haşimi N, Tolan V, Kizil S ve Kilinc E (2014). Anason (*Pimpinella anisum* L.) ve kimyon (*Cuminum cyminum* L.) tohumlarının uçucu yağ kompozisyonu ile antimikrobiyal ve antioksidan özelliklerinin belirlenmesi. *Tarım Bilimleri Dergisi, 20: 19-26*.

Hussain A, Anjum F, Rab A and Sajid M (2006). Effects of nitrogen on the growth and yield of asparagus (*Asparagus officinalis*). *Journal of Agricultural and Biological Science*, *2: 41-47*.

İpek A, Demirayak S, Gürbüz B and Tarihi G (2004). A study on the adaption of some anise (*Pimpinella anisum* L.) population to Ankara conditions. *Tarım Bilimleri Dergisi*, *10(2): 202-205*.

Karaç T ve Efe L (2017). *Anason (Pimpinella anisum* L.*) bitkisinin farmakolojik özellikleri ve tedavi amaçlı kullanımı*. 12. Tarla Bitkileri Kongresi, Kahramanmaraş Sütçü İmam Üniversitesi, Kahramanmaraş.

Karık Ü (2020). Türkiye anason (*Pimpinella anisum* L.) genetik kaynakları ve yabancı anason genotiplerinin uçucu yağ bileşenleri. *Anadolu Ege Tarımsal Araştırma Enstitüsü Dergisi*, *2: 163-178*.

Katar D, Can M ve Katar N (2020). Farklı lokasyonların lavandin (*Lavandula × intermedia* Emeric ex Loisel.)'de uçucu yağ oranı ve kimyasal kompozisyonu üzerine etkisi. *Uluslararası Tarım ve Yaban Hayatı Bilimleri Dergisi*, *6(3): 546-553*.

Katar N and Katar D (2020). Effect of different row spaces on yield and quality of anise (*Pimpinella anisum*) under Eskisehir ecological conditions. *Biyolojik Çeşitlilik ve Koruma*, *13(3): 314-321*.

Khalid AK (2015). Quality and quantity of *Pimpinella anisum* L. essential oil treated with macro and micronutrients under desert conditions. *International Food Research Journal*, *22(6): 2396-2402*.

Kotyuk L (2015). Hyssop composition depending on age and plants development phases. *Biotechnologia Acta*, *8: 55-63*.

Mammadov R (2014). Tohumlu bitkilerde sekonder metabolitler. *Nobel Akademik Yayıncılık*, Yayın No: 841, Ankara.

Nabizadeh E, Salari B and Hosainpour M (2012). The effect of fertilizers and biological nitrogen and planting density on yield quality and quantity *Pimpinella anisum* L. *European Journal of Experimental Biology*, *2(4): 1326-1336*.

Orav A, Raal A and Arak E (2008). Essential oil composition of *Pimpinella anisum* L. fruits from various European countries. *Natural Product Research*, *22(3): 227-232*.

Salim EA, Yagi S and Elyass HMM (2016). Histology, phytochemistry and bacterial activity of anise (*Pimpinella anisum* L.) seed and essential oil. *Journal of Bacteriology & Mycology Open Access*, *3(4): 1-6*.

Shojaii A and Abdollahi Fard M (2012). Review of pharmacological properties and chemical constituents of *Pimpinella anisum*. *ISRN Pharmaceutics*, *1-8*.

Sourestani MM, Malekzadeh M and Tava A (2014). Influence of drying, storage and distillation times on essential oil yield and composition of anise hyssop [Agastache foeniculum (Pursh.) Kuntze]. *Journal of Essential Oil Research*, *26(3): 177-184*.

Sönmez Ç and Bayram E (2017). The influence of different water and nitrogen applications on some yield parameters and antioxidant activity in sage (*Salvia officinalis* L.) *Turkish Journal of Field Crops*, *22(1): 96-103*.

Sönmez Ç (2018). Effect of phosphorus fertilizer on some yield components and quality of different anise (*Pimpinella anisum* L.) populations. *Turkish Journal of Field Crops*, *23(2): 100-106*.

Turhan H (2006). Lemon balm. In K.V. Peter (eds.) *Handbook of herbs and spices* (Chapter 23, pp.390-399). Cambridge, England: *Woodhead Publishing*.

Yıldırım V (2010). *Türk anason genotiplerinin (Pimpinella anisum* L.*) Tekirdağ koşullarında tohum verimi ve bazı bitkisel özellikleri üzerinde bir çalışma.* Yüksek Lisans Tezi, Namık Kemal Üniversitesi, Fen Bilimleri Enstitüsü, Tarla Bitkileri Ana Bilim Dalı, 47s, Tekirdağ.

Turkish Journal of Agricultural Engineering Research

https://dergipark.org.tr/en/pub/turkager
https://doi.org/10.46592/turkager.2021.v02i02.009

Turk J Agr Eng Res (TURKAGER)
ISSN: 2717-8420
2021, 2(2), 348-362

Research Article

Development and Performance Evaluation of a Solar Powered Lawn Mower

Babatunde Oluwamayokun SOYOYE* ID

Department of Agricultural and Environmental Engineering, School of Engineering and Engineering Technology, Federal University of Technology Akure, Ondo State, NIGERIA

(*): Corresponding author, bosoyoye@futa.edu.ng

ABSTRACT

The continuous increase in the cost of fuel and the effect of emission of gases from burned fuel into the atmosphere when operating engine powered lawn mower has necessitated the use of the abundant solar energy from the sun as a power source of a lawn mower. A solar powered lawn mower was designed, fabricated and assembled on the basis of the general principle of mowing. The components of the lawn mower are; direct current (DC) motor, rechargeable battery, solar panel, galvanized steel blade of various thicknesses and shapes, and a speed controller. The required torque needed to drive the galvanized steel blade was achieved through the DC motor. The speed of the DC motor was controlled by the speed controller with the resistance in the circuit and allowed the motor to drive the blade at varied speeds. The battery recharged through the solar charging circuit, which comprises of a solar panel and charge controller. Performance evaluation was conducted on the developed mower with various thicknesses (1 mm, 1.5 mm and 2 mm) and shapes of the cutting blade (two, three and four blades). It was found that the cutting efficiency of the mower ranges from 70.50% - 84.10%, also the cutting capacity ranges from 0.05 ha h^{-1} - 0.27 ha h^{-1}, the uncut area was also found to range from 15.90% - 29.50%.

RESEARCH ARTICLE

Received: 30.09.2021
Accepted: 04.11.2021

Keywords:

- Lawn mower,
- Solar panel,
- Environmental pollution,
- Cutting efficiency,
- Cutting capacity

To cite: Soyoye BO (2021). Development and Performance Evaluation of a Solar Powered Lawn Mower. Turkish Journal of Agricultural Engineering Research (TURKAGER), 2(2), 348-362. *https://doi.org/10.46592/turkager.2021.v02i02.009*

INTRODUCTION

The previous technology of grass cutting was manually operated using hand tools like pruning shreds, scissors etc., these tools weren't efficient because they require more human effort and time. With the incorporation of lawn mowers into grass cutting, human effort and time was being saved (Prasanthi and Balaiah, 2017). Lawn mowers are classified based on different criteria and according to the axis of rotation of blades; reel lawn mowers (that which axis is horizontal) and rotary lawn mowers (that which axis is vertical).

The reel mower is made of a cylindrical blade, it achieves a clean cut by scissors action. Rotary mowers are often powered by gasoline or electricity (Dutta *et al*., 2016).

The sun supply viable amount of energy used for several purposes on earth. Every minute the sun radiates about 5.68x1018 calories of energy and the earth intercept only 2.55x1018 calories (NRF, 2010). This represents only 2000 millionth of the total solar energy is sent into space. The total solar energy is estimated to be 30000 times greater than the total annual energy of the world (Mgbemu, 2005). The solar powered lawn mower works on the same principle as other lawn mowers; the only difference is the energy source. It uses the photovoltaic panel to generate the energy needed to power the mower (Tanimola *et al*., 2014). In recent times, the environment has become one of the paramount global concern, especially with the surge of pollution, the depletion of natural resources and environmental degradation. As a result of this, lot of researches are ongoing to find alternative solutions that encourage environmental preservation (Fernandez and Krishnasamy, 2018). Due to the present revolution in green energy, industries are starting to change their perspective about power utilization. They now tend to lean toward the usage of green energy i.e., renewable energy which reduces effort, cost and pollution (Fernandez and Krishnasamy, 2018). A solar powered lawn mower is a lawn mower that uses solar energy as its source of power. It uses the electricity gotten from the solar energy to power the electric motor which in turn drives the blade that mows the lawn (Satwik *et al*., 2015). Solar lawn mower is a manually operated grass cutting vehicle powered by solar energy. The electric current is derived from the solar panel powers the electric motor, which then drives the blades Tanimola *et al.* (2014). The only difference between it and gas-powered lawn mowers is the application of different power sources. Satwik *et al.* (2015) researched on design and fabrication of lever operated solar lawn mower and contact stress analysis of spur gears. They worked on the adjustment of the mower's rotor blades heights with the aid of a spur gear displacement mechanism and a lever to achieve efficient cutting of grasses of different heights. The mechanism involves a pair of spur gears of different face width and the lever, which is used to adjust the rotor height in a way that the smaller spur gear slides against the face width of the larger spur gear. An Arduino board was incorporated to control the speed of the motor manually, also an ultrasonic sensor is placed in front of the machine which sends signal to the board before collision with an obstacle. A Buzzer receives a signal from the board and produces an alarm that prevents the collision. Dalal *et al.* (2016) researched on manufacturing of solar grass cutter which consists basically of direct current (D.C) motor, a rechargeable battery, solar panel, a stainless-steel blade and control switch. It was reported that solar panels were mounted in such a way that it can receive solar radiation with high intensity easily from the sun. These arranged solar panels converted solar energy into electrical energy. This electrical energy was stored in batteries through the solar charger. The motor was connected to the batteries through two mechanical circuit breaker switches, which aided the ON and OFF of the motor. The rotary power from the motor was transmitted to the blade, which resulted in the cutting of grasses. Igbokwe *et al.* (2019) worked on the development of a solar powered lawn mower which is made of a twin solar panel of 75A/130W capacity each. The purpose of this research work is to design, fabricate, assemble and evaluate a solar powered lawn mower using Design Expert software and MS Excel.

MATERIALS and METHODS

Machine Conception

The components of the solar lawn mower include; the machine frame, electric motor, solar panel, steel blades, connecting wires, tyres, battery, charging circuit and machine handle. The machine frame holds every other component of the machine together. The solar panel charges the battery while the battery powers the electric motor, which in turn rotates the attached blades at a high speed using the control switch. The machine has a handle which is used to maneuver it in the direction the handler intends it to go, with the help of the rotary wheels (Figure 1).

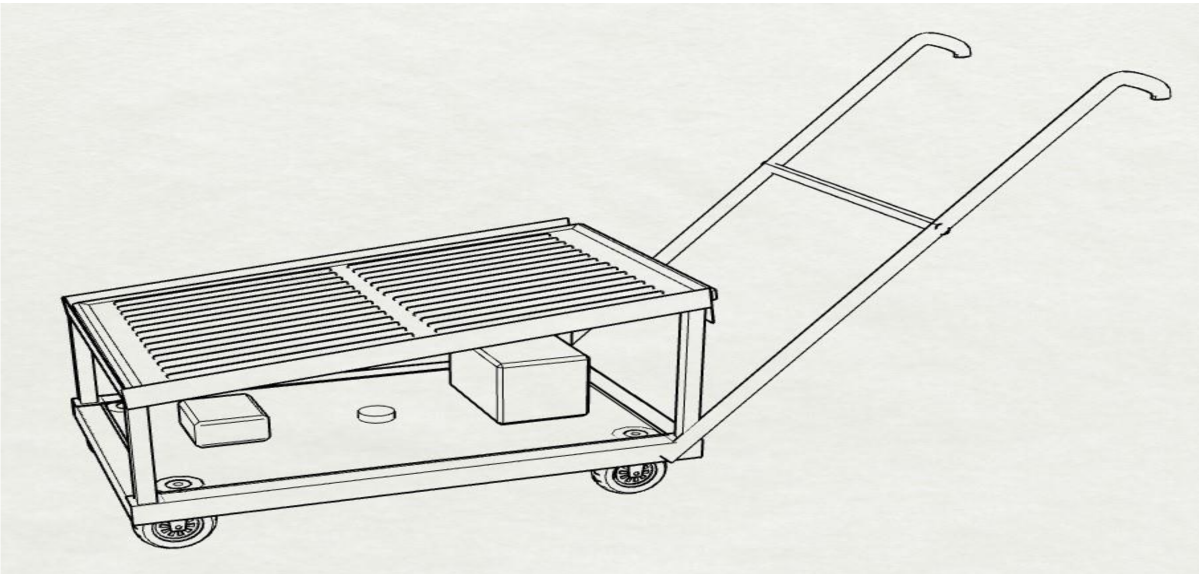

Figure 1. 3D Front view of the machine concept.

Design Analysis

The necessary components needed for the fabrication of the machine was designed following the standard design procedure used by Igbokwe *et al.* (2019).

Power selection

Mower blades are the cutting components of lawn mowers. They are usually made of sturdy metals as they must be able to withstand high-speed contact with various objects in addition to grass. The materials used (as well as size, thickness, and design of the blades) vary by manufacturer. Galvanized steel was selected with a density of 7922 kg m^{-3} in accordance with what was used by Igbokwe *et al* (2019). The shearing force of most annual and perennial grasses found on most lawns is usually between 9.20 N and 11.51 N, however, it depends on the height of the grass, type of grass as well as grass density in the area. The calculations (a to j) were done in accordance to Igbokwe *et al* (2019).

a) $Area\ of\ blade = Length \times Breadth = 300\ mm \times 50\ mm = 15000\ mm^2$

b) $Volume\ of\ blade = Area \times Thickness = 15000\ mm^2 \times 2\ mm = 30000\ mm^3$

c) $Mass\ of\ blade\ (M) = Density \times Volume = 7922 \times 30000 \times 10^{-9} = 0.238\ kg$

d) $Weight\ of\ the\ blade = Mass \times Acceleration\ due\ to\ gravity = 0.238 \times 9.81 = 2.335\ N$

e) $Torque\ produced\ by\ blade\ =\ Weight \times\ Radius = 2.335 \times \frac{0.3}{2} = 0.35\ N\ m$

f) $Where\ N\ is\ the\ rotational\ speed\ of\ the\ selected\ motor\ (1800\ rpm), then$

g) $Angular\ velocity = \frac{2\pi N}{60} = \frac{2 \times \pi \times 1800}{60} = 188.50\ rads/s$

h) $The\ power\ developed\ is\ therefore\ the\ product\ of\ torque\ and\ angular\ velocity$ $= 0.35 \times 188.50 = 66\ Watts.$

i) $Converting\ determined\ power\ to\ horsepower =\ 66 \times 0.00134 = 0.088\ HP$

Battery sizing

The design power was determined using Equation 1 (Igbokwe *et al.*, 2019);

$$\text{Design power} = \frac{I \times V}{Power\ factor\ of\ the\ machine} \quad (1)$$

Where I is the expected current to be drawn by the motor, V is the expected voltage of the battery (12 V), and the power factor is 0.8. Current used to power the motor is given as;

$$I = \frac{Design\ power \times Power\ factor\ of\ the\ machine}{V} = \frac{66 \times 0.8}{12} = 4.40\ Amps$$

The battery selected is 45 Ah at 12 volts, it is expected to discharge after; (45 Ah/4.40 A); 10.23 hours.

Solar sizing

The average sunshine in Akure, Nigeria is about 5 hours (Sinha and Mathur, 2020).
The solar panel selected is 2.88 Amps rated at 50 Watts

$$Average\ battery\ charge\ per\ day\ =\ 2.88\ Amps\ \times\ 5\ hours = 14.4\ Ah$$

Battery will be fully charged in (charging rate) = 45 Ah / 14.4 A = 3.125 hours.

Component Assembly

Frame: The mower frame was fabricated from an angle iron, cut and welded with the aid of cutter, grinder and welding machine. Positions of two bearings were also provided on the metal plate at the base of the machine to prevent excessive vibration of machine while it's at work. A room is provided for the solar panel at the top of the frame in such a way that it can easily be removed and slotted in (Figure 2).

Handle: The handle is made of galvanized hollow pipe having an internal diameter of 25 mm. The pipe was cut into 100 mm on both sides spaced 46 mm, then joined together by another 45.50 mm long pipe of the same internal diameter through welding. The other open end was welded to the base of the machine frame. The handle was designed in such a way that it can be detachable for future modifications.

Tyres/wheels: Two (2) Swivel caster wheels were attached to the front of the machine and two (2) fixed caster wheels were attached to the back of the machine. This is to enable easy maneuverability of the machine during operation when handled from the handle.

DC motor: A DC motor with speed of 1800 rpm was used. The shaft of the motor was fixed into the bearing and threaded at the end to screw the blades. The motor was supported by three rods screwed and welded to the top of the base frame.

Blades: The blade is made of galvanize steel, 300 mm long, 50 mm wide and 0.1 mm thick. The blade was sharpened and screwed to the end of the threaded motor shaft. The panel was connected to a charge controller before connected to the battery.

Battery and solar panel: The battery is placed beside the motor and the panel was affixed to the space provided by the frame at the top of the machine.

Painting: After the completion of the fabrication, the machine was painted to cover weld and scratch marls and enhance the beauty as shown in Figure 3.

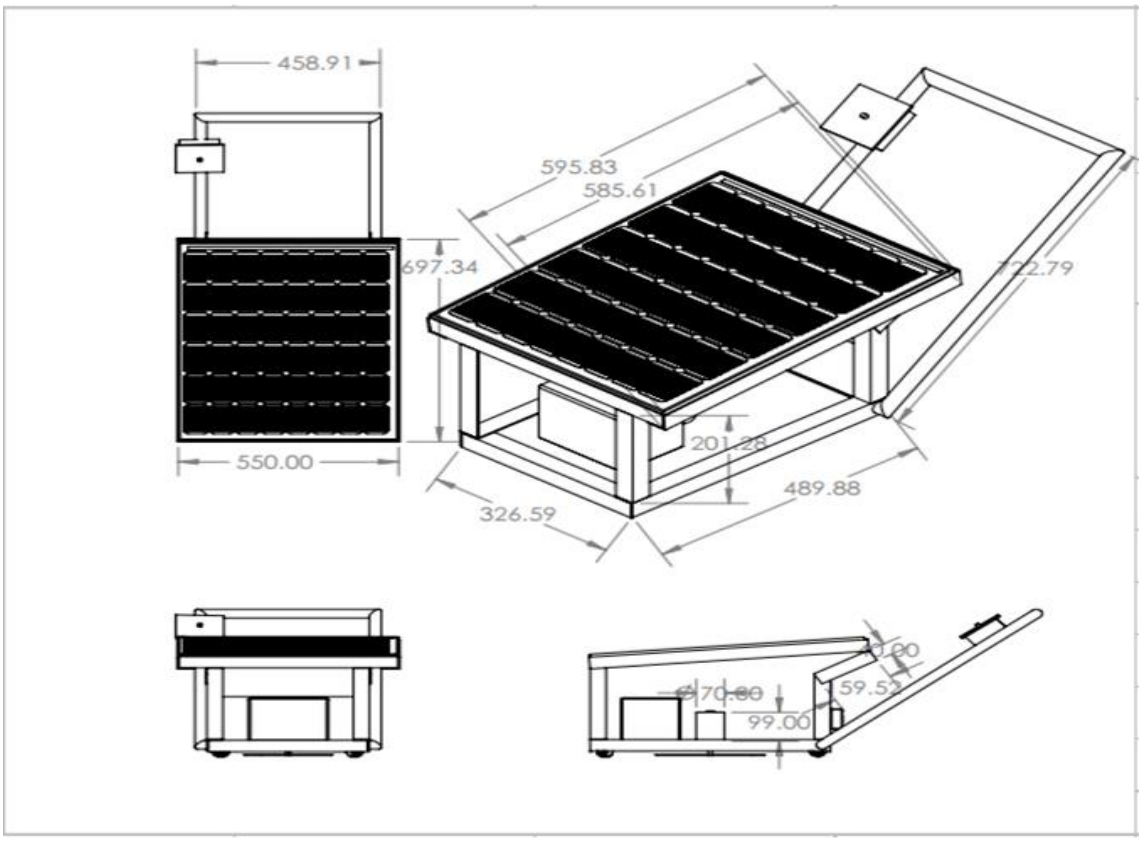

Figure 2. Orthogonal view of the designed lawn mower.

Figure 3. Assembled lawn mower.

Speed controller

The circuit used for the lawn mower uses similar PWM (Pulse Width Modulation) technique to control the motor speed and uses IC 555 to generate PWM signals. The PWM, is a modulation technique in which the width of the output pulse varies with respect to time. Therefore, changes the duty cycle of the wave, which in turn modify on and off time of this PWM signal. The heart of this circuit is an astable multivibrator built out of IC 555. This multivibrator produces a series of square wave pulses as the output of the fixed frequency. A 555 astable multivibrator output duty cycle can never fall below 50%. In order to achieve the PWM signal in the output, the duty cycle should be able to be modified to the required optimum level. This is achieved through the use of D2, D1 and RV1 (Figure 4).

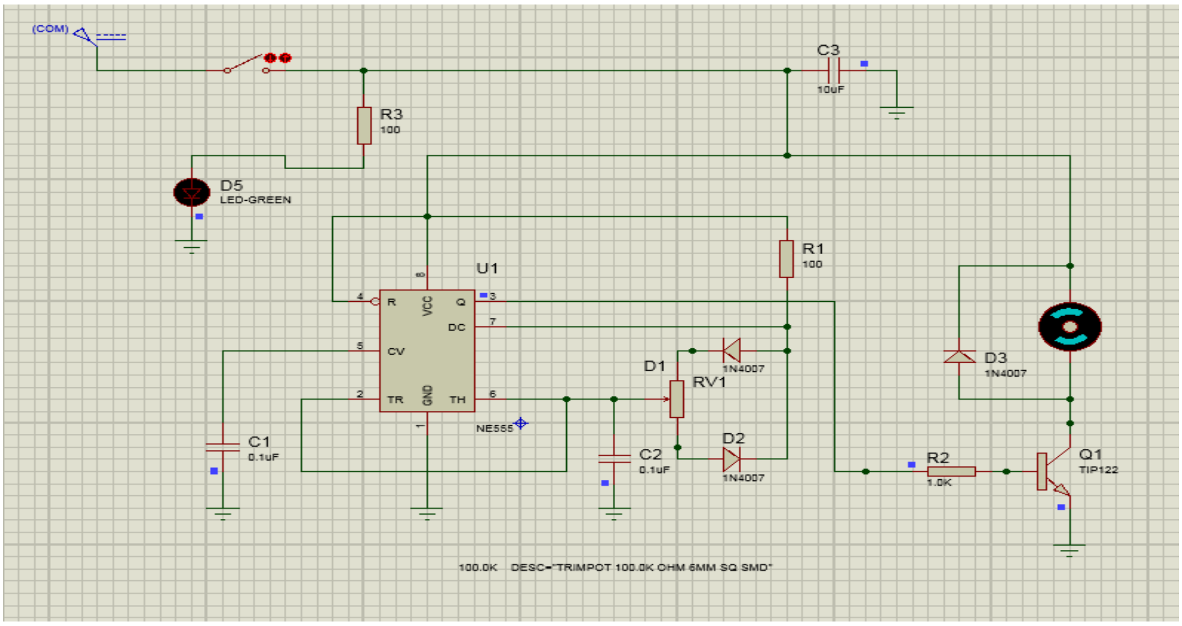

Figure 4. Circuit design of the speed controller.

Working of this astable multivibrator depends on the resistors and capacitor used with pin 7, pin 6 and pin 2. When the circuit is powered ON capacitor *C2* charges via resistor *R1* and *RV1*. But in the circuit, the current from *R1* can pass through only one terminal of the variable resistor since *D2* is reverse biased. Hence, *D1* allows current to flow through it and RV1 exhibits some resistance to the current, which depends on the position of the pot. When the capacitor is charging output of IC 555 will be in a high state. Once the capacitor charges up to 2/3 VCC (Voltage Common Collector), internal discharge transistor connected to pin 7 goes high. Now, the output of IC 555 will go low. This forces the capacitor to discharge through RV1. But this time the discharging current goes through diode *D2* since *D1* is reverse biased. The resistance exhibited by *RV1* to discharging current will be different from what exhibited to charge current of capacitor. Therefore, the discharge time of capacitor will be different from charging time. These varied charging and discharging time will modify the width of the output pulse. This results in a *PWM* output signal in the output. When *RV1* is set up, it exhibits very high resistance to charging current coming from *D1*, output pulse will have longer ON time. On the other hand, this will leave low resistance path for the discharge current going out via *D2*, therefore, capacitor discharges quickly make the OFF time shorter. Thus, a high duty cycle *PWM* pulse will be generated. If the resistance is reversed, low time will be longer and high time will be much shorter comparatively. This will make *PWM* signal much lower than 50% be generated.

Charging time and discharge time were determined using Equations 2 and 3;

$$Charging\ time\ or\ ON\ time\ =\ 0.693(R1\ +\ RV1)C2 \quad (2)$$

$$Discharge\ time\ or\ OFF\ time\ =\ 0.693\ x\ RV1\ x\ C2 \quad (3)$$

If the variable resistor was set to exhibit 10 kΩ resistance between terminals 1 and 2. Then, this will be the resistance to charging path by *RV1*. At this point terminal 2 and 3 in *RV1* will exhibit 90kΩ resistance to discharge path. Substituting the values into equation (2) and (3);

$$ON\ time\ =\ 0.693\ (100 + 10)0.1\ =\ 0.7\ ms$$

$$OFF\ time\ =\ 0.693 \times 90 \times 0.1\ =\ 6.237\ ms$$

$$T\ =\ ON\ time\ +\ OFF\ time\ =\ 0.7\ ms + 6.237\ ms\ =\ 6.937\ ms$$

$$Duty\ cycle\ =\ 0.7\ ms\ /\ 6.937\ ms\ =\ 10\%$$

Now if *RV1* is altered to make the resistance in terminal 1 and 2 as 90 kΩ and terminal 2 and 3 as 10kΩ. The duty cycle changes vastly;

$$ON\ time\ =\ 0.693\ (100 + 90)0.1 =\ 6.24\ ms$$

$$OFF\ time\ =\ 0.693 \times 10 \times 0.1\ =\ 0.693\ ms$$

$$T\ =\ 6.24\ ms + 0.693\ ms\ =\ 6.933\ ms$$

$$Duty\ cycle\ =\ 6.24\ ms\ /\ 6.933\ ms = 90\%$$

From the above calculations, providing different charging and discharging path with different resistance will give room for the production of *PWM* pulse from IC 555. Modifying the resistance value of *RV1* between its terminals will modify the duty cycle.

Motor driver

The output of the IC 555 is pretty low to drive a motor that can consume 500 mA. Therefore, a transistor TIP122, a Darlington transistor that can drive motor load up to 5A was used as a switch and a current driver. The *PWM* signal will drive the base of transistor *Q1*. This drives the motor according to the incoming signal from the output of the 555 IC. When the duty cycle of the *PWM* signal is high then the speed of the motor will be high and vice versa.

Diode *D3* is used to arrest the reverse current from motor when it is turned off. Figure 5 shows the fabricated speed controller. The 0 point on the speed controller signifies OFF while 1, 2, 3 and 4 signify the varying speeds of the blade.

Figure 5. Speed controller.

Cutting blades

For the purpose of performance evaluation, three pairs of blades made of galvanized steel were fabricated, each having different shapes. As shown Figure 6, the first pair is double-bladed, the second is triple-bladed, while the third is quadruple-bladed. Each pair have two different thickness, 1 mm and 1.3 mm. Designs were first made on a drawing paper, then cut out and pasted on the galvanized steel plate, the shape was then reproduced on the plate, which was then cut out with the aid of a hand grinder.

Figure 6. Blades of different shapes and thickness.

RESULTS and DISCUSSION

Cutting Efficiency

The graphical representations of the cutting efficiency of the mower at different number of blades, blade thickness and machine speed are shown in Figures 7 to 9. According to the figures, the cutting efficiency of the mower ranges from 70.50% to 84.10%. The number of blades and blade thickness has an inverse relationship with the cutting efficiency (Figure 7). The machine speed is proportional to the cutting efficiency (Figures 8 and 9). As deduced from the linear relationship in Equation 4, a unit increase in the machine speed resulted in an average increase in the cutting efficiency by 0.008%, whereas a unit increase in the number of blades and thickness resulted in an average decrease in the cutting efficiency of the solar powered lawn mower by 0.278% and 1.789%, respectively, which might be as a result of the increase in weight of the blades as the number and thickness increases.

$$E = +69.229 - 0.2778n - 1.7889t + 0.0083S \quad (4)$$

The mathematical relationship between the cutting efficiency and the input parameters (number of blades, thickness and machine speed) are shown in Equation 5 with a determination coefficient of thickness and this shows that the equation can significantly ($p<0.05$) predict the 99.01% change in the cutting efficiency as a function of number of blades, thickness and machine speed.

$$E = +57.76 + 11.37n - 3.08t + 1.27x10^{-3}S - 0.38nt - 2.90x10^{-4}nS - 2.20x10^{-5}tS - 1.78n^2 + 0.82t^2 + 2.98x10^{-6}S^2 \quad (5)$$

Where E is the machine efficiency, n is no of blades (blades), t is thickness of the blade (mm) and S is machine speed (rpm).

Table 1 shows the results of the analysis of variance (ANOVA) of the cutting efficiency. Based on the table, the number of blades do not have significant effect on the efficiency of the mower but the blade thickness and the machine speed significantly affect its efficiency. The combination of number of blades, thickness and machine speed can significantly explain the variation in the cutting efficiency at 95% probability level. However, the change in the cutting efficiency significantly ($p<0.05$) depends on the machine speed followed by blade thickness and number of blades has the least significant effect on the cutting efficiency of the Solar Powered Lawn Mower. The result has a similar trend with that reported by Sinha and Mathur (2020) when they evaluated the performance of a solar powered lawn mower, where they also experimented with various thickness of blade and the cutting efficiency obtained was 78.06%.

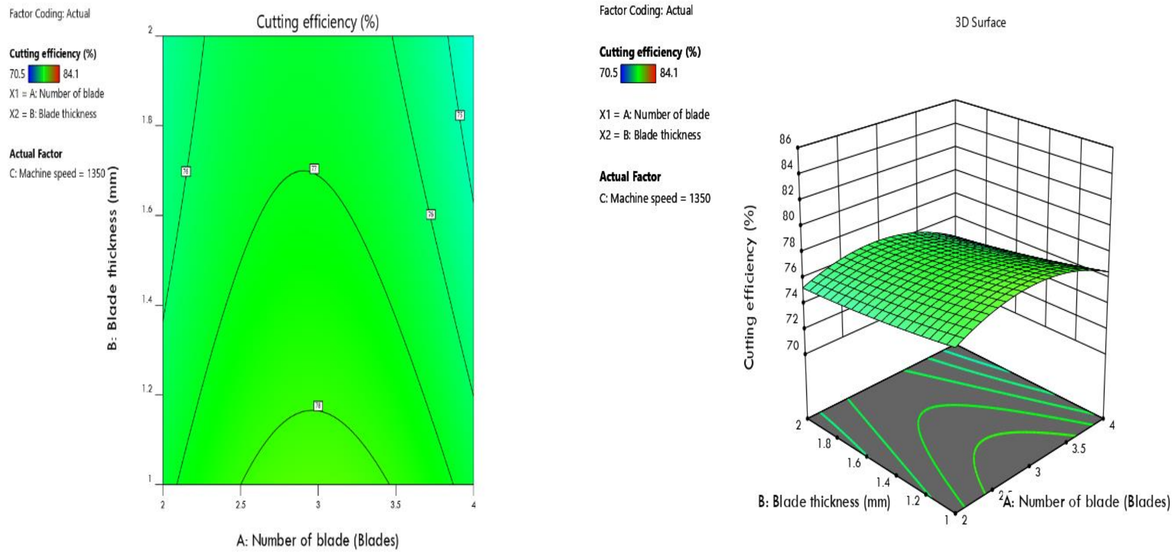

Figure 7. Contour and 3D surface plot of cutting efficiency at different blade thickness and number of blades.

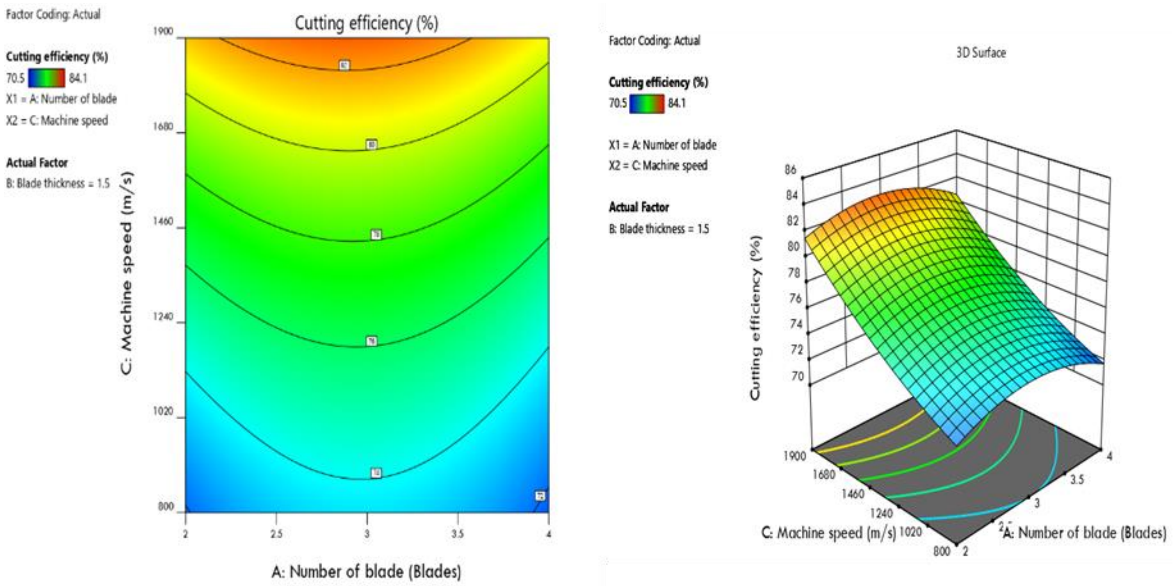

Figure 8. Contour and 3D surface plot of cutting efficiency at different machine speeds and number of blades.

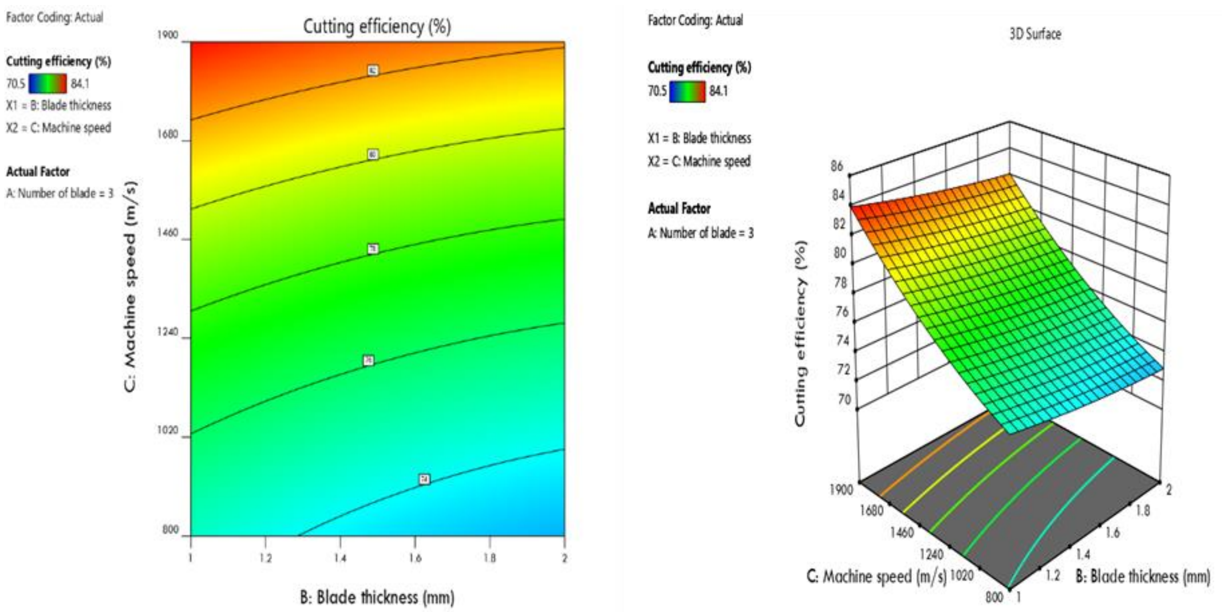

Figure 9. Contour and 3D surface plot of cutting efficiency at different machine speeds and blade thickness.

Table 1. ANOVA Table for the cutting efficiency.

Source	Sum of Squares	Df	Mean	F-value	p-value	Remark
Model	422.353	9	46.9281	189.1794029	3.04×10^{-15}	Significant
A-Number of blades	1.233	1	1.2326	4.968975514	0.039585437	
B-Blade thickness	14.211	1	14.2113	57.2896481	7.69×10^{-7}	Significant
C-Machine speed	385.494	1	385.4939	1554.027487	3.75×10^{-18}	Significant
AB	0.441	1	0.4408	1.777115376	0.200094605	
AC	0.314	1	0.3135	1.263996204	0.276521067	
BC	0.000	1	0.0004	0.001733877	0.967270957	
AÂ^2	18.963	1	18.9630	76.44470257	1.07×10^{-7}	
BÂ^2	0.254	1	0.2535	1.021999979	0.326218455	
CÂ^2	4.076	1	4.0757	16.4303131	0.000825884	Significant
Residual	4.217	17	0.2481			
Cor Total	426.570	26				

Df = degree of freedom, F-value = F- statistics (Fisher's) value and p-value = Probability value

Cutting Capacity

Figures 10 to 12 show the graphical representation of the cutting capacity of the developed solar powered lawn mower in different number of blades, thickness and machine speed. According to the figure, the cutting capacity of the mower ranges from 0.05 ha h^{-1} - 0.27 ha h^{-1}. As deduced from the linear relationship in the Figures (10 to 12) and Equation 6, a unit increase in the thickness resulted in an average increase in the cutting capacity by 0.027%, whereas a unit increase in the number of blades and machine speed resulted in an average decrease in the cutting capacity of the solar powered lawn mower by 0.01% and 0%, respectively, this is due to the increase in weight of the blades.

$$C = +0.3443 - 0.0102n + 0.0269t - 0.0002S \quad (6)$$

The mathematical relationship between the cutting capacity and the input parameters (number of blades, thickness and machine speed) is shown in Equation 7 with a determination coefficient of thickness and this shows that the equation can significantly ($p<0.05$) predict the 99.70% change in the cutting capacity as a function of number of blades, thickness and machine speed.

$$C = +57.76 + 11.37n - 3.08t + 1.27x10^{-3}S - 0.38nt - 2.90x10^{-4}nS - 2.20x10^{-5}tS - 1.78n^2 + 0.82t^2 + 2.98x10^{-6}S^2 \quad (7)$$

Where *C* is the machine capacity, *n* is no of blades (blades), *t* is thickness of blade (mm) and *S* is machine speed (rpm).

Table 2 shows the result of the analysis of variance (ANOVA) of the cutting capacity. Based on the table, all the considered parameters (number of blades, thickness and machine speed) significantly affect the cutting capacity of the mower and this can significantly explain the variation in the cutting capacity at 95% probability level. However, the change in the cutting capacity significantly ($p<0.05$) depends on the machine speed followed by blade thickness and number of blades has the least significant effect on the cutting efficiency of the solar powered lawn mower.

Tanimola *et al.* (2014) reported in their research that the effective field capacity of the solar powered lawn mower was 0.000111 ha h^{-1}. Sinha and Mathur (2020) also reported that the maximum and minimum field capacity of the mower was 0.0306 ha h^{-1} and 0.0282 ha h^{-1}, respectively.

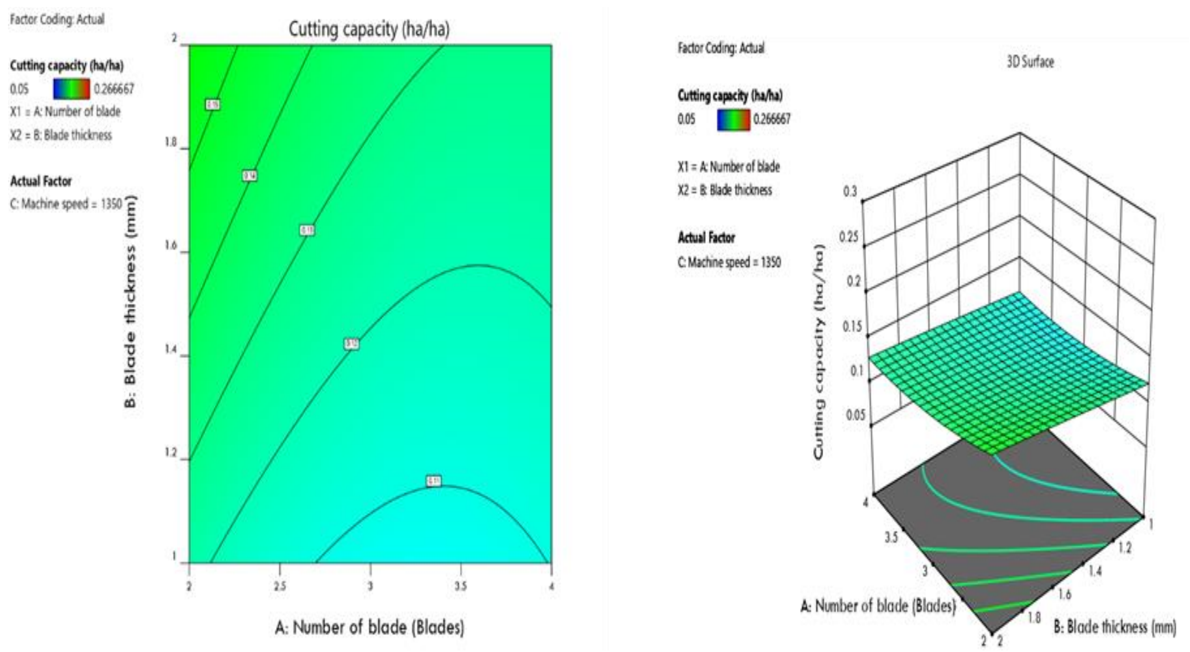

Figure 10. Contour and 3D surface plot of the cutting capacity at different blade thickness and number of blades.

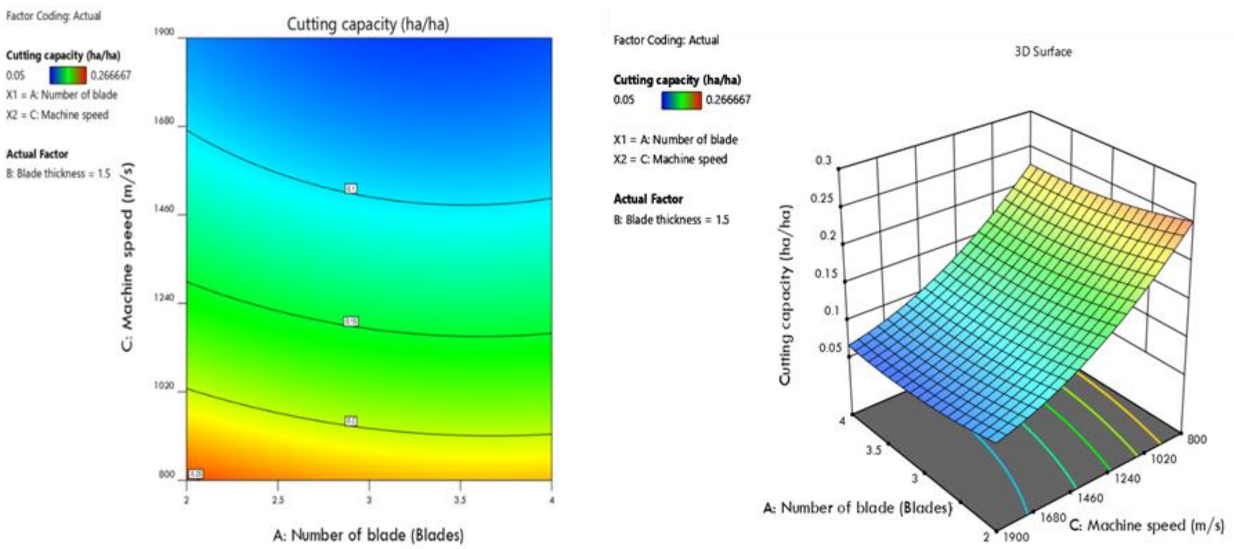

Figure 11. Contour and 3D surface plot of the cutting capacity at different machine speeds and number of blades.

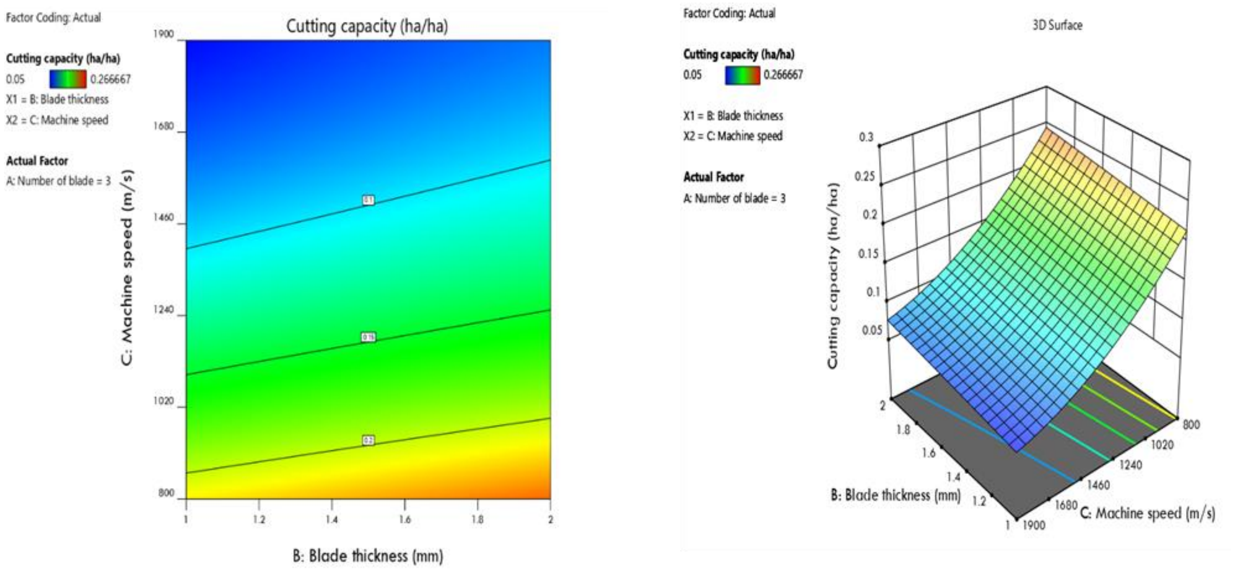

Figure 12. Contour and 3D surface plot of the cutting capacity at different machine speeds and blade thickness.

Table 2. ANOVA Table for the cutting capacity.

Source	Sum of Squares	Df	Mean Square	F-value	p-value	Remark
Model	0.1427	9	0.0159	629.18	< 0.0001	Significant
A-Number of blades	0.0019	1	0.0019	76.64	< 0.0001	Significant
B-Blade thickness	0.0033	1	0.0033	129.79	< 0.0001	Significant
C-Machine speed	0.1236	1	0.1236	4905.99	< 0.0001	Significant
AB	0.0002	1	0.0002	8.27	0.0105	
AC	0.0001	1	0.0001	3.27	0.0884	
BC	0	1	0	1.07	0.3161	
A^2	0.0005	1	0.0005	20.42	0.0003	Significant
B^2	1.29E-06	1	1.29E-06	0.051	0.824	
C^2	0.0034	1	0.0034	135.61	< 0.0001	Significant
Residual	0.0004	17	0			
Cor Total	0.1431	26				

Df = degree of freedom, F-value = F- statistics (Fisher's) value and p-value = Probability value

CONCLUSION

In recent times, machines are designed with the aim of reducing or eliminating greenhouse gas emissions, which are the major causes of climate change. This project has met the challenges of environmental pollution and high cost of operation by producing a solar powered lawn mower from locally sorted materials. The cutting efficiency and cutting capacity were evaluated using Design-Expert software and MS Excel and found to range from 70.5% to 84.10% and 0.05 ha/h to 0.27 ha h^{-1} respectively. The following conclusions can be drawn from this study:

a) Utilization of solar energy in lawn mowing is more efficient compared to other means.
b) Light weighted materials used in construction aids easy movement of the operator.
c) The machine's capacity is adequate for its purpose.
d) The machine has proved to be a possible replacement for the gasoline powered lawn mowers.

DECLARATION OF COMPETING INTEREST

The author of this manuscript declare that there is no conflict of interest.

CREDIT AUTHORSHIP CONTRIBUTION STATEMENT

The author would like to declare that he solely developed all the sections in this manuscript.

REFERENCES

Dalal SS, Sonune VS and Gawande DB (2016). Manufacturing of solar grass cutter. *International Journal of Research in Advent Technology, 352–355. Special Issue. National Conference "CONVERGENCE 2016", 06th-07th, April 2016.*

Dutta PP, Baruah A, Konwar A and Kumar VA (2016). *Technical review of lawn mower technology. ADBU Journal of Engineering Technology, 4(1): 4-7.*

Fernandez G and Krishnasamy VA (2018). Fully automated lawn mower using solar panel. *Journal of Advanced Research in Dynamical and Control Systems. 7(07): 977-983.*

Igbokwe JO, Okafor BE and Ehujuo US (2019). Development of a solar powered lawn mower. *International Journal of Engineering and Technology, 6(03): 104-108.*

Mgbemu EN (2005). Modern physics, First Edition. *Spectrum Limited, Ibadan. pp72.*

National Research Foundation (NRF) (2010). Communication astronomy in school. Astronomy Activities/Demostrations, Cape Town, South Africa.

Prasanthi SG and Balaiah R (2017). Fabrication of solar powered lawnmower. *International Journal of Scientific Research in Science, Engineering and Technology (IJSRSET). 3(8): 477-480.*

Satwik D, Rao NR and Reddy GS (2015). Design and Fabrication of lever operated solar lawn mower and contact stress analysis of spur gears. *International Journal of Science, 4(8): 2815-2821.*

Sinha Y and Mathur SM (2020). Development and performance evaluation of solar powered lawn mower. *International Journal of Current Microbiology and Applied Sciences, 9(5): 3378-3384.*

Tanimola O, Diabana P and Bankole Y (2014). Design and development of a solar powered lawn mower. *International Journal of Science and Engineering Research, 5(6): 215-220.*

Turkish Journal of Agricultural Engineering Research

https://dergipark.org.tr/en/pub/turkager
https://doi.org/10.46592/turkager.2021.v02i02.010

Turk J Agr Eng Res (TURKAGER)
ISSN: 2717-8420
2021, 2(2), 363-375

Research Article

Mathematical Modelling of Drying Characteristics of Coconut Slices

John ISA[a] **Kabiru Ayobami JIMOH**[b*]

[a*] Department of Agricultural and Environmental Engineering, Federal University of Technology Akure, NIGERIA,

[b] Department of Agricultural and Environmental Engineering, Federal University of Technology Akure, NIGERIA

(*): Corresponding author, jimohage114882@futa.edu.ng

ABSTRACT

Mathematical modelling is one of the most important Engineering considerations for the effective representation of drying processes. Therefore, the drying behaviour of the coconut slices was modelled using non-linear regression (fitting existing mathematical models). The three thickness of the coconut samples (4 mm, 8 mm and 12 mm) were dried using laboratory oven under five different temperature (40°C, 50°C, 60°C, 70°C and 80°C) and constant air velocity (1 m s^{-1}). Drying properties such as moisture content, moisture ratio, drying rate, drying time, effective moisture diffusivity coefficient (Deff) and activation energy of the process was used to define the behaviour of the coconut slices, the experimentally observed moisture ratios were fitted into fifteen (15) existing thin-layer mathematical model to forecast the behaviour of the coconut slices during process. The result of the modelling showed that the modified Henderson and pabis, Page and Peleg model had the most acceptable level of accuracy in predicting the drying behaviour of the coconut slices at 4mm, 8mm and 12mm, respectively. The obtained values for the effective moisture diffusivity ranges between 6.06×10^{-11} m^2 s^{-1} and 3.16×10^{-10} m^2 s^{-1} for 4mm thickness; 5.46×10^{-10} m^2 s^{-1} and 1.44×10^{-9} m^2 s^{-1} for 8mm thickness; 5.97×10^{-10} m^2 s^{-1} and 2.83×10^{-9} m^2 s^{-1} for 12mm thickness, whilst the activation energy ranges between 27.44892 and 27.563 kJ mol^{-1} for 4mm thickness; 27.45371 and 27.53017 kJ mol^{-1} for 8mm thickness; 35.64817 and 35.84369 kJ mol^{-1} for 12 mm. Therefore, the Modified Henderson and Pabis, Page and Peleg thin-layer mathematical models were chosen for the best prediction of the dehydration behaviour of coconut slices of 4 mm, 8 mm and 12 mm thickness respectively.

RESEARCH ARTICLE

Received: 18.07.2021
Accepted: 09.11.2021

Keywords:

- Coconut,
- Drying characteristics,
- Mathematical models,
- Oven drying

To cite: Isa J, Jimoh KA (2021). Mathematical Modelling of Drying Characteristics of Coconut Slices. Turkish Journal of Agricultural Engineering Research (TURKAGER), 2(2), 363-375. *https://doi.org/10.46592/turkager.2021.v02i02.010*

INTRODUCTION

Coconut (*Cocos nucifera*) is a tree and a member of the Arecaceae family that is grown for a variety of reason, the most important of which are its nutritional and therapeutic properties. In the traditional coconut arming locations, all the components are used in some form in the everyday lives of the inhabitants, it is a good source of natural materials for the creation of medications for a variety of ailments as well as industrial goods. The tender coconut kernel and water, for example contain anti-bacteria, antifungal, antiviral, antiparasitic, anti-dermatophytes, and antioxidant hypoglycemic, characteristics, also, it contains micro-minerals and nutrients that were important for health, thus, it is widely consumed by people all over the world, mostly in the tropical areas. Coconut is one of the most highly significant crop in the tropics, its highly cultivated in over 80 countries worldwide, with total annual production of 61 mt (FAO, 2010). Between 2004 and 2008, Nigeria produced 1.088.500 million tons of coconut palm (Uwubanwen, 2011). Coconut milk, juice, flour and oil are just a few examples of coconut-derived goods (Madhiyanon *et al*., 2009). Desiccated coconut, which has a moisture level of around 3% dry weight, may be used to decorate ice cream, cakes, and doughnuts, as well as to flavor chocolate bars, candies, and biscuits (Madhiyanon e*t al*., 2009; FAO, 2010).

Drying method is one of the oldest methods for improving the shelf life ethnic foods. It's becoming more well-known as one of the rising technologies that necessitates new study methods. There are two basic principles that govern drying. To begin, hot air must be delivered to the material, followed moist air (vapour) migration from the material to its immediate environment (Sigge *et al*., 1998). Because moisture removal in an energy intensive process, it's effectiveness might be enhanced by increasing the rate of drying, which affects the time taken. Long drying times might result in worse final goods (Sigge *et al*., 1998; Horner, 1993). Higher drying rates are desired in order to produce acceptable end products that are both economically and nutritionally viable (Sigge *et al*., 1998). The modelling of the drying method is one of the vital parts of drying technology and developments. Modelling represents the development of a set of equations that accurately represent the real time systems and processes. Scientific models for prediction of drying process are mostly used in the design of new drying structures, enhance the performance of the existing systems, and even control the process of drying. Several models and methods for forecasting of the drying behaviour was proposed in literatures, with thin layer drying models being the most widely used. Several studies were recently carried out to highlight the drying behaviour of fruit (Yaldiz *et al*., 2001; Akpinar, 2006), vegetables (Karaaslan and Tuncer, 2008), spices (Murthy and Manohar, 2012), oilseeds (Gowen *et al*., 2008), nuts (Moreira *et al*., 2005), red pepper (Doymaz and Pala, 2002), and other foods. To this end, the study models the characteristics of coconut slice during drying using existing thin-layer mathematical models and the specific objectives of the study are to determine the influence of the temperature and slice thickness on drying behaviour of coconut slices in a laboratory oven, model the drying behaviour of the coconut slices using fifteen (15) existing models and choose the best model for predicting the behaviour of the coconut slices during the drying.

MATERIALS and METHODS

Sample preparation

Experimental drying of the coconut slices was done in the Crop Processing Laboratory of the Department of Agricultural and Environmental Engineering, using some available materials which include laboratory oven, weighing scale, desiccators: weighing balance, and thermometer. The coconuts in this research were acquired from a local municipal market in Akure (Oja-Oba market), Nigeria's south-western area. The coconut meat was manually taken from the coconuts and cleaned with water before being cut into a standard rectangular form (30 x 10 mm) with thicknesses of 4 mm, 8 mm, and 12 mm, respectively. The coconut slices were carefully cleaned, and those that had black stains were removed. The oven-drying approach was utilized for the measurement of the initial moisture content of the coconut slices, which was done 105°C for 24 hours in the laboratory oven and moisture content was measured in replicate using three samples in total.

Drying experimentation

Before each drying cycle, The laboratory oven (Searchtech Instruments, DHG-9053 Model) was turned on for roughly 30 minutes to create steady-state conditions. The coconut slices were then put in a stainless tray and placed inside the laboratory oven; the hot air flows perpendicular to the samples in the drying trays. Prior to the experiment, the tray's and sample's original weights were recorded. Thereafter, the trays were taken out every 30 minutes and weighed using a smart weighing balance. After cooling of the sample in the desiccator at room temperature, the dry product was packed in low-density polyethene bags and kept in a desiccator, the moisture removal experiment were done at different temperature (40, 50, 60, 70 and 80°C), the drying tests were conducted three times (Kaveh *et al.*, 2018).

Determination of moisture content and moisture ratio

The subsequent equations are related to the modeling of the behaviour of coconut slices during drying. Though some of the equation is computed by the computer in the validation of the statistical data. However, the moisture content equation given by the Equation (1 and 2) is used in the computation of the coconut moisture content with the weight of coconut at time T=0 and T= t.

$$M_t = \frac{W_t - W_o}{W_o} \times 100 \tag{1}$$

$$M_t = \frac{W_t - W_e}{W_e} \times 100 \tag{2}$$

The experimental data for the coconut slices during the drying experiments were used to represent the dimensionless form of moisture ratio (MR) as reported by Midilli and Kucuk (2003) and Ng *et al.* (2015) presented in Equation 3.

$$MR = \frac{(M_t - M_e)}{(M_0 - M_e)} \tag{3}$$

Where *MR* is the moisture ratio, M_t is the moisture content of the coconut slices at each time (%), M_o is the initial moisture content of coconut slices (%) and M_e is the moisture coconut of the coconut slice (%) at saturation point.

Determination drying rate

The rate of drying for the coconut slices were estimated using the Equation (4), which was utilized in the drying studies by Guine and Fernandes (2006).

$$\frac{dm}{dt} = \frac{m_0 - m_t}{t - t_0} \quad (4)$$

Where $\frac{dm}{dt}$ is the drying rate, $m_0 - m_t$ is the change in coconut moisture content and $t - t_0$ is the change in the time of drying.

Determination of effectiveness moisture diffusivity and activation energy

Garcia *et al.* (2007) reported a model equation using Fick's second law of diffusion that state the relation between the effective moisture diffusivity, dimensionless moisture ratio, diffusivity constant and minimal shrinkage, which is given in the Equation (5).

$$MR = \left(\frac{8}{\pi^2}\right) \exp\left[\frac{-D_{eff}}{4L^2} \pi^2 \text{ t}\right] \quad (5)$$

Where D_{eff} is moisture diffusivity constant (m^2 s^{-1}), t is time of drying (s) and L is sample thickness.

For estimation of the activation energy, the moisture diffusivity was defined as a function of temperature using Arrhenius equation (Dissa *et al.*, 2011) as shown Equation (6):

$$D_{eff} = D_o \exp\left(-\frac{E_a}{R(T + 273.15)}\right) \quad (6)$$

Where D_{eff} is moisture diffusivity constant (m^2 s^{-1}), D_O is pre-exponential constant (m^2 s^{-1}), E_a is the activation energy (kj mol^{-1}), T is hot air temperature (°C) and R is the universal gas constant (kJ mol^{-1} K) as stated by Celen *et al.* (2010); Caliskan and Dirim, (2017) and Demiray et al. (2017). The Equation (6) above can further be simplified as shown in Equation (7).

$$\ln D_{eff} = \ln D_o - \frac{E_a}{R(T+273.15)} \quad (7)$$

Model Fitting

The experimental moisture ratio data was fitted into 15 mathematical models (Table 1) using solver addin on Microsoft Excel software version 2016, the most suitable model was chosen based on some parameters such as determination coefficient (R^2), chi square (χ^2) and root mean squared error (*RMSE*).

Table 1. Selected models for prediction of the drying characteristics.

S/N	Model	Equation	Reference
1	Newton	$MR = \text{Exp}\ (-kt)$	Ayensu (1997); Toğrul and Pehlivan (2004)
2	Henderson and pabis	$MR = a\text{Exp}\ (-kt)$	Kashaninejad *et al.* (2007)
3	Page	$MR = Exp(-kt^n)$	Kaleemullah and Kailappan (2006)
4	Logarithmic	$MR = a\text{Exp}\ (-kt)\ + c$	Onwude *et al.* (2018)
5	Two term	$MR = a\text{Exp}\ (-kt)\ + bExp(-gt)$	Wang *et al.* (2007)
6	Verma et al.	$MR = a\text{Exp}\ (-kt)\ + (1 + a)Exp(-gt)$	Yaldiz and Ertekin (2001)
7	Diffusion approach	$MR = a\text{Exp}\ (-kt) + (1 - a)Exp(-gt)$	Wang *et al.* (2007)
8	Midilli *et al.*	$MR = aExp(-kt^n) + bt$	Midilli and Kucuk (2003)
9	Wang and Singh	$MR = 1 + at + at^2$	Wang and Singh (1978)
10	Hii et al.	$MR = a\mathrm{e}^{-kt^n} + cExp(-gt^n)$	Hii *et al.* (2009)
11	Modified henderson pabis	$MR = a\text{Exp}\ (-kt) + bExp(-gt) + cExp(-ht)$	Doymaz (2005); Karathanos (1999);
12	Modified Page	$MR = aExp(-(kt)^n)$	Lahsasni *et al.* (2004); Wang *et al.* (2007)
14	Two term exponential	$MR = aExp(-kt) + (1 + a)Exp(-kat)$	Midilli and Kucuk (2003); Sacilik *et al.* (2006); Tarigan *et al.* (2007)
15	Peleg	$\text{MR} = 1 - \frac{t}{(a+bt)}$	Da Silva *et al.* (2014)

RESULTS and DISCUSSION

Drying Curves

The curves of the time against time against moisture content, time against moisture ratio, time against drying rate and moisture content against drying rate for coconut samples of 4 mm, 8 mm and 12 mm thickness are presented in Figures 1-3 respectively at different hot-air temperature (40, 50, 60, 70 and 80°C). It was observed from the Figures that the drying rate, moisture ratio and moisture content decrease continuously with increase in the time (Doymaz, 2005). The total period taken to dry the coconut sample increases and the moisture content reduces, the rate of drying significantly reduce as well. The rate at which moisture migrates in the laboratory oven started slow and then gradually increased before decreasing as the sample approached equilibrium similar observation was reported by Arslan and Ozcan (2010), Sharma *et al.* (2009) and Bozkir *et al.* (2018) for onion, garlic cloves and garlic respectively. More specifically, due to low diffusion process, about 2/3 of the total time taken might be spent in drying of the final 1/3 of moisture in the sample. Also, higher amount of moisture removal was recorded at high temperature and the required total time taken to dry the sample was reduced significantly with the rise in the hot-air temperature. Decrease in the amount of moisture removed from the sample at higher time might be due to the fact the moisture content in the sample is low and it requires more energy to vaporize the moisture which therefore shows that the drying of the coconut slices is guided by diffusion and this finding agrees with the study of Kingsley *et al.* (2007) and Piga *et al.* (2004). The drying time and final moisture content of the product was reduces with increase in the thickness of the sample similar findings was reported by Ikrang and Umani (2019) during optimization of process condition for the drying of catfish using response surface methodology.

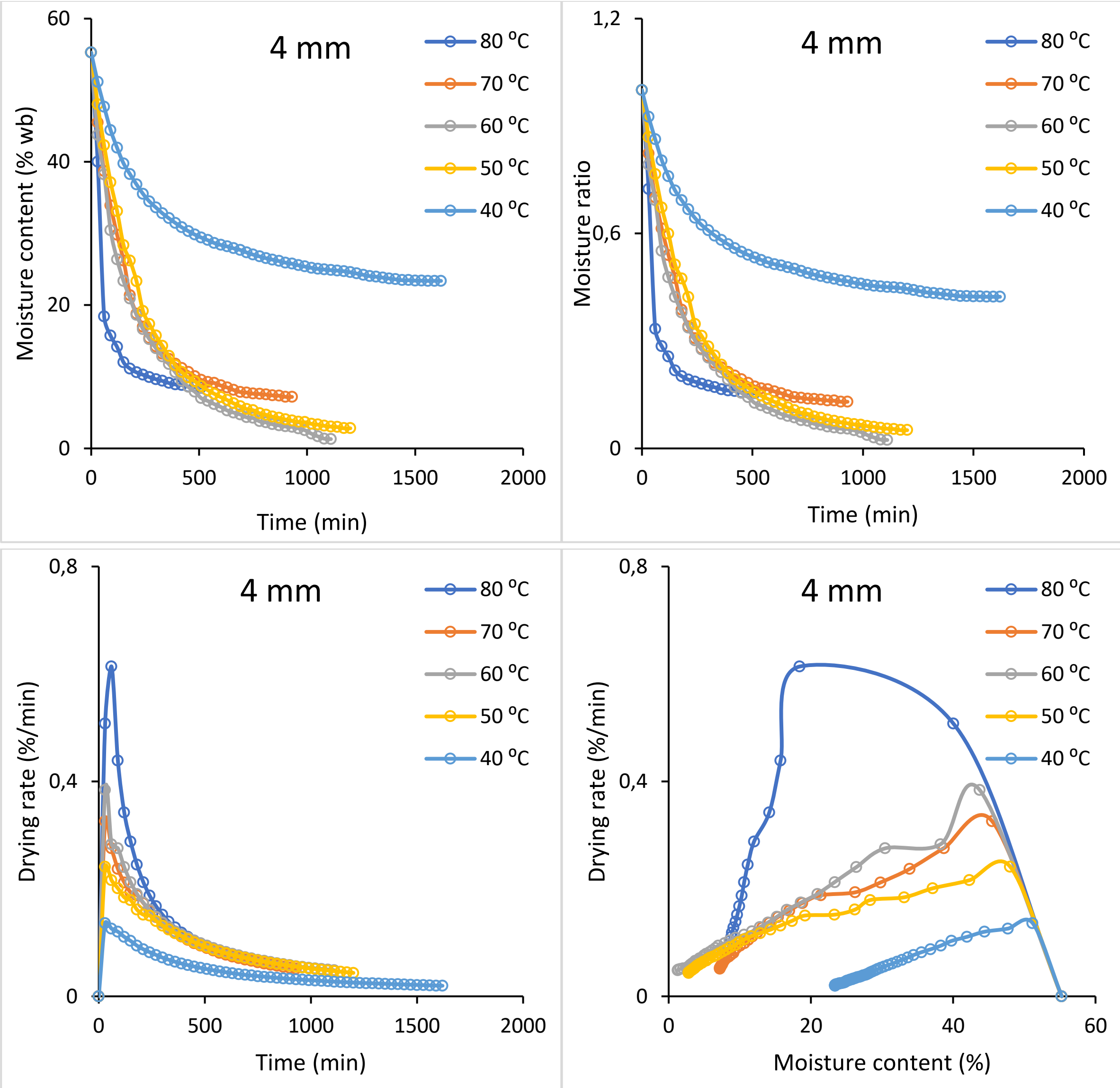

Figure 1. Drying curves of coconut slices of 4 mm diameter at different temperature for laboratory oven.

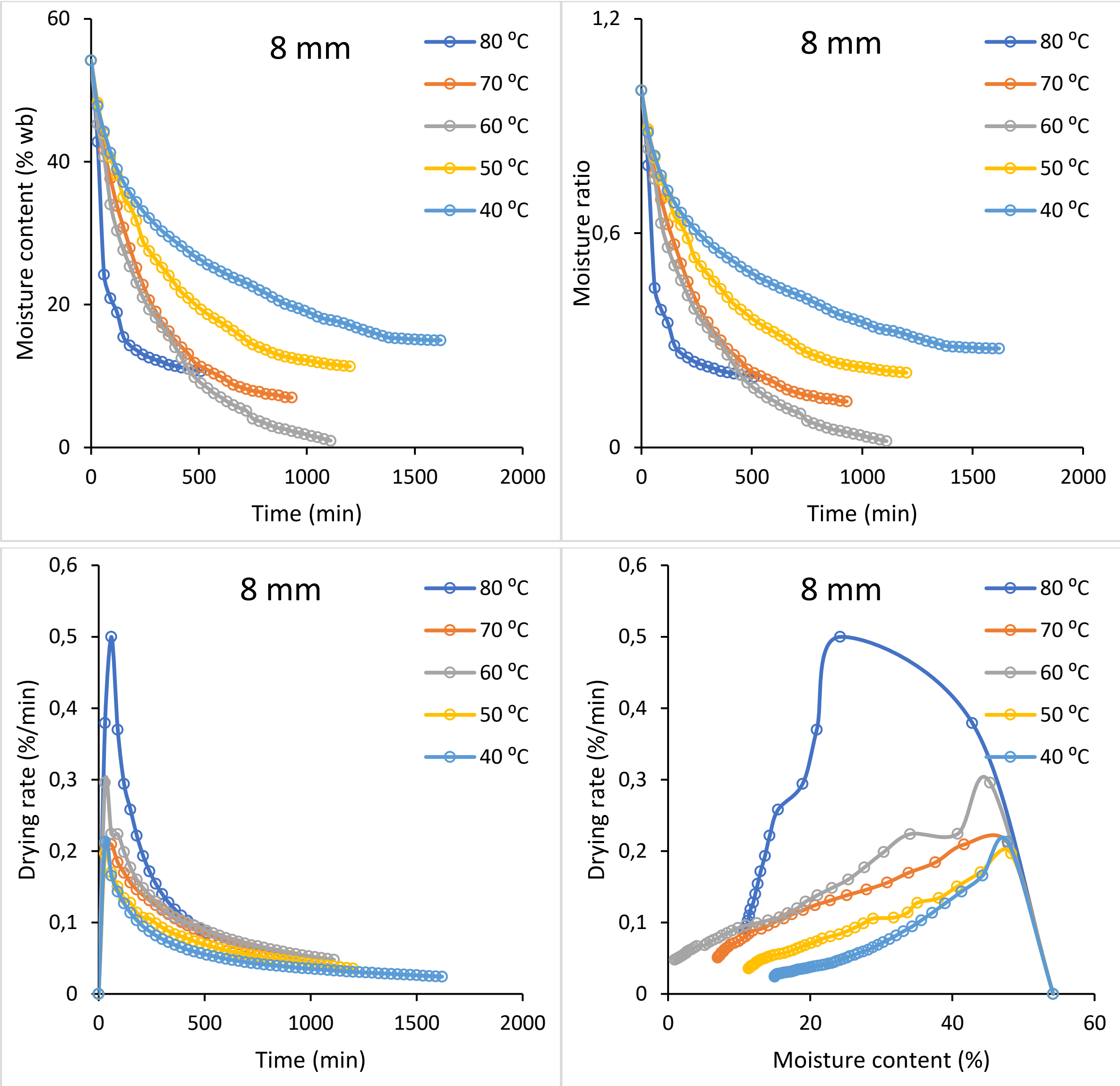

Figure 2. Drying curves of coconut slices of 8 mm diameter at different temperature for laboratory oven.

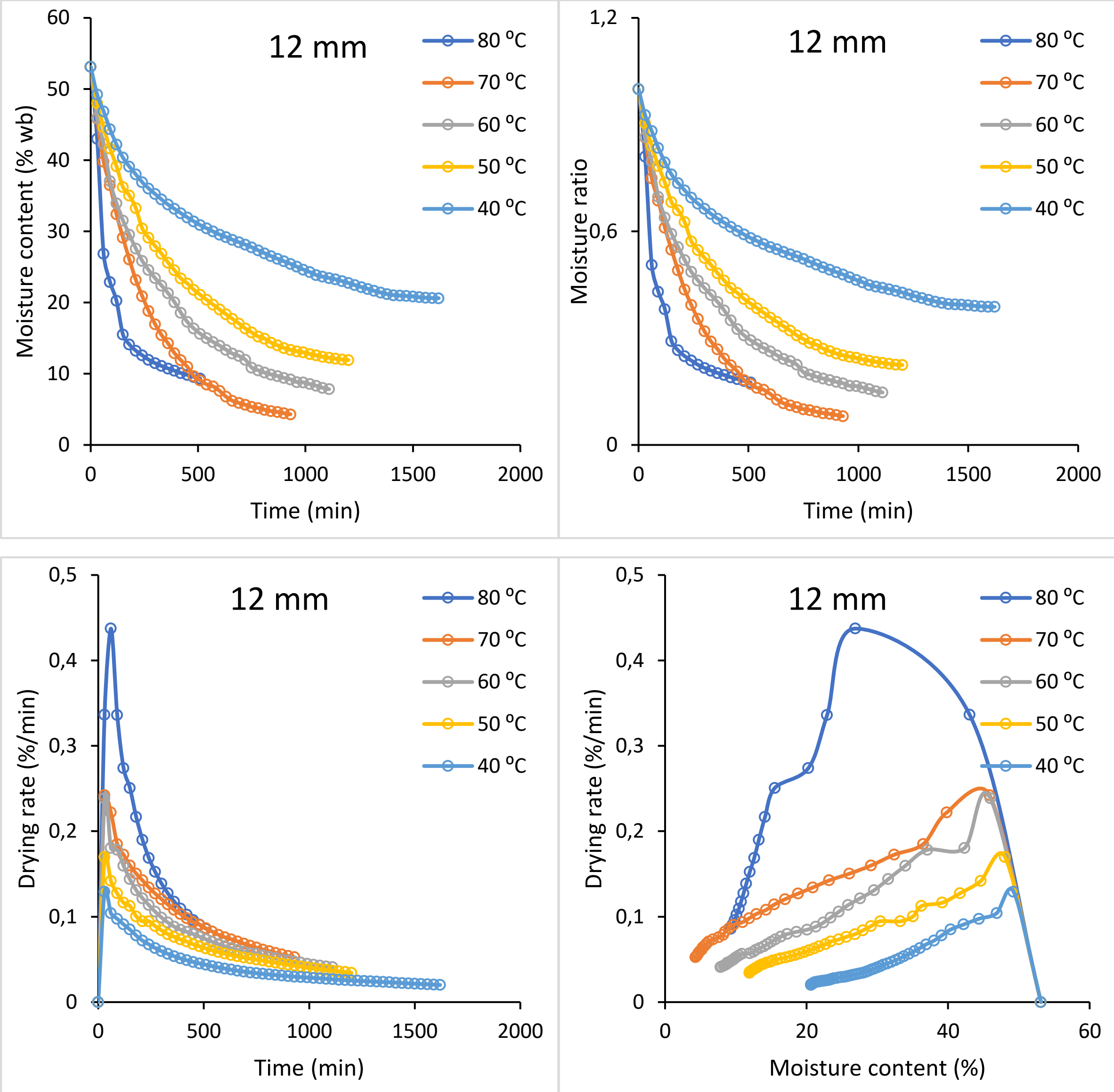

Figure 3. Drying curves of coconut slices of 12 mm diameter at different temperature for laboratory oven.

Evaluation of drying models

Experimental moisture ratio was fitted into 15 mathematical models (Table 1), the most suitable mode was chosen based on some statistical parameters which include the highest value of determination coefficient *(R^2)*, low value of reduced-chi-square *(χ^2)* and root-mean-square-error *(RMSE)*. The goodness of fit statistics and model coefficient of each of the model under different slice thicknesses (4 mm, 8 mm and 12 mm) and air temperature (40, 50, 60, 70 and 80°C) are shown in Table 2.

For the thickness of 4 mm, Modified henderson and pabis model, Modified Henderson and pabis model, Peleg model, Modified Henderson and pabis model and Peleg model recorded the best performance with high R^2 (0.9720, 0.9971, 0.9991, 0.9989, and 0.9995 respectively), low χ^2 (0.0021, 0.0002, 0.0001, 0.0001, and 0.0001 respectively) and RMSE (0.0.037, 40.0117, 0.0080,0.0069, and 0.0030 respectively) for the drying air temperature of 80°C, 70°C, 60°C, 50°C, and 40°C, respectively.

For the thickness of 8 mm, the diffusion approach model, Peleg model, Modified page II model Peleg model and page model recorded has the most suitable performance with high

R^2 (0.9747, 0.9815, 0.9843, 0.9897 and 0.9972 respectively), low χ^2 (0.0049, 0.0040, 0.0027, 0.0296, and 0.0056 respectively) and low RMSE (0.0678, 0.0610, 0.0490, 0.1678 and 0.0732 respectively) for the drying air temperature of 80°C, 70°C, 60°C, 50°C, and 40°C, respectively.

For the thickness of 12 mm, the best fitting performance was observed in the Verma et al. model, Verma et al. model, Page model, Logarithmic and Modified page II model, with high R^2 (0.9894, 0.9992. 0.9984, 0.9990, and 0.9967 respectively), low χ^2 (0.0007, 0.0001, 0.0001, 0.0001, and 0.0001 respectively) and low RMSE (0.0233, 0.0078, 0.0089, 0.0064, and 0.0085 respectively) for the drying air temperature of 80°C, 70°C, 60°C, 50°C, and 40°C, respectively. The range of accuracy of the model agrees with the report of Younis *et al.* (2018) for garlic slice with the Page, Logarithmic, Midilli and Hii *et al.* models as the best model for prediction the drying characteristics, also, Onwude *et al.* (2018) reported the Page, Logarithmic, and Midilli model as the best model for predicting the drying behavior of sweet potato.

Table 2. Drying model constants and goodness of fit parameters for coconut samples of 4 mm thickness.

Temp.	Model	Model constant	R^2	RMSE	X^2
80 °C	Newton	K = 0.5771	0.8788	0.1176	0.0146
	Henderson and Pabis	K = 0.4248, a = 0.8255	0.8042	0.1099	0.0136
	Page	K = 0.8608, n = 0.4524	0.9236	0.0608	0.0042
	Logarithmic	K = 0.0505, a = 1.4893, c = -0.9414	0.5127	0.1531	0.0281
	Two term	K = 0.3747, g = 0.3734, a = 13.7957, c = -12.9931	0.7868	0.1103	0.0156
	Verma et al.	K = 0.7329, g = 0.0059, a = 0.8756	0.9278	0.0662	0.0053
	Diffusion	K = 0.5094, g = 0.9994, a = 122.4643	0.8655	0.1184	0.0168
	Midili et al.	K = 0.0133, b = -0.0567, a = 0.5225, n = 0.3652	0.4773	0.1585	0.0323
	Wang and smith	a = -0.3457, b = 0.0313	0.7702	0.1409	0.0223
	Hii et al.	K = 0.041, g = -0.0009, a = 15.5101, c = -14.4773, n = 0.1829	0.8909	0.0725	0.0073
	Modified Henderson and pabis	**K = -10.827, a = 0.5601, g = 4.4332, b = 0.3778, h = 7.4428, c = 0.7429**	**0.972**	**0.0374**	**0.0021**
	Modified Page I	K = 0.718, n = 0.4524	0.9236	0.0608	0.0042
	Modified Page II	K = 1.0037, a = 0.0358, n = 0.4846, L = 0.0015	0.9231	0.0612	0.0048
	Two term exponentials	K = -0.0902, a = -0.2636	0.4224	0.1669	0.0313
	Peleg	a = 0.6386, b = 1.0769	0.959	0.0447	0.0022
70 °C	Newton	K = 0.2438	0.9636	0.0726	0.0054
	Henderson and Pabis	K = 0.201, a = 0.8574	0.9353	0.0617	0.0041
	Page	K = 0.4277, n = 0.6444	0.979	0.032	0.0011
	Logarithmic	K = 0.3534, a = 0.8397, c = 0.1246	0.9969	0.0123	0.0002
	Two term	K = 0.1685, g = 0.1663, a = 9.0072, c = -8.1707	0.9257	0.0631	0.0046
	Verma et al.	K = 0.6881, g = 0.1135, a = 0.5282	0.989	0.0241	0.0006
	Diffusion	K = 0.2376, g = 0.9992, a = 25.5376	0.9629	0.0727	0.0058
	Midili et al.	K = 0.3634, b = 0.0065, a = 0.9905, n = 0.8409	0.9963	0.0135	0.0002
	Wang and smith	a = -0.1767, b = 0.0083	0.9225	0.0888	0.0084
	Hii et al.	K = 0.4111, g = -0.3791, a = 1.0194, c = 0.0054, n = 0.7564	0.9955	0.0146	0.0003

Table 2 (continues). Drying model constants and goodness of fit parameters for coconut samples of 4 mm thickness.

70 ºC	**Modified Henderson and pabis**	**K = -1.487, a = 0.0969, g = 0.3982, b = 0.0321, h = 1.0607, c = 0.3147**	**0.9971**	**0.0117**	**0.0002**
	Modified Page I	K = 0.2677, n = 0.6444	0.979	0.032	0.0011
	Modified Page II	K = 1.0417, a = 0.0056, n = 0.616, L = 0.0008	0.9802	0.0313	0.0011
	Two term exponentials	K = -0.0615, a = -0.2375	0.6034	0.138	0.0203
	Peleg	a = 2.057, b = 0.9846	0.9923	0.0195	0.0004
60 ºC	Newton	K = 0.2846	0.9882	0.0475	0.0023
	Henderson and Pabis	K = 0.2477, a = 0.8868	0.9791	0.0371	0.0015
	Page	K = 0.427, n = 0.7265	0.9981	0.0102	0.0001
	Logarithmic	K = 0.3446, a = 0.8914, c = 0.0656	0.9892	0.0235	0.0006
	Two term	K = 0.1673, g = 0.1472, a = 2.5277, c = -1.6963	0.9648	0.0436	0.0021
	Verma et al.	K = 0.2856, g = 0.2848, a = -1.3819	0.9886	0.045	0.0022
	Diffusion	K = 0.234, g = 0.9923, a = 20.6985	0.9862	0.0478	0.0025
	Midili et al.	K = 0.3036, b = 0.002, a = 0.9234, n = 0.9212	0.9916	0.0207	0.0005
	Wang and smith	a = -0.1605, b = 0.0063	0.9067	0.1103	0.0128
	Hii et al.	K = 0.3665, g = 0.7653, a = 0.9606, c = 0, n = 0.7916	0.9958	0.0148	0.0003
	Modified Henderson and pabis	K = -7.2489, a = 0.0807, g = 1.7682, b = 0.0375, h = 6.33, c = 0.1105	0.97	0.039	0.0018
	Modified Page I	K = 0.3099, n = 0.7257	0.9982	0.0097	0.0001
	Modified Page II	K = 1.9946, a = 0.0008, n = 0.7492, L = 0.0002	0.9979	0.0106	0.0001
	Two term exponentials	K = -0.0508, a = -0.265	0.6404	0.1355	0.0194
	Peleg	**a = 2.0627, b = 0.9157**	**0.9991**	**0.0069**	**0.0001**
50 ºC	Newton	K = 0.2323	0.9933	0.0336	0.0012
	Henderson and Pabis	K = 0.2177, a = 0.9434	0.989	0.0302	0.001
	Page	K = 0.3107, n = 0.8237	0.9946	0.0184	0.0004
	Logarithmic	K = 0.2887, a = 0.935, c = 0.0665	0.9988	0.0085	0.0001
	Two term	K = 0.2718, g = 0.3036, a = 2.7455, c = -1.7971	0.9895	0.0349	0.0014
	Verma et al.	K = 0.235, g = -0.4294, a = 1	0.9923	0.0279	0.0008
	Diffusion	K = 0.2586, g = 1.006, a = 18.0861	0.9938	0.0352	0.0013
	Midili et al.	K = 0.3508, b = 0.0027, a = 1.0567, n = 0.8338	0.9965	0.0142	0.0002
	Wang and smith	a = -1.1448, b = 0.0052	0.9347	0.0874	0.008
	Hii et al.	K = 0.3497, g = -0.4188, a = 1.0427, c = 0, n = 0.7765	0.9949	0.0177	0.0004
	Modified Henderson and pabis	**k = -16.4817, a = 0.2603, g = 1.034, b = 0.1467, h = 16.4595, c = 0.2694**	**0.9989**	**0.008**	**0.0001**
	Modified Page I	K = 0.2417, n = 0.8163	0.9943	0.0189	0.0004
	Modified Page II	K = 1.0387, a = 0.0008, n = 0.7801, L = 0.0004	0.9947	0.018	0.0004
	Two term exponentials	K = -0.0505, a = -0.2494	0.6332	0.1453	0.0222
	Peleg	a = 2.7545, b = 0.8894	0.9937	0.0196	0.0004
40 ºC	Newton	K = 0.0588	0.8644	0.0942	0.0091
	Henderson and Pabis	K = 0.0388, a = 0.8116	0.8315	0.056	0.0033
	Page	K = 0.2186, n = 0.4641	0.9732	0.0225	0.0005
	Logarithmic	K = 0.048, a = 0.7172, c = 0.1031	0.8471	0.0534	0.0031
	Two term	K = 0.0414, g = 0.0426, a = 2.2248, c = -1.4108	0.832	0.0561	0.0035
	Verma et al.	K = 0.0741, g = -0.2838, a = 0.9989	0.9159	0.0628	0.0043
	Diffusion	K = 0.0665, g = 1.0052, a = 22.6842	0.8642	0.0948	0.0097
	Midili et al.	K = 0.236, b = 0.0012, a = 1.0138, n = 0.4474	0.9735	0.0214	0.0005

Table 2 (continues). Drying model constants and goodness of fit parameters for coconut samples of 4 mm thickness.

40 ºC	Wang and smith	a = -0.065, b = 0.0017	0.9055	0.0652	0.0044
	Hii et al.	K = 0.2136, g = -0.1505, a = 0.9868, c = 0, n = 0.4497	0.9625	0.0255	0.0007
	Modified Henderson and pabis	k = -9.6475, a = 0.0945, g = 3.2654, b = 0.0498, h = 7.3452, c = 0.1176	0.9943	0.01	0.0001
	Modified Page I	K = 0.0321, n = 0.4181	0.9665	0.0244	0.0006
	Modified Page II	K = 1.0396, a = 0.0014, n = 0.397, L = 0.00	0.9687	0.0234	0.0006
	Two term exponentials	K = -0.0338, a = -0.1564	0.6574	0.0774	0.0062
	Peleg	**a = 5.2046, b = 1.534**	**0.9995**	**0.003**	**0.0001**

Effective Moisture Diffusivity and Activation Energy

The moisture diffusivity that was obtained for the coconut slices were presented in Table 3, the values ranges between $6.06 \times 10^{-11}\, m^2\, s^{-1}$and $3.16 \times 100^{-10}\, m^2\, s^{-1}$ for 4 mm thickness, $5.46 \times 10^{-10}\, mm^2\, s^{-1}$and $1.44 \times 10^{-9}\, m^2 s^{-1}$ for 8 mm thickness, $5.97 \times 10^{-10}\, m^2\, s^{-1}$and $2.83 \times 10^{-9}\, m^2\, s^{-1}$ for 12 mm thickness. In addition, the rise in the temperature of the laboratory oven increases the moisture diffusivity coefficient of the coconut slices sample. The D_{eff} values recorded for the coconut slices was within the 10^{-12}-10^{-08} m^2 s^{-1} posited for moisture removal from agricultural material by Doymaz (2005).

The activation energy was measured based on the slope of $\ln(D_{eff})$ against temperature inverse $\left(\frac{1}{T+273.15}\right)$. The activation energy of the coconut slices ranges between 27.44892 and 27.563 $kJ\, mol^{-1}$ for 4 mm thickness, 27.45371 and 27.53017 $kJ\, mol^{-1}$ for 8 mm thickness, 35.64817 and 35.84369 $kJ\, mol^{-1}$ for 12 mm, respectively.

Table 3. Activation energy, E_a and Effective moisture diffusivity, $D_{eff.}$

Thickness		80 ºC	70 ºC	60 ºC	50 ºC	40 ºC
4 mm	$D_{eff} \times 10^{-10}$	2.91	2.14	3.16	2.64	6.06×10^{-1}
	E_a	27.449	27.496	27.515	27.527	27.563
	$d_o \times 10^{-10}$	0.244	0.179	0.264	0.221	0.051
8 mm	$D_{eff} \times 10^{-9}$	1.09	9.44×10^{-1}	1.44	5.46×10^{-1}	3.57×10^{-1}
	E_a	27.454	27.500	27.511	27.530	27.46955
	$d_o \times 10^{-9}$	0.192	0.142	0.209	0.174	0.040
12 mm	$D_{eff} \times 10^{-9}$	2.83	2.64	1.57	1.19	5.97×10^{-1}
	E_a	35.648	35.737	35.719	35.741	35.844
	$d_o \times 10^{-9}$	0.465	0.435054	0.259	0.196	0.098

CONCLUSION

In conclusions of the mathematical modelling of the drying characteristics of coconut slices:

1. The drying process happened in a continuous falling rate and no constant drying rate was recorded.
2. The moisture diffusivity value ranges between $6.06 \times 10^{-11}\, m^2\, s^{-1}$ and $3.16 \times 10^{-10}\, m^2\, s^{-1}$ or 4 mm thickness, $5.46 \times 10^{-10}\, m^2 s^{-1}$ and $1.44 \times 10^{-9}\, m^2\, s^{-1}$ for 8 mm thickness, $5.97 \times 10^{-10}\, m^2\, s^{-1}$ and $2.83 \times 10^{-9}\, m^2\, s^{-1}$ for 12 mm thickness.

3. The activation energy of the sample ranges between 27.44892 and 27.563 $kJ\ mol^{-1}$ for the 4mm thickness, 27.45371 and 27.53017 $kJ\ mol^{-1}$ for 8mm thickness, 35.64817 and 35.84369 $kJ\ mol^{-1}$ for 12mm, respectively.
4. Among the fifteen thin-layer mathematical model considered in this study, the Modified Henderson Pabis, Page and Peleg model were chosen as the most appropriate model for effective prediction of the experimental data for 4 mm, 8 mm and 12 mm thickness respectively. Therefore, they are recommended for effective prediction of the drying characteristics of the coconut slices.

DECLARATION OF COMPETING INTEREST

The authours declare that they have no conflict of interest.

CREDIT AUTHORSHIP CONTRIBUTION STATEMENT

John Isa: Conceptualization, methodology, investigation, review and writing original.
Kabiru Ayobami Jimoh: Formal analysis, data curation, validation, visualisation and editing.

REFERENCES

Akpinar EK (2006). Determination of suitable thin layer drying curve model for some vegetables and fruits. *Journal of Food Engineering, 73: 75-84.*

Arslan D and Ozcan MM (2010). Study the effect of sun, oven and microwave drying on the quality of onion slices. *LWT Food Science Technology, 43: 1121-1127.*

Ayensu A (1997). Dehydration of food crops using a solar dryer with convective heat flow. *Solar Energy, 59: 121-126.*

Bozkir H, Ergun AR, Tekgu Y and Baysa T (2018). Ultrasound as pretreatment for drying garlic slices in microwave and convective dryer. *Food Science and Biotechnology*, *28: 347-354*.

Caliskan G, Dirim SN (2017). Drying characteristics of pumpkin (*Cucurbita moschata*) slices in convective and freeze dryer. *Heat Mass Transfer, 53: 2129-2141.*

Celen S, Kahveci K, Akyol U and Haksever A (2010). Drying behaviour of cultured mushrooms. *Journal of Food Processing and Preservation*, *34(1): 27-42.*

Da Silva, WP, eSilva, CMDPS, Gama FJA and Gomes JP (2014). Mathematical models to describe thin-layer drying and to determine drying rate of whole bananas. *Journal of the Saudi Society of Agricultural Sciences, 13(1): 67-74.*

Demiray E, Seker A and Tulek Y (2017). Drying kinetics of onion (*Allium cepa* L.) slices with convective and microwave drying. *Heat Mass Transfer, 53: 1817-1827.*

Dissa AO, Bathiebo DJ, Desmorieux H, Coulibaly O and Koulidiati J (2011). Experimental characterisation and modelling of thin layer direct solar drying of Amelie and Brooks mangoes. *Energy*, *36(5): 2517-2527.*

Doymaz I (2005). Sun drying of figs: An experimental study. *Journal of Food Engineering, 71: 403-407.*

Doymaz I and Pala M (2002). Hot-air drying characteristics of red pepper. *Journal of Food Engineering*, *55(4): 331-335.*

FAO (2010). Food and Agricultural Organization of the United Nation. Economic and Social Department. Statistic Division.

Garcia CC, Mauro MA and Kimura M (2007). Kinetics of osmotic dehydration and air drying of pumpkins (*Cucurbita moschata*). *Journal of Food Engineering, 82: 284-291.*

Gowen AA, Abu-Ghannam N, Frias J and Oliveira J (2008). Modelling dehydration and rehydration of cooked soybeans subjected to combined microwave-hot-air drying. *Innovative Food Science and Emerging Technologies*, *9(1): 129-137.*

Guine RPF and Fernandes RMC (2006). Analysis of the drying kinetics of chestnuts. *Journal of Food Engineering, 76: 460-467.*

Hii CL, Law CL, Cloke M and Suzannah M (2009). Thin layer drying kinetics of cocoa and dried product quality. *Biosystems Engineering, 102(2): 153-161.*

Horner WFA (1993). Drying: chemical changes in: Macrae R, Robinson R. K., Sadler M. J. (Eds) Encyclopedia of Food Science, Food Technology and Nutrition, *Academic Press*, London, Pp. 1485-1489.

Ikrang EG and Umani, KC (2019). Optimization of process conditions for drying of catfish (*Clarias gariepinus*) using Response Surface Methodology (RSM). *Food Science and Human Wellness, 8: 46-52.*

Kaleemullah S and Kailappan R (2006). Modelling of thin- layer drying kinetics of red chilies. *Journal of Food Engineering, 76(4): 531-537.*

Karaaslan SN and Tuncer IK (2008). Development of a drying model for combined microwave fan assisted convection drying of spinach. *Biosystems Engineering, 100(1): 44-52.*

Karathanos VT (1999). Application of thin layer equation to drying data of fresh and semi dried fruits. *Journal of Agricultural Engineering Research, 74(4): 355-361.*

Kashaninejad M, Mortazavi A, Safekordi, A and Tabil LG (2007). Thin-layer drying characteristics and modelling of pistachio nuts. *Journal of Food Engineering, 78: 98-108.*

Kaveh M, Sharabiani VR, Chayjan RA, Taghinezhad E, Gilandeh YA and Golpour I (2018). ANFIS and ANNs model for prediction of moisture diffusivity and specific energy consumption potato, garlic and cantaloupe drying under convective hot air dryer. *Information Processing in Agriculture, 5: 372-381.*

Lahsasni S, Kouhila M, Mohrouz M and Jaouhari JJ (2004). Thin layer convective solar drying and mathematical modeling of prickly pear peel (*Opuntia ficus* indica). *Energy, 29: 211-224.*

Madhiyanon T, Phila A and Soponronnarit S (2009). Models of fluidized bed drying for thin-layer chopped coconut. *Applied Thermal Engineering, 29: 2849-2854.*

Midilli A and Kucuk H (2003). Mathematical modeling of thin layer drying of pistachio by using solsr energy. *Energy Conversion Management, 44(11): 11-22.*

Moreira R, Chenlo F, Chaguri L and Vázquez G (2005). Mathematical modelling of the drying kinetics of chestnut (*Castanea Sativa Mill.*): Influence of the natural shells. *Food and Bioproducts Processing, 83(4): 306-314.*

Murthy TPK and Manohar B (2012). Microwave drying of mango ginger (*Curcuma amada* Roxb): prediction of drying kinetics by mathematical modelling and artificial neural network. *International Journal of Food Science and Technology, 47(6): 1229-1236.*

Onwude DI, Hashim N, Abdan K, Janius R and Chen G (2018). Modelling the mid-infrared drying of sweet potato: Kinetics, mass and heat transfer parameters, and energy consumption. *Heat Mass Transfer, 54: 2917-2933.*

Piga A, Pinna I, Ozer KB Agabbio M and Aksoy U (2004). Hot air dehydration of figs (*Ficus carica* L.): drying kinetics and quality loss. *International Journal of Food Science Technology, 39: 793-799.*

Sacilik K, Keskin R and Elicin AK (2006). Mathematical modeling of solar tunnel drying of thin layer organic tomato. *Journal of Food Engineering, 73: 281-289.*

Sharma GP, Prasad S, Chahar VK (2009). Moisture transport in garlic cloves undergoing microwave-convective drying. *Food and Bioproducts Processing, 87: 11-16.*

Sigge GO, Hansmann CF and Joubert E (1998). Effect of temperature and relative humidity on the drying rates and drying times of green bell papers (*Capsicum annum* L.). *Drying Technology, 16: 1703-1714.*

Tarigan E, Prateepchaikul G, Yamsaengsung R, Sirichote A and Tekasakul P (2007). Drying characteristics of unshelled kernels of candle nuts. *Journal of food Engineering, 79: 828-833.*

Toğrul IT and Pehlivan D (2002). Mathematical modeling of solar drying of apricots in thin layers. *Journal of Food Engineering, 55: 209-216.*

Uwubanwen IO (2011). Harnessing the potentials of the coconut palm in the Nigeria economy. *Journal of Agricultural Engineering, 23: 3-27.*

Wang CY and Singh RP (1978). A single layer drying equation for rough rice. American society Agricultural Engineering, Paper No. 78-3001*, St. Joseph, MI,* USA.

Wang Z, Sun J, Liao X, Chen F, Zhao G, Wu J and Hu X (2007). Mathematical modeling on hot air drying of thin layer apple pomace. *Food Research International, 40: 39-46.*

Yaldiz O and Ertekin C (2001). Thin layer solar drying of some vegetables. *Drying Technology, 19: 583-596.*

Yaldiz O, Ertekin C and Uzun HI (2001). Mathematical modelling of thin layer solar drying of Sultana grapes. *Energy, 26(5): 457-465.*

Younis M, Abdelkarim D and El-abdein AZ (2018). Kinetics and mathematical modeling of infrared thin-layer drying of garlic slices. *Saudi Journal of Biological Science, 25: 332–338.*

Turkish Journal of Agricultural Engineering Research

https://dergipark.org.tr/en/pub/turkager
https://doi.org/10.46592/turkager.2021.v02i02.011

Turk J Agr Eng Res (TURKAGER)
e-ISSN: 2717-8420
2021, 2(2): 376-389

Research Article (Araştırma Makalesi)

Determination of Factors Affecting Tractor Brand Preference Farmer of Erzurum Province

Servan BAYBAS[ID][a], **Adem AKSOY**[ID][b]*

[a]*Bingöl Tarım Kredi Kooperatifi 1200, Merkez, Bingöl, TÜRKİYE*

[b]*Tarım Ekonomisi Bölümü, Ziraat Fakültesi, Atatürk Üniversitesi, 25240, Erzurum, TÜRKİYE*

(*): Corresponding author, aaksoy@atauni.edu.tr

ABSTRACT

In this study; it is aimed to identify and reveal the factors which affect the choice of tractor farmers about brand of tractor in Erzurum where mechanization in agriculture, particularly the number of tractors, is increasing day by day. Another aim of the studyis to revealif the farmers are conscious or not about purchasing tractors. With this aim one to interviews were reconciled with 200 bussinesses which own tractors in Erzurum in 2020 and a number of questions were asked to the producers to decide the factors, affect the manufacturers brand selection. probit and Multinominal regression model were used in the study. According to the results of the research farmers attach the most importance to endurance fuel consumption spare parts status, service status, dealer network and brand image, in turn. 75% of the farmers prefer the same brand when they change their tractors. Spare parts and brand image were effective in the prefence of brand A fuel and service in the prefence of brand B and durability in the prefence of other brand groups. According to the results of the study, farmers must be trained about the maintenance and use of tractors. This training can be provided by tractor manufacturers or various official institutions.

RESEARCH ARTICLE

Received: 08.09.2021
Accepted: 18.11.2021

Keywords:

- Mark preference,
- Tractor,
- Erzurum,
- Probit,
- Farmer

To cite: Baybas S, Aksoy A (2021). Determination of Factors Affecting Tractor Brand Preference of Erzurum Province Farmers. Turkish Journal of Agricultural Engineering Research (TURKAGER), 2(2), 376-389. *https://doi.org/10.46592/turkager.2021.v02i02.011*

Erzurum İli Çiftçilerinin Traktör Marka Tercihini Etkileyen Faktörlerin Belirlenmesi

ÖZET

Bu çalışmada; tarımda mekanizasyonun özellikle de traktör sayısının her geçen gün arttığı Erzurum ilinde çiftçilerin traktör alırken marka tercihinde etkili olan faktörlerin tespit edilerek ortaya konması amaçlanmıştır. Çiftçilerin traktör satın alımında bilinçli davranıp davranmadığının ortaya konması çalışmanın bir diğer amacıdır. Bu amaçla 2020 yılında Erzurum ilinde traktör sahibi olan 200 işletme ile anket yapılarak çiftçilerin marka seçiminde etkili olan faktörler belirlenmeye çalışılmıştır. Çalışmada, Probit ve Multinominal Probit Regresyon Modelleri kullanılmıştır. Araştırma sonuçlarına göre çiftçiler sırasıyla en çok dayanıklılık, yakıt tüketimi, yedek parça durumu, servis hizmetleri, bayi ağı ve marka imajına önem vermektedir. Çiftçilerin %75'i traktörlerini değiştirmeleri durumunda aynı markayı tercih etmektedirler. A markasının tercih edilmesinde yedek parça ve marka imajı, B Markasının tercih edilmesinde yakıt ve servis hizmetleri, diğer marka gruplarının tercih edilmesinde ise dayanıklılık kriteri etkili olmuştur. Çalışma sonucunda çiftçilere mutlaka traktör bakım ve kullanımı konusunda eğitim verilmesinin gerekli olduğu ortaya çıkmıştır.

ARAŞTIRMA MAKALESİ

Alınış tarihi: 08.09.2021
Kabul tarihi: 18.11.2021

Anahtar Kelimeler:

- Marka tercihi,
- Traktör,
- Erzurum,
- Probit,
- Çiftçi

Alıntı için: Baybas S, Aksoy A (2021). Erzurum İli Çiftçilerinin Traktör Marka Tercihini Etkileyen Faktörlerin Belirlenmesi. Turkish Journal of Agricultural Engineering Research (TURKAGER), 2(2), 376-389. https://doi.org/10.46592/turkager.2021.v02i02.011

GİRİŞ

Tarımda çağdaş üretim tekniklerinin uygulanabildiği gelişmiş araç ve makinelerin kullanılmasına tarımsal mekanizasyon denir. Tarımda makine kullanımı kırsal alanda yapılacak olan işlerin hem kolaylaşmasını hem de verimliliğin ve karlılığın artmasını sağlamaktadır (Koçtürk ve Avcıoğlu, 2007).

Tarımsal mekanizasyonda ilk uygulamalar, "toprak işleme" alanında basit el aletlerinin kullanımı ile başlamıştır. Sonraki zamanlarda bu basit el aletlerinin çekimi güçlü iş hayvanları ile sağlanmıştır. 1800'lü yılların sonlarına doğru, buhar gücü ile çalışan traktörler üretilip 1900'lü yılların ilk çeyreğine kadar kullanılmıştır. 1950 yılına kadar mekanizasyon uygulamalarının artmasıyla birlikte üretimde ciddi artışlar yaşanmıştır. 1970'lerden sonra belli başlı tarım teknikleri uygulanmaya başlanmıştır. 1990'lı yılların başında kontrol sistemleri ve bilgisayar, elektronik teknikler tarımda kullanılmıştır. 1995'ten bu yana arazilerdeki parametreleri hesaba katan "hassas uygulamalı tarım teknolojileri" uygulanmıştır. Bu ve benzer teknolojiler üzerine yapılan bilimsel çalışmalar yoğun bir şekilde sürmektedir. Bugün, tarımda sürücüsüz biçerdöver ve traktör kullanımı uygulamaları mevcuttur (Anonim, 2014).

Tarımsal mekanizasyonda yaşanan hızlı gelişmeler sayesinde birim alandan elde edilen ürünlerde önemli artışlar olmuştur. Ayrıca kırsal alanlarda üretim tekniklerinin ve yeni yöntemlerin gelişmesini sağlamıştır. Buna ek olarak tarımsal mekanizasyon birçok teknolojik uygulamanın ekonomik ve teknik anlamda etkinliğini arttırıp, çalışma koşullarını iyileştirmektedir. Böylelikle uygun teknoloji kullanımı ile çiftçilerin daha fazla verim almasına yardımcı olmaktadır (Saral ve ark., 2000).

Tarım işletmelerinde mekanizasyon, en büyük paya sahip girdi yatırımıdır. İşletmeler zamanı daha verimli kullanmak ve daha fazla ekonomik fayda sağlayabilmek için makineleşmeye gitmektedirler. Yine ülkeler üretim maliyetini minimuma çekmek için iş gücü yerine makine ikamesine gitmektedirler. Bu durum da mekanizasyonun önemini her geçen gün arttırmaktadır. Bu nedenlerle özellikle traktör; bölge ve ülkelerin tarımsal mekanizasyon seviyelerinin belirlenmesinde göz önünde bulundurulması gereken en önemli araçtır (Moens ve Wanders, 1984; Işık, 1988; Sümer ve ark., 2003).

Özellikle traktör, uzun yıllar boyunca tarımsal mekanizasyonun tek göstergesi olmuştur (Akdemir ve ark., 1999). Bu sebeple işletmecilerin rantabl karlı bir üretim yapabilmesi için ihtiyaçlara en iyi şekilde yanıt verecek traktör seçimi yapması gerekmektedir. Traktör seçimine işletmenin büyüklüğü, arazi yapısı, toprak özelliği, iklim koşulları, üretim şekli ve işletmecinin sosyo-ekonomik yapısı etki eden faktörlerdendir (Işık, 1996).

Çiftçiler traktör marka seçiminde yeni teknolojili birçok seçenekle karşı karşıyadırlar. Reklam, broşür, satış elemanı ve arkadaş tavsiyesi faktörü gibi bir takım kaynaktan etkilenmektedirler (Cankurt ve ark., 2009; Cankurt ve Miran, 2010). İşletmeciler ürünün performansı hakkında net bir bilgiye sahip olmayıp seçeneklerin zaman içerisinde değişmesi marka tercihlerinin de değişimine neden olabilmektedir (Aytuğ ve Karadibak, 1998).

Bu çalışmanın amacı, Erzurum ilinde çiftçilerin traktör marka tercihinde etkili olan faktörlerin tespit edilerek ortaya konması ve üretici firma yetkilileri ve politika yapıcılarına faaliyetlerini yönlendirmelerinde yardımcı olabilecek bilgiler sunmaktır. Bu çerçevede; çiftçilerin traktör satın almasını etkileyen faktörlerin irdelenmesi ve traktör marka tercihi ile çiftçi ve işletme özellikleri arasında bir ilişki olup olmadığının tespiti ve çiftçilerin traktör kullanım memnuniyetinin belirlenmesi amaçlanmıştır.

MATERYAL ve YÖNTEM

Tarımsal mekanizasyon; teknolojik uygulama faaliyetlerinin arttırılması, çalışma koşullarının iyileştirilmesi ve böylece üretimde ekonomikliğin sağlanması yönünden önemli bir öğedir (Altuntaş ve Demirtola 2004). Mekanizasyon, tarım işletmelerinin ekonomik ve teknik yapısına bağlı olarak farklı düzeylerde uygulanmaktadır (Zeren ve ark., 1995).

Erzurum il geneli toplam 12429 adet traktör bulunmaktadır. Bu traktörlerin 12067'si (%97) iki akslı traktörlerden oluşmaktadır. İki akslı traktörler içerisinde 51-70 kW güç grubunda bulunan traktörler sayıca en fazladır (TÜİK, 2020).

Materyal

Çalışmada 2020 yılı Erzurum merkez ve ilçelerinde traktör sahibi olan 200 üreticiden anket yoluyla elde edilen veriler birincil veri kaynağını oluşturmuştur. İkincil veriler ise ilgili internet sayfaları, Birleşmiş Milletler Gıda ve Tarım Teşkilatı (FAO), Türkiye İstatistik Kurumu (TÜİK) Yayınları, ulusal ve uluslararası düzeyde yapılan çalışmalardan elde edilmiştir. Çalışmada *Etik Kurul Kararı* alınmıştır.

Metot

Erzurum ilinin, ilçeleri her biri kendi aralarında benzerlik içeren 4 farklı alt bölgeye ayrılmıştır. İlçelerin seçiminde her bir agroekolojik alt bölge içerisinden diğer ilçeleri de yansıtan bir ilçe seçilmiştir. Böylece Erzurum ilini temsil edecek 4 ilçe araştırma alanı olarak belirlenmiştir (Oltu, Horasan, Pasinler, Karayazı). Alt bölgelerdeki ilçelerin seçiminde ilçelerin sahip olduğu traktör sayıları dikkate alınarak seçim yapılmıştır (Anonim, 2004).

Bu çalışmada, 2020 yılı Erzurum ilinde traktör sahibi olan işletmelerle bire bir görüşülüp üreticilere bazı sorular sorularak üreticilerin marka seçiminde etkili olan faktörler belirlenmeye çalışılmıştır. Bunun için örnek hacmi; oransal örnekleme yöntemi ile belirlenmiştir. Örnek hacminin belirlenmesinde yüzde 90 güven aralığı, yüzde 5 hata payı ile çalışılmıştır. Aksoy ve ark. (2019) bölgede yaptıkları benzer çalışmada traktör değişiminde çiftçilerin %77'sinin aynı markayı tercih edeceklerini ifade ettikleri için çalışmada p: 0.77 alınmıştır. Örnek sayısının belirlenmesinde kullanılan formül aşağıda verilmiştir (Newbold, 1995; Miran, 2007).

$$n = \frac{N*p*(1-p)}{(N-1)*\sigma^2{}_p+p*(1-p)} \quad (1)$$

n: Örnek hacmi

N: Erzurum ilinde traktöre sahip işletme sayısı

p: Traktör değişiminde aynı markayı tercih eden çiftçilerin oranı, (maksimum örnek hacmine ulaşmak için 0.77 alınmıştır)

$\sigma^2{}_p$: Varyansı vermektedir. (0.00092)

Erzurum ilinde toplam 12429 adet traktör mevcuttur. %90 güven aralığı ve %5 hata ile örnek hacmi 192 bulunmuştur. Anketlerden bazılarının eksik doldurulabileceği düşüncesi ile 8 adet artırılarak örnek hacmi 200'e çıkarılmıştır.

Probit Model

Bağımlı değişkenin temelde iki değer alabilmesi durumunda sınırlı bağımlı değişken modelleri kullanılır. Olayın varlığı ya da yokluğu gibi iki durum var ise olayın olma durumunda bağımlı değişken "1", olmama durumunda ise "0" değerini almaktadır (Yavuz 2001; Gujarati, 2006).

Bu durumlarda model tahmininde dört yöntem kullanılmaktadır. Bunlar; Doğrusal Olasılık Modeli, Logit Modeli, Probit Modeli ve Tobit Modeli'dir. Doğrusal Olasılık Modelinde olasılık sınırları bazı durumlarda 0-1 sınırları dışına düşmektedir. Probit ve Logit modellerinde tahmin edilen olasılık 0-1 aralığındadır. Bağımlı değişkeni "evet-hayır" ya da "var-yok" yanıtlarından oluşan regresyon modellerinde Logit ya da Probit modelleri güvenilir sonuçlar vermektedir (İnal ve ark., 2006). Logit ve Probit modelleri birbirine benzer olduğundan bunlardan hangisinin kullanılacağına araştırmacı karar vermektedir (Sarımeşeli, 2000; Gujarati, 2006). Tobit modelinde ise sınırlanmış alt veya üst limite sahip bağımlı değişken bulunmaktadır. Bu modelde sansürlenmiş ya da kesilmiş bağımlı değişkenler bulunmaktadır.

Probit modelinde, bir olayın olma ya da olmama durumu veya kararı gözlenmeyen bir fayda indeksine bağlı olduğu varsayılmaktadır. Söz konusu fayda indeksi I_i ile ifade edilecek olur ise; I_i, bağımsız değişkenlere bağlıdır: Öyle ki, I_i indeksinin büyüklüğü ölçüsünde söz konusu olayın olma yani gerçekleşme ihtimali artmaktadır. I_i, indeksi,

$$I_i = \beta_1 + \beta_2 X_i \quad (2)$$

Burada;

$\beta_1 =$ Sabit değer,

$\beta_2 =$ X ile ifade edilen değişkene ait katsayı,

$X_i =$ Bağımsız değişken değeri şeklinde ifade edilmektedir. I_i ile bir olayın gerçekleşme ya da geçekleşmeme durumu arasındaki ilişki olay gerçekleşmiş ise "1", gerçekleşmemiş ise "0" ile ifade edilmektedir. Her bağımlı değişken için I_i'nin kritik veya başlangıç değerinden itibaren söz konusu olayın gerçekleşme durumu ortaya çıkmaktadır. Başlangıç değeri I_i * ile ifade edilecek olursa; I_i değeri ancak I_i * değerini aştığında olay meydana gelecek aksi halde gelmeyecektir. I_i *'ın Ii'den küçük veya eşit olma ihtimali aşağıdaki şekilde yazılabilir. Formül 3'te P_i olayın gerçekleşme ihtimalini, P_r ise Probit modelini ifade etmektedir (Gujarati, 2006).

$$P_i = P_r\,(Y = 1) = P_r\,(I_i^* \leq I_i) = F(I_i) \quad (3)$$

Probit modellerinde belirlilik katsayısını ifade eden R^2 değeri, modelin fonksiyonel biçiminin iyi seçilip seçilmediği konusunda göz önüne alınmamaktadır. Bu nedenle modelin en uygun şekilde belirlenmesi konusunda değişkenlerin katsayıları ve P değerleri dikkate alınmaktadır (Gujarati, 2006; Akkaya ve Pazarlıoğlu, 1998).

Multinominal Probit Model

Multinominal Probit Modeli, çıktı kategorileri içerisinde tüm olası karşılaştırmalar için iki değerli logit modellerinin eş anlı biçimde tahminlenmesidir. Multinominal Probit Modeli iki değerli logit modelinin genişletilmiş halidir. İki değerli probit modelinden elde edilen tahminler Multinominal Probit Modeli'nin parametrelerinin tahminlerinin tutarlı olmasını sağlamaktadır (Begg ve Gray, 1984).

Araştırmada, Erzurum ili çiftçilerinin satın alınan traktörün parasını ödeme şekli üzerinde etkili olan yaş, eğitim, hanedeki birey sayısı, arazi miktarı, tarım dışı gelir, sulu arazi, traktörle işlenen ve arazi gibi faktörler kriterler olduğundan, etkili olabilecek kriterlerin değerlendirilmesinde multinominal probit modeli kullanılmıştır. Bu kapsamda, çiftçilerin mevcut traktörlerinden memnunum, memnun değilim, kararsızım şeklinde cevap verenler için ayırt edici olan etkenler tespit edilmeye çalışılmıştır. Multinomial probit regresyonda bağımlı değişkenler K sayıda kategoriye sahipse; karşılığında bağımlı ve bağımsız parametreleri tanımlayan ve kategorileri referans kategoriyle mukayese eden K-1 sayıda eşitlik olmalıdır (Menard, 2002).

$$g_h(X_1, X_2, \ldots\ldots, X_k) = e^{(a_h + b_{h1}X_1 + b_{h2}X_2 + \ldots + b_{hk}X_k)}$$

h = 1, 2, ... , M – 1 , (0.1)

k simgesi özel bağımsız X değişkenlerini işaret ederken, simge h, Y bağımsız değişkenin, $g_0(x_1, x_2, \ldots x_k) = 1$. Y'nin h_0 dışındaki h'nin herhangi bir değerine eşit olma olasılığı;

Y'nin h_0 dışındaki h'nin herhangi bir değerine eşit olma olasılığı;

$$P(Y = h\ I\ X_1, X_2, \ldots X_k) = \frac{e(a_h + b_{h1}X_1 + b_{h2}X_2 + \ldots + b_{hk}X_k)}{1 + \sum_{h=1}^{M-1} e(a_h + b_{h1}X_1 + b_{h2}X_2 + \ldots + b_{hk}X_k)}$$

h= 1, 2, ... , M – 1, (0.2)

h_0 = M ya da 0 için,

$$P(Y = h\ I\ X_1, X_2, \ldots X_k) = \frac{1}{1 + \sum_{h=1}^{M-1} e(a_h + b_{h1}X_1 + b_{h2}X_2 + \ldots + b_{hk}X_k)}$$

h = 1, 2, ... M – 1. (0.3)

$$Y = \alpha_0 + \alpha_1 x_1 + \alpha_2 x_2 + \ldots\ldots\ldots\ldots\ldots \alpha_n x_n + u \qquad (4)$$

Y = Ödeme şekli: peşin (0), taksitli (1), banka kredili (2)
x_1 = İşletmecinin yaşını,
x_2 = İşletmecinin eğitim durumunu,
x_3 = Hanedeki birey sayısı,
x_4 = Toplam arazi büyüklüğü (51-100)
x_5 = Toplam arazi büyüklüğü (101-200)
x_6 = Toplam arazi büyüklüğü (201- >)
x_7 = Tarım dışı gelir
x_8 = Sulu arazi miktarı
x_9 = Traktörle işlenen arazi miktarı
α = Değişkenlerle ilgili katsayıları (α_0, α_1, α_2,..., α_n)
u = Hata terimini göstermektedir.

BULGULAR ve TARTIŞMA

Araştırma bölgesindeki işletmelerin sahip oldukları traktör markalarının dağılımı Çizelge 1'de verilmiştir. Çizelgede traktörler markalarına göre sınıflara ayrılmış üç grup belirtilmiştir. Grupların belirlenmesinde; anketlerde A marka grubu en çok tercih edilen marka, B marka grubu ikinci sırada tercih edilen marka ve son olarak diğer marka grubu bulunmaktadır. Traktör marka grupları içerisinde A markasını tercih edenlerin %40'lık, B markasını tercih edenler %23.5, diğer markaların ise %36.5 paya sahip oldukları görülmektedir.

Çizelge 1. İşletmelerin bulundurdukları traktör markalarına göre dağılımı
Table 1. *Distribution of tractors in the enterprises according to the brand category*

Traktör Markası	İşletme Sayısı	Toplam İçerisindeki Payı (%)
A Marka	80	40.0
B Marka	47	23.5
Diğer Markalar	73	36.5
Toplam	**200**	**100.0**

Orijinal hesaplamalar

Çizelge 2'de araştırma bölgesinde bulunan işletmelerin traktörlerini değiştirmeleri durumunda aynı traktör markasını tercih etmelerine göre dağılımı verilmiştir. Çizelgede aynı traktörleri tercih edecek olan işletmelerin toplam işletmelerdeki payı (%75.5) ve farklı marka traktör grubunu tercih edecek olan işletmelerin payı (%24.5) olarak belirlenmiştir. İşletmecilerin büyük bir bölümü mevcut traktörlerinden memnundurlar. Daha önce yapılan çalışmada çiftçilerin %77.8'i traktörlerini değiştirmeleri durumunda yine aynı marka traktör grubunu tercih etmişlerdir (Aksoy ve ark., 2019).

Çizelge 2. İşletmelerin aynı traktör markasını tercih etme durumlarına göre dağılımı.
Table 2. *Distribution according to the same tractor preference brand of enterprices.*

Tercih durumu	İşletme Sayısı	Toplam İçerisindeki Payı (%)
Evet	151	75.5
Hayır	49	24.5
Toplam	**200**	**100.0**

Orijinal hesaplamalar

Anket sonuçlarına göre çalışma alanında işletmelerin ilçe merkezine uzaklığı ortalama 16.48 km olduğu tespit edilmiştir. İşletmelerin ekilen arazi miktarı 5 ile 2000 da arasında değişmektedir. Ortalama 175 da olarak bulunmuştur. İşletmelerin sahip oldukları arazilerin parsel sayısına oranı 9.21 olarak tespit edilmiştir. Bu oran, Türkiye'de işletme başına düşen tarım arazisi parça sayısından (5.9) oldukça yüksek iken parsellerin ortalama büyüklüğüne bakıldığında anket uygulanan işletmelerin ortalama parsel büyüklüğü 19.21 da ile Türkiye ortalamasından (12.9 da) oldukça yüksek olduğu dikkati çekmektedir (TÜİK, 2020). İşletmelerin %91'i mülk arazide üretim yapmakta ve %12'lik kesim kiralama yoluyla üretim yaparken ortaklık yok denecek kadar azdır (Çizelge 3).

Anket uygulanan işletmelerde ortalama büyükbaş hayvan varlığı 18 olarak tespit edilmiştir. Bölgede daha önce yapılan bir çalışma incelendiğinde ortalama büyükbaş hayvan varlığını 19 adet hesaplamışlardır (Yıldırım, 2016).

Çizelge 3. İncelenen işletmelerle ilgili temel istatistikler.
Table 3. *Descriptive statistics about the enterprises.*

İşletme bilgileri	Min.	Maks.	Ortalama	Std. Sapma
İl merkezine uzaklık (km)	5	199	72.38	35.826
İlçe merkezine uzaklık (km)	0	134	16.48	14.352
		Arazi varlığı ve dağılımı		
Ekilen alan (da)	5	2000	175.50	286.748
Ekilen sulu alan (da)	0	800	33.42	96.981
Ekilen Kuru alan (da)	0	850	119.58	148.957
Nadasa bırakılan alan (da)	0	300	14.15	42.055
Çayır alanı(da)	0	700	21.80	59.329
Sebze alanı (da)	0	20	0.29	1.959
Parsel sayısı	1	42	9.21	7.016
Ort parsel büyüklüğü (da)	1	133	19.21	21.820
Parselin işletmeye uzaklığı (km)	0	60	6.45	8.314
		Arazinin Mülkiyet durumu		
Mülk arazi	0	1	0.91	0.294
Kira	0	1	0.12	0.332
Ortak	0	1	0.04	0.196
Büyükbaş hayvan varlığı	0	110	17.81	19.741
Küçükbaş hayvan varlığı	0	400	7.04	33.697
Hayvanları merada kalma süresi (ay)	0	8	4.41	2.576
Süt sağım makinası	0	1	0.24	0.428
Tarım sigortası yaptırma	0	1	0.62	0.488

Orijinal hesaplamalar

Araştırma bölgesinde anket uygulanan tüm çiftçilerin en az bir traktörü olup iki veya daha fazla traktöre sahip olan çiftçilerin oranı %3.5 olarak tespit edilmiştir. Çiftçilerin %53'ü tek çeker traktör tercih etmişlerdir. Traktör sahibi çiftçilerin %59'u traktörlerini sıfır ve %41'i ise ikinci el almışlardır. Çiftçilerin %49'u traktörü kredili almışlardır. Traktörlerin model yılına göre dağılımı Çizelge 4'te verilmiş olup 0-5 yaş (%32.5) ve 6-10 yaş (%31) aralığındaki traktörler yoğunluk göstermektedir. Çiftçilerin büyük bir bölümü yüksek modelli traktörleri tercih etmişlerdir. Traktörlerin bakım periyodu ağırlıklı olarak yıllık (%56.3) ve sezonluk (%35.5) yapılmakta olup günlük traktör bakımı yapılmamaktadır.

Çizelge 4. İşletmelerin sahip oldukları traktöre ait temel bilgiler.
Table 4. *Basic information of tractors owned by enterprises.*

Özellikler	***Sayı***	***%***
Tek Traktörü olan	193	100
İki ve daha fazla traktörü olan	7	3.5
Çekiş tipi		
2WD	106	53.0
4WD	94	47.0
Yılı		
2015->	65	32.5
2014-2010	62	31.0
2009-2000	40	20.0
1999- <	16	16.5
Gücü (hp)		
50-<	38	19.0
51-70	114	57.0
71->	48	24.0
Alınış Şekli		
Sıfır	118	59.0
İkinci el	82	41.0
Kredili	102	51.0
Peşin	98	49.0
Traktörün bakım periyodu		
Günlük	0	0.0
Haftalık	4	2.0
Aylık	12	6.0
Sezonluk	71	35.5
Yıllık	113	56.5

Orijinal hesaplamalar

Çizelge 5'e göre anket yapılan işletmelerin toplam alet makina varlığı 1086 adettir. Alet makina varlığında (traktör ve biçerdöver varlığı hariç) en yüksek paya sırasıyla tarım arabası (%18,3), ot toplama tırmığı (%15.5) ve pulluk (%14.5) sahiptir. Traktörü olan her işletmenin tarım arabası da mevcut olup, şeker pancarı hasat makinasına anket yapılan hiçbir işletmede rastlanmamıştır.

Çizelge 5. İşletmelerin sahip oldukları alet makina varlığı ve traktör başına düşen makina sayısı.

Table 5. *The number of tools and machinery owned by the enterprises and the number of machines per tractor.*

Makine cinsi	*Sayı*	*%*	*Makina Traktör^{-1}*
Römork	199	18.3	1.00
Pulluk	157	14.5	0.79
Kültivatör	35	3.2	0.18
Dipkazan	74	6.8	0.37
Toprak Frezesi	16	1.5	0.08
Merdane	80	7.4	0.40
Ekim makinası	68	6.3	0.34
Gübre dağıtma makinası	45	4.1	0.23
Patates dikim makinası	5	0.5	0.03
Çapa makinası	27	2.5	0.14
Çayır biçme makinası	125	11.5	0.63
Ot toplama tırmığı	168	15.5	0.84
İlaçlama makinası	25	2.3	0.13
Balya makinası	32	2.9	0.16
Harman makinası	14	1.3	0.07
Silaj makinası	9	0.8	0.05
Patates hasat makinası	7	0.6	0.04
Şeker Pancarı Hasat Makinası	0	0.0	0.00

Orijinal hesaplamalar

Yapılan anketler sonucunda çiftçilerin traktör marka tercihinde ilk sırada traktör fiyatına (4.73), ikinci sırada traktörün dayanıklılığına (4.66), üçüncü sırada traktörün seri olmasına (4.62) ve dördüncü sırada traktörün gücüne (4.56) önem vermektedirler (Çizelge 6). Marka seçiminde en az önem verilen kriterler ise tanıtım ve reklam (2.68), renk (2.72), satış elemanı/bayi tavsiyesi (3.03), dış görünümü (3.04) ve satış sonrası müşteri ziyaretleri (3.19) olarak sıralanmaktadır. Araştırma alanında daha önce yapılan çalışma incelendiğinde; ilk sırada yakıt tüketimi (4.8), ikinci sırada traktörün fiyatı (4.7) ve üçüncü sırada yedek parça (4.6) kriterinin önemli olduğu görülmektedir (Aksoy ve ark., 2019). Her iki çalışmada da traktör fiyatı benzer düzeyde önemli bulunmuştur.

Çizelge 6. Mevcut traktör markasının tercihinde etkili olan faktörler.
Table 6. *Factors influencing the brand preference of current tractor.*

Faktörler	1	2	3	4	5	Ort
Marka imajı	13.0	15.0	5.5	29.0	37.5	3.63
Dayanıklılık	0.0	2.5	2.0	23.0	72.5	4.66
Yakıt tüketimi	0.0	4.0	2.5	26.0	67.5	4.57
Yedek parça	1.5	2.5	3.5	30.0	62.5	4.50
Servis hizmetleri	4.0	5.0	6.5	35.0	49.5	4.21
Ürünün arkasında durması	8.5	5.5	8.0	36.5	41.5	3.97
Bayi ağı	17.0	12.5	18.0	28.5	24.0	3.30
Tanıtım ve reklam	38.0	13.0	8.5	24.5	16.0	2.68
Fiyat	5.0	4.0	0.0	12.5	83.0	4.73
İkici elinin kıymetli olması	4.0	7.0	5.0	27.0	57.0	4.26
İkinci elde kolay satımı	4.0	6.0	8.0	29.0	53.0	4.20
Satış sonrası müşteri ziyaretleri	17.5	20.5	11.0	27.0	24.0	3.19
Çift çeker olması	13.0	13.5	2.0	16.0	55.5	3.87
Soğutma (Klima) sistemi olması	10.5	15.5	2.0	24.5	47.5	3.83
Traktörün kabinli olması	9.0	7.5	1.5	21.0	61.0	4.17
Hidrolik direksiyon	3.5	6.0	1.0	34.5	55.0	4.31
Traktörün gücü	0.0	3.5	2.0	29.5	65.0	4.56
Tecrübe	1.0	7.0	2.5	43.5	46.0	4.27
Yeni nesil şanzıman sistemi	7.0	11.0	7.0	37.0	38.0	3.88
Aile (anne baba eş çocuklar) tavsiyesi	10.0	13.0	2.0	32.0	43.0	3.85
Arkadaş tavsiyesi	14.0	12.5	4.0	32.0	37.5	3.66
Bölgede yaygın kullanımı	12.0	9.5	6.0	35.0	37.5	3.76
Yakın çevrede kullanılıyor olması	11.5	8.5	8.5	34.5	37.0	3.77
Yetkili servis/tamirci tavsiyesi	16.5	17.0	5.5	34.0	27.0	3.38
Satış elemanı/bayi tavsiyesi	22.0	21.5	9.5	25.0	22.0	3.03
Renk	33.0	19.0	7.0	24.5	16.5	2.72
Dış görünümü	27.5	17.0	2.0	31.0	22.5	3.04
Seri olması	1.5	1.0	1.5	26.0	70.0	4.62
Servis masrafı	2.5	5.5	2.0	23.0	67.0	4.47
Kredi faizlerinin oranı	24.5	5.5	1.5	13.5	55.0	3.69

1= Hiç önemi yok, 2= Biraz önemli, 3=Kararsızım, 4=Oldukça önemli 5= Çok önemli

Çizelge 7 incelendiğinde Tarım dışı gelir ile A markası arasında çok önemli ($p<0.01$) ters yönlü bir ilişki olduğu dikkati çekmektedir.

Çiftçilerin traktör seçimi, yaptıkları üretime yönelik olması önemli olup arazi tipi ve arazi büyüklüğü en önemli değişkenlerdendir (Sağlam ve Çetin, 2017). Yine B markası ile arazi parsel sayısı ve parsel uzaklığı arasında %10 önem seviyesinde ters yönlü ilişki olduğu tespit edilmiştir. Parsel sayısı fazla olan ve parsel uzaklığı fazla olan çiftçiler B markasını tercih etmedikleri görülmektedir. Diğer traktör markaları ile parsel sayısı arasında pozitif önemli ($p<0.05$) ilişki bulunmuştur. Parsel sayısı artıkça çiftçiler diğer traktörleri satın almaktadırlar. Küçükbaş hayvan sayısı artıkça diğer markalara yönelme azalmaktadır. Bu durum istatistiki açıdan %5'te önemli bulunmuştur.

Çizelge 7. Çiftçilerin Traktör tercih kriterine ilişkin Probit Model Sonucu
Table 7. *Probit Model result regarding the tractor preference criteria of the farmers*

	A markası		B markası		Diğerleri	
Değişkenler	**Katsayı**		**Katsayı**		**Katsayı**	
Sabit	-0.011482 (0.428483)		-0.422923 (0.510028)		-0.878070 (0.379852)	**
Yaş	-0.000739 (0.006119)		-0.002088 (0.006768)		0.003134 (0.005469)	
Eğitim	-0.035082 (0.050660)		-0.002764 (0.062619)		0.043455 (0.045539)	
Parsel sayısı	-0.000432 (0.007885)		-0.020311 (0.011434)	*	0.016298 (0.008245)	**
Ortalama parsel uzaklığı	0.008607 (0.005979)		-0.009644 (0.004953)	*	-0.002479 (0.006276)	
Büyükbaş hayvan sayısı	0.004236 (0.002598)		-0.003498 (0.003650)		-0.001558 (0.002519)	
Küçükbaş hayvan sayısı	0.001809 (0.001209)		0.000273 (0.001387)		-0.002557 (0.001089)	**
Sulu arazi miktarı	0.000583 (0.000642)		0.000244 (0.000817)		-0.000809 (0.000498)	
Kuru arazi miktarı	-0.000326 (0.000266)		0.001973 (0.000307)		0.000103 (0.000298)	
Tarım dışı gelir	-0.000005 (0.000002)	***	0.000003 (0.000002)		0.000002 (0.000002)	
Log pseudo likelihood	**-134.96339**		**-105.07641**		**-123.46302**	

*Robust standart hata değerleri parantez içerisinde gösterilmiştir.
*,**,*** sırasıyla 0.01, 0.05 ve 0.10 istatistiki anlamlılığı göstermektedir.

Bağımlı değişken olarak çiftinin traktörünü alış şekli alınmıştır. Burada çiftçi peşin, taksitli ve banka kredili olmak üzere üç alternatif satın alma şeklinden birisini tercih etmiştir. Multinominal Probit Modelinde peşin alım baz alınarak yorumlar buna göre yapılmıştır. Toplam arazi miktarı 101-200 da arasında olanlar peşin almak yerine banka kredili almayı tercih etmektedirler (Çizelge 8). Sahip olunan sulu arazi miktarının artması taksitli ve banka kredili almayı azaltmaktadır. Sulu arazi miktarı fazla olan çiftçiler peşin para ile traktörlerini almaktadırlar. İstatistiki olarakta %5 önem seviyesinde önemli bulunmuştur. İşlenen arazi miktarı fazla olan çiftçiler peşin almak yerine taksitli veya banka kredili almayı tercih etmektedirler.

Çizelge 8. Çiftçilerin traktör satın alma şekillerini etkileyen faktörlerin Multinominal Probit Model sonucu.
Table 8. *Multinominal Probit Model result of factors affecting the way farmers buy tractors.*

	Taksitli			Banka Kredili		
Değişkenler	**Katsayı**		**Stand. Hata**	**Katsayı**		**Stand. Hata**
Sabit	-1,55615		1,44816	-0,97521		1,18188
Yaş	0,00438		0,19319	0,00434		0,01587
Eğitim	-0,01999		0,16827	0,10068		0,14157
Hane sayısı	0,00614		0,06456	0,00027		0,05691
Toplam arazi (51-100)	-0,08636		0,42360	-0,16369		0,35369
Toplam arazi (101-200)	0,29246		0,47998	0,65789	*	0,39924
Toplam arazi (201 üzeri)	-0,68989		0,76256	-0,54316		0,63355
Tarım dışı gelir	0,54409		0,35578	-0,11266		0,30644
Sulu arazi	-0,00786	**	0,00330	-0,00626	**	0,00288
Traktörle işlenen arazi	0,00396	**	0,00161	0,00334	**	0,00150
Log likelihood		**-188.1743**				
LR Chi squared (x^2)		**19.07**				

Marjinal etkilerin verildiği Çizelge 9 incelendiğinde sadece tarım dışı gelir, sulu arazi ve traktörle işlenen arazi miktarı için istatistiki açıdan anlamlı sonuçlar bulunmuştur. Eğer tarım dışı geliri olanın olmayana göre taksitle satın alma olasılığı %10.33 daha fazladır. Sulu arazi 1 dekar arttığında peşin alma olasılığı %0.02 artıyor, taksitle satın alma olasılığı %0.008 azalıyor, banka kredisiyle alma olasılığı %0.011 azalıyor. Traktörle işlenen arazi 1 dekar arttığında peşin alma olasılığı %0.01 azalıyor, taksitle satın alma olasılığı %0.04 artıyor, banka kredisiyle alma olasılığı %0.06 artıyor.

Çizelge 9. Multinominal Probit Modeline ait marjinal etkiler.
Table 9. *Marginal effect of the Multinominal Probit Model.*

	Peşin		Taksitli		Banka Kredili	
Değişkenler	**Katsayı**		**Katsayı**		**Katsayı**	
Yaş	-0.00131		0.00039		0.00091	
Eğitim	-0.01963		-0.01190		0.03152	
Hane sayısı	-0.00060		0.00104		-0.00044	
Toplam arazi (51-100)	0.04244		-0.00116		-0.04128	
Toplam arazi (101-200)	-0.16577		-0.00476		0.17054	
Toplam arazi (201 üzeri)	0.17659		-0.07346		-0.10312	
Tarım dışı gelir	-0.02472		0.10352	*	-0.07907	
Sulu arazi	0.00203	**	-0.00083	*	-0.00119	*
Traktörle işlenen arazi	-0.00106	**	0.00040	**	0.00066	*

*,** sırasıyla 0.01 ve 0.05 istatistiki anlamlılığı göstermektedir.

SONUÇ

Araştırmada Erzurum ili çiftçilerinin traktör marka seçimine etki eden faktörler ve çiftçilerin traktör yenilemeleri durumunda traktör marka seçim davranışına etki eden faktörler belirlenmeye çalışılmıştır.

Parsel uzaklığı fazla olan çiftçiler traktör seçiminde dayanıklılığa önem vermektedirler. Sulu arazisi olan çiftçilerin gelir seviyelerinin daha yüksek olması nedeniyle daha sık traktör değiştirdikleri bilinmektedir. Bu çiftçiler için dayanıklılığın ön planda olmadığı sonucu çıkarılabilir. Parsel sayısı ve parsel uzaklığı fazla olan çiftçiler diğer marka grubu traktörleri tercih etmekte, B markasını tercih etmemektedirler.

Araştırmadan elde edilen sonuçlar itibariyle sunulacak öneriler, maddeler halinde şu şekilde sıralanabilir:

Sulu arazilerde traktörlerin yıpranma payı daha yüksektir. Analiz sonucunda sulu tarım yapan çiftçilerin dayanıklılık kriterine önem vermedikleri görülmüştür. Sulu tarım yapan çiftçiler traktör marka tercihinde dayanıklı ve sorun çıkarmayan traktör markalarını tercih etmeleri üretim maliyetlerini düşürecektir.

Araştırma alanındaki işletmelerin birçoğu küçük parsellerden oluşmaktadır. Bu konuda arazi toplulaştırma çalışmalarının yetersiz kaldığı söylenebilir. Yapılacak toplulaştırma sonucu parseller arası traktörle gidip gelme azalacağından yakıt tüketiminin de düşmesi ile maliyetler azalıp verimlilik artacaktır. Bu ve buna benzer bilgiler, ilgili kamu kurum kuruluşları ve traktör sahipleri ile paylaşılmalıdır.

Son olarak traktörünü değişmeyi düşünen üreticilere basit birkaç sorudan oluşan test yapılarak traktör değişimine ihtiyacı olup olmadığı değişim yapacak ise ihtiyacını karşılayacak en uygun güç bandının ve çeker sisteminin tespiti yapılarak traktör alması sağlanabilir.

ÇIKAR ÇATIŞMASI

Yazarlar herhangi bir çıkar çatışması olmadığını beyan ederler.

YAZAR KATKISI*

Yazarlar olarak makaleye aşağıdaki katkıların sunulduğunu beyan ederiz.
Servan Baybas: Literatür taraması, giriş ve sonuç bölümlerinin yazımı.
Adem Aksoy: Araştırmanın planlanması, analizlerin yapımı, araştırma bulgularının yazımı.
**Çalışma, Servan Baybas'ın Yüksek Lisans tezinden türetilmiştir.*

KAYNAKLAR

Akdemir B, Sağlam C ve Aktaş T (1999). Tarım traktörleri kitabı. Tekirdağ.

Akkaya Ş ve Pazarlıoğlu MV (1998). Ekonometri II. İkinci Baskı, İstanbul.

Aksoy A, Demir N ve Demir O (2019). Erzurum ilinde çiftçilerin traktör satın alma davranışlarının belirleyicileri üzerine bir analiz. *Atatürk Üniversitesi Ziraat Fakültesi Dergisi, 50(1): 75-83.*

Altuntaş E ve Demirtola H (2004). Ülkemizin tarımsal mekanizasyon düzeyinin coğrafik bölgeler bazında değerlendirilmesi. *Gaziosmanpaşa Üniversitesi Ziraat Fakültesi Dergisi, 21(2): 63-70.*

Anonim (2004). Erzurum Master planı, İl Tarım ve Kırsal Kalkınma Master Planlarının Hazırlanmasına Destek Projesi, Tarım ve Köyişleri Bakanlığı Erzurum İli Müdürlüğü, Erzurum.

Anonim, (2014). Dünyada ve ülkemizde tarımsal mekanizasyonun tarihi ve gelişimi http://www.tarmakbir.org/haberler/tmtarihi.pdf (03.02.2020).

Aytuğ S ve Karadibak A G T (1998). Türk traktör kullanıcılarının marka tercihlerinin belirlenmesi üzerine bir araştırma. *Süleyman Demirel Üniversitesi İktisadi ve İdari Bilimler Fakültesi Dergisi, 3(3): 73-80.*

Begg CB and Gray R (1984). Calculation of polychotomous logistic regression parameters using individualized regressions. *Biometrica, 71: 11-18.*

Cankurt M, Miran B ve Gülsoylu E (2009). Çiftçilerin traktör tercihlerinin konjoint analizi ile belirlenmesi. *Tarım Makinaları Bilimi Dergisi, 5(1): 29-34.*

Cankurt M ve Miran B (2010). Aydın yöresinde çiftçilerin traktör satın alma eğilimleri üzerine bir araştırma. *Ege Üniversitesi Ziraat Fakültesi Dergisi, 47(1): 43-51.*

Gujarati DN (2006). Basic econometrics. Forth Edition, Mc Graw-Hill, USA.

Işık A (1988). *Sulu tarımda kullanılan mekanizasyon araçlarının optimum makina ve güç seçimine yönelik işletme değerlerinin belirlenmesi ve uygun seçim modellerinin oluşturulması üzerinde bir araştırma.* Tarımsal Mekanizasyon Anabilim Dalı, Doktora Tezi. Çukurova Üniversitesi, s. 226, Adana-Türkiye.

Işık A (1996). *İşletme özelliklerine uygun traktör seçimine yönelik uzman sistem geliştirilmesi üzerine bir araştırma.* 6. Uluslararası Tarımsal Mekanizasyon ve Enerji Kongresi Bildiri Kitabı, s. 302-314, Ankara-Türkiye.

İnal ME, Topuz D ve Uçan O (2006). Doğrusal olasılık ve logit modelleri ile parametre tahmini. Sosyoekonomi / 2006-1 / 060103.

Koçtürk D ve Avcıoğlu A (2007). Türkiye'de bölgelere ve illere göre tarımsal mekanizasyon düzeyinin belirlenmesi. *Tarım Makinaları Bilimi Dergisi, 3(1): 17-24.*

Menard SW (2002). Applied logistic regression analysis. 2nd Edn Series, Quantitative Applications in the Social Sciences, Sage Publications (CA), No. 106.

Miran B (2007). Temel istatistik. *Gama Kitabevi*, Ders Kitabı, ISBN:975-93088-00, İzmir.

Moens A and Wanders AA (1984). *Planning requirements of agricultural machinery.* Xth Congress of CIGR, Budapest, 1-16.

Newbold P (1995). Statistics for business and economics, *Prentice-Hall International*, New Jersey.

Sağlam C ve Çetin N (2017). Kayseri yöresindeki çiftçilerin traktör seçimi ve satın alma davranışlarını etkileyen faktörlerin belirlenmesi. *Uludağ Üniversitesi Ziraat Fakültesi Dergisi, 31(2): 109-121.*

Saral A, Vatandaş M, Güner M, Ceylan M ve Yenice T (2000). *Türkiye tarımının makinalaşma durumu.* Türkiye Ziraat Mühendisliği Teknik Kongresi. 17-21 Ocak. S. 901-924. Ankara-Türkiye.

Sarımeşeli M (2000). Ekonometri el kitabı. *Gazi Kitabevi*, s.210, Birinci Baskı, Ankara-Türkiye.

Sümer SK., Say SM, Has M ve Sabancı A (2003). Türkiye'de ekonomik traktör parkı ve gelişimi. *Çukurova Üniversitesi Ziraat Fakültesi Dergisi, 18: 45-52.*

TÜİK (2020). Türkiye İstatistik Kurumu, https://tuikweb.tuik.gov.tr/PreÇizelge.do?alt_id=1003 (04.12.2020).

Yavuz F (2001). Ekonometri teori ve uygulama. *Atatürk Üniversitesi Ziraat Fakültesi Ders Yayınları*, Yayın No: 185, Erzurum-Türkiye.

Yıldırım A (2016). *IPARD programı kapsamındaki hibelerin etkinliğinin belirlenmesi üzerine bir çalışma: Erzurum, Kars ve Ağrı illeri örneği*. Yüksek Lisans Tezi, Atatürk Üniversitesi Fen Bilimleri Enstitüsü, Tarım Ekonomisi Ana Bilim Dalı, s.123, Erzurum-Türkiye.

Zeren Y, Tezer E, Tuncer İK, Evcim Ü, Güzel E ve Sındır KO (1995). *Tarım alet-makine ve ekipman kullanım ve üretim sorunları*. Ziraat Mühendisliği Teknik Kongresi Tarım Haftası 95 Kongresi, 9-13 Ocak 1995, Ankara-Türkiye.

Turkish Journal of Agricultural Engineering Research

https://dergipark.org.tr/en/pub/turkager
https://doi.org/10.46592/turkager.2021.v02i02.012

Turk J Agr Eng Res (TURKAGER)
e-ISSN: 2717-8420
2021, 2(2): 390-402

Research Article

Prediction the Performance Rate of Chain Type Trenching Machine

Mohamed Ibrahim GHONIMY[ID][a,b*]

[a]*Department of Plant Production and Protection, College of Agriculture and Veterinary Medicine, Qassim University, Buraydah, SAUDI ARABIA*

[b] *Department of Agricultural Engineering, Faculty of Agriculture, Cairo University, Giza, EGYPT*

(*): Corresponding author; mohamed.ghonimy@agr.cu.edu.eg

ABSTRACT

The mathematical analysis for estimating the performance rate "*RP*" of chain-type trenching machine was studied. The mathematical analysis ended with an equation for this type. This mathematical equation was checked under different operating conditions. The practical study of the performance rate showed that the deviation of the theoretical performance rate from the actual performance rate ranged from -3.4 to +2% only for the 150.7 cm and 120.7 cm trench depth respectively. The machine field efficiency ranged from 46.7 to 57% for the 150.7 cm and 120.7 cm depth respectively. It also showed an increase in machine field efficiency by decreasing the trench depth.

RESEARCH ARTICLE

Received: 23.09.2021
Accepted: 26.11.2021

Keywords:

- Chain-type,
- Mathematical analysis,
- Performance rate,
- Drainage,
- Trencher

To cite: Ghonimy MI (2021). Prediction the Performance Rate of Chain type Trenching Machine. Turkish Journal of Agricultural Engineering Research (TURKAGER), 2(2): 390-402. *https://doi.org/10.46592/turkager.2021.v02i02.012*

INTRODUCTION

The drainage of agricultural land is one of the main operations which affecting the production of agricultural crops (Vlotman *et al.*, 2020). The productivity of the agricultural crops increased by 22-35% when implementing agricultural drainage projects (Kovalenko *et al.*, 2020). Several trenching machines excavate the tile drainage trenches. There are mainly three types of trenching machines different in their construction and way of performance. These three types are chain-type trenching machines, wheel type trenching machine and plow type trenching machines.

Day (1973) defined the productivity of trenching machines as the rate the excavator can move along the trench line. The rate of excavation for a continuous trenching machine is its controlled productivity. It will vary with the width and depth of trench, the toughness of the material to be excavated and the power available or selected by the operator. Peurifoy (1970) studied the productivity in trenching operations. He found many factors affecting the production rate of trenching machine. These include the class of soil, depth and width of trench, extent of shoring required, topography, climatic condition, extent of vegetation such a trees, stumps and roots, and physical obstruction, such as buried pipes, sidewalks, paved streets, building etc.

In case of laying a pipeline, the speed with which the pipe can be placed in the trench, also affect the production rate of the machine. Sitorus *et al.* (2016) reported that the digging machine forward speed, cutting depth, uniaxial compressive strength, and trench width are the most sensitive parameters affecting the power and angular speed. Design optimization using the information drawn from this parameter study can be preceded by focusing on the selection of traverse speed, uniaxial compressive strength, trench width, carrier weight, nose radius, bar length, and pivot point location. Spencer *et al.* (2007) described the principal features of the upgraded trenching and methods of calculating predicted trenching performance and they found that the target performance rate for wheel type trenching machine ranged from 80 to 400 m h^{-1} according to soil type. Schwab *et al.* (1982) studied the productivity in trenching operations. They found many factors affecting it such as; soil moisture, soil characteristics as hardness and stickiness, stones, and submerged stumps, depth of trench, conditions of the trenching machine, the ski1l of the operator, and the delays due to interruptions during operation. They found that an extremely wet soil may stop machine operation. Soil with a low moisture content may not affect the digging rate to any extent, but soil that stick to the buckets of the machine, sandy soils that fall apart easily, and deep cuts reduce digging speed. They also found that increasing the depth from 90 to 150 cm decreased the digging speed by 56% under Iowa and Minnesota conditions. Donahue *et al.* (1985) mentioned that the soil moisture, soil characteristics, skill of operator, width of the trench, and depth of the trench influence the factors affecting the capacity of the trenching machines.

There is a several research concerned with the use of mathematical models for trenching machines. Diep (2017) found that the chipping depth of a chain trenching machine is related to the tangential tooth speed *(ut)*, the traverse speed *(U)*, the spacing between teeth *(S)* and the angle of the cutting assembly *(Φ)*. If working length of the tooth is known, the maximum of traverse speed U can be determined by the following formula h_{max}=U/ut.S , where h_{max} is the theoretical maximum cutting depth occurs with cutting angle Φ = 90°. Du *et al.* (2016) found that the operator control inputs to execute a work cycle of an excavator trenching operation. The simulation results in a work cycle that is generated by executing a series of tasks in the way a human operator would perceiving the state of the machine, deciding when to transition from one task to the next, and controlling the machine to move the bucket through the tasks. The virtual operator model appropriately adapted to different operator control strategies, machine parameters changes (i.e. pump speed) and a change in work site goals (trench depth, pile location). The model-generated outputs based on human-like perception, decision-making, and action selection. Reddy and Shailesh (2018) mentioned that, in order to increase the life of backhoe excavator bucket tooth other two materials i.e.

HSS and HCHCr has been analyzed for the similar force and boundary conditions. 3D model was prepared in solid works and software in finite element method (FEM) domain was utilized for analyzing the model or excavator bucket tooth behavior. Computational approach will give the closer results to practical values through simulation. Computer Aided Engineering (CAE) can drastically reduce the costs associated with the product lifecycle.

Whatever the type of the trenching machine is, it has the advantage of quite high rate of performance, since it simultaneously digs the trench, lays down the tiles or the pipes and, in some types, it also refills the ditches with the soil. This means fulfilling its did define this complete function in a short period within the same day. It is characterized with the high accuracy in laying the pipes or the tiles at the required depth and slope. Besides, these types of trenching machines suppress the manual way of digging and laying drainage pipes by its lower costs of operation (Schaufelberger and Migliaccio, 2019).

The aim of this work was to find out the main factors affecting chain-type trenching machine performance rate, relate these affecting factors in mathematical relationship, and validate the mathematical relationship to predict the performance rate of chain-type trenching machine.

MATERIALS AND METHODS

Mathematical analysis approach

The mathematical analysis had to be preceded with the two main steps which were to state the theory, the construction the specifications and the dimensions of the applied mechanism for chain-type trenching machine, Figure 1, and to state the expected affecting factors on the performance of the applied mechanism, the nature and the magnitude of their effects. The performance rate of the trenching machine depends, to a great extent, on the forward speed of the machine. This forward speed in return, is related to both the size of the power source of the trenching machine and the magnitude of the consumed power during the performance of the machine. Therefore, the mathematical analysis depended on expressing the magnitude of any required power of the trenching machine as a function of machine forward speed. By equating the size of the power source with the summation of the required powers during machine performance (equation 1), the magnetite of the maximum machine forward speed can be estimated, and hence, the rate of performance of the machine can be determined.

$$P_b = P_c + P_r + P_i + P_s + P_t + P_e \pm P_a + P_n \quad (1)$$

Where:

P_b = brake power of the engine of the machine, kW;

P_c = pulling power needed for cutting, kW;

P_r = pulling power to overcome rolling resistance, kW;

P_i = pulling power to overcome slope resistance, kW;

P_s = power lost in slop resistance, kW;

P_t = power 1ost in transmission systems, kW;

P_e = power required to lift the cut soil, kW;

P_a = power required to overcome air resistance, kW;
P_n = power required to accelerate the machine to the operating speed due to its inertia, kW.

Both P_a and P_n could be neglected since the operating forward speeds of the trenching machine are very limited compared with any other moving truck. Therefore, equation (1) can be simplified as shown in the following equation (2).

$$P_b = P_c + P_r + P_i + P_s + P_t + P_e \quad (2)$$

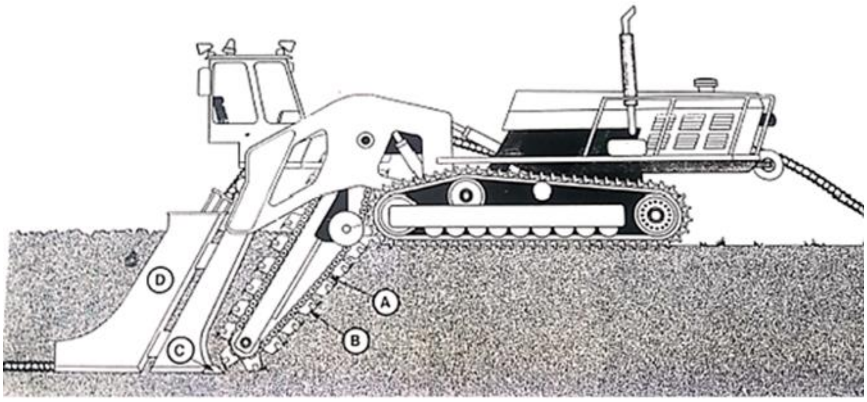

A) Endless rotating chain B) Cutters attached to chain
C) Shoe to smooth trench bottom D) Tubing (or tile) shute

Figure 1. Chain-type trenching machine. "After Shady 1989"

The theory, construction, and specifications of the mechanisms of chain-type trenching machine:

The excavating unit of the chain-type trenching machine, Figure 2, mainly consists of an endless chain, which moves along a boom at a speed (V_c). The angle of the chain with the vertical direction is (θ). On the chain, there are attached cutter buckets equipped with teeth. The inclined distance between the cutting edges of any two consecutive buckets is (S_b). The depth of the digged trench is (d). The performance theory of chain-type trenching machine is that the machine moves horizontally at a veracity (V_m), the chain moves in an inclined direction with an angle equals (θ) at a speed (V_c). The absolute speed of the cutting edge of the bucket (V_b) can be considered as the summation of the vectors of (V_m) and (V_c) as shown in Figure 3. The cutting edges of the consecutive buckets cut the soil in thin inclined layers. The buckets elevate the cut soil and throw it outside the digged trench.

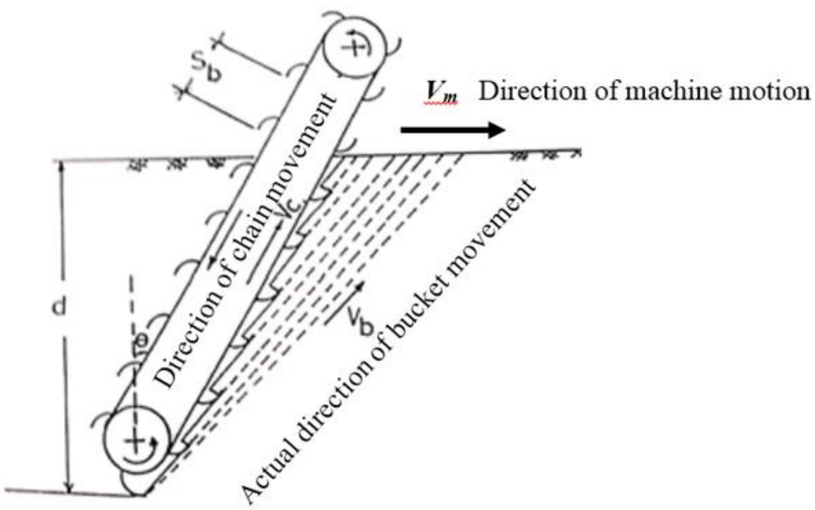

Figure 2. The mechanism of chain-type trenching machine.

Factors affecting the performance of the trenching machines

There are many factors affecting the performance rate of the trenching machines. These factors can be classified into two groups; **soil factors** which include soil specific weight *(ω)*, N cm^{-3}, soil unit draft *(U)*, N cm^{-2}, traction coefficient, rolling resistance coefficient *(RR)*, angle between inclined soil surface and the horizontal direction *(ψ)*, and friction coefficients between soil and soil and between soil and metal *(F_{ms})*.

Machine factors, which include machine weight *(W_m)*, N, machine brake power *(P_b)*, kW, machine forward speed (V_m), m s^{-1}, trench cutting width *(W_t)*, cm, vertical depth of the cut trench *(d)*, cm, slip percentage of the tractor device of the machine *(S)*, machine transmission efficiency (η_t), and machine field efficiency (η_f), chain speed *(V_c)*, m s^{-1}, and angle of chain with vertical direction *(θ)*.

Some assumptions and simplifications were done in order to facilitate mathematical manipulation. These include Homogeneous and isotropic soil, with a constant unit draft. Constant velocities for any moving element, i.e., constant forward machine speed, and constant chain speed were assumed. The paths of the cutting edge for the chain-type trenching machines were considered as straight lines.

Mathematical analysis for estimating the performance rate

The mathematical analysis for estimating the performance rate *(RP)* of the chain-type-trenching machine is expected to be in the form of the equation (2):

$$RP = 60 \times V_m \times \eta_f \quad (3)$$

Where:

RP = the actual performance rate of the machine, m min^{-1};
V_m = the machine forward speed, m s^{-1};
η_f = the field efficiency, decimal.
To find out the value of V_m, the components of equation (2) were obtained as the following:

a) Determination of P_c

Referring to Figure 4:

$$P_c = 0.001\left(F_c + F_f\right) \times V_b = 0.001(U.W_t.\delta.N + F_{ms}(1000\,P_b.\eta_t/V_m)cos\phi) \times V_b \qquad (4)$$

$$P_c = 0.001 \times U^* \times W_t \times \delta \times N \times V_b \qquad (5)$$

Where:

$U^* = K^*.\ U$

$$K^* = \frac{U^*}{U} = \frac{[U.W_t.\delta.N(1000.F_{ms}.P_b.\eta_t/V_m)cos\phi].V_b}{U.W_t.\delta.N.V_b}$$

$$K^* = 1 + \frac{(1000.F_{ms}.P_b.\eta_t/V_m).cos\phi}{U.W_t.\delta.N.V_b} \cong from\ 5\ to\ 15$$

Using reasonable values for chain-type trenching machines, means that utilizing unit draft (U^*) including friction can be as much as about twelve times the unit draft *(U)* used in soil ploughing.

Referring to Figures 2 and 3;

$$N = \frac{d}{cos\theta.S_b}\ and\ \delta = \frac{V_m}{V_b}.cos\theta.S_b$$

$$\therefore P_c = 0.001\,K^*.U.W_t.d.V_m \ \therefore P_c = 0.001\,K^*.U.W_t.d.V_m \qquad (6)$$

b) Determination of *P_r*

$$P_r = 0.001\,F_r.V_m \qquad (7)$$

The resistance force (F_r) due to rolling resistance depends on machine weight *(W_m)*, the weight of cut soil *(W_s)*, the rolling resistance coefficient (*RR*), the vertical component of the cutting force *(F_{cv})*, and the angle ψ between inclined soil surface and the horizontal direction.

$$F_r = RR.cos\psi.(W_m + W_s + F_{cv})F_r = RR.cos\psi.(W_m + W_s + F_{cv}) \qquad (8)$$

$$W_s = \frac{1}{2}W_t.\delta.N.l.\omega \qquad but \quad V_b.t = l$$

$$V_c.t = S_b.N = \frac{d}{\cos\theta}$$

$$W_s = \frac{\omega.W_t.d^2.V_m}{2\,cos\theta\,.V_c}$$

$$F_{cv} = \left(\frac{K^*.U.W_t.d.V_m}{V_b}\right).cos\phi$$

$$but \quad cos\phi = \frac{V_c.cos\theta}{V_b} \qquad and \qquad v_b = [(V_m)^2 + 2V_c.V_m.cos\theta + (V_c)^2]^{1/2}$$

$$F_{cv} = \frac{K^*.U.W_t.d.(V_c/V_m).cos\theta}{1 + 2(V_c/V_m).cos\theta + (V_c/V_m)^2}$$

Substituting into equations (8) and (7) gives

$$P_r = 0.001\,V_m.RR.cos\psi.\left[W_m + \frac{\omega.W_t.d^2}{2\,cos\theta.(V_c/V_m)} + \frac{K^*.U.W_t.d.(V_c/V_m).cos\theta}{1 + 2.(V_c/V_m).cos\theta + (V_c/V_m)^2}\right]$$

$$P_r = 0.001\, V_m.RR.cos\psi.\left[W_m + \frac{\omega.W_t.d^2}{2\,cos\theta.(V_c/V_m)} + \frac{K^*.U.W_t.d.(V_c/V_m).cos\theta}{1+2.(V_c/V_m).cos\theta+(V_c/V_m)^2}\right] \quad (9)$$

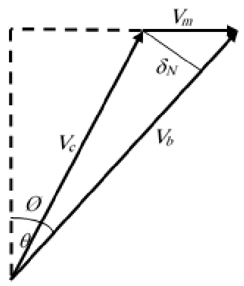

V_m= machine speed.
V_c = chain speed
V_b = resultant speed of the bucket edge
N= number of bucket in the cutting action.
δ = thickness of cut for one bucket.

Figure 3. Bucket resultant speed.

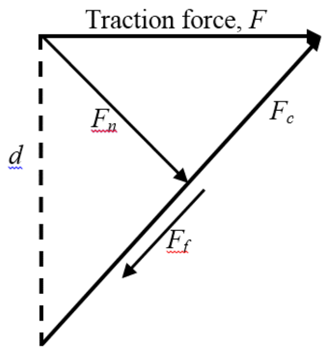

Figure 4. Determination of the friction force F_f acting on bucket edge.

c) Determination of P_i

$$P_i = 0.001\,(W_m + W_S).sin\psi.V_m \quad (10)$$

$$P_i = 0.001\, V_m.sin\psi.\left[W_m + \frac{\omega.W_t.d^2}{2\,cos\theta.(V_c/V_m)}\right] \quad (11)$$

d) Determination of P_s

$$P_s = 0.001\, F_s.V_s = 0.001\,(F_c + F_r).V_s \quad (12)$$

Where;

P_s is the power lost in slip resistance.

F_c is the cutting force,

F_r is the resistance force due to rolling and

V_s is the loss in machine speed due slippage (S).

$$V_s = \left(\frac{S}{100-S}\right).V_m \quad (13)$$

$$P_s = 0.001\left[\left(\frac{S}{100-S}\right).V_m\right].\left[\frac{K^*.U.W_t.d}{\left[1+2.(V_c/V_m).cos\theta+(V_c/V_m)^2\right]^{1/2}} + RR.cos\psi.\left(W_m + \frac{\omega.W_t.d^2}{2\,cos\theta.(V_c/V_m)}\right) + \frac{K^*.U.W_t.d.(V_c/V_m).cos\theta}{1+2.(V_c/V_m).cos\theta+(V_c/V_m)^2}\right] \quad (14)$$

e) Determination of P_t

$$P_t = P_b.(1-\eta_t) \quad (15)$$

f) Determination of P_e

$$P_e = 0.001\, W_S.V_c.cos\theta = 0.001 \times \frac{\omega.W_t.d^2.V_m}{2} \quad (16)$$

From equations 2, 3, 9, 11, 14, 15 and 16

$$P_c + P_r + P_i + P_s + P_t + P_e - P_b = 0 \quad (17)$$

$$V^2{}_m\left[\left(\frac{\omega.W_t.d^2}{2cos\theta.V_c}\right).\left(RR.cos\psi+sin\psi+RR.cos\psi.\frac{S}{100-S}\right)\right]+V_m\left[K^*.U.w_t.d+RR.cos\psi.W_m+\right.$$

$$\left.W_m.sin\psi+\frac{K^*.U.W_t.d.\left(\frac{S}{100-S}\right)}{\left[1+2.(V_c/V_m).cos\theta+(V_c/V_m)^2\right]^{1/2}}+RR.cos\psi.W_m.\left(\frac{S}{100-S}\right)+\frac{\omega.W_t.d^2}{2}\right]+$$

$$\left[\left(\frac{RR.cos\psi.K^*.U.W_t.d.cos\theta.V_c}{1+2.(V_c/V_m).cos\theta+(V_c/V_m)^2}\right).\left(1+\frac{S}{100-S}\right)-1000P_b.\eta_t\right]=0$$

$$V^2{}_m+\frac{G}{Q}.V_m-\frac{J}{Q}=0 \qquad (18)$$

Where:

$$Q=\left(\frac{\omega.W_t.d^2}{2cos\theta.V_c}\right).\left(RR.cos\psi\left(\frac{100}{100-S}\right)+sin\psi\right) \qquad (19)$$

$$G=G_1+G_2+G_3 \qquad (20)$$

$$G_1=K^*.U.w_t.d.\left[1+\left(\frac{S}{100-S}\right).\left[1+2.(V_c/V_m).cos\theta+(V_c/V_m)^2\right]^{-1/2}\right] \qquad (21)$$

$$G_2=RR.cos\psi.\left[V_m+W_m.\left(\frac{S}{100-S}\right)\right] \qquad (22)$$

$$G_3=W_m.sin\psi+\frac{\omega.W_t.d^2}{2}G_3=W_m.sin\psi+\frac{\omega.W_t.d^2}{2} \qquad (23)$$

$$J=\left(\frac{RR.cos\psi.K^*.U.W_t.d.cos\theta.V_c}{1+2.(V_c/V_m).cos\theta+(V_c/V_m)^2}\right).\left(1+\frac{100}{100-S}\right)-1000P_b.\eta_t \qquad (24)$$

Applying the rule:

$$V_m=-\frac{b}{2}\pm\sqrt{\left(\frac{b}{2}\right)^2-\frac{C}{a}} \qquad (25)$$

$$\frac{b}{2}=\frac{G}{2Q} \qquad (26)$$

$$C=\frac{J}{Q} \qquad (27)$$

$$\frac{b}{2}=\left(\frac{cos\theta.V_c}{\omega.W_t.d^2.\left(RR.cos\psi\left(\frac{100}{100-S}\right)+sin\psi\right)}\right)\times\left\{K^*.U.w_t.d.\left(1+\left(\frac{S}{100-S}\right).\left[1+2.(V_c/V_m).cos\theta+\right.\right.\right.$$

$$\left.\left.\left.(V_c/V_m)^2\right]^{-1/2}\right)+RR.cos\psi.W_m.\left(1+\frac{S}{100-S}\right)+\left(W_m.sin\psi+\frac{\omega.W_t.d^2}{2}\right)\right\} \qquad (28)$$

$$C=\frac{2\,cos\theta.V_c}{\omega.W_t.d^2.\left(RR.cos\psi\left(\frac{100}{100-S}\right)+sin\psi\right)}\times\left[\left(\frac{RR.cos\psi.K^*.U.W_t.d.cos\theta.V_c}{1+2.(V_c/V_m).cos\theta+(V_c/V_m)^2}\right).\left(\frac{100}{100-S}\right)-1000P_b.\eta_t\right] \qquad (29)$$

Equation (25) could be solved by trial-and-error method using reasonable initial values of V_m in equations (28) and (29) and the value of $K^*\approx12$. When different values of K^* ranging from 1 to 15 were used, the estimated values of V_m ranged from 2.92 to o.26 m sec^{-1} respectively.

The actual performance rate *(RP)* could be obtained from equation (3) using field efficiency $\eta_f = \eta_s.\ \eta_w.\ \eta_{ti}$, where η_s is the efficiency of utilizing the geared speed, η_w is the efficiency of utilizing the proposed width of the machine, and η_{ti} is the efficiency of utilizing the time. However, due to the very low speed of the machine, both η_s and η_w could be considered equal to 1.0.

Field experimental work

The experimental work was carried out through a period of almost one year. It was conducted in Gharbia Governorate, in Sawahel El-Neel region, in which the chain-type trenching machine (Figure 5) was tested. The specification of the machine is shown in Table 1. Trench depths of 120 and 150 cm were tested.

Figure 5. The tested chain-type trenching machine. "i-bidder.com 2015"

Table 1. Technical specifications of the chain-type trenching machine.

Model	Barth Holland K171
Engine	Deutz diesel type
Power	149 kW (203 HP) - 2150 rpm
Tank capacity	Fuel 320 lit., Hydraulic oil 120 lit
Electricity	24 V.
Speed	variable (0 - 5000 m h^{-1})
Ground pressure	3 N cm^{-2}
Transmission efficiency	90%
Cutting system speed	1 gear: 1.04 m s^{-1} 2 gear: 2.15 m s^{-1} 3 gear: 3.26 m s^{-1} 4 gear: 4.35 m s^{-1} 5 gear: 5.75 m s^{-1} r. gear: 1.02 m s^{-1}
Max. trench depth	1750 mm
Trench width	230 or 280 mm
The angle of the chain with the vertical direction	30 degree
Chain pitch	100 mm
TRANSPORT DATA	
length	10905 mm
Width	2500 mm
Height	1000 mm
Weight	13 tons

RESULTS AND DISCUSSION

The average rolling resistance coefficient of the experimental field was taken as 4.0%, since it was found ranging between 3.0 and 5.0% (Jia *et al.*, 2018). The average specific weight of the soil *(ω)* was found to be 0.011 N cm^{-3} (Jia *et al.*, 2018). In addition, the average draft was taken as 10 N cm^{-2} (Jia *et al.*, 2018). The average values of field measurements were as shown in Table 2.

Table 2. Average values of field measurements for chain-type trenching machine.

Nominal trench depth, cm	120		150	
Field measurements	Ave.	SD	Ave.	SD
d, cm	120.70	2.37	150.7	2.15
W_t, cm	23.10	0.34	23.1	0.34
S, %	5.00	---	6.00	---
V_m, m s^{-1}	0.40	0.05	0.34	0.04
V_c, m s^{-1}	3.26	---	2.15	---
K^*	12.00	---	12.00	---
ψ, degree	0.00	---	0.00	---

d = Trench depth, W_t = Trench width, S = slip percentage, V_m = Machine forward speed, V_c = Chain forward speed, K^* = A dimensionless coefficient = (U^*/U), ψ = angle between inclined soil surface and the horizontal direction.

Actual performance rate *(RP)* and field efficiency *(η_f)*

The average values of breakdown items of the daily machine time, machine performance rate *(RP)*, field efficiency (η_f) as practically measured in the field are shown in Table 3. It is clear that the average values of *RP* were 13 and 9 m min^{-1} for 120 and 150 cm trench depth respectively while the η_f were 57 and 46.7% for 120 and 150 cm trench depth respectively.

Table 3. Breakdown items of the daily machine item for chain-type trenching machine and its average performance rate and field efficiency.

Activities	*Average spent time, min day^{-1} Trench depth, cm		SD, min day^{-1} Trench depth, cm	
	120	150	120	150
Net excavating and pipe laydown	229	215	7.26	5.81
Turning and travelling to start digging another trench	55	65	2.49	3.12
Setup time for reaching the depth	23	29	1.76	2.18
Rest periods	60	66	1.76	3.26
Field quick maintenances	30	30	2.17	1.73
Refill of water and oil tank	30	34	2.23	1.48
Other lost time	10	18	1.49	1.73
Average total time, min day^{-1}	485	455	8.15	7.21
**Total installed length, m day^{-1}	6305	4095	6.12	4.23
Actual performance rate, m min^{-1}	13.0	9.0	1.15	0.92
*** Field efficiency, %	57.0	46.7	0.89	0.81

* Average value of ten estimates, each for a different operating day.
**Average value (m/day) of the total excavated trench lengths within the ten days period.
***Average field efficiency within the ten days period.

Theoretical deterioration of the performance rate of the chain-type trenching machine

To theoretically predict the performance rate, equations (3), (25), (28), and (29) were applied. Using the above-mentioned data into equation (28) for the value of *b/2* and into equation (29) for the value of *C* gave the following equations:

For 120.7 cm depth

$$\frac{b}{2} = 6154.28 + \frac{316.97}{\sqrt{1 + \frac{5.65}{V_m} + \frac{10.63}{V^2{}_m}}}$$

$$C = \frac{1431.77}{1 + \frac{5.65}{V_m} + \frac{10.63}{V^2{}_m}} - 4827.6$$

For 150.7 cm depth

$$\frac{b}{2} = 3196.18 + \frac{199.98}{\sqrt{1 + \frac{3.72}{V_m} + \frac{4.62}{V^2{}_m}}}$$

$$C = \frac{4964.60}{1 + \frac{3.72}{V_m} + \frac{4.62}{V^2{}_m}} - 2011.5$$

Solving equation (18) by trial-and-error method, gave the computed values of the V_m, Table 4. Applying the computed values of the V_m into equation (3) gave the predicted value of the performance rate of the chain-type trenching machine:

RP (120.7 cm depth) = 60 x 0.388 x 0.57 = 13.26 m min^{-1}

This computed value was very close to the experimentally determined value of the performance rate for the 120.7 cm trench depth, which was found to be 13 m min^{-1}., Table 3 and Figure 6. The deviation of the theoretically computed value from the field determined value for the performance rate was only about + 2%.

RP (150.7 cm depth) = 60 x 0.31 x 0.467 = 8.69 m min^{-1}

This computed value was very close to the experimentally determined value of the performance rate for the 150.7 cm trench depth, which was found to be 9.00 m min^{-1}, Table 3 and Figure 6. The deviation of the theoretically computed value from the field determined value for the performance rate was only about - 3.4%.

Table 4. The initially proposed and the computed values in the interaction process for the determination of the forward speed of the chain-type trenching machine at different trench depths. (Using trial and error method).

Trench depth, cm	V_m, m s^{-1}	Trial 1	Trial 2	Trial 3	Trial 4
120.7	proposed value	3.000	1.000	0.400	0.388
	computed value	0.355	0.301	0.389	0.388
150.7	proposed value	3.000	1.000	0.400	0.310
	computed value	0.278	0.300	0.309	0.310

The findings of the used chain-type trenching machine show the degree of accuracy of the mathematically derived equations. This derived equation can be used with enough confidence to theoretically predict the performance rate of chain-type trenching machine depending on the prevailing operating conditions.

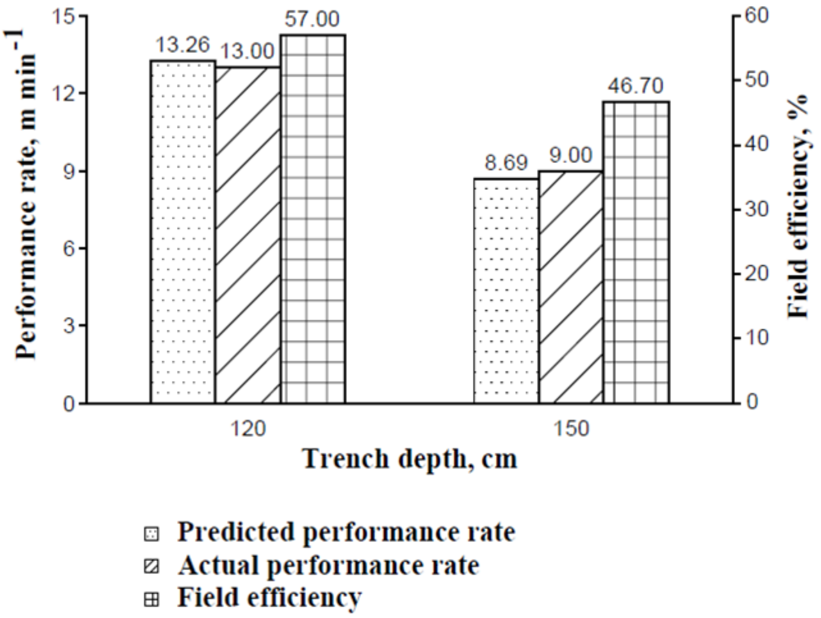

Figure 6. The actual & predicted performance rate and field efficiency of the chain-type trenching machine.

CONCLUSION

The digging of the trenches is an important process in order to implement the tail drainage projects. This research is concerned with studying the relationship that correlate the performance of the chain-type trenching machine with the factors affecting them, so that the rate of performance can be predicted or controlled through the factors affecting it. A mathematical analysis of chain-type trenching machine was performed. Also, a field operation study was conducted under actual operating conditions to test the validity of the derived mathematical equations.

The study showed the validity of the derived equations in predicting the performance rate of chain-type trenching machine. The percentage difference between the performance rate calculated from the equations and the actual field estimated performance rate were -3.4% and +2% at a trench depth of 150.7 and 120.7 cm respectively. The results of the field study also showed that the field efficiency was 46.7 and 57% for the chain-type trenching machine at a trench depth of 150.7 and 120.7 cm respectively. The finial equation of the mathematical model can be used to increase the performance rate of the chain-type trenching machine by maximizing all the factors in the numerator or by minimizing all the factors in the denominator.

Finally, the derived mathematical equation can be used with enough confidence to theoretically predict the performance rate of chain-type trenching machine depending on the prevailing operating conditions.

DECLARATION OF COMPETING INTEREST

The author declares that he has no conflict of interest.

CREDIT AUTHORSHIP CONTRIBUTION STATEMENT

The author, Mohamed Ghonimy, is responsible for the various parts of this paper.

ACKNOWLEDGMENTS

The author wishes to express here sincere thanks and appreciation to the spirit of Prof. Dr. Monier A. Morcos and Prof. Dr. Abdalla E. Badr, former professors, Agricultural Engineering Dept., Faculty of Agriculture, Cairo University for continues help supports.

REFERENCES

Day DA (1973). Construction equipment guide. John Wiley and Sons.,Inc., N. Y., USA, 206-208.

Diep DD (2017). Analysis the Factors Affecting Conveyance Rate of Unbucket Chain Trenching Machine. *Agricultural, Forest and Transport Machinery and Technologies, 4(1): 38-44.*

Donahue RL, Miller RW and Shickluna GC (1985). Soil an introduction to soil and plant growth. 4th Ed. Prentice Hall, Inc., Englewood cliffs, *New Jersey*, USA. 98-106.

Du Y, Dorneich MC and Steward B (2016). Virtual operator modeling method for excavator trenching*. Automation in Construction, 70: 14-25.*

i-bidder.com 2015. Barth holland k171 trencher. [Online] Available from: https://www.i-bidder.com/en-gb/auction-catalogues/ml/catalogue-id-morris10019/lot-dd3f8267-bddc-47be-ab61-a50900a797df. (Accessed November 24, 2021).

Jia J, Jia and Schmidt (2018). Soil dynamics and foundation modeling. *Springer*, New York.

Kovalenko P, Rokochinskiy A, Mazhayskiy Y, Volk P, Volk L and Chernikova O (2020). Construction and agricultural drainage parameter optimization considering economic and environmental requirements. *Engineering for Rural Development*, *19: 1009-1017.*

Peurifoy RL (1970). Construction planning, equipment, and methods. 2nd ed. McGraw, Hill Kogakusha, Ltd., Tokyo, Japan, pp 695.

Reddy Y and Shailesh P (2018). Design and analysis of excavator bucket tooth. *International Journal of Modern Trends in Engineering and Research, 5(4): 79-86.*

Shady AM (1989). Irrigation drainage and flood control in Canada. Canadian international development agency, *Quebec*, Canada.

Schaufelberger JE and Migliaccio GC (2019). Construction equipment management. *Routledge*.

Schwab GO, Frevert RK, Edminster TW and Barnes KK (1982). Soil and water conservation engineering. *Soil Science, 134(2): 146.*

Sitorus PE, Ko JH and Kwon OS (2016). Parameter study of chain trenching machines of Underwater Construction Robots via analytical model. In OCEANS 2016 MTS/IEEE Monterey (pp. 1-6). IEEE.

Spencer A, Machin J and Jackson E (2007). Rock cutting With the T750 super trenching. Unmanned Intervention, *New Orleans*, LA, 30.

Vlotman WF, Smedema LK and Rycroft DW (2020). Modern land drainage: Planning, design and management of agricultural drainage systems. *CRC Press*.

Turkish Journal of Agricultural Engineering Research

https://dergipark.org.tr/en/pub/turkager
https://doi.org/10.46592/turkager.2021.v02i02.013

Turk J Agr Eng Res
(TURKAGER)
e-ISSN: 2717-8420
2021, 2(2): 403-412

Research Article

Important Physical and Mechanical Properties of Dominant Potato Variety Widely Grown in Ethiopia

Dereje ALEMU[ID][a*]

[a] *Department of Agricultural Engineering Research, Melkassa Agricultural Research Centre, Ethiopian Institute of Agricultural Research, Addis Ababa, ETHIOPIA*

(*): Corresponding author. *drjalemu@gmail.com*

ABSTRACT

The physical attributes of agricultural product are utmost essential in developing technologies for different unit operations. Pertinent potato tuber attributes were studied. 100 samples of dominant and popular potato tuber varieties grown in Ethiopia which are free from any injuries from each variety were obtained from Holeta Agricultural Research Center. In this study, the physical attributes of potato tubers were determined at a moisture content of 70.75, 69.99, 71.75, 69.70 and 72.38% (wet basis) for Belete, Jalenie, Gera, Gudene and Chala varieties, respectively. Except specific gravity of potato tuber, other physical properties studied were significantly different at 5% of level of significance. Analysis of variance showed that there is also a significant difference in coefficient of static friction and angle of repose of all potato tuber varieties under four different materials and dynamic coefficient of friction under mild steel sheet metal and galvanized sheet.

RESEARCH ARTICLE

Received: 08.10.2021
Accepted: 28.11.2021

Keywords:

- Physical,
- Mechanical,
- Potato tuber,
- Property,
- Variety,
- Attribute

To cite: Alemu D (2021). Important physical and mechanical properties of dominant potato variety widely grown in Ethiopia. Turkish Journal of Agricultural Engineering Research (TURKAGER), 2(2): 403-412. *https://doi.org/10.46592/turkager.2021.v02i02.013*

INTRODUCTION

Potato is the first in terms of production from tuber and root crops grown in more than 125 countries (Alemu *et al.*, 2021). It is used for daily consumption for a billion people (Gebru *et al.*, 2017). It plays a significant role in improving food security and Ethiopian smallholder potato grower's income due to its high yield potential per hectare (Ayalew, 2014; CSA, 2015; Alemu *et al.*, 2021). It is widely grown in eastern, southern, central and northwestern region of Ethiopia, which is around 83% of potato growers (CSA, 2009). Around 1,288,146 households are dependent on potato production and about 67,361.87 ha of land is under potato production which has 31.13% area coverage among root crops (CSA, 2015: Alemu *et al.*, 2021). It can be used for cooking, processing, feed, seed tubers, starch and alcohol production (Alemu *et al.*, 2021). Within 30 years, the average potato crop productivity in Africa, Asia and Latin America has increased by 44, 25 and 71 percent, respectively (FAO, 2009).

Physical attributes of agricultural products are important in many grains/seeds and vegetables, and food materials handling and processing operation. Physical characteristics of agricultural products plays a significant role during development of equipment used for different operation (Malcolm *et al.*, 1986; Razavi *et al.*, 2007; Joshi and Raisoni, 2016). In addition to physical attributes, mechanical properties have to be taken into account during development of machines. Therefore, the objective of this study was to determine pertinent physical and mechanical attributes of potato tuber variety widely grown in Ethiopia.

MATERIALS AND METHODS

Source of experimental material

The study was conducted at Melkassa Agricultural Research Center (MARC); which is found in Oromia National Regional State, Ethiopia. It is located at an altitude of 1550 meters above sea level (masl) and lies between 8° 24' 0" to 8° 30' 12" N, 39° 21' 0" to 39° 35' 14" E latitude and longitude, respectively. Agro-ecologically, the area is characterized as arid and semi-arid.

100 samples free from any injuries of dominant and popular potato varieties (Belete, Jalenie, Gera, Gudene and Chala) grown in Ethiopia were used from Holeta Agricultural Research Centers as shown in Figure 1. The samples were kept in a refrigerator at a temperature of 4°C and relative humidity of 95% for 24 hours as recommended by Hurst *et al.* (1993) to offset the effect of the environment.

Figure 1. Potato variety used during physical and mechanical attributes measurements.

Determination of Physical Attributes

Shape and size

To measure potato tuber mass digital balance with accuracy of 0.10 g was used. As shown in Figure 2, major, minor and intermediate diameters of each tuber were measured using digital caliper with an accuracy of 0.01 mm and measuring range of 0-150 mm.

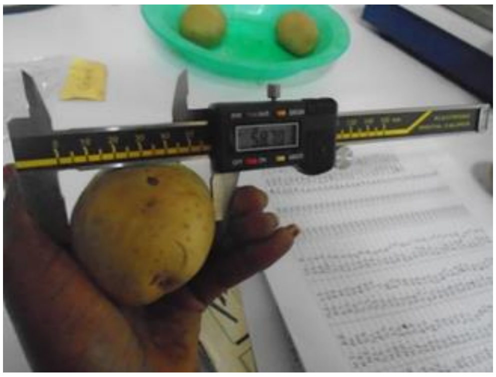

Figure 2. Measurement of principal dimensions of potato tuber.

Geometric mean diameter

Geometric mean diameter (GMD) was determined using the three measured perpendicular diameters as shown in Equation 1 (Kamat *et al.*, 2020).

$$GMD = \sqrt[3]{abc} \quad (1)$$

Where: -

GMD = geometric mean diameter, mm

a, b and *c* = major, intermediate and minor diameter respectively, mm

Surface area

Surface area (S, mm^2) of the potato tuber was determined using Equation 2 (Mohsenin, 1986).

$$S = \pi(GMD)^2 \quad (2)$$

Volume

As shown in Figure 3 the volume of a potato tuber was determined based on the water displacement method (Mohsenin, 1986).

Figure 3. Measurement of volume of potato tuber by using water displacement method.

Sphericity

The sphericity *(φ)* of potato tubers was determined with presumption that the volume of solid can be approximating to the volume of a triaxial ellipsoid with a diameter equal to the minor, intermediate and major diameters using Equation 3 (Mohsenin, 1986).

$$\varphi = \sqrt[3]{\frac{abc}{a}} \quad (3)$$

Moisture content

Potato tuber moisture content was determined using hot air oven method and Equation 4 (Asoegwu, 1995). The weight of the potato tuber was measured before and after oven-drying at 105°C until constant weight was obtained using a digital balance with an accuracy of 0.01 g.

$$M_C = \frac{W_1 - W_2}{W_2} \quad (4)$$

Where:-

M_c= moisture content (% wb),

W_1= mass of potato tuber before oven-drying (g) and

W_2= mass of potato tuber after oven-drying (g).

Tuber density (ρ_p)

Tuber density is described as mass of a tuber divided to its actual volume (Equation 5). Internal pores are included (Mohsenin, 1986).

$$\rho_P = \frac{M_t}{V_C} \quad (5)$$

Where:

ρ_p = particle density (g cm^{-3}),

M_t = mass of a tuber (g) and

V_c = volume of a tuber (cm^3).

Bulk density (ρ_{bulk})

Bulk density (ρ_{bulk}) was determined from mass and volume of potato tuber using Equation 6. (Rahman, 2014).

$$\rho_{bulk} = \frac{Mass\ (g)}{Volume\ (m^3)} \quad (6)$$

Specific gravity (G_s)
The specific gravity of potato tuber was determined based on the water displaced method and Equation 7.

$$G_s = \frac{Weight\ in\ air\ (N)}{Weight\ in\ air\ (N) - Weight\ in\ water(N)} \quad (7)$$

Where *N*=Newton

Frictional properties of potato tuber

Static coefficient of friction
The static coefficients of friction between potato tuber and four different surfaces (Mild steel sheet metal, galvanized sheet, wood and rubber) were determined by using Equation 8 (Almaiman and Ahmad, 2002).

$$\mu_s = tan\alpha \quad (8)$$

Where:

μ_s = static coefficient of friction,
α = angle of inclination at which potato tuber start to slide down.

Dynamic coefficient of friction
The dynamic coefficient of friction was determined using a topless and bottomless plywood box with dimensions of 250 × 250 × 90 mm^3. The box was placed on a test surface and filled with a known quantity of potato tubers; then force was applied to bottomless plywood box until it moved uniformly with a horizontal pull. The friction test was replicated three times for the surfaces under investigation. For each replication, the box was refilled with a different sample. The dynamic coefficient of friction was determined using Equation 9 (Puchalski *et al.*, 2003; Amin *et al.*, 2004).

$$\mu_d = \frac{F}{mg} \quad (9)$$

Where:
μ_d = dynamic coefficient of friction,
F = friction force that will be measured using pull force gauge (N),
m = mass tuber (kg) and
g = gravitational acceleration (m s^{-2}).

Angle of repose
Angle of repose for potato tuber was determined with a bottomless cylinder. The cylinder was placed over a smooth surface and filled with potato tuber. The cylinder was then raised slowly allowing the tuber to flow down and form a natural slope. The height

and diameter of the heap formed were measured and angle of repose was estimated using Equation 10.

$$\alpha = \tan^{-1} \frac{Height\ of\ potato\ tuber\ pile}{base\ of\ potato\ tuber\ pile/2} \quad (10)$$

Where α is expressed in degree.

RESULTS AND DISCUSSION

Physical properties

The physical properties of potato tubers were determined at a moisture content of 70.75, 69.99, 71.75, 69.70 and 72.38% (w.b) for Belete, Jalenie, Gera, Gudene and Chala varieties, respectively. The temperature recorded in the laboratory during the experiments was 20-28°C.

The weight measurement of each potato tubers showed that Belete variety had the maximum weight of 102.24 g while the minimum value was recorded for Chala Variety 59.66 g.

The mean major diameters of 66.96, 56.28, 55.43, 63.45 and 54.09 mm were observed for Belete, Giera, Jalenie, Gudene and Chala varieties, respectively. The maximum and minimum tubers major diameters of 106.82 mm and 76.90 mm were obtained for Belete and Jalenie varieties, respectively.

The intermediate diameters ranged between 38.72 and 73.63, 30.18 and 71.31, 32.95 and 65.49, 33.17 and 58.67, and 34.15 and 58.19 mm for Belete, Gera, Gudene, Jalenie and Chala varieties, respectively. The maximum tuber intermediate diameter was observed with Belete variety (73.63 mm) and the minimum was observed was Chala (58.19 mm).

The minor diameter ranged between 31.97 and 57.39, 25.56 and 57.05, 30.47 and 52.04, 26.83 and 46.82 and 29.09 and 50.23 mm for Belete, Gera, Gudene, Jalenie and Chala varieties respectively. The maximum tuber intermediate diameter was observed with Belete variety (57.39 mm) and the minimum was observed in Jalenie variety (46.82 mm).

As shown in Table 1, multiple regression equations were determined to describe the relationship between the weight of tubers and its main dimensions for each variety. The equations show that the dimensions of each tuber's varieties were directly proportional with its weight.

Table 1. Multiple regression model of weight of potato tuber and main dimension of potato tuber varieties.

Variety	*Regression Model*	*R Square*
Belete	Weight = 1.61a +2.48b +1.67c -204.54	$R^2 = 0.91$
Jalene	Weight = 1.21 a +1.39b +0.70c -95.29	$R^2 = 0.97$
Chala	Weight = 1.32 a +1.53b +1.77c -148.27	$R^2 = 0.95$
Gera	Weight = 1.06 a +1.76b +1.64c -139.83	$R^2 = 0.88$
Gudene	Weight = 1.32 a +1.53b +1.77c -148.27	$R^2 = 0.95$

Where: a, b and c = major, intermediate and minor diameter respectively, mm

The geometric mean diameters of the selected potato tubers were 52.68, 45.28, 49.87, 47.88 and 44.52 mm for Beleta, Jalenie, Giera, Gudene and Chala varieties, respectively. The maximum geometric mean diameter was observed with Belete variety (75.60 mm) followed by Gudenie variety (67.13 mm) and the minimum was obtained with Giera variety (30.39 mm). The measured surface areas were 8959.30, 6545.70, 7924.10, 7333.10 and 6311.70 mm^2 for Beleta, Jalenie, Gera, Gudene and Chala varieties, respectively.

The measured volumes were 83924.00, 83924.00, 68979, 60943 and 48697 mm^3 for Beleta, Jalenie, Giera, Gudene and Chala varieties respectively. The calculated volumes were 83089, 50994, 67696, 60750 and 48152 mm^3 for Beleta, Jalene, Gera, Gudene and Chala varieties, respectively. The sphericity of the selected potato varieties was found to be 0.80, 0.82, 0.87, 0.76 and 0.82 for Beleta, Jalene, Gera, Gudene and Chala, respectively.

Tuber densities of selected varieties of potato were determined to be 1.23, 1.22, 1.19, 1.20 and 1.25 g cm^{-3} for Beleta, Jalene, Gera, Gudene and Chala, respectively. The maximum and minimum tuber densities were recorded for Chala and Gera varieties, respectively. Bulk densities of 525.94, 529, 523.60, 519.10 and 518.03 kg m^{-3} were recorded for Belete, Gera, Jalene,Gudene and Chala varieties, respectively.

The specific gravity of potato tubers of selected varieties ranged from 1.05 to 1.09. As shown in Table 2, the maximum specific gravity was recorded for Belete variety and the minimum one is recorded for Gera variety. All potato tuber varieties in this study, except Chala and Gera with specific gravity of 1.06 and 1.05, respectively, had a specific gravity greater than 1.07. Except specific gravity of potato tuber, all other physical properties of each variety of potato tuber are significantly different at 5% of level of significance. There was no significant difference among varieties of potato tuber in their specific gravity. The summarized value of important physical and engineering properties of potato tuber variety is shown in Table 2.

Table 2. Physical and engineering attributes of potato tuber varieties.

Variety	Variable	Mean	SD	C.V.	Minimum	Maximum
Belete	Weight(g)	102.42	54.80	53.51	38.00	363.60
	Geometric mean diameter (mm)	52.68	8.81	16.72	39.17	75.76
	Calculated volume (mm^3)	82699	43093	52.11	31477	227654
	Particle density ($g\ cm^{-3}$)	1.24	0.12	9.97	1.08	2.19
	Specific gravity	1.09	0.13	11.74	1.01	2.10
	Shape index	1.42	0.18	12.51	1.09	1.84
Jalenie	Weight(g)	61.55	21.81	35.66	27.20	134.30
	Geometric mean diameter (mm)	45.28	5.81	12.82	32.91	58.27
	Calculated volume(mm^3)	50681	19149	37.78	18668	103612
	Particle density ($g\ cm^{-3}$)	1.22	0.14	11.49	1.03	1.84
	Specific gravity	1.07	0.09	8.06	0.99	1.90
	Shape index	1.35	0.13	9.45	1.07	1.66
Gera	Weight(g)	80.24	28.34	35.32	18	166.80
	Geometric mean diameter (mm)	49.87	5.99	12.	30.39	64.67
	Calculated volume(mm^3)	67263	23958	35.62	14698	141623
	Particle density ($g\ cm^{-3}$)	1.19	0.11	9.43	0.83	1.56
	Specific gravity	1.05	0.09	8.27	0.58	1.49
	Shape index	1.20	0.10	8.01	1.05	1.87
Gudene	Weight(g)	72.50	31.15	42.96	34.6	201.10
	Geometric mean diameter (mm)	47.88	6.52	13.63	37.74	67.13
	Calculated volume(mm^3)	60750	27093	44.60	28137	158396
	Particle density ($g\ cm^{-3}$)	1.20	0.07	5.95	1.04	1.48
	Specific gravity	1.07	0.21	19.38	0.49	2.32
	Shape index	1.52	0.17	11.51	1.14	1.94
Chala	Weight(g)	59.66	21.49	36.01	32.9	141.30
	Geometric mean diameter (mm)	44.52	5.20	11.68	36.61	61.33
	Calculated volume(mm^3)	48152	18362	38.13	25701	120812
	Particle density ($g\ cm^{-3}$)	1.25	0.06	5.21	1.02	1.43
	Specific gravity	1.06	0.02	2.22	1.00	1.21
	Shape index	1.34	0.14	10.50	1.09	1.89

Where, SD = standard deviation and CV = coefficient of variation.

Mechanical properties of potato tubers

As shown in Table 3, the mean angle of repose of potato tubers ranged from 23.12 to 31.74° on mild steel sheet metal, 23.01 to 41.14° on Galvanized sheet, 22.61 to 38.39° on wood and 25.68 to 36.61° on rubber surface. The maximum and minimum angle of repose was recorded as 41.14 and 22.61° for Belete and Chala varieties on Galvanized sheet and wood surface, respectively.

The static coefficients of friction of the different variety's potato tubers ranged from 0.22 to 0.27 on mild steel sheet metal, from 0.18 to 0.30 on galvanized sheet, from 0.29 to 0.43 on wood and from 0.27 to 0.47 on rubber. The minimum and maximum static coefficients of friction were recorded as 0.18 and 0.47 for Gera and Belete variety on Galvanized sheet and rubber, respectively.

The dynamic coefficients of friction ranged from 0.48 to 0.67 on mild steel sheet metal, from 0.52 to 0.65 on galvanized sheet, from 0.62 to 0.68 on wood and from 0.61 to 0.68 on rubber surfaces. The minimum and maximum dynamic coefficients of friction were recorded as 0.48 and 0.68 for Belete and Chala varieties on mild steel sheet metal and rubber surfaces, respectively.

Table 3. Mechanical attributes of dominant and popular potato varieties.

		Varieties					
Property	**Material**	**Belete**	**Jalenie**	**Giera**	**Gudenie**	**Chala**	**Average**
Coefficient of static friction	Mild steel sheet metal	0.23	0.274	0.2309	0.2614	0.2187	0.2430
	Galvanized sheet metal	0.3	0.243	0.1824	0.2248	0.1885	0.277
	Wood	0.43	0.332	0.3122	0.3512	0.2937	0.3438
	Rubber	0.47	0.365	0.2742	0.3252	0.2805	0.3430
	Average	0.3575	0.3035	0.2499	0.2906	0.2453	0.2894
Coefficient of dynamic friction	Mild steel sheet metal	0.4762	0.6556	0.6664	0.6455	0.6698	0.6227
	Galvanized sheet metal	0.5203	0.5981	0.6477	0.5497	0.5524	0.5736
	Wood	0.6716	0.623	0.6803	0.6505	0.6664	0.6584
	Rubber	0.6147	0.6805	0.6786	0.6435	0.6846	0.6604
	Average	0.5707	0.6393	0.6683	0.6223	0.6433	0.6288
Angle of repose	Mild steel sheet metal	31.6033	26.7033	31.74	35.4967	23.12	29.7327
	Galvanized sheet metal	41.1433	23.01	36.2	28.9667	24.14	30.692
	Wood	38.3867	27.4433	38	37.9733	22.61	32.8827
	Rubber	36.6133	29.9167	31.56	33.6967	25.68	31.4933
	Average	36.9367	26.7683	34.36	34.0333	23.8875	31.2002

As shown in Table 4, the result of analysis of variance showed that static coefficient of friction and angle of repose of all potato tuber varieties under four different materials and dynamic coefficient of friction under mild steel sheet metal and galvanized sheet is significantly different. There is no significant difference in dynamic coefficient of friction of all varieties of potato tuber between wood and rubber surface.

Table 4. Analysis of variance on mechanical properties of potato tuber (source of variation: between varieties).

Property	**Material**	**SS**	**df**	**MS**	**F**	**P-value**
Static Coefficient of friction	Mild steel sheet metal	0.0077	4	0.0019	8.0600	0.0036
	Galvanized sheet metal	0.0300	4	0.0067	19.3900	0.0001
	Wood	0.0340	4	0.0085	4.9300	0.0200
	Rubber	0.0700	4	0.0200	10.1200	0.0015
Dynamic coefficient of friction	Mild steel sheet metal	0.0800	4	0.0200	53.6400	0.0000
	Galvanized sheet metal	0.0300	4	0.0073	7.0000	0.0000
	Wood	0.0066	4	0.0017	1.1780	0.3800
	Rubber	0.0100	4	0.0027	1.6100	0.2500
Angle of repose	Mild steel sheet metal	280.9700	4	70.2400	22.8100	0.0001
	Galvanized sheet metal	733.3300	4	183.3300	21.5800	0.0001
	Wood	652.5300	4	163.1300	13.2200	0.0005
	Rubber	202.0600	4	50.5200	9.3800	0.0020

Where, SS: sum of square, MS: mean square, df: degree of freedom, F: F ratio and P: significance level at 5%

CONCLUSION

Pertinent physical and mechanical attributes of the potato tuber relevant to develop equipment for potato production were studied. The study revealed that for five different varieties of potato tubers; the mean major, intermediate and minor diameters were 66.00, 50.94 and 42.27 mm, respectively. The mean geometric diameters, surface area, percent and Sphericity of the potato tubers were found to be 48.06 mm, 7414.77 mm^2 and 81.92%, respectively. For tubers of five different varieties, tuber density, bulk density and specific gravity were found to be 1.22 g cm^{-3}, 518.03 kg m^{-3} and 1.07 respectively.

DECLARATION OF COMPETING INTEREST

The author declares that they have no conflict of interest.

CREDIT AUTHORSHIP CONTRIBUTION STATEMENT

The author confirms sole responsibility for the following: investigation, methodology, conceptualization, formal analysis, data curation, validation, writing - original draft, review, editing and visualization etc.

REFERENCES

Alemu DA, Fanta A and Getnet B (2021). Performance evaluation of engine operated potato grader; *Ethiopian Journal of Agricultural Science, 31(2): 61-71.*

Almaiman S and Ahmad D (2002). Changes in physical and chemical properties during pomegranate (*Punica granatum* L.) fruit maturation. *Journal of Food Chemistry, 76: 437-441.*

Amin MN, Hossain MA and Roy C (2004). Effects of moisture content on some physical properties of lentil seeds. *Journal of Food Engineering, 65: 83-87.*

Asoegwu SN (1995). Some physical properties and cracking energy of conophor nuts at different moisture content. *International Agrophysics, 9(2): 131-142.*

Ayalew T (2014). Potato seed systems in Ethiopia. *Asian Journal of Agricultural Research, 8(3): 122-135.*

Central Statistical Agency (CSA) 2009. Agricultural sample survey Report on area and production of crops, Addis Ababa, (p. 126), Ethiopia.

Central Statistical Agency (CSA) 2015. Report on area and production of major crops (Vol. I). Addis Ababa, Ethiopia.

Food and Agricultural Organization (FAO) (2009). Sustainable potato production-Guidelines for Developing Countries. Agricultural and Forest Meteorology (Vol. 127) https://doi.org/10.1016/j.agrformet.2004.08.003.

Gebru H, Mohammed A, Dechassa N and Belew D (2017). Assessment of production practices of smallholder potato (*Solanum tuberosum* L.) farmers in Wolaita zone, Southern Ethiopia. *Journal of Agricultural and Food Security, 6 (31): 1-11.*

Hurst WC, Reynolds AE, Schuler GA and Christian JA (1993). Maintaining Food Quantity in Storage. University Of Georgia Cooperative Extension Service Bulletin 914.

Joshi AV and Raisoni GH (2016). Review Paper on Physical and Mechanical Properties of Citrus Fruits and Various Techniques used in Fruit Grading system based on their sizes. *International Journal of Science Technology & Engineering, 3(4): 129-132.*

Kamat V, Sisodiya JH, Mahawar MK and Jalgaonkar K (2020). Determination of some physical properties of Plum (*cv.* Kala Amritsari) fruits. *International Journal of Chemical Studies, 8(3): 225-228.*

Malcolm EW, Tappan JH and Sister FE (1986). The size and shape of typical sweet potatoes. *Transactions of the ASAE, 29: 678-682.*

Mohsenin NN (1986). Physical properties of plant and animal materials. Department of Agricultural Engineering, Pennsylvania State University, *Gordon & Breach Science Publishers*, New York.

Puchalski C, Brusewitz G and Slipek Z (2003). Coefficients of friction for apple on various surfaces as affected by velocity. *Agricultural Engineering International: the CIGR Journal of Scientific Research and Development". Manuscript FP 03 002. Vol. V. December 2003.*

Rahman MS (2014). Engineering properties of foods, 4th Edition. Newyork: *CRC Press Taylor & Francis Group*. https://doi.org/International Standard Book Number-13: 978-1-4665-5643-0 (eBook - PDF). Boca Ratan, London,

Razavi SMA, Emadzadeh B, Rafe A and Mohammad Amini A (2007). The physical properties of pistachio nut and its kernel as a function of moisture content and variety: Part I. Geometrical properties. Journal of Food Engineering, *81: 209-217.*

Turkish Journal of Agricultural Engineering Research

https://dergipark.org.tr/en/pub/turkager
https://doi.org/10.46592/turkager.2021.v02i02.014

Turk J Agr Eng Res (TURKAGER)
ISSN: 2717-8420
2021, 2(2), 413-424

Research Article

Optimization of Operational Parameters of an Improved Maize Sheller Using Response Surface Methodology

Adewale Moses SEDARA[ID][a]* Emmanuel Olutope ODEDIRAN[ID][b]

[*a]*Department of Agricultural and Environmental Engineering, School of Engineering and Engineering Technology, The Federal University of Technology, Akure, NIGERIA*

[b]*Department of Agricultural and Environmental Engineering, School of Engineering and Engineering Technology, The Federal University of Technology, Akure, NIGERIA*

(*): Corresponding author, adewale.sedara@gmail.com

ABSTRACT

The research was carried out to optimize parameters for evaluating an improved motorize maize sheller. Statistical analysis was performed using response surface methodology (RSM) with 3 by 3 factorial experiment with 3 replicates. The three parameters are speed (850 rpm, 950 rpm and 1100 rpm), moisture content (12, 15, and 17%) and feed rate (120 kg h^{-1}, 130 kg h^{-1} and 140 kg h^{-1}) used to illustrate the ability of the machine to shell maize (throughput capacity, shelling rate and machine efficiency). Results obtained showed that for optimum throughput capacity of 630.97 kg h^{-1}; shelling rate 485.34 kg h^{-1} and machine efficiency 93.86% of the machine; is maximum for 129.6 kg h^{-1} feed rate and moisture content 16.49% and machine speed of 1026.9 rpm. The machine can be used on commercial farms with these operational results.

RESEARCH ARTICLE

Received: 12.09.2021
Accepted: 20.11.2021

Keywords:

- Maize sheller,
- Optimization,
- ANOVA,
- Machine efficiency,
- Throughput capacity
- Shelling rate

To cite: Sedara AM, Odediran EO (2021). Optimization of Operational Parameters of an Improved Maize Sheller Using Response Surface Methodology. Turkish Journal of Agricultural Engineering Research (TURKAGER), 2(2), 413-424. *https://doi.org/10.46592/turkager.2021.v02i02.014*

INTRODUCTION

Maize (*Zea mays*) is an essential cereals crop that have its place to a grass family (Poaceae) creating trivial eatable seeds (Aremu *et al.*, 2015). In maize processing shelling is consider a major operation that is very important to study. Shelled maize grains are important because they are consumed worldwide and are used for different purposes in different industries that's why its shelling is considered to be crucial (Sedara *et al.*, 2020). When maize seeds are removed from cob this is referred to as shelling and it's a postharvest process. It's performed on the farm or processing facilities

(Nwakaire *et al*., 2011). To produce finished products like flour from maize it is important to shell. Maize shelling operation could be performed manually, mechanically or electro-mechanically. The operation is should be able to remove the grain without inflicting damages to the kernels. According to Okure and Ssekanyo (2017), the traditional method of maize dehusking was done manually with hand and shelling was by beating the dehusked cob of maize with sticks, sickle, finger, etc., mostly done by rural women. Olaoye (2004) claimed that appropriate change of functioning condition in motorised thresher has been discovered by scholars to be the best critical success feature in grain threshing. Key variables of notice are mostly categorised as machine factors, crop characteristics and swaying eco-friendly or handling conditions. Nkakini *et al.* (2007) reported that the sheller used abrasion mechanism to strip maize. Manually functioned lever was used to alternate two shafts, one of which explained revolving motion to direct motion a slider crank. Maize cobs are push into the machine by the slider which is a continuous process. Despite the fact that of its operation, it provided constant flow with kernels dropping through the chute. Ojomo and Alemu (2012) reported that most of locally fabricated maize sheller/thresher have low efficiency due to limited knowledge on how to optimize parameters for improve performance. Different designs for maize shelling still the operational conditions still need to be optimized. Nsubuga *et al.* (2020) worked on optimizing the maize shelling operation of a multipurpose maize thresher and got optimum moisture content and speed of 13% and 896 rpm. The aim of the research was to establish optimum performance indicators between operation variables (moisture content, speed and feedrate) and their effect on shelling rate, throughput capacity and machine efficiency using 3D surface response methodology, thereby improving the quality of shelling/threshing and productivity.

MATERIALS and METHODS

Principles of Operation

The shelling is achieved by the shearing by the rotating spikes auger, which releases the grains from the maize cobs holding them. Different grain crops and different varieties of the same grain crop have varying characteristics, which require different speeds of the cylinder for achieving the best result of shelling, therefore adjustment of cylinder speed and proper feeding of cobs is essential.

Design and Fabrication

The hopper was designed to be a frustum, trapezoidal in shape and has the following dimensions that were chosen based on proportionality and aesthetics. The angle of the base to the vertical is 490 with volume of hopper 0.04749 m^3. The total number of spikes on the shelling cylinder 28, and the power required was 1.5753 hp. The shelling/threshing chamber was 65 mm in diameter and length was 750 mm. The overall dimensions of frame were 77 cm length, 42.5 cm width and 128 cm height. Hopper receives and conveys maize cobs to the shelling unit, shelling chamber is where the maize encounters impact force on maize cob during shelling. Shaft and bearing allows the rotation cylinder and spikes and screen receives and screen the shelled grains, while frame supports the weight of the entire machine. V-Belt transmits power from engine to the shaft

The machine was designed using AutoCAD 16 as shown in Figure 1. Shows the side view of the fabricated motorize maize sheller.

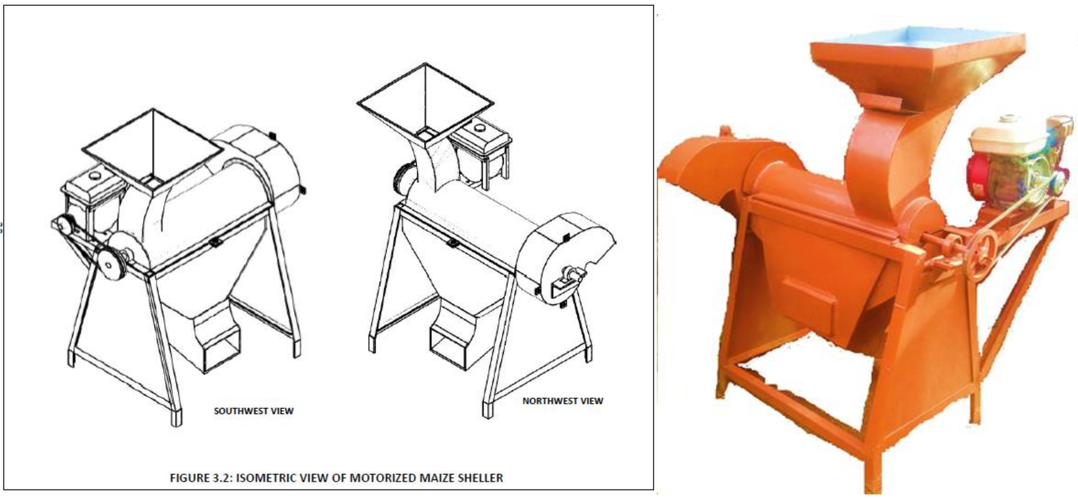

Figure 1. Side view of developed motorized maize sheller.

Experimental design and performance evaluation

Complete Randomised Design was used in the test as experimental design. A tachometer was used to measure the speed in rpm of the motor and the machine pulleys. The range of instrument was 10-10000 rpm. Stopwatch was used to measure time taken to run the machine during performance test and weighing balance to measure mass of maize. Moisture content was determined gravimetric method, Samples at all levels of moisture contents was randomly assigned to the sequence of test runs. Each test at a particular moisture content was replicated three times. This is carried out to ascertain the efficiency and effectiveness of the machine in terms of throughput capacity, shelling rate and machine efficiency. The developed machine performance was tested using maize at different variables such as moisture content (12, 15, and 17%) with variation in the machine speed (850 rpm, 950 rpm and 1100 rpm) and the feed rates (120 kg h^{-1}, 130 kg h^{-1} and 140 kg h^{-1}).

The feed rate was calculated using equation 1

(i) Feeding rate (kg h^{-1}) $= \frac{W_{mf}}{T_t}$ (1)

where, W_{mf} is total weight of maize cob fed into the hopper, T_t is total time taken

(ii) Shelling rate (kg h^{-1}) The weight of the maize kernels (whole + broken) detached from the cobs in unit time was taken as shelling rate. It was calculated using Equation 2:

$$\text{Shelling rate (kg h}^{-1}\text{)} = \frac{W_{mh}}{T_{th}} \quad (2)$$

W_{mh} is total weight of material handled and T_{th} is total time taken.

(iii) Machine efficiency (%): It is the percentage by weight of shelled kernels from all outlets of the sheller with respect to total kernel input. It is calculated using Equation 3:

$$\text{Machine Efficiency (\%)} = \frac{T_{ws}}{T_{wc}} \times 100 \qquad (3)$$

T_{ws} is total weight of shelled grains from the outlets and T_{wc} total weight of cobs input

(iv) Throughput capacity (kg h^{-1}): The weight of the maize cobs with kernels attached attempted by the machine in unit time was taken as rate of throughput and it was calculated using Equation 4;

$$\frac{T_{wgc}}{T_t} \times 100 \qquad (4)$$

T_{wgc} is total weight of grains attached with cobs and T_t is total time taken.

Data analysis
The analysis entails Response surface methodology (RSM) on Design Expert 12. The factors (speed, moisture content and feed rate) were set in range while the responses (throughput capacity, shelling rate and machine efficiency) were set to maximize. It can be expressed as the dependent variable y is a function of X_1, X_1 and X_3.

$$Y = f(X_1) + f(X_2) + f(X_3) + e \qquad (5)$$

where Y is the response (dependent variable), X_1 and X_2 are independent variables and e is the experimental error.

RESULTS and DISCUSSION

The factors were optimized to result the level of responses of throughput volume, shelling rate and efficiency. To maximized productivity in terms of shelling the machine operations at different speed, feed rate and moisture content. The RSM (response surface methodology) stayed functional on motorize sheller/threshing with a total of 18 experiments was performed. For accurate results, three-dimensional surfaces representation describing the behaviour of the structure inside the experiment design.

Throughput capacity (kg h^{-1})
Table 1 shows that the model established is not significant with F-value of 1.05. This means that the value is large (46.49%) and this could be caused by no-symmetry between the factors to give a better response. The "Prob> F" show model relationships are significant. It was observed that only feed rate that have significant effect on the throughput volume for the machine while the other factors are insignificant, and they can be revisited to improve the model. "Lack of Fit F-value" 3.29 infers it's not significant with only 10.84% given the model a fit.

Throughput capacity (kg h^{-1}) = 541.44-23.89*A+1.19*B+5.04*C+15.49*AB-8.57*AC-3.59 *BC+36.34*A^2+5.2 *B^{2}6-7.46 *C^2 (6)

where A is feed rate, B is moisture content and C is machine speed. Equation 6 shows that speed and moisture content had positive coefficient (little effect) while feed rate was negative showing less effect on throughput capacity. Equation 1 is suitable for classifying the virtual effect of the factors by linking the factor coefficients. Throughput capacity shows a ratio of 5.158 (ratio>4) which indicates an adequate signal as shown in Table 4.3. The model is quadratic in nature which describes the fits. Equation (6) was used to calculate the predicted value and compared with actual value of throughput for the experiment as shown in Figure 2 with a coefficient of determination ($R^2 = 0.6513$) as shown in Table 2. This means the model can significantly explain 65.13% variation in throughput capacity of the machine.

Table 1. Effect of feed rate, moisture content and machine throughput capacity.
Response 1. Throughput capacity.

Source	Sum of Squares	df	Mean Square	F-value	P-value	
Model	31688.75	9	3520.97	1.05	0.4649	not significant
A-feed rate	7797.59	1	7797.59	2.33	0.1579	not significant
B-moisture content	19.34	1	19.34	0.0058	0.9409	not significant
C-machine speed	346.38	1	346.38	0.1035	0.7543	not significant
AB	1918.59	1	1918.59	0.5734	0.4664	not significant
AC	587.73	1	587.73	0.1757	0.6840	not significant
BC	103.32	1	103.32	0.0309	0.8640	not significant
A^2	19030.61	1	19030.61	5.69	0.0383	significant
B^2	398.47	1	398.47	0.1191	0.7372	not significant
C^2	801.42	1	801.42	0.2395	0.6351	not significant
Residual	33459.27	10	3345.93			
Lack of Fit	25664.87	5	5132.97	3.29	0.1084	not significant
Pure Error	7794.39	5	1558.88			
Cor Total	65148.01	19				

Where df is degree of freedom, F-value is critical value and P-value is significant value

Table 2. Fit statistics for the throughput capacity of maize sheller.

Std. Dev.	51.80	R^2	0.6513
Mean	517.66	Adjusted R^2	0.3374
C.V. %	10.01	Predicted R^2	-1.2381
		Adeq Precision	5.1576

Where Std. Dev. is standard deviation, C.V. % is coefficient of variation, R^2 is coefficient of determination, Adjusted R^2 is adjusted coefficient of determination, Predicted R^2 is predicted coefficient of determination and Adeq Precision is adequate precision.

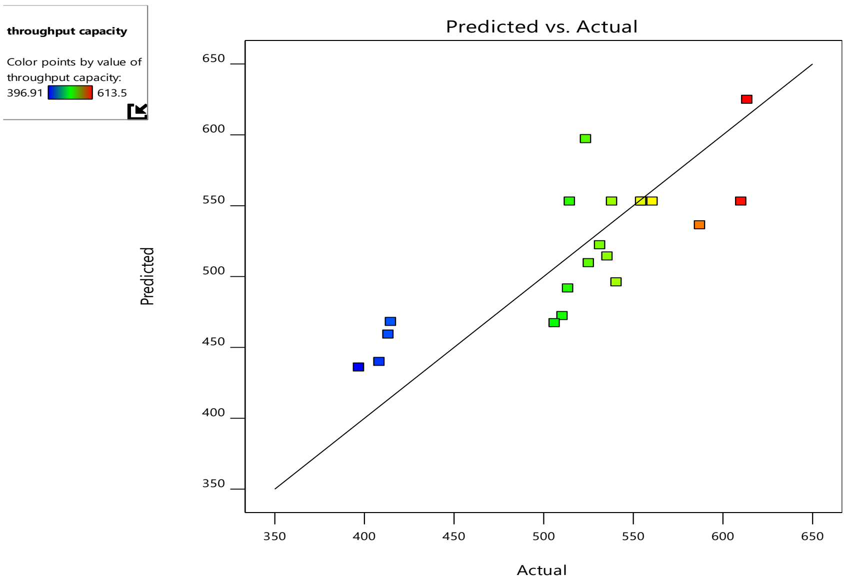

Figure 2. Predicted against actual values of throughput of maize sheller.

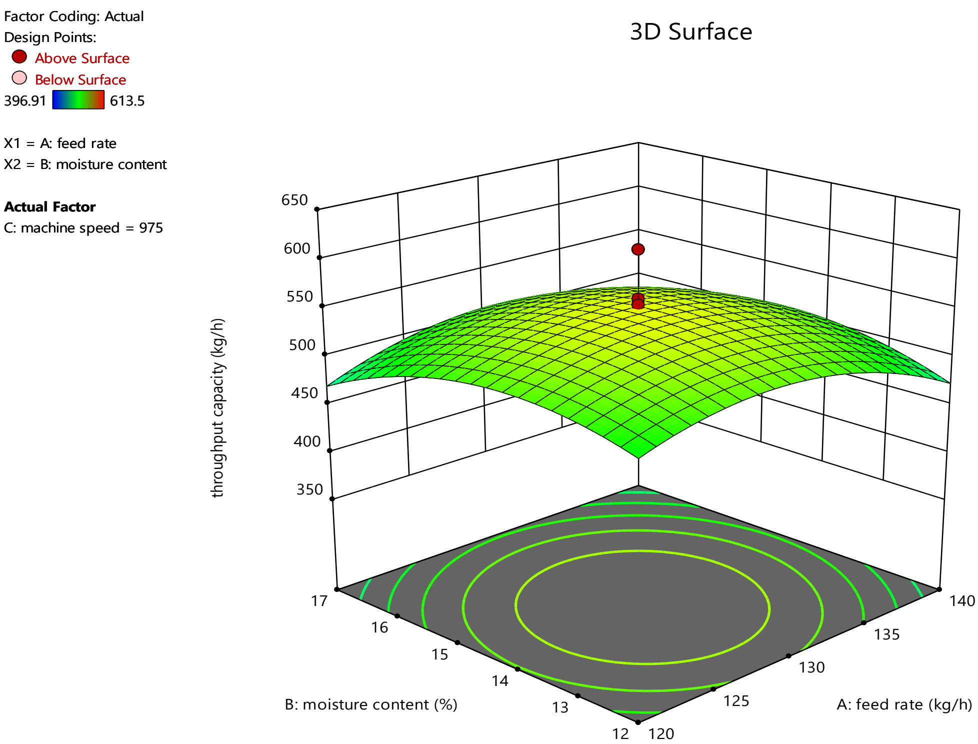

Figure 3. Effect of feed rate and moisture content on throughput capacity of machine.

Figure 3 depicts the interaction feed rate and moisture content on throughput capacity of machine. It is clear that the throughput capacity of machine to be minimum at 520 kg h^{-1} and maximum at 580 kg h^{-1} i.e., as the feed rate and moisture increased. This may be due to the reduction in the resistance to detachment from the cobs and the operational energy required to remove the grains from the cobs as moisture content reduced which agrees with Oriaku *et al.* (2014) and Ogunlade *et al.* (2014), when the moisture content reduced, it resulted into increase in throughput capacity.

Shelling rate (kg h^{-1})

Table 3 shows the analysis of the variance (ANOVA) of the shelling rate, it was observed that the three conditions have no significant effects on shelling rate. However, the most effective of the factors was the feed rate with a contribution of 35.5%. The model is significant with **p-value** of 0.0236. The product of (federate)^2, (moisture content) ^{2}, (speed)^2 are significant model terms compared to other terms having a lower contribution to 0.05.

$$\textbf{Shelling rate} = 426.626 + -1.8713 * A - 2.94736 * B - 12.5042 * C + 0.1575 * AB - 2.2525 * AC + -4.04 * BC + -30.7692 * A^2 + -28.4711 * B^2 + 21.8749 * C^2 \quad (7)$$

where A is feed rate, B is moisture content and C is machine speed. The model for shelling rate is given by Equation 7 and can be used to calculate the predicted value and compared with actual value of shelling rate for the experiment as shown in Figure 4 with a coefficient of determination (R^2 = 0.7759) as shown in Table 4

Table 3. Effect of feed rate, moisture content and machine throughput capacity on **shelling rate.**

Source	Sum of Squares	df	Mean Square	F-value	p-value	
Model	36396.23	9	4044.03	3.85	0.0236	significant
A-feed rate	47.82	1	47.82	0.0455	0.8354	not significant
B-moisture content	118.64	1	118.64	0.1128	0.7439	not significant
C-machine speed	2135.31	1	2135.31	2.03	0.1846	not significant
AB	0.1985	1	0.1985	0.0002	0.9893	not significant
AC	40.59	1	40.59	0.0386	0.8482	not significant
BC	130.57	1	130.57	0.1242	0.7318	not significant
A^2	13643.77	1	13643.77	12.98	0.0048	significant
B^2	11681.82	1	11681.82	11.11	0.0076	significant
C^2	6895.98	1	6895.98	6.56	0.0283	significant
Residual	10514.11	10	1051.41			
Lack of Fit	9835.22	5	1967.04	14.49	0.0054	significant
Pure Error	678.89	5	135.78			
Cor Total	46910.34	19	135.78			

Where df is degree of freedom, F-value is critical value and P-value is significant value

Table 4. Fit statistics for the throughput capacity of maize sheller.

Std. Dev.	32.43	R^2	0.7759
Mean	401.11	Adjusted R^2	0.5741
C.V. %	8.08	Predicted R^2	-0.6080
		Adeq Precision	7.5486

Where Std. Dev. is standard deviation, C.V. % is coefficient of variation, R^2 is coefficient of determination, Adjusted R^2 is adjusted coefficient of determination, Predicted R^2 is predicted coefficient of determination and Adeq Precision is adequate precision.

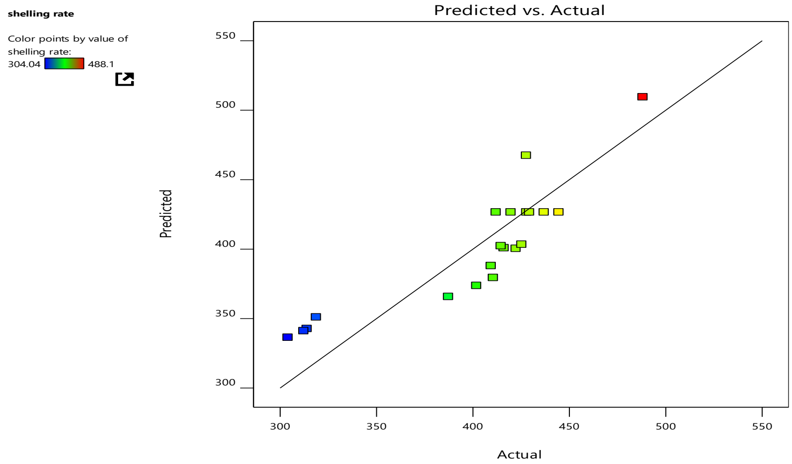

Figure 4. Predicted against actual values of throughput of maize sheller.

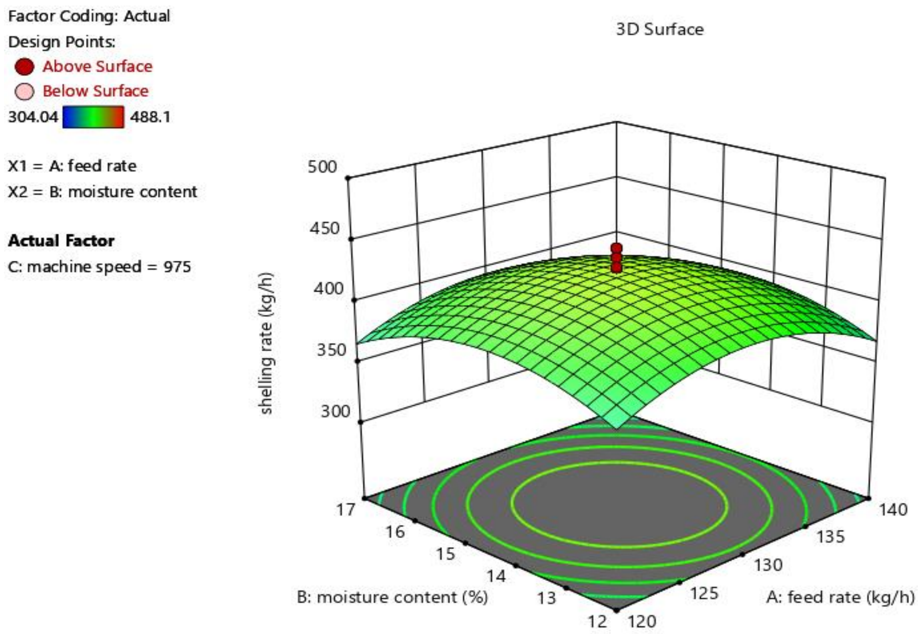

Figure 5. Feed rate and moisture content effect on shelling rate.

Figure 5 shows the interaction of feed rate and moisture content on shelling rate. It was observed that shelling rate was highest at 130 kg h^{-1} and minimum at 120 kg h^{-1} which means as shelling rate of grain from cob improved with feed rate and vice-versa, this shows shelling rate slightly improved with increased in moisture content. Also increased shelling speed increased the shelling rate. This may be due to the increased ease of detachment of the maize grains from the cobs with higher impacts and friction created between the shelling drum and the concave as the shelling speed increases which is in agreement with Oriaku *et al.* (2014).

Machine Efficiency

Table 5 shows the ANOVA for the machine efficiency, it was observed that the three conditions have significant effect on the efficiency of the machine **($p<0.05$).** the product of (feed rate)², (moisture content)², (speed)² also shows they significantly contributes to model terms.

Machine Efficiency (%) = 90.0015 + 0.23421 * A + -0.220268 * B + 0.120386 * C + 0.35 * AB + -0.0975 * AC + -0.095 * BC + 1.13928 * A^2 + 1.33197 * B^2 + 0.74684 * C^2 (8)

Equation 8 was used to calculate the predicted value and compared with actual value of machine efficiency for the experiment as shown in Figure 6 with a coefficient of determination (R^2=0.5905) as shown in Table 6.

Table 5. Effect of feed rate, moisture content and speed on m**achine efficiency.**

Source	Sum of Squares	df	Mean Square	F-value	P-value	
Model	47.09	9	5.23	3.94	0.0219	Significant
A-feed rate	0.7491	1	0.7491	0.5637	0.04701	Significant
B-moisture content	0.6626	1	0.6626	0.4986	0.04963	Significant
C-machine speed	0.1979	1	0.1979	0.1489	0.04076	Significant
AB	0.9800	1	0.9800	0.7374	0.4106	not significant
AC	0.0761	1	0.0761	0.0572	0.8158	not significant
BC	0.0722	1	0.0722	0.0543	0.8204	not significant
A^2	18.71	1	18.71	14.07	0.0038	Significant
B^2	25.57	1	25.57	19.24	0.0014	Significant
C^2	8.04	1	8.04	6.05	0.0337	Significant
Residual	13.29	10	1.33			
Lack of Fit	8.70	5	1.74	1.90	0.2494	not significant
Pure Error	4.59	5	0.9171			
Cor Total	60.38	19				

Where df is degree of freedom, F-value is critical value and P-value is significant value

Table 6. Fit statistics for the machine efficiency of maize sheller.

Std. Dev.	1.67	R^2	0.5905
Mean	91.69	Adjusted R^2	0.2220
C.V. %	1.82	Predicted R^2	0.0340
		Adeq Precision	4.8365

Where Std. Dev. is standard deviation, C.V. % is coefficient of variation, R^2 is coefficient of determination, Adjusted R^2 is adjusted coefficient of determination, Predicted R^2 is predicted coefficient of determination and Adeq Precision is adequate precision.

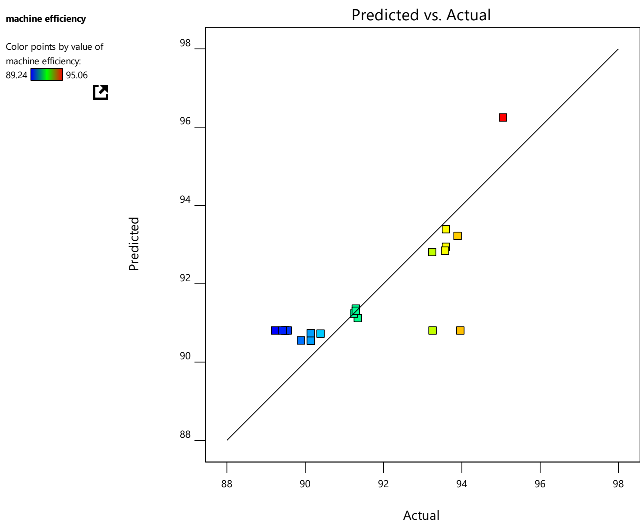

Figure 6. Predicted against actual values of machine efficiency of maize sheller.

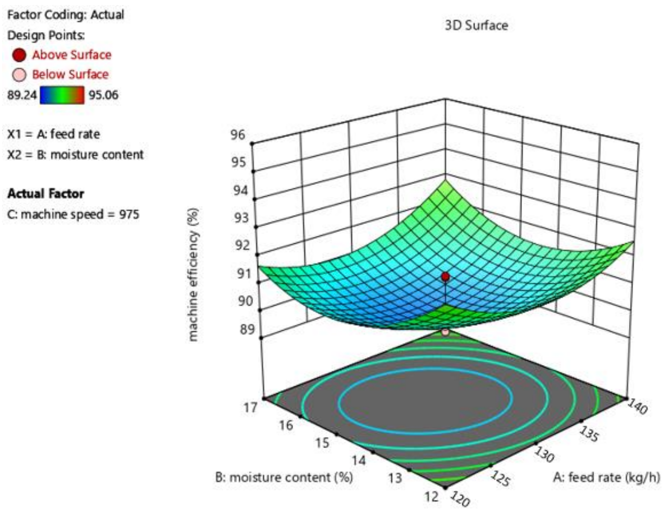

Figure 7. Feed rate and moisture content effects on machine efficiency.

Figure 7 shows the interaction of moisture level and feed rate on efficiency of the machine. The highest efficiency of 92.6% was observed at the peak interaction of feed rapture and moisture level and lowest value of 85%, as machine efficiency decreased with increased in feed rate and vice-versa, machine efficiency slightly improved and reduced with increased in moisture content. These results were in agreement with the findings of Roy *et al.* (2017). A reduction in moisture resulted into an increase in the machine efficiency of the improved maize sheller at the same shelling speed. This may be due to less time required to detach the maize grains from the cob as the moisture content reduced as explained by Chaudhary (2016). The machine efficiency was greatest at a moisture content of 12% and lowest at 17%.

Optimize parameters

The optimization of the interactions between factor terms and the evaluation of the machine is has presented in Figure 8 using surface response methodology. The results were found that at 129.6 kg h^{-1} feed rate, moisture content 16.49% and machine speed of 1026.9 rpm the throughput capacity of 630.97 kg h^{-1}; shelling rate 485.34 kg h^{-1} and machine efficiency 93.86 % of machine is maximum as shown in Figure 8. It was observed that the desirability at run 1 of 73 was the best compared to other runs.

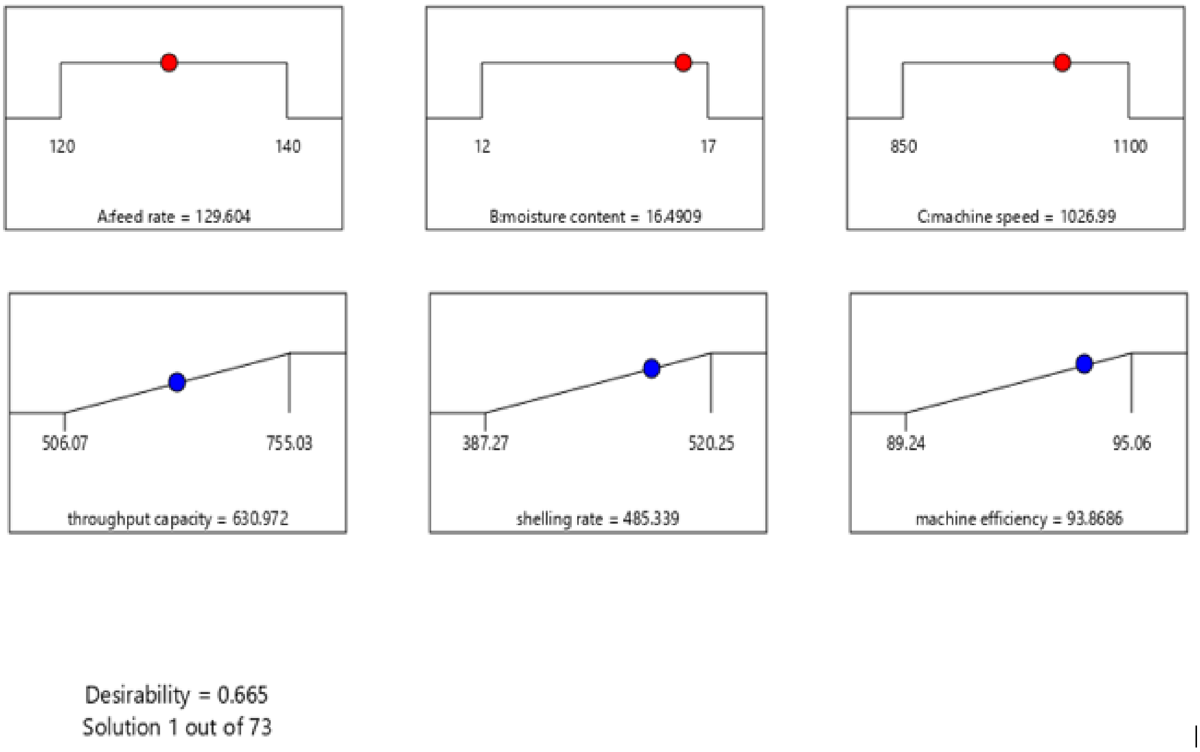

Figure 8. Optimize parameters of machine.

CONCLUSION

A motorized maize sheller machine has been designed and fabricated with the use of locally available materials. The machine was tested at three levels of moisture content (12, 15 and 17%), three levels of feed rate (120, 130 and 140 kg h^{-1}) and three levels of machine speed (850, 950 and 1100 rpm) had different machine efficiency (%), throughput capacity (kg h^{-1}) and shelling rate (kg h^{-1}). The throughput capacity of machine varied from 480 kg/h to 755.03 kg h^{-1} at different moisture content and different speed of operation. Regression analysis showed a quadratic relationship for throughput capacity, shelling rate and machine efficiency having coefficient of determination R^2 of 0.6513, 0.7759 and 0.5905 respectively. The moisture content had no effect on the throughput capacity of motorized maize shelling machine. The shelling rate decreased with increase in moisture content and decreased with increase in moisture content. The machine speed had great effect on the shelling rate. With the increased in speed of operation, the machine efficiency increased. It showed an increasing trend with the increased in speed of operation. The overall machine efficiency of machine had approximately 95.06%. The optimized results show shelling rate and throughput capacity was determined; with throughput capacity of 630.97 kg h^{-1}; shelling rate 485.34 kg h^{-1} and machine efficiency 93.86% of machine is maximum for 129.6 kg h^{-1} feed rate and moisture content 16.49% and machine speed of 1026.9 rpm.

DECLARATION OF COMPETING INTEREST

The authors of this manuscript declare that there is no conflict of interest.

CREDIT AUTHORSHIP CONTRIBUTION STATEMENT

Adewale Moses Sedara: Methodology, conceptualization,, validation, writing - original draft, review and editing.
Emmanuel Olutope Odediran: Investigation, formal analysis, data curation, visualization.

REFERENCES

Aremu DO, Adewumi IO and Ijadunola JA (2015). Design, fabrication and performance evaluation of a motorized maize shelling machine. *Journal of Biology, Agriculture and Healthcare, 5(5): 154-164*

Chaudhary S (2016). Development and performance evaluation of modified maize dehusker cum sheller. *Ph.D diss., Sam Higginbottom Institute of Agriculture, Technology and Sciences.*

Nkakini SO, Ayotamuno MJ, Maeba GPD, Ogaji SOT and Probert SD (2007). Manually-powered continuous flow maize sheller. *Applied Energy, 84: 1175-1186.*

Nsubuga D, Kabenge I, Zziwa A, Kiggundu N, Wanyama J and Banadda N (2020). Performance evaluation and optimization of the maize shelling operation of the multi-purpose farm vehicle. *Agricultural Engineering International: CIGR Journal, 22(4): 174-183.*

Nwakaire JN, Ugwuishiwu BO and Ohagwu CJ (2011). Design, construction and performance analysis of a maize thresher for rural dweller, *Nigerian Journal of Technology, 30(2): 49-54.*

Ogunlade CA, Aremu DO, Babajide NA and Akinyele AO (2014). *Design, fabrication and performance evaluation of a power (motorised) maize shelling machine*. In Proceedings of the Third International Conference on Engineering and Technology Research, 117-125, *ISBN 978-2902-58-6 5-7*

Ojomo AO and Alemu MO (2012). Response surface methodology approach to optimising performance parameters of a locally fabricated maize shelling machine. *Journal of Science and Multidisciplinary Research, 4(2): 70-79.*

Okure D and Ssekanyo S (2017). User perception towards a motorized thresher ('Kungula') in Uganda: A need finding survey. *African Journal of Agricultural Research, 12(12): 997-1004.*

Olaoye JO (2004). *An Analytical modeling of the performance of tooth peg grain crop thresher*. Ph.D. Thesis, Department of Agricultural Engineering and Bio-systems, University of Ilorin, Ilorin, Nigeria, 2004.

Oriaku EC, Agulanna CN, Nwannewuihe HU, Onwukwe MC and Adiele ID (2014). Design and performance evaluation of a corn de-cobbing and separating machine. *American Journal of Engineering Research, 3(6): 127-136.*

Roy SK, Albu M and Rob A (2017). Business rationale for investment on power operated maize sheller in Bangladesh. *Agricultural Engineering International: CIGR Journal, 9(3): 1-13.*

Sedara A, Odediran E and Manuwa S (2020). Design and Fabrication of an Improved Motorized Maize Sheller/Threshing Machine*, Journal of Engineering Studies and Research, 26(4): 119-130.*

Turkish Journal of Agricultural Engineering Research

https://dergipark.org.tr/en/pub/turkager
https://doi.org/10.46592/turkager.2021.v02i02.015

Turk J Agr Eng Res
(TURKAGER)
e-ISSN: 2717-8420
2021, 2(2): 425-433

Research Article

Physicochemical Characterization of Selected Pomegranate (*Punica granatum* L.) Cultivars

Vijay Singh MEENA[a], Bhushan BIBWE[b], Bharat BHUSHAN[c], Kirti JALGAONKAR[d], Manoj Kumar MAHAWAR[d*]

[a]*ICAR- National Bureau of Plant Genetic Resources, New Delhi, INDIA*
[b]*ICAR- Central Institute of Post-Harvest Engineering and Technology, Abohar (Punjab); INDIA*
[c]*ICAR- Indian institute of Maize Research, Ludhiana (Punjab), INDIA*
[d]*ICAR- Central Institute for Research on Cotton Technology, Mumbai (Maharashtra), INDIA*

(*): Corresponding author. manojmahawar362@gmail.com

ABSTRACT

The physical and chemical characteristics of five pomegranate cultivars (Mridula, Ganesh, White muscut, G-137 and Jalor seedless) were examined in the present investigation. Physical properties of different cultivars were determined such as major diameter (85.05 to 91.62 mm), intermediate diameter (76.85 to 87.83 mm), minor diameter (79.86 to 90.01 mm), sphericity (0.903 to 0.937), fruit weight (294.4 to 404.14 g), fruit volume (289 to 387 mL), number of arils per fruit, weight of 100 arils were evaluated and analysed for the varietal difference. In addition, properties such as peel moisture content (68.72 to 74.15% w.b.), aril moisture content (78.25 to 81.82% w.b.), peel ash content (0.81 to 1.51%), aril ash content (0.29 to 0.53%), juice pH (3.47 to 3.96), total soluble solids (11.60 to 13.00 °Brix), titratable acidity (0.42 to 0.58%), total phenolic content, juice yield per fruit (104 to 186 mL) juice turbidity (142.20 to 364.50 NTU) and textural properties, like fruit compressive strength/firmness of arils (23.09 to 34.54 N), cutting strength of peel (84.33 to 111.35 N) and aril skin puncture force (0.28 to 0.38 N) were also investigated. Overall results suggested that the measured physico-chemical properties were quite different by the cultivar differences.

RESEARCH ARTICLE

Received: 08.10.2021
Accepted: 06.12.2021

Keywords:

- Cultivars,
- Juice,
- Physical properties,
- Pomegranate,
- Textural properties

To cite: Meena VS, Bıbve B, Bhushan B, Jalgaonkar K, Mahawar MK (2021). Physicochemical Characterization of Selected Pomegranate (*Punica granatum* L.) Cultivars. Turkish Journal of Agricultural Engineering Research (TURKAGER), 2(2): 425-433. *https://doi.org/10.46592/turkager.2021.v02i02.015*

INTRODUCTION

Pomegranate (*Punica granatum* L.) is a fruit of Punicacea family and is one of the prominent and commercial fruits in the world. The fruits are mostly consumed either in fresh form or processed as juice, jellies and syrup for domestic as well as industrial market. Pomegranate is commercially grown for its sweet and acidic taste of the arils.

Arils are the edible part of the fruit which represents around 52-58% of the whole fruit weight comprised of 64-78% juice and 22-36% of seeds (Al-Maiman and Ahmad, 2002; Kandylis and Kokkinomagoulos, 2020). The remaining parts like flowers, leaves, and roots can be utilized for medicinal purpose (Lansky and Newman, 2007). Arils contain plentiful of vitamins, sugars, polysaccharides, polyphenols, and minerals making it nutritionally important for human health (Al-Said *et al.*, 2009; Meena *et al.*, 2020).

The estimation of physical and engineering properties of any agricultural commodity is important from the design and development aspect of machineries for harvest, handling and storage. For horticultural crops, especially fruits and vegetables, shape is very imperative factor in sorting, sizing and estimating the number of fruits that can be kept in shipping or storage containers.

Although, some research studies involving the quantification of physical properties of pomegranate are reported (Al-Maiman and Ahmad 2002; Fadavi *et al.*, 2005; Kingsly *et al.*, 2006).

It is very important to understand the variation in the physico-chemical properties of fruits like juice yield, number of arils per fruit, total phenol content and so on, due to the existing cultivar difference. Therefore, this study was envisaged to determine the various physico-chemical properties of selected pomegranate cultivars of the semi-arid region of Punjab (India).

MATERIALS AND METHODS

Fresh pomegranate fruits of all the cultivars were harvested from the farm orchard of ICAR-Central Institute of Post-Harvest Engineering and Technology (CIPHET), Abohar region (30.1489°N, 74.2253°E) of Punjab in India in 2018. Fruits were subjected to cleaning and washing to remove any foreign material present before using them for experimental purpose. A sample of 10 freshly harvested fruits of each variety was taken for the estimation of physical and chemical attributes.

Fruit dimensions such as the major diameter *(L)*, intermediate diameter *(W)*, minor diameter *(T)*, length of calyx (L_{calyx}) was determined using digital vernier callipers (M/s Mitutoyo, ±0.01mm). Individual fruit weight (g) was recorded using digital weighing balance (M/s Mettler Toledo, ±0.01 g) and volume was determined using water displacement method (Mohsenin 1970). Geometric mean diameter, *GMD* (D_p) and sphericity (Φ_s) was calculated using the following relationship as reported by (Mohsenin 1970; Mahawar *et al.*, 2017; Mahawar *et al.*, 2019; Altuntas and Mahawar, 2021).

$$Dp = (\mathrm{L} \times W \times T)^{1/3} \quad (1)$$

$$\Phi s = \frac{(LWT)^{1/3}}{L} \quad (2)$$

Surface area (*S*) of the fruits was calculated by keeping the equivalence with a sphere having equivalent *GMD*, using the following formula as reported by Altuntas *et al.* (2005); Mahawar *et al.* (2017):

$$S = \pi Dp^2 \quad (3)$$

Where, *S* is the surface area (mm^2); D_p is the geometric mean diameter (mm).

Arils (edible portion) were separated manually from the fruit and total aril weight per fruit was observed. In addition, the total number of arils in a fruit were also counted and presented. The ratio of peel weight and fruit weight signifies the average peel yield (%) and similarly, aril yield (%) was determined as the ratio between aril weight and fruit weight. After the determination of aril properties, juice of each variety was extracted using a juice extractor (M/s Kalsi, Machine No. 10) in the laboratory for evaluation of chemical properties.

Moisture content of both peel and arils was determined using hot air oven method (78±2°C) until constant values are not obtained (Riyahi *et al.*, 2011).

The juice samples were subjected to the estimation of total juice yield, pH, total soluble solids (TSS), turbidity, acidity and vitamin C content. TSS was determined using a digital refractometer (M/s Atago, 0-85% Brix) as reported by Mahawar *et al.* (2018). Titratable acidity (TA) was determined by adopting the method of AOAC (2009). Juice pH was measured using a digital pH meter (M/s Eutech, range 0-14) at 20ºC. Juice turbidity was determined using digital turbidity meter (M/s Systronics, range: 0-1000 NTU). Ash content of arils and peel samples was determined using muffle furnace keeping the samples at 650°C for 8 hours.

The total phenolic content (TPC) was determined by the Folin–Ciocalteu method following a described procedure as reported by Mena *et al.* (2012). Results were expressed as mg 100 mL^{-1} of gallic acid equivalents (GAE).

Colorimetric aluminium chloride method was used for the measurement of total flavonoid content as described by Huang *et al.* (2005). Catechin was used as a standard for preparation of calibration curve.

The anthocyanin content of pomegranate aril was determined by pH differential method (Wrolstad *et al.*, 2005).

All the samples were kept for centrifugation at 7500 rpm using refrigerated centrifuge (M/s. Remi, India) for 15 min at 4°C. The in vitro free radical scavenging activity of the samples was determined using the DPPH free radical (Gonzalez-Molina *et al.*, 2008).

Textural properties like firmness of fruit, skin puncture of aril and cutting strength of peel of respective cultivars were determined using Texture Analyser (M/s Stable Micro Systems Ltd). Aril firmness was determined using 25 mm diameter cylindrical probe (contact area 490.87 mm^2) with the settings as: pre-test speed (1.50 mm s^{-1}), test speed (1 mm s^{-1}), post- test speed (10 mm s^{-1}), target mode (strain 30%), trigger force (30 g). Cutting strength of peel was determined by blade probe with the settings as; pre-test speed (2 mm s^{-1}), test speed (2 mm s^{-1}), post- test speed (10 mm s^{-1}), target mode (strain 70%), trigger force (60 g).

Statistical analysis of the observed data was performed using SPSS version 16.0 software. Univariate analysis in general linear model was done for analysis of variance (ANOVA) at 5% level of significance.

RESULTS AND DISCUSSION

The difference among the measured physical properties of selected pomegranate cultivars was observed to be significant at 5% level of significance (Table 1). White Muscut cultivar had the highest major diameter of 91.62 mm, minor diameter of 90.01 mm and intermediate diameter of 87.83 mm, while the lowest values were observed in

Mridula cultivar that is major diameter of 85.43 mm, minor diameter of 76.85 mm and thickness of 79.86 mm. An individual fruit of White Muscut cultivar having highest weight of 404.14 g, while among all cultivars weight of Jalore seedless cultivar was lowest 293.18 g. The existing variation in fruit is dependent on climatic conditions and production practices (Radunic *et al.*, 2015). Tehranifar *et al.* (1997) observed the fruit weight in the range of 196.89–315.28 g.

The average volume of a single fruit of White Muscut was higher 387 mL and the lowest value 289 mL was recorded for *cv.* Mridula. Total arils weight was highest and lowest for White Muscut 255.09 g and G-137 139.44 g, respectively. Similarly, peel weight was highest 160 g and lowest 99.45 g for G-137 and Jalore seedless, respectively. Being larger as well as heavier, the total number of arils per individual fruit was higher 974 in White Muscut variety and the number was lowest 606 in Mridula cultivar. Fruit size may fluctuate depending on climatic conditions and production practices (Radunic *et al.*, 2015). Calyx length varied between 16.38 (G-137) to 21.79 (White Muscut) cultivar. These results are consistent with previous studies, where calyx length ranged between 13.45 to 24.0 mm (Tehranifar *et al.*, 1997) and Radunic *et al.* (2015) observed 14.3-19.2 mm of calyx length in their study. Moisture values were higher for arils as compared to peels irrespective of the varieties.

The aril moisture content of G-137 (81.82%) cultivar found higher as compared to other accessions, whereas peel moisture content was higher in Jalore seedless (74.15 ± 0.01). It was also observed that, peel moisture contents of all cultivars had significant inter- varietal differences. The juice yield and total soluble solids was higher in White Muscat (186.00±2.00 ml and 13°Brix) followed by G-137 cultivar (152.00 ± 0.15 ml and 12.50°Brix). It was lowest in Jalore seedless (104±0.05 ml and 11.60°Brix). Mir *et al.* (2012) reported higher TSS in Ganesh (14.46°Brix), Mridula (15.60°Brix) and G-137 (15.57°Brix) cultivars. Similarly, some Spanish cultivars reported to have TSS in the range 12.36 to 16.32% (Martinez *et al.*, 2006).

Table 1. Physical properties of selected pomegranate cultivars.

Cultivar	*L* (mm)	*W* (mm)	*T* (mm)	L_{calyx} (mm)	*GMD* (mm)	*S* (mm²)	Φ_s	Volume (ml)	Weight (g)	No. of arils	Weight of 100 arils (g)	Total arils weight (g)	Total peel weight (g)
Mridula	85.43± 1.57^{c}	79.86± 1.09^{e}	76.85± 1.83^{e}	17.26± 1.80^{cb}	80.63± 1.42^{ed}	20424.11± 654.28^{ed}	0.90± 0. 01^{e}	289± 17.13^{d}	294.4± 16.83^{d}	795± 5.00^{d}	26.65± 0.23^{c}	188.21± 6.80^{c}	106.55± 10.06^{d}
Ganesh	87.11± 0.96^{ba}	84.78± 0.98^{c}	82.12± 1.33^{ca}	18.31± 1. 09^{b}	84.64± 0.92^{cb}	22506.15± 442.91^{cb}	0.93± 0. 01^{ba}	317.4±11 .15^{cb}	324.58± 7.89^{c}	1000± 20.00^{cb}	30.02± 0.11^{b}	207.07± 2.44^{b}	122.05± 15.70^{c}
White Muscut	91.62± 1.54^{a}	90.01± 1.63^{a}	87.83± 1.28^{a}	21.79± 0.70^{a}	89.80± 1.26^{a}	25333.93± 644.52^{a}	0.94± 0. 01^{a}	387± 23.58^{a}	404.14± 18.26^{a}	1141± 9.00^{a}	36.67± 0.21^{a}	255.09± 7.98^{a}	143.45± 7.71^{a}
Jalore seedless	85.05± 2.73^{c}	81.08± 1.24^{d}	77.12± 2.85^{d}	18.78± 0.75^{b}	81.30± 2.19^{d}	20764.95± 1012.70^{d}	0.91± 0. 01^{dc}	290± 25.59^{d}	293.18± 22.46^{d}	734± 6.00e^{d}	23.14± 0.58^{d}	186.34± 3.28^{dc}	99.45± 3.56^{d}
G-137	89.86± 2.75^{a}	87.44± 2.73^{ba}	84.16± 3.12^{ba}	16.38± 2.46^{d}	87.12± 2.72^{ba}	23844.35± 1371.70^{b}	0.92± 0. 01^{cb}	329± 19.21^{b}	348.44± 32.78^{b}	1045± 5.00^{b}	21.53± 0.21^{e}	139.44± 1.98^{e}	160± 20.14^{b}
							ANOVA						
F value	1.70^{NS}	6.88^{S}	3.98^{S}	6.24^{S}	4.25^{S}	4.20^{S}	3.66^{S}	3.72^{S}	4.24^{S}	210.75^{S}	61.99^{S}	109.16^{S}	
Significance	0.198	0.002	0.020	0.003	0.016	0.016	0.027	0.025	0.016	0.000	0.000	0.000	
LSD	6.55	4.85	7.05	7.22	5.43	2.78	0.00	6.25	6.93	4.53	0.91	19.53	

L: Major intercept, *W*: intermediate intercept, *T*: minor intercept of fruit, *GMD*: Geometric mean diameter (excluding calyx), L_{calyx}: Length of calyx, $W_{100\ aril}$: Weight of 100 arils, W_{aril}: total weight of arils per fruit, W_{peel}: Total weight of peel per fruit. *S*: Surface area,

^{S}: Significant (P≤0.05), ^{NS}: Non- significant, All the values presented as mean ± SD

Table 2. Chemical properties of juice obtained from selected pomegranate cultivars.

Cultivar	Moisture (% w.b.)		Ash (%)		pH	TSS	TA (%)	Juice yield/ fruit (ml)	Turbidity (NTU)
	Aril	Peel	Aril	Peel					
Mridula	80.82±0.39^{ba}	68.72±0.01^{e}	0.38±0.03^{cb}	1.51±0.01^{a}	3.96±0.02^{a}	12.50±0.50^{ba}	0.56±0.02^{d}	108±0.02^{d}	142.20±0.20^{ed}
Ganesh	79.69±0.01^{cb}	69.06±0.01^{d}	0.53±0.02^{a}	0.86±0.00^{dc}	3.47±0.01^{edc}	11.75±0.25^{cba}	0.58±0.01^{b}	142±0.10^{c}	145±2.00^{d}
White muscut	79.59±0.01^{dcb}	70.35±0.02^{c}	0.29±0.01^{ed}	0.81±0.01^{e}	3.50±0.00^{c}	13.00±0.00^{a}	0.50±0.04^{ed}	186±2.00^{a}	364.50±3.50^{a}
Jalore seedless	78.25±0.01^{edcb}	74.15±0.01^{a}	0.44±0.00^{b}	1.02±0.00^{b}	3.49±0.01^{cd}	11.60±0.60^{dcba}	0.42±0.02^{a}	104±0.05^{ed}	157.25±3.15^{c}
G-137	81.82±0.11^{a}	72.62±0.02^{b}	0.30±0.00^{d}	0.89±0.01^{c}	3.66±0.01^{b}	12.50±0.50^{ba}	0.48±0.02^{c}	152±0.15^{b}	195.50±0.70^{b}
					ANOVA				
F value	64.16^{S}	2.94×10^{4S}	40.65^{S}	1.31×10^{3S}	458.95^{S}	1.75^{NS}	2.00^{S}	3.57^{S}	1.41×10^{3}
Significance	0.001	0.00	0.002	0.00	0.00	0.301	0.00	0.00	0.00
LSD	0.66	0.00	0.00	0.00	0.00	1.73	0.12	7.02	9.83

All the values presented as mean ± SD

^{S}: Significant ($P \leq 0.05$), ^{NS}: Non- significant

Table 3. Bio-chemical properties of juice obtained from selected pomegranate cultivars.

	Phenols (GAE mg 100 g^{-1})	Flavanoids (CE mg 100 g^{-1})	Anthocyanins (mg 100 g^{-1})	DPPH (TE mg 100 g^{-1})
Mridula	104.33^{a}±0.80	18.62^{b}±0.05	1.33^{a}±0.04	16.01^{a}±0.01
Ganesh	70.56^{c}±0.76	17.3^{c}±0.07	1.18^{b}±0.01	12.17^{c}±0.03
G 137	64.12^{d}±0.60	15.72^{e}±0.15	0.74^{c}±0.00	7.47^{e}±0.03
Muscat	53.63^{e}±0.31	17.06^{d}±0.02	0.26^{e}±0.00	8.86^{d}±0.03
Jallore	87.12^{b}±0.23	20.3^{a}±0.05	0.44^{d}±0.00	13.35^{b}±0.07
		ANOVA		
F value	1.52×10^{3S}	576.10^{S}	5.52×10^{5S}	7.04×10^{3S}
Significance	0.00	0.00	0.00	0.00
LSD	1.67	0.24	0.06	0.13

All the values presented as mean ± SD

^{S}: Significant ($P \leq 0.05$), ^{NS}: Non- significant

The juice pH depicted the acidic taste of the juice was higher in Mridula cultivar (3.96) which was in confirmation with the results obtained by Cemeroglu *et al.* (1992). The juice pH of G137, White Muscut and Jalore seedless was significantly acidic than other cultivars. Titratable acidity of the different cultivars taken in this study was in the range of 0.42 to 0.58. The acidity of pomegranate varieties grown in Iran were found in the range of 0.35 to 3.36% (Akbarpour *et al.*, 2009). The turbidity of juice was highest for the White Muscut cultivar (364.50 NTU), whereas it was below 200 NTU in all other cultivars and lowest for Ganesh cultivar (145 NTU). The information is presented in Table 2.

Total phenolics and flavonoid content of fresh arils of the five pomegranate varieties are presented in Table 3. The phenol content of juice extracted from five different cultivar varied from 53.63 to 104.33 (GAE mg 100 g^{-1}), whereas the flavonoid content varied from 15.72 to 20.3 (CE mg 100 g^{-1}). Mridula cultivar had highest TPC whereas Jallore has the highest content of flavonoids. The quantifiable amounts of flavonoids range from 15.72 to 20.3 mg CE 100 g^{-1}. The reported values in this study were considerably lower than those reported by Tehranifar *et al.* (1997); Cam *et al.* (2009); Pande and Akoh (2009) in their respective studies. The anthocyanin content of juice extracted from different cultivars varied from 0.26 (Muscat) to 33.33 (Mridula) (C3G mg 100 g^{-1}). Mridula cultivar had the highest amount of total anthocyanins compared with other cultivars and the range (5.56 and 30.11 mg 100 g^{-1}) was in accordance with previously published reports for different pomegranate cultivars (Tehranifar *et al.*, 2010).

The presence of anthocyanin and phenolic acids, and other biomolecules determines the antioxidant activity of pomegranate arils and juice color (Shahkoomahally *et al.*, 2021).

The free radical scavenging capacity of juice extracted from five different cultivar varied from 7.47 to 16.01 (TE mg 100 g^{-1}). The antioxidant capacity in reference with DPPH radical inhibition values were found in the sequence Mridula> Jallore> Ganesh >White Muscat> G-137. The results were found in corroboration with the findings of high antioxidant activity in pomegranate cultivars as reported by Zaouay and Mars (2011). This existing variation was attributed to the inherent differences in cultivars and extraction methodologies. The information about the evaluated bio-chemical properties of fruit juice is depicted in Table 3.

Table 4. Textural properties of selected pomegranate cultivars.

Cultivar	Peel cutting force (N)	Fruit compressive strength (N)	Aril skin puncture (N)
Mridula	111.35±4.52^{a}	29.34±1.18^{cb}	0.29±0.01^{b}
Ganesh	101.67±8.51^{b}	27.64±1.11^{d}	0.26±0.01^{c}
White muscut	89.68±6.48^{d}	31.73±1.66^{ba}	0.29±0.01^{b}
Jalore seedless	84.33±11.60^{ed}	34.54±2.09^{a}	0.38±0.01^{a}
G-137	99.99±5.49^{cb}	23.09±1.47^{ed}	0.25±0.02^{dc}
		ANOVA	
F value	1.70^{NS}	6.95^{S}	19.91^{S}
Significance	0.178	0.000	0.000
LSD	23.57	4.66	0.00

All the values presented as mean ± SD
^{S}: Significant (P≤0.05), ^{NS}: Non- significant

It was observed that, firmness of whole fruit (34.54 N) and arils (0.38 N) of Jalore seedless cultivar was higher. Owing of the higher peel thickness of Mridula cultivar, the peel cutting force was highest as 112.62 N. Aril skin puncture force of Ganesh and G137 cultivars were at par and was significantly different for all other cultivars (Table 4). The variation in the physical as well as chemical properties among the cultivars is attributed to the genotype of the cultivars. The agro-climatic conditions, postharvest practices, processing techniques, type of cultivar have influenced the quality and quantity of pomegranates juice (Martinez *et al.*, 2012).

CONCLUSION

In this study, various physico-chemical and textural properties of five different pomegranate cultivars were determined. The results authenticated that there was significant variation in the determined properties among the selected cultivars. The variations could be originated from genotype of cultivar or due to agro-climatic and environmental conditions. This information about variation of physico-chemical attributes is pertinent for easy identification of pomegranate cultivars, particularly for juice extraction and preparation of suitable value-added products. It will also be helpful for pomegranate producers and processors from cultivation and processing point of view and to the breeders for improvement in desirable traits.

DECLARATION OF COMPETING INTEREST

The authors declares that they have no conflict of interest.

CREDIT AUTHORSHIP CONTRIBUTION STATEMENT

Vijay Singh Meena: Conceptualization, data curation, formal analysis, resources, software, validation, writing-original draft, writing-review & editing.
Bhushan Bibwe: Conceptualization, methodology, resources, writing-review & editing.
Bharat Bhushan: Conceptualization, formal analysis, validation, writing-original draft.
Kirti Jalgaonkar: Formal analysis, methodology, supervision, writing-original draft.
Manoj Kumar Mahawar: Supervision, validation, visualization, writing-review & editing.

REFERENCES

Akbarpour V, Hemmati K and Sharifani M (2009). Physical and chemical properties of Pomegranate (*Punica granatum* L.) fruit in maturation stage. *American Eurasian Journal of Agriculture Environment and Science, 6(4): 411-416.*

Al-Maiman S, and Ahmad D (2002). Changes in physical and chemical properties during pomegranate *(Punica granatum* L.) fruit maturation. *Journal of Food Chemistry, 76(4): 437-441.*

Al-Said FA, Opara LU and Al-Yahyai RA (2009). Physico-chemical and textural quality attributes of pomegranate cultivars (*Punica granatum* L.) grown in the Sultanate of Oman. *Journal of Food Engineering, 90(1): 129-134.*

Altuntas E, Özgöz E, and Taşer, ÖF (2005). Some physical properties of fenugreek (*Trigonella foenum-graceum* L.) seeds. *Journal of Food Engineering, 71(1): 37-43.*

Altuntas E, and Mahawar MK (2021). Mass prediction of cherry laurel genotypes based on physical attributes using linear regression models. *Journal of Agricultural Faculty of Gaziosmanpasa University. 38(2): 87-94.*

AOAC (2009). Association of official analytical chemistry. Official methods of analysis. 16th ed. *Washington.* 1141.

Cam M, Hisil Y and Durmaz G (2009). Classification of eight pomegranate juices based on antioxidant capacity measured by four methods. *Food Chemistry, 112: 721-726.*

Cemeroglu B, Artik N and Erbas S (1992). Extraction and composition of pomegranate juice. *Fluessiges Obst, 59(6): 335-340.*

Fadavi A, Barzegar M, Azizi MH and Bayat M (2005). Physicochemical composition of ten pomegranate cultivars (*Punica granatum* L.) grown in Iran. *Food Science Technology International, 11: 113-119.*

Gonzalez-Molina E, Moreno DA and Garcia-Viguera C (2008). Genotype and harvest time influence the phytochemical quality of fino lemon juice (*Citrus lemon* L. Burm. f.) for industrial use. *Journal of Agricultural and Food Chemistry, 56(5): 1669-1675.*

Huang D, Ou B, and Prior RL (2005). The Chemistry behind antioxidant capacity assays. *Journal of Agricultuiral and Food Chemistry, 53(6): 1841-1856.*

Kandylis P and Kokkinomagoulos E (2020). Food applications and potential health benefits of pomegranate and its derivatives. *Foods, 9(2): 122.*

Kingsly ARP, Singh DB, Manikantan MR and Jain RK (2006). Moisture dependent physical properties of dried pomegranate seed (*Anaradana*). *Journal of Food Engineering, 75: 492-496.*

Lansky EP and Newman RA (2007). Punica granatum (pomegranate) and its potential for prevention and treatment of inflammation and cancer. *Journal of Ethnopharmacology*, *109: 177-206.*

Mahawar MK, Jalgaonkar K, Kumar M, Meena VS and Bhushan B (2017). Determination of some physical properties of date *palm fruits* (*cv.* Khadrawy and Medjool). *Acta Agrophysica, 24(2): 217-223.*

Mahawar MK, Jalgaonkar K, Bibwe B, Kulkarni T, Bhushan B and Meena VS (2018). Optimization of blended Aonla-Guava fruit bar through Response surface methodology. *Nutrition and Food Science. 48(4): 621-630.*

Mahawar MK, Bibwe B, Jalgaonkar K and Ghodki BM (2019). Mass modeling of kinnow mandarin based on some physical attributes. *Journal of Food Process Engineering, 42(5).*

Martinez JJ, Melarejo P, Hernandez F, Salazar DM and Martinez R (2006). Arils characterization of five new pomegranate (*Punica granatum* L.) varieties. *Scientia Horticulturae, 110: 241-246.*

Martinez JJ, Hernández F, Abdelmajid H, Legua, P, Martínez R, El Amine, A and Melgarejo P (2012). Physico-chemical characterization of six pomegranate cultivars from Morocco: processing and fresh market aptitudes. *Scientia Horticulturae, 140: 100-106.*

Meena VS, Jalgaonkar K, Mahawar MK, Bhushan B, Bhushan B, Kashyup P (2020). Optimization of process variables for preparation of Pomegranate juice fortified aonla candy. *Current Science, 118(1): 114-118.*

Mena P, Gironés-Vilaplana A, Marti N and García-Viguera C (2012). Pomegranate varietal wines: Phytochemical composition and quality parameters. *Food Chemistry, 133: 108-115.*

Mir MM, Umar I, Mir SA, Rehman MU, Rather GH and Banday SA (2012). Quality evaluation of pomegranate crop – a review. *International Journal of Agriculture Biology, 14: 658-667.*

Mohsenin NN (1970). Physical properties of plant and animal materials. *Gordon and Breach Science Publishers,* New York.

Pande G and Akoh CC (2009). Antioxidant capacity and lipid characterization of six Georgia-grown pomegranate cultivars. *Journal of Agricultural and Food Chemistry, 57: 9427-9436.*

Radunic M, Špika MJ, Ban SG, Gadze J, Diáz-Pérez JC and MacLean D (2015). Physical and chemical properties of pomegranate fruit accessions from Croatia. *Food Chemistry, 177: 53-60.*

Rice-Evans CA, Miller NJ and Paganga G (1997). Antioxidant properties of phenolic compounds. *Trends in Plant Sciences, 2: 152-159.*

Riyahi R, Rafiee S, Dalvand MJ and Keyhani A (2011). Some physical characteristics of pomegranate seeds and arios. *Journal of Agricultural Technology, 7(6): 1523-1537.*

Shahkoomahally S, Khadivi A, Brecht JK and Sarkhosh A (2021). Chemical and physical attributes of fruit juice and peel of pomegranate genotypes grown in Florida, USA. *Food Chemistry, 342:* 128302.

Tehranifar A, Zarei M, Nemati Z, Esfandiyari B and Vazifeshenas MR (1997). Investigation of physic-chemical properties and antioxidant activity of twenty Iranian pomegranate (*Punica granatum* L.). *Scientia Horticulturae, 126: 180-185.*

Wrolstad RE, Durst RW and Lee J (2005). Tracking color and pigment changes in anthocyanin products. *Trends in Food Science and Technology, 16: 423-428.*

Zaouay F and Mars M (2011). Diversity among Tunisian pomegranate (*Punica granatum* L.) cultivars as assessed by pomological and chemical traits. *International Journal of Fruit Science, 11(2):151-166.*

Turkish Journal of Agricultural Engineering Research

https://dergipark.org.tr/en/pub/turkager
https://doi.org/10.46592/turkager.2021.v02i02.016

Turk J Agr Eng Res (TURKAGER)
e-ISSN: 2717-8420
2021, 2(2): 434-449

Research Article

Optimization of Mechanical Oil Expression from Sandbox (*Hura crepitans* Linn.) Seeds

David Nwabueze ONWE[a]* Adeleke Isaac BAMGBOYE[b]

[a]*Department of Agricultural and Food Engineering, Faculty of Engineering, University of Uyo, P. M. B. 1017, Uyo, Akwa Ibom State, NIGERIA*

[b]*Department of Agricultural and Environmental Engineering, Faculty of Technology, University of Ibadan, NIGERIA*

(*): Corresponding author. davidonwe@uniuyo.edu.ng

ABSTRACT

Optimization of process variables has become very vital in oil extraction processes to obtain maximum oil yield from oilseeds and nuts. This work focussed on the optimization of process oil extraction process from sandbox seed by mechanical expression. Effects of moisture content, roasting temperature, roasting time, expression pressure and expression time on oil yield from sandbox seed was studied using a 5×5 Central Composite Rotatable Design of Response Surface Methodology experimental design. Results obtained were subjected to Analysis of Variance (ANOVA) and SPSS statistical tool at ($p = 0.05$). Optimum conditions predicted were validated by experiments. All the processing factors were significant at ($p = 0.05$) for the sandbox oil yield except roasting temperature. The experimental results and predicted values showed low deviation (0.01-0.62). Oil yields obtained from the sandbox seed at varying process conditions varied from 16.38-38.68%. The maximum oil yield of 38.68% was obtained when the sandbox seed was subjected to process conditions of 6% moisture content, 85°C roasting temperature, 15 min roasting time, expression pressure of 20 MPa and 8 min pressing time. Mathematical equations to predict sandbox seed oil yield at varying process conditions were developed with an R^2 (0.8908). The optimum extractable oil yield of 38.95% was predicted for sandbox seed at processing conditions of 7.03% moisture content, 97.72°C roasting temperature, 11.32 min roasting time, 15.11 MPa expression pressure and 8.57 min expression time. The study results provide data for designs of process and equipment for oil extraction from sandbox and other oilseeds.

RESEARCH ARTICLE

Received: 03.10.2021
Accepted: 08.12.2021

Keywords:

- Process optimization,
- Sandbox seed,
- Oil extraction,
- Mechanical expression

To cite: Onwe, DN, Bamgboye AI (2021). Optimization of Mechanical Oil Expression from Sandbox (*Hura crepitans* Linn.) Seeds. Turkish Journal of Agricultural Engineering Research (TURKAGER), 2(2): 434-449. *https://doi.org/10.46592/turkager.2021.v02i02.016*

INTRODUCTION

The sandbox (*Hura crepitans* Linn.) tree is of the (Euphorbiaceae) family, indigenous to the humid zones of the American continents. The sandbox is referred to as the dynamite tree because of the shooting reverberations of the matured pods as they split before dropping. The sandbox seeds are flattened, about 2 cm, arranged as carpel of 14-16 seeds in fruit capsules of height 3-5 cm and diameter of 5-8 cm (Feldkamp, 2006; Okolie *et al.,* 2012). Consumption of sandbox seed has been reported to cause sicknesses such as burning throat, suffocation, headache, nausea, stomach pain, vomiting and diarrhea, while the plant sap coming in contact with the eye can cause blindness. Sandbox leaves have been recognized to be used as curatives, but the seed has not really been harnessed and used (Allen, 2000; Clarke, 2000). Sandbox seed has been noted to contain a number of important properties that can be useful for the production of feeds, paints, and cosmetics amongst others (Olatidoye *et al.,* 2010; Idowu *et al.,* 2012). Sandbox seed was noted amongst seeds with high oil content (Idowu *et al.,* 2012; Basumatary, 2013). Sandbox seed properties, proximate composition and its oil's chemical characterization have been studied (Fowomola and Akindahunsi, 2007; Idowu *et al.,* 2012; Okolie et al., 2012). However, sandbox has been classified amongst underutilized species of plants; in most parts of the world, the trees have been used as shade due to their large spreading branches (Idowu *et al.*, 2012). In Nigeria, the trees are grown as cover plants, while the seeds were thrown away as waste (Adewuyi *et al.,* 2012).

Oil extraction from sandbox seeds by earlier studies was focused mainly on solvent extraction (Okolie *et al.*, 2012; Muhammed *et al.,* 2013; Adewuyi *et al.,* 2014; Nwanorh, 2015; Ottih *et al.,* 2015; Shonekan and Ajayi, 2015). Oil extraction by solvent methods has increased oil recovery up to 98% and has made it economically attractive for some oilseeds (Matthäus, 2012). However, oil extraction by mechanical methods still remains a good option for oil extraction from seeds and nuts.

Mechanical oil expression from many agricultural products has been studied, viz: almond seed (Akubude *et al.,* 2017); groundnut (Pominski *et al.,* 1970; Adeeko and Ajibola, 1990; Olajide *et al.,* 2014); dika kernels (Abidakun *et al.,* 2012; Ogunsina *et al.,* 2014); African oil bean (Aremu and Ogunlade, 2016); various clones of rubber seed (Ebewele *et al.,* 2010); fine and coarse roselle seed (Bamgboye and Adejumo, 2011); sesame seeds (Tunde-Akintunde *et al.,* 2000; Akinoso *et al.,* 2006; Hashim *et al.*, 2014; Elkhaleefa and Shigidi, 2015); soybean seed (Mwithiga and Moriasi, 2007; Lawson *et al.,* 2010); bitter gourd (Umamaheshwari and Dinesh Sankar Reddy, 2016); neem seed (Awolu *et al.*, 2013; Orhevba *et al.,* 2013); avocado fruit (Southwell and Haris, 1990); rice bran respectively (Sivala *et al.,* 1991); coconut (Hammonds *et al.,* 1991); shea butter (Olaniyan and Oje, 2007); melon (Ajibola *et al.*, 1990); conophor nuts (Fasina and Ajibola, 1989); peanut (Badwaik *et al.*, 2012); sunflower kernels (Southwell and Harris, 1992); African star apple seed (Ajala and Adeleke, 2014); *Moringa* seed (Adejumo *et al.,* 2013; Fakayode and Ajav, 2016).

According to Mwithiga and Moriasi (2007), seed quality is the first determinant of the quantity and quality of producible oil from an oilseed, before the consideration of the process and machine to be used. Variations in seed and machine parameters including seed size, moisture level, preparation temperature and time, expression pressure and duration of extraction greatly influence oil yields from oilseeds and nuts during mechanical expression

(Khan and Hanna, 1984). It is therefore of optimum importance to control these parameters during oil extraction for optimal oil extraction. Improper management of these variables during mechanical expression may possibly lead to low oil yield and oil quality. Therefore, quality lipid feedstocks and effective handing before expression are vital to achieving quality and higher oil yield (Bamgboye and Adejumo, 2011).

Data for mechanical oil extraction from sandbox seed and process optimization of same is however scarce. To quantify and predict oil yield from sandbox seed by mechanical expression relatively to process factors, the Response Surface Methodology (RSM) was employed. According to Giwa *et al.* (2015), process optimization where other process factors are kept constant and varying one, does not correctly capture the inter-relationship existing amongst the factors. Hence, such procedure may not accurately predict the best combination of interaction of factors that gives the optimum outcome of the process. The (RSM) was developed as an appropriate statistical tool for optimization of processes. It employs the use of Central Composite Design (CCD), Box-Behnken design and D-optimal experimental designs (Triveni *et al.*, 2001). According to Hamzat and Clarke (1993), accurate knowledge of interactions between oil expression devices and processing variables improves the efficiency of oil extraction. RSM has shown to be a tool in effectively relate the inter-relationship occurring amongst process variables such as effect of moisture, heat application and heating time, pressing pressure and duration on oil yield. Superior to normal methods, the RSM uses minimal experimental investigations to predict the values of process factor combination for optimum result(s) and also generates model equation(s) connecting the factors and response(s) (Giwa *et al.*, 2015). RSM utilizes results from practical experiments to generate models that can predict response such as oil yield in relation to process factors. In this work, how process factors: moisture content, treating temperature and time, expression pressure and time influence oil expression and yield from sandbox seed was investigated and optimized using the RSM.

MATERIALS AND METHODS

Design of experimental

Among processing factors, seed moisture, treating temperature and time, expression pressure and time have been observed to significantly at (p = 0.05) increase oil yield by mechanical expression methods (Fakayode and Ajav, 2016). The process of oil extraction from sandbox seed by mechanical means was optimized by varying these factors. The design of experiment adopted was 5×5 factorial Central Composite Rotatable Design (CCRD) of Response Surface Methodology developed by Box *et al.* (1978). According to Fakayode and Ajav (2016), CCRD is combining factorial, (d_f), axial, (d_a) and central, (d_c) design points respectively. $t = 2^c(d_f) + 2c(d_a) + c(d_c)$, represents the total number of treatments, where 'c' is the number of process factors. The average experiment of the CCRD design was 32 combinations, representing $T = 2^{c-1} + 2c + (t_0)$ design points, consisting of 16 factorial CCD, 10 axial points and 6 replications of the center points.

The initial moisture content of the mature sandbox seed influenced the decision of the moisture content range selected for the experiment. There is a lack of information on mechanical extraction of oil from sandbox seed, its oil yield and optimization of the process. Thus, data from previous studies on oil extraction by mechanical methods from other oilseeds was used to carry out preliminary investigations on the sandbox seed. Results obtained informed the varying values of process factors selected for the experiment. Values used were; moisture content, mc (4, 6, 8, 10 and 12% wet-basis); roasting temperature, γ_{tp} (80, 85, 90, 95 and 100°C) and time, γ_{tm} (0, 5, 10, 15 and 20 min); expression pressure, ε_{Pr} (5, 10, 15, 20 and 25 MPa) and time, εx_{tm} (2, 4, 6, 8 and 10 min).

Development of laboratory screw press

A five-barrel pilot screw press (Figure 1) was developed and used for the experiment. Designed for 25MPa maximum capacity, the screw pitch diameter was calibrated by length to vary the applied pressure. Preliminary test was conducted by placing a piece of wire gauze into the base of the screw press barrel, and 500 gram sample of the ground sandbox was placed on the wire gauze and another piece of wire gauze was placed on the specimen. The 25 MPa mark was got with a spring gauge as a point where the press screw could not push the sample any further. Pitch lengths were used to mark the other pressure points; 20, 15, 10 and 5 MPa respectively. The multiple barrel press designed was adopted to easily cover the multiple experiments carried out.

Preparation of sample

About 100 kg of mature sandbox fruits were collected from under the trees in Uyo metropolis, Akwa Ibom State, Nigeria between 2106-2018. The fruits (Figure 2) were cracked to remove the seeds (Figure 3) and the seeds peeled to get the kernel (mesocarp) (Figure 4).

Figure 1. Screw press.

Figure 2. Sandbox fruits.

Figure 3. Sandbox seeds.

Figure 4. Sandbox kernels.

Moisture content determination

Initial moisture content of the sandbox seeds was determined using ASABE standard for oven drying method as adopted by Olaoye (2000), Ozguven and Vursavus (2005), Fakayode and Ajav (2016) and Onwe *et al.* (2020) for castor nut, pine nuts, African star apple and

Moringa seeds respectively. Three 50 g ground samples of the sandbox box seed designated A, B, C were used for the experiment. The three different samples were placed and dried in the oven at 105°C and weighed after 6 hours and subsequently at intervals until a constant weight was attained. Equation 1 below was used to calculate the mc (wet-basis).

$$MC\ (\%\ w.b.) = \frac{W_i - W_f}{W_i} \times 100 \qquad (1)$$

W_i = initial sample weight and W_f = final sample weight

1 kg each of the samples were subjected to 4, 6, 8, 10 and 12% wet basis moisture content respectively using Equation 2 as adopted by Olajide (2000); Fakayode and Ajav (2016).

$$Q = \left(\frac{100 - S_i}{100 - S_d} - 1\right) \times W_s \qquad (2)$$

Q = quantity of required moisture to be absorbed (ml); S_i = initial sample moisture (%wb); S_d = required sample moisture (%wb); W_s = weight of sample (g)
The conditioned samples were wrapped in fabrics and placed in polyethylene bags and stored in a refrigerator at 5°C for two days for the required moisture content to even up.

After that, the samples were stored in a desiccator to retain them at the conditioned moisture content for the experiment.

Experimental procedures

From the already conditioned samples of the sandbox seed at 4, 6. 8, 10, 12% wb moisture content, the various experiments were conducted using 500 g weight. A hotplate was used for roasting the sandbox seed samples. The various roasting temperature levels of 80, 85, 90, 95 and 100°C were achieved by regulating the hotplate temperature. A frying pot was placed on top of the hotplate, and a digital thermometer probe was used to check the pot temperature until the required temperatures were obtained before pouring the sandbox seed samples for frying. A stopwatch was used to time the roasting periods for 0, 5, 10, 15 and 20 min respectively. Afterwards, the samples were fed into the extraction chamber (barrel); wire gauze was placed at the base of the barrel and on top of the samples before pressing. The samples were subjected to 5, 10, 15, 20 and 25 MPa extraction pressure, at 2, 4, 6, 8 and 10 min extraction duration. The experiments were replicated three times. Pressed samples were left to drain into containers for three days before the weight of the oil was determined (Weiss, 2000). Oil yields were determined by Equation 3, used by Bello and Daniel, (2015) for groundnut oil yield determination.

$$Oil\ Yield\ (\%) = \frac{Wieght\ of\ oil\ expressed}{Wieght\ of\ sandbox\ seed\ sample\ before\ pressing} \times 100 \qquad (3)$$

Response Surface Methodology (RSM)

The experiment was designed using a software package of RSM Design Expert (6.0.6). The software generated sets of combinations of experimental factors when their ranges were keyed in. These combinations of factors were used for the experiments. The oil expressions were carried out using these combinations. The percentage of expressed oil for each experiment was keyed in as the response of the particular combination. The Design Expert contains four different models, which include the linear, the two factorial interactions (2FI), the quadratic and the cubic models respectively. These four models analyses the outcome of the experiments in terms of the probability of error value (p-value) and coefficient of determination (R^2), which are statistical parameters indicating the degree of relationship between process factors and oil yield. The decision on the best model for the oil expression process was based on their p and R^2 values. The chosen model was subjected to Analysis Of Variance (ANOVA) to further prove the model's level of significance and fitness in explaining the relationship between the process factors and oil yield. Then the tests of between-subjects of effects of processing conditions on oil yield were analyzed using Windows 20.0 SPSS statistical software package. Combination conditions suggested to be optimal for oil expression by the model were used to conduct fresh experiments for validation. Then, the results from real experimental and model predicted values were also compared to test for similarities.

RESULTS AND DISCUSSION

The moisture content of 6.12% wb was obtained as the initial moisture content of the sandbox seed. The oil yields from the combination of varying process conditions are as shown in Table 1. Plots relating the process factors and the oil yield are presented in Figures. 5-9. The sandbox oil yield varied from 16.38-38.68%. The optimum oil yield of 38.68% was obtained when the sandbox seed was subjected to process conditions of 6% moisture content, 85^{o}C roasting temperature, 15 min roasting time, expression pressure of 20 MPa and 8 min pressing time. Relatively to sandbox seed oil extraction by solvent methods; Ottih *et al.* (2015) and Okolie *et al.* (2012) obtained 57.26% and 53.61% oil yield respectively using n-hexane. Nwanorh (2015) obtained 42.70% oil yield using petroleum ether. According to Bockisch (1998), the reason why solvent extraction produces better oil yield when compared to other extraction methods could be as a result of solvents permeation ability to solubilize lipids in the cell structures to extract as much oil as possible. However, Adewuyi *et al.* (2014) and Shonekan and Ajayi (2015) obtained 37.75 and 36.70% oil yield respectively using n-hexane. Difference in oil yield during extraction is a function of extraction methods employed, and also biological and environmental conditions (Anwar *et al.*, 2006; Orhevba *et al.*, 2013).

Table 1. Oil yield from sandbox seed at various processing conditions.

Run	Factor 1 A: mc (%)	Factor 2 B: Υ_{tp} (%)	Factor 3 C: Υ_{tm} (min)	Factor 4 D: ε_{Pr} (MPa)	Factor 5 E: εx_{tm} (min)	Response Oil yield (%)
1	8	90	10	15	6	36.14
2	6	85	5	10	8	32.77
3	6	95	15	10	8	35.09
4	10	95	15	10	4	23.66
5	8	90	10	15	2	16.38
6	8	90	10	15	6	35.00
7	10	85	15	20	4	24.43
8	8	90	10	15	10	37.02
9	8	80	10	15	6	32.66
10	4	90	10	15	6	32.22
11	8	90	10	15	6	36.22
12	6	85	15	10	4	24.68
13	8	90	10	15	6	35.00
14	10	95	5	20	4	19.44
15	10	85	5	20	8	25.00
16	8	100	10	15	6	36.00
17	6	95	15	20	4	25.00
18	6	95	5	10	4	21.66
19	8	90	20	15	6	34.33
20	8	90	10	15	6	36.77
21	10	95	15	20	8	32.88
22	8	90	10	5	6	18.66
23	8	90	10	25	6	30.00
24	12	90	10	15	6	20.49
25	6	95	5	20	8	30.66
26	10	85	5	10	4	24.99
27	8	90	10	15	6	35.66
28	8	90	0	15	6	18.62
29	10	95	5	10	8	32.54
30	10	85	15	10	8	34.65
31	6	85	15	20	8	38.68
32	6	85	5	20	4	23.11

Where mc = moisture content of sandbox seed, Υ_{tp} = Roasting temperature, Υ_{tm} = Roasting time, ε_{Pr} = Expression pressure and εx_{tm} = Extraction time

The oil recovery from the sandbox seed increased substantially at the moisture content range of 4-8% wb, but declined when the moisture level exceeded 8% wb (Figures 5-6). This could be attributed to the observation by Sivala *et al.* (1992), that moisture addition pushes particles faster to saturation points during oil expression. Nevertheless, in the presence of excess moisture, the particle's liquid phase absorbs the expression pressure and debar it from reaching the oil capillaries, thereby, decreasing oil yield.

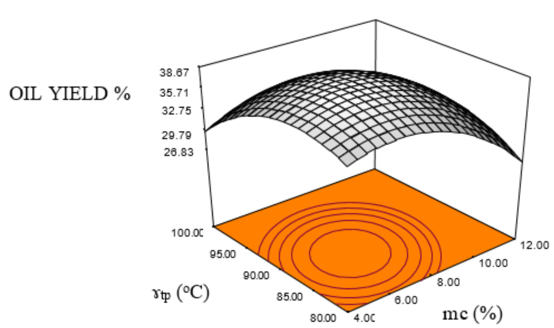

Figure 5. Extraction time and moisture content against oil yield.

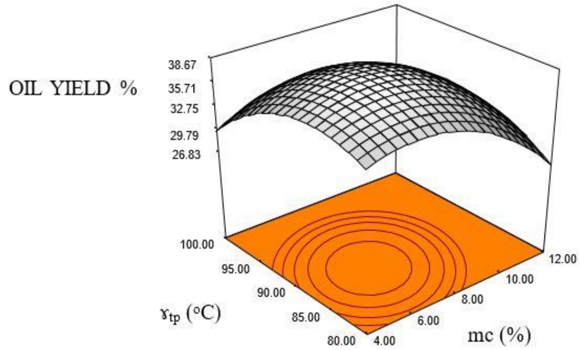

Figure 6. Roasting temperature and moisture content against oil yield.

The highest oil yield was obtained for sandbox seed at the moisture level of 8% wb (Figures 5-6). The trend agrees to earlier results from groundnut, neem, avocado, roselle, dika and locust beans (Southwell *et al.*, 1990; Owolarafe *et al.*, 2003; Ogunsina *et al.*, 2008; Bamgboye and Adejumo, 2011; Orhevba *et al.*, 2013; Olajide *et al.*, 2014) and many other authors as the most suitable moisture level for mechanical oil extraction.

Increase in the sandbox box oil yield was observed as the roasting temperature increased from 80-90°C. The oil yield decreases as the roasting temperature increased from 90-100°C (Figs. 6-7). Roasting temperature has been recognized as one of the factors that greatly enhance oil yield (Costa *et al.*, 2014; Terigar *et al.*, 2011; Martinez *et al.*, 2013). According to Fakayode and Ajav, (2016), expected oil yield cannot be got from oil samples at lower heating temperatures. At the same time, roasting at high temperatures hardens oil samples, causing them to resist applied pressure during extraction, and thus, leading to lower oil yield. In comparison, the roasting temperature value for maximum oil recovery from sandbox seed was similar to 81.93°C heating temperature reported by Olajide, (2000) for groundnut kernel (*Arachis hypogeae*), 90°C reported by Aremu and Ogunlade, (2016) for African oil bean seed. The sandbox seed grain is very soft and roasting at 90°C was suitable heat treatment to release optimum oil yield from it.

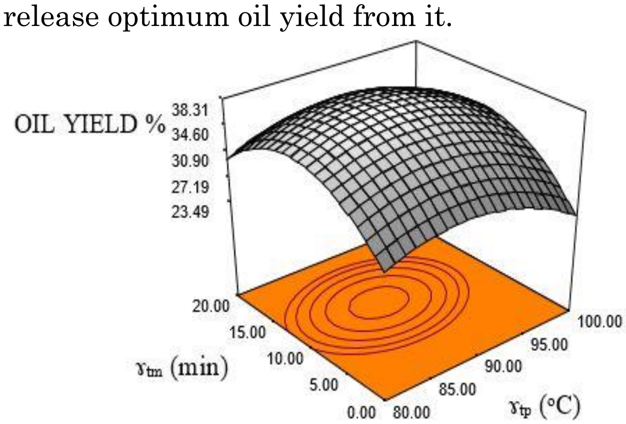

Figure 7. Roasting time and roasting temperature against oil yield.

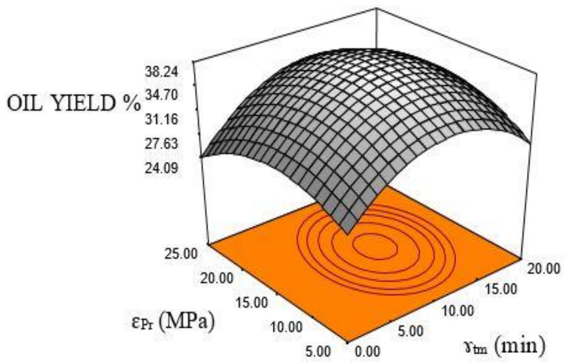

Figure 8. Expression pressure and roasting time against oil yield.

Findings from Ajibola *et al.* (1993); Alonge *et al.* (2003); Bamgboye and Adejumo (2011) are all in agreement with this heat treatment observed for sandbox seed, which was attributed to the phenomenon of oilseeds undergoing concurrent decrease in moisture content, oil viscosity and protein coalescence by heat injection, which enhances oil expression. However, at higher temperatures, excessive moisture loss can occur, causing seed hardening, thereby reducing the oil yield. This observation conforms to findings on dika nut, groundnut, and shea kernel respectively (Olaniyan and Oje, 2007; Abidakun *et al.*, 2012; Olajide *et al.*, 2014;).

Roasting the sandbox samples up to 15 min increased the oil yield (Figures 7-8). It was observed that the oil yield was least for the un-roasted sample which represents the 0-minute roasting time. The unroasted samples yielding the lowest oil is an indication of the importance of heat-treating oil samples before extraction. Sandbox oil yield decreased at roasting time above 15 min. Kagwacie and Anozie (1995) observed that the flow of oil is inversely proportional to the kinematic viscosity. Thus, as heat treatment progresses, kinematic viscosity of samples is lowered for oil to flow. According to Fakayode and Ajav (2016), heating oilseed samples at lowered temperatures requires more time to allow for the adjustment of moisture content to the optimum level that would lead to the folding of oil vessels, congealing of protein and allow flowability, but heating at higher temperature would take shorter time to reach these conditions, that additional heat would cause a reduction in oil yield. Movement of moisture during heat treatment creates a vacuum which becomes an accommodating capacity for the rupturing oil capillaries as heating continue. Oil yield is higher and faster and proportional to the rate of protein coalescence and decline in kinematic viscosity (Ajibola *et al.*, 2000; Akintunde *et al.*, 2001). This phenomenon enables the emergence of oil from the oil tubes into the inter-grain vacuum (Adeeko and Ajibola, 1990). This occurrence could be obtained at higher roasting temperatures and short time respectively, while extended roasting time at higher temperatures causes drastic drop in moisture content, leading to hardening of oilseeds which results in decrease in oil yield. The sandbox oil yield was highest when seed samples were roasted at 85^{o}C for 15 min (Figures 7-8). Similar conditions were reported for groundnut and sheanut (Adeeko and Ajibola, 1990; Olajide, 2000; Ajav and Olatunde, 2011).

The sandbox oil yield was observed to increase with increase in expression pressure of 5-20 MPa, which decreased as the pressure increased to 25 MPa (Figures 8-9). It was observed that the pressed sandbox mash slurried and clogged the screw press oil holes and overflowing the pressing plate at pressure above 20 MPa. This may be that at pressing pressure beyond 20 MPa, the sandbox oil bearing capillaries were crushed, hence blocking the flow of oil. Bamgboye and Adejumo (2011) observed that seed cells rupture during oil expression due to pressure on seed cell walls, which causes them to release their lipid contents. Conversely, as the applied pressure increases, oil capillaries are repeatedly compressed, disrupted and could eventually become blocked (Ward, 1976). This finding on sandbox seed is similar to reports on other oilseeds and nuts: groundnut, rice bran, melon, roselle, dika, soybean, conophor (Fasina and Ajibola, 1989; Adeeko and Ajibola, 1990; Ajibola *et al.*, 1990; Sivala *et al.*, 1992; Akintunde *et al.*, 2001; Bamgboye and Adejumo, 2011; Ogunsina *et al.*, 2014).

The sandbox oil yield increased with increase in expression time from 2-8 min and dropped as the pressing time exceeded 8 min (Figure 9). The result is similar to those reported by Olajide *et al.* (2014) on groundnut kernel and Mwithiga and Moriasi (2007) on soybeans.

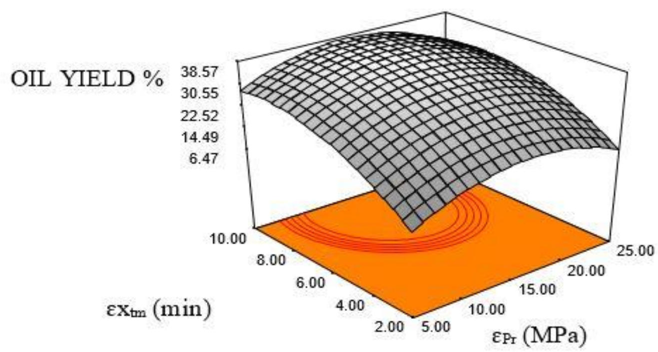

Figure 9. Roasting temperature and moisture content against oil yield.

Response surface optimization of oil extraction from sandbox seed

Out of the four models of the RSM software, the one chosen for the prediction of oil yield from sandbox seed by mechanical means was based on the model with the best statistics as regards the polynomial order with the largest number non- aliasing significant additional terms, insignificant lack-of-fit and high Adjusted and Predicted *(R^2)*. The quadratic model with the highest R^2 and lower standard deviation values (Table 2) was selected.

Table 2. Model comparison.

Statistics	Models			
	Linear	2Factorial Interaction	Quadratic	Cubic
Standard Deviation, SD	4.84	5.86	3.72	2.21
R^2	0.5623	0.6053	0.8907	0.9789
Mean	29.39	29.39	29.39	29.39
Adjusted R^2	0.4781	0.2353	0.6921	0.8909
Coefficient of Variation, C.V.	16.47	19.93	12.65	7.53
Predicted R^2	0.3910	-2.1284	-1.8079	-19.9477
PRESS	847.71	4352.06	3906.19	29140.84
Adequate Precision	9.272	5.449	7.280	10.349

PRESS = Predicted Sum of Square.

Mathematical relationship for predicting oil yield from sandbox relatively to the process factors is given in Equation 5.

$$OY = 35.35 - 1.5mc - 0.03\gamma_{tp} + 2.5\gamma_{tm} + 0.49\varepsilon_{Pr} + 4.8\varepsilon x_{tm} - 1.91mc^2 + 0.086\gamma_{tp}^2 - 2.41\varepsilon_{Pr}^2 - 1.83\varepsilon x_{tm}^2 + 0.39mc\gamma_{tp} - 0.098mc\gamma_{tm} - 1.09mc\varepsilon_{Pr} - 0.64mc\varepsilon x_{tm} - 0.27\gamma_{tp}\gamma_{tm} + 0.058\gamma_{tp}\varepsilon_{P} + 0.47\gamma_{tp}\varepsilon x_{tm} + 1.04\gamma_{tm}\varepsilon_{Pr} + 0.74\gamma_{tm}\varepsilon x_{tm} - 0.30\varepsilon_{Pr}\varepsilon x_{tm} \quad (5)$$

[SD = 3.72, R^2 = 0.8908, Mean = 29.39, Adjusted R^2 = 0.6922, C.V. = 12.66, Predicted R^2 = –1.8061, PRESS = 3910.93, Adequate Precision = 7.301 and F-value of 4.49 (Tables 2 and 3)]

OY = Oil Yield (%), *mc* = moisture content of sandbox seed, γ_{tp} = Roasting temperature, γ_{tm} = Roasting time, ε_{Pr} = Expression pressure and εx_{tm} = Extraction time

From the equation, the oil yield varies directly with factors with positive sign and inversely with factors with negative sign. The values of "Prob > F" in Figure 3, lower than 0.05, such as γ_{tm}, εx_{tm}, mc^2, γ_{tm}^2, ε_{Pr}^2, and εx_{tm}^2, represents significant model parameters for sand box oil extraction.

Table 3. ANOVA for Response Surface Quadratic Model of the Oil Extraction

Source	Sum of squares	DF	Mean square	F value	Prob > F
Model	1241.52	20	62.08	4.49	0.0069^s
mc	58.56	1	58.56	4.23	0.0642
γ_{tp}	0.022	1	0.022	0.0016	0.9688
γ_{tm}	151.76	1	151.76	10.97	0.0069^s
ε_{pr}	5.82	1	5.82	0.42	0.5299
ε_{tm}	568.13	1	568.13	41.06	0.0001^s
mc^2	106.76	1	106.76	7.47	0.0180^s
γ_{tp}^2	0.22	1	0.22	0.016	0.9026
γ_{tm}^2	103.43	1	103.43	7.47	0.0194^s
ε_{pr}^2	171.01	1	171.01	12.36	0.0048^s
ε_{tm}^2	98.39	1	98.39	7.11	0.0219^s
$mc\gamma_{tp}$	2.44	1	2.44	0.18	0.6825
$mc\gamma_{tm}$	0.15	1	0.15	0.011	0.9179
$mc\varepsilon_{pr}$	18.86	1	18.86	1.36	0.2677
$mc\varepsilon_{tm}$	6.46	1	6.46	0.47	0.5084
$\gamma_{tp}\gamma_{tm}$	1.14	1	1.14	0.082	0.7795
$\gamma_{tp}\varepsilon_{pr}$	0.054	1	0.054	0.004	0.9513
$\gamma_{tp}\varepsilon_{tm}$	3.51	1	3.51	0.25	0.6246
$\gamma_{tm}\varepsilon_{pr}$	17.28	1	17.28	1.25	0.2875
$\gamma_{tm}\varepsilon_{tm}$	8.69	1	8.69	0.63	0.4449
$\varepsilon_{tp}\varepsilon_{tm}$	1.47	1	1.47	0.11	0.7506
Residue	152.21	11	13.84		
Lack of fit	149.68	6	24.95	49.25	0.0003^s
Pure Error	2.53	5	0.51		
Cor Total	1393.74	31			

The quadratic model had a high R^2 of 0.8908 and very low p-value of less than 0.0001 and thus was concluded to be significant (Table 4). The R^2 of 0.89 is an indication of a direct relationship between the oil yield and the process factors, showing 89.08% confidence that the model explained 89.08% of every irregularity as regards the process factors and oil yield.

Table 4. Test of between-subjects effect of process conditions on oil yield from sandbox seed

Source	df	Mean Square	F	Significance
Corrected Model	27	51.439	86.003	0.0001 s
Intercept	1	10656.051	17816.504	0.0001 s
mc	3	67.567	112.970	0.0001 s
Υ_{tp}	2	4.189	7.004	0.049
Υ_{tm}	2	122.883	205.456	0.0001 s
ε_{Pr}	2	124.977	208.957	0.0001 s
εx_{tm}	2	164.746	275.449	0.0001 s
Error	4	0.598		
Total	32			
Corrected Total	31			

The 4.49 model F-value (Table 3) indicated that the model effectively explained the inter-relationships between process factors and oil yield. The quadratic curve relationship is one of optimum and minimum. That means that there are process parameters values in which oil yield would be optimum or minimum. The sandbox seed grain is very soft, similar to melon seed, thus a mild roasting temperature of 85°C for 15 min was enough heat treatment to release optimum oil yield from it. The sandbox mash slurried and clogged the screw press oil holes and overflowing the pressing plate at pressure above 20 MPa and pressing time above 8 min and moisture content above 6% wb. The optimum oil yield for sandbox seed was obtained at the process variable ranges. From the findings, process parameter values for optimal sandbox oil yield were determined. Findings from Ebewele *et al.* (2010); Bamgboye and Adejumo (2011); Olajide *et al.* (2014); Yusuf *et al.* (2014); Aremu and Ogunlade (2016); Akubude *et al.* (2017) agrees with this finding as regards mechanical oil expression.

Model validation

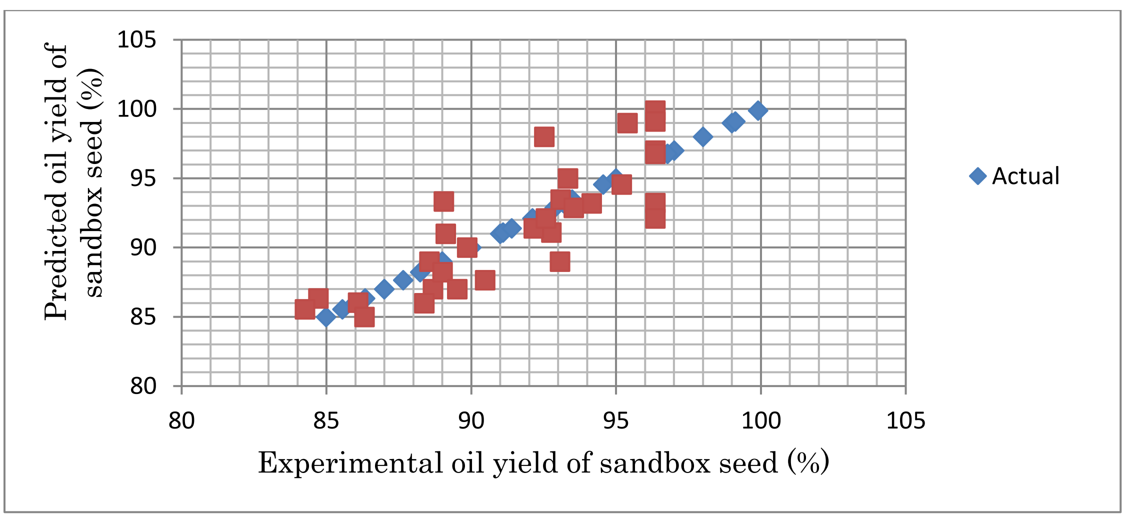

Figure 10. Predicted oil yield against actual oil yield

A similarity plot of correlation relationship of the laboratory results and predicted results of oil yield from the sandbox seed is shown in Figure 10. The R^2 of 0.8908 of the relationships is an indication of high correlation between the predicted oil yield values and the values gotten from the actual experiment. This is an indication that without distortions that accompany practical experiments, the model represents a reliable equivalent for the estimation of extractable oil from sandbox seed by mechanical means within the range of process variables studied. At the range of process factors: 8-12% wb moisture content, 80-100°C roasting temperature, 0-20 min roasting time, 5-25 MPa expression pressure and 2-10 min expression time, the maximum oil yield of 38.68% was obtained at 6% wb moisture content, 85°C roasting temperature, 15 min roasting time, expression pressure of 20 MPa and 8 min pressing time, while the predicted optimum oil yield was 38.95% at processing conditions of 7.03% moisture content, 97.72°C roasting temperature, 11.32 min roasting time, 15.11 MPa expression pressure and 8.57 min extraction time. Experiments carried out under the predicted optimum conditions produced an oil yield of 38.90%, validating the predicted oil yield and the processing conditions. The variations between the experimental and predicted results were low at the ranged 0.01-0.62. This is an indication that model used reasonably predicted the oil yield from sandbox seed by mechanical screw press.

CONCLUSION

Oil extraction process from sandbox seed using screw press was optimized. From the variations of process factors studied, the extracted oil from sandbox seed varied from 16.38-38.68%. The 38.68% oil yield, which was the highest, was attained at the process factor combination of 6% wb moisture content, 85°C roasting temperature, 15 min roasting time, 20 MPa expression pressure and 8 min pressing time. The model maximum predicted oil yield was 38.95% at 7.03% moisture content, 97.72°C roasting temperature, 11.32 min roasting time, 15.11 MPa expression pressure and 8.57 min extraction. Experiments carried out under the predicted optimum conditions produced an oil yield of 38.90%, validating the predicted oil yield and the processing conditions. The variations between the experimental and predicted results were low at the range of 0.01-0.62. All process factors considered seem to have greatly influenced the oil yield, with roasting temperature been insignificant. The model developed for the sandbox oil expression, with R^2 of 0.8908 indicates a high correlation between the process factors. The similarity between the values oil yield from actual experiment and predicted values, indicates that the model adequately predicted the oil yield from sandbox seed by mechanical expression.

DECLARATION OF COMPETING INTEREST

The authors declare that they have no conflict of interest.

CREDIT AUTHORSHIP CONTRIBUTION STATEMENT

David Nwabueze ONWE: Conceptualization, Sample collection, Methodology, Investigation, Data collection, Analysis, Validation, Writing of Report.
Adeleke Isaac BAMGBOYE: Supervision, Visualization, Review, Correction and Editing of Report.

REFERENCES

Abidakun OA, Koya OA and Ajayi OO (2012). *Effect of expression conditions on the yield of Dika Nut (Irvingia gabonesis) oil under uniaxial compression*. In: 2012 International Conference on Clean Technology and Engineering Management (ICCEM 2012), 12th-15th, p. 315-320. Mechanical Engineering,Covenant University, Ota, Nigeria.

Adeeko KA and Ajibola OO (1990). Processing factors affecting yield and quality of mechanically expressed groundnut oil. *Journal of Agricultural Engineering Research, 45(1): 31-43.*

Adejumo BA, Alakowe AT and Obi DE (2013). Effect of heat treatment on the characteristics and oil yield of *moringa oleifera* seeds. *The International Journal of Engineering and Science (IJES), 2 (1): 232-239.*

Adewuyi A, Paul O, Awolade PO and Oderinde RA (2014). *Hura crepitans* seed oil: an alternative feedstock for biodiesel production. *Journal of Fuels,* (*8): 464590.*

Adewuyi A, Gopfert A, Wolff T, Rao BVSK and Prasad RBN (2012). Synthesis of azidohydrin from *Hura crepitans* seed oil: a renewable resource for oleochemical industry and sustainable development. *ISRN Organic Chemistry*, *2012/ID 873046.*

Ajala AS and Adeleke SA (2014). Effect of drying temperatures on physicochemical properties and oil yield of african star apple (*Chrysophyllum alibidum*) seeds. *Global Journal of Engineering Design and Technology* (*G.J. E.D.T.*), *3(3): 12-16.*

Ajav EA and Olatunde OB (2011). *Mechanical oil expression from groundnut (Arachishypogaea).* held between October 17–20 at Ilorin, Kwara State In: Proceedings of the 11th International Conference and 32nd Annual General Meeting of The Nigerian Institution of Agricultural Engineers, 32: 427-430.

Ajibola OO, Adetunji SO and Owolarafe OK (2000). Oil point pressure of sesame seed. *Ife Journal of Technology, 9(2): 57-62.*

Ajibola OO, Eniyemo SE, Fasina OO and Adeeko KA (1990). Mechanical expression of oil from melon seeds. *Journal of Agricultural Engineering Research, 45: 45-53.*

Ajibola OO, Owolarafe OK, Fasina OO and Adeeko KA (1993). Expression of oil from sesame seeds. *Canada Agricultural Engineering*, *35: 83-88.*

Akinoso R, Igbeka J and Olayanju T (2006). Process optimization of oil expression from sesame seed (*Sesamum indicum* Linn.). *Agricultural Engineering International: The CIGR Ejournal. Manuscript FP 06 011: Vol. VIII.*

Akintunde TY, Akintunde BO and Igbeka JC (2001). Effects of processing factors on yield and quality of mechanically expressed soybean oil. *Journal of Agricultural Engineering Technology*, *9: 39-45.*

Akubude VC, Maduako JN, Egwuonwu CC, Olaniyan AM, Ozumba IC, Nwosu C and Ajala OE (2017). Effect of process parameters on oil yield mechanically expressed from almond seed (Using Response Surface Methodology). *American Journal of Food Science and Nutrition Research, 4(1): 1-8.*

Allen TF (2000). *Hura crepitan* L. *The Encyclopedia of pure material medical. Homeopathe International,* , pp. 1-2, New Delhi, India.

Alonge AF, Olaniyan AM, Oje K and Agbaje CO (2003). Effects of dilution ratio, water temperature and pressing time on oil yield from groundnut oil expression. *Journal of Food Science and Technology, 40: 652-655.*

Anwar F, Zafar SN and Rashid U (2006). Characterization of Moringa oleifera seed oil from drought and irrigated regions of Punjab, Pakistan. *Grasas Aceites, 57(2): 60-168.*

Aremu AK and Ogunlade CA (2016). Effect of operating parameters on mechanical oil expression from African oil bean seed. *Global Journal of Science Frontier Research: Agriculture and Veterinary, 16(1): 1.*

Awolu OO, Obafaye RO and Ayodele BS (2013). Optimization of solvent extraction of oil from neem (*Azadirachta indica*) and its characterizations. *Journal of Scientific Research and Reports, 2(1): 304-314.*

Badwaik LS, Prasad K and Deka SC (2012). Optimization of extraction conditions by Response Surface Methodology for preparing partially defatted peanut. *International Food Research Journal*, *19(1): 341-346.*

Bamgboye AI and Adejumo OI (2011). Effects of processing parameters of roselle seed on its oil yield. *International Journal of Agricultural and Biological Engineering, 4(1): 82-86.*

Basumatary S (2013). Non-conventional seed oils as potential feedstocks for future biodiesel industries: *A Brief Review Research Journal of Chemical Sciences. 3(5): 99-103.*

Bockisch M (1998). Fats and Oils Handbook. *Manuals by AOCS Press.*

Bello EI and Daniel F (2015). Optimization of Groundnut Oil Biodiesel Production and characterization. *Applied Science Report, 9(3): 172-180.*

Box GPE, Hunter WG and Hunter JS (1978). Statistics for Experiments. *John Wileyand Sons Inc,* pp. 335-375, New York.

Clarke JH (2000). Hura crepitan. A Dictionary of Practical Material Medical. *Homeopathe International,* 1-2, New Delhi, India

Costa SS, Gariepy Y, Rocha SCS and Raghavan V (2014). Microwave extraction of mint essential oil-temperature calibration for the oven. *Journal of Food Engineering, 126: 1-6.*

Ebewele RO, Iyayi AF and Hymore FK (2010). Considerations of the extraction process and potential technical applications of Nigerian rubber seed oil. *International Journal of the Physical Sciences, 5(6): 826-831.*

Elkhaleefa A and Ihab Shigidi I (2015). Optimization of sesame oil extraction process conditions. *Advances in Chemical Engineering and Science, 5: 305-310.*

Fakayode OA and Ajav EA (2016). Process optimization of mechanical oil expression from Moringa *(Moringa oleifera)* seeds. *Industrial Crops and Products, 90: 142-151.*

Fasina OO and Ajibola OO (1989). Mechanical expression of oil from Conophor nut (*Tetracarpidium conophorum*). *Journal of Agricultural Engineering Research, 46: 45-53.*

Feldkamp S (2006). Modern Biology. *Holt, Rinehart, and Winston.* p. 618, United States

Fowomola MA and Akindahunsi AA (2007). Nutritional quality of sandbox tree (*Hura crepitans* Linn.). *Journal of Medicinal Food, 10(1): 159-64.*

Giwa A, Bello A and Giwa SO (2015). Artificial Neural Network Modeling of a Reactive Distillation Process for Biodiesel Production. *International Journal of Scientific and Engineering Research, 6(1): 1175-1191.*

Hammonds TW, Harris RV and Head SW (1991). The influence of moisture content on the extraction of oil from fresh grated Coconut. *Tropical Science, 31: 73-81.*

Hamzat KO and Clarke B (1993). Prediction of oil yield from Groundnuts using the concept of Quasi-equilibrium oil yield. *Journal of Agricultural Engineering Research, 55: 79-87.*

Hashim AB, Giwa SO, Ibrahim M and Giwa A (2014). Finding the optimum parameters for oil extraction from sesame seed using Response Surface Methodology. *International Journal of Scientific Research and Management Studies (IJSRMS), 2(1): 1-13.*

Idowu DO, Abegunrin TP, Ola FA, Adediran AA and Olaniran JA (2012). Measurement of some engineering properties of sandbox seeds (*Hura crepitans*). *Agriculture and Biology Journal of North America, 3(8): 318-325.*

Islau M, Marks B and Bakker-Arkema F (2002). Optimization of commercial ear-corn dryers. Agricultural Engineering International: *The CIGR Journal of Scientific Research and Development,* 04 (007): VI.

Kagwacie OC and Anozie NA (1995). Effect of processing conditions on solvent extraction of oil from rubber seeds. *Journal of Agricultural Technology, 3(1): 31-40.*

Khan LM and Hanna MA (1984). Expression of soybean oil, *Transaction of the ASAE, 27(1): 190.*

Lawson OS, Oyewumi A, Ologunagba FO and Ojomo AO (2010). Evaluation of the parameters affecting the solvent extraction of soybean oil. *ARPN Journal of Engineering and Applied Sciences, 5(10).*

Martínez ML, Penci MC, Marin MA, Ribota PD and Maestri DM (2013). Screw press extraction of almond (*Prunus dulcis* (Miller) D.A. Webb): Oil recovery and oxidative stability. *Journal of Food Engineering, 119: 40-45.*

Matthäus B (2012). Oil technology. S.K. Gupta (ed.), *Technological Innovations in Major World Oil Crops*, 2.

Muhammed NA, Isiaka AA and Adeniyi OA (2013). Chemical composition of hura crepitans seeds and antimicrobial activities of its oil. *International Journal of Science and Research (IJSR), 2(3).*

Mwithiga G and Moriasi L (2007). A study of yield characteristics during mechanical oil extraction of preheated and ground soybeans. *Journal of Applied Sciences Research, 3(10): 1146-1151.*

Nwanorh KO (2015). Extraction and characterization of oil from *Hura crepitans* (sandbox tree). *International Research Journal of Education and Innovation, 1(5).*

Ogunsina BS, Koya OA and Adeosun OO (2008). Deformation and fracture of Dika nut (*Irvingia gabonensis*) under uni-axial compressive loading. *International Agrophysics, 22: 249-253.*

Ogunsina BS, Olatunde GA and Adeleye O (2014). Effect of pre-treatments on mechanical oil expression from Dika kernels. *Journal of Agricultural Technology, 10(2): 309-319.*

Okolie PN, Uaboi-Egbenni PO and Ajekwene AE (2012). Extraction and quality evaluation of sandbox tree seed (*Hura crepitan*). *Oil World Journal of Agricultural Sciences, 8(4): 359-365.*

Olajide JO (2000). Process Optimization and Modling of Oil Expression from Groundnut and Sheanut Kernels. A Ph.D. Thesis. *Department of Agricultural Engineering, University of Ibadan, Nigeria.*

Olajide JO, Afolabi JO and Adeniran JA (2014). Optimization of oil yield from groundnut kernel (*Arachis hypogeae*) in a hydraulic press Using Response Surface Methodology. *Journal of Scientific Research and Reports*, *3(14): 1916-1926.*

Olaniyan AM and Oje K (2007). Development of mechanical expression rig for dry extraction of Shea butter from shea kernel. *Journal of Food Science and Technology*, *44(5): 465-470.*

Olaoye JO (2000). Some Physical Properties of Castor Nut relevant to the Design of Processing Equipment. *Journal of Agricultural Engineering Research, 77 (1): 113-118.*

Olatidoye OP, Adeleke AE, Adegbite SA and Sobowale SA (2010). Chemical composition and nutritional evaluation of sandbox (*Hura crepitan*) seed flour for domestic consumption and industrial. *Journal of Medical and Applied Biosciences. 2: 72-83.*

Onwe DN, Umani KC, Olosunde WA and Ossom IS (2020). Comparative analysis of moisture-dependent physical and mechanical properties of two varieties of African star apple *(Chrysophyllum albidum)* seeds relevant in engineering design. *Scientific African, 8, e00303.*

Orhevba BA, Chukwu O, Osunde ZD and Ogwuagwu V (2013). Influence of moisture content on the yield of mechanically expressed neem seed kernel oil. *Academic Research International, 4(5).*

Ottih OP, Aneke NAG and Ejikeme PC (2015). Production and characterization of paint driers from sand box seed oil (*Hura crepitans*). *International Journal of Innovative Science, Engineering and Technology, 2(2).*

Owolarafe OK, Adegunloye AT and Ajibola OO (2003). Effects of processing condition on oil point pressure of locust bean. *Journal of Food Processing Engineering, 26(51): 489-497.*

Ozguven F and Vursavus K (2005). Some physical, mechanical and aerodynamic properties of pine nuts. *Journal of Food Engineering, 68: 191-196.*

Pominski J, Pearce HM and Spadero JJ (1970). Partially defatted Peanuts-factors affecting oil removal during pressing. *Food Technology*, *24(6): 92-94.*

Sivala K, Bhole NG and Mukherjee RK (1991). Effect of moisture on rice bran oil expression. *Journal of Agricultural Engineering Research, 50: 81-91.*

Shonekan FO and Ajayi JO (2015). The biochemical analysis of *Hura crepitans* (Sandbox Tree) seed oil and meal. *Globalacademicgroup.com*, (*January 15, 2016).*

Southwell KH and Harris RV (1992). Extraction of oil from oilseeds using the hot water flotation method. *Tropical Science, 82: 251-256.*

Terigar BG, Balasubramanian S, Sabliov CM, Lima M and Boldor D (2011). Soybean and rice bran oil extraction in a continuous microwave system: From laboratory- to pilot-scale. *Journal of Food Engineering*, *104: 208-217.*

Triveni R, Shamala TR and Rastogi NK (2001). Optimized production and utilization of exopolysaccharide from *Agrobacterium radiobacter. Process Biochemistry, 36: 787-795.*

Tunde-Akintunde, TY, Akintunde BO and Igbeka JC (2001). Effect of processing factors on yield and quality of mechanically expressed soybeans oil. *Journal of Agricultural Engineering Technology, 55: 86-92.*

Umamaheshwari P and Dinesh Sankar Reddy P (2016). Effect of operating parameters on extraction of oil from Bitter gourd seeds: a kinetic and thermodynamic study. *International Journal of Science and Research (IJSR), 5(2).*

Ward JA (1976). Processing high oil content seeds in continuous screw press. *Journal of American Oil Chemist Society*, 53, 261-264.

Weiss EA (2000). Oilseed Crop. pp.131-164, 2nd ed. *Blackwell Longman Group Ltd*, USA.

Yusuf KA, Olaniyan AM, Atanda EO and Sulieman LA (2014). Effects of heating temperature and seed condition on the yield and quality of mechanically expressed groundnut oil. *International Journal of Technology Enhancements and Emerging Engineering Research, 2(7): 73-78.*

Turkish Journal of Agricultural Engineering Research

https://dergipark.org.tr/en/pub/turkager
https://doi.org/10.46592/turkager.2021.v02i02.017

Turk J Agr Eng Res
(TURKAGER)
e-ISSN: 2717-8420
2021, 2(2): 450-459

Research Article

Assessment of Spatial Variability of Heavy Metals (Pb and Al) in Alluvial Soil around Delta State University of Science and Technology, Ozoro, Southern Nigeria

Hilary UGURU[a*], Ovie Isaac AKPOKODJE[b], Goodnews Goodman AGBI[c]

[a]*Department of Agricultural Engineering, Delta State University of Science and Technology, Ozoro, NIGERIA*

[b]*Department of Civil and Water Resources Engineering, Delta State University of Science and Technology, Ozoro, NIGERIA*

[c]*Department of Civil Engineering, Delta State University, Oleh Campus, NIGERIA*

(*): Corresponding author. erobo2011@gmail.com

ABSTRACT

Soil heavy metals pollution is a major global threat, because of its impact to plants, animals, and the soil geotechnical properties. Geostatistical method was used to investigate the spatial distributions of aluminum and lead within a section of the Delta State University of Science and Technology, Ozoro, Nigeria. A total area of 1 km^2 (100 hectares) was covered within the school environment. Twenty -five (25) topsoil samples were collected, at the end of the dry season (March 2021); when the water table in the study area was very low. The lead and aluminum concentrations of the 25 samples were measured by using the Association of Official Analytical Chemists (AOAC) approved methods. Using a geostatistical tool, the lead and aluminum concentrations and distribution in the soil were plotted on predication maps. The maps revealed irregular spatial distributions of lead and aluminum ions within the study area. The lead concentration was highest at the North-central region of the study area; while lead concentration was lowest at the Eastern region of the study area. In terms of the aluminum metal, the highest aluminum concentration was observed in the North eastern region; while aluminum concentration was lowest at the South western region. Data obtained from this study will be useful for agricultural and civil engineering purposes, mainly in the area of decision-making.

RESEARCH ARTICLE

Received: 22.09.2021
Accepted: 09.12.2021

Keywords:

- Geotechnical properties,
- Heavy metals,
- Predication map,
- Soil properties,
- Spatial distribution

To cite: Uguru H, Akpokodje OI, Agbi GG (2021). Assessment of Spatial Variability of Heavy Metals (Pb and Al) in Alluvial Soil around Delta State University of Science and Technology, Ozoro, Southern Nigeria. Turkish Journal of Agricultural Engineering Research (TURKAGER), 2(2): 450-459. *https://doi.org/10.46592/turkager.2021.v02i02.017*

INTRODUCTION

Soil is a vital component of the ecosystem that is mainly used for agricultural and constructional purposes; hence, it needs to be protected. According to Alloway (1990) the knowledge of the heavy metals and minerals status of the soil is necessary, in order to ascertain the concentrations of the essential micronutrients in the environment. Spatial heterogeneity of heavy metals concentrations in soil is an important factor affecting agricultural productivity and geotechnical properties of the soil (Cemek *et al.*, 2007). Geotechnical properties of soil are one of the major factors to be considered during foundation design of farm structures and other residential buildings. Soil productivity in agricultural technology is influenced by its texture, structure, chemical composition, heavy metals concentration, amongst others. The availability (solubility) of a metal in the soil is a factor of the immediate environmental condition (Ogbaran and Uguru, 2021a); as solubility is higher in fine grained soils with high moisture content, compared to coarse grained soils with low water content. Hence, aquatic environments tend to have higher metals content, which will results in high buildup of these metals by aquatic organisms in their bodies (Sobhanardakani *et al.*, 2011).

Lead (Pb) and aluminum (Al) are some of the most toxic and abundant heavy metals (elements) in the world. They occur in soils mostly as a result of the weathering of rocks; although, leachates from waste dumpsites and other anthropogenic sources also contribute greatly to their concentrations in the soil. The environment acquires its heavy metals contamination through direct atmospheric deposition, geologic weathering, anthropogenic sources, etc. (Wang and Rainbow, 2008; EPA, 2020; Ogbaran and Uguru, 2021a; Ogbaran and Uguru, 2021b). Multiple factors such as, soil pH, soil moisture content and its holding capacity, texture, organic materials content, vegetation type, etc., usually influenced the concentration and distribution of metals in the soil (Marques *et al.*, 2009; Rakesh *et al.*, 2013).

According to previous researches (Giller *et al.*, 1998; Friedlov´a, 2010; Chibuike and Obiora, 2014; Akpokodje and Uguru, 2019), heavy metals toxicity is dependent on the soil temperature, soil pH, organic materials present, chemical forms of the metal, etc. Lead and aluminum contamination of the environment had become an alarming issue, mainly due to their impact on the soil's geotechnical and physiochemical properties (Kidd and Proctor, 2001; Ohadi *et al.*, 2015). Therefore, the presence of these heavy metals in the soils did not only have adverse effects on plants and human beings, but altered the soil's mechanical/geotechnical properties (Begun *et al.*, 2009). Ohadi *et al.* (2015) worked on the impact of lead metal on the liquid limit of sand–clay soil samples, and they observed a decline in the liquid limit as the lead concentration increased. Accordingly, Negahdar *et al.* (2017) studied the influence of lead on sandy clay soils, and observed that the soil's cohesion decreased non-linearly, as the lead concentration increases; although, the soils internal friction angle was not affected by the lead concentration. Furthermore, Jafer *et al.* (2021) stated that aluminum had great effect on the unconfined compressive strength (UCS) of contaminated soils samples, as a reduction in the soil's UCS was observed as the aluminum concentration increased.

Regarding the impact of these heavy metals on plants, Nas and Ali (2018) reported that high lead concentration in the soil could result in retardation of crops' growth, inhabitation of the photosynthesis process, and several other factors. Likewise, Barceló and Poschenrieder (2002) in their study reported that a high concentration of aluminum can results in extensive plants roots injuries, resulting in poor ion and water uptake by the plants' roots. According to Sivaguru and Horst (1998), the toxicity of aluminum in plants includes callose buildup in the plants' roots cells, thus hindering cell-cell trafficking, and disrupting the structure of the plant cytoskeleton (Panda *et al.*, 2009).

Although many studies (Atikpo and Ihimekpen, 2018; Hua *et al.*, 2012; Burgos *et al.*, 2006; Stirbescu *et al.*, 2018) had investigated spatial variation patterns of heavy metals in the environment, there is no recorded literature on the spatial variability of lead and aluminum metals in the soils in the Niger Delta area with particular reference to the Ozoro community of Delta State, Nigeria. Ozoro is a center for agricultural and commercial development, and is presently undergoing construction/development activities. Therefore, this study is aimed at investigating the concentration and spatial distribution of lead and aluminum metals in the topsoil in a selected area of Ozoro community, Delta State, by using geostatistical method.

MATERIALS AND METHODS

Description of experimental area

The study was done at Delta State University of Science and Technology, Ozoro, located in Delta State, Nigeria. Ozoro falls within the tropical forest zone of Nigeria, and is characterized by two major climatic seasons (rainy and dry season); with rainfall of about 1800 mm annually. The study area usually experiences tropical rain storms and flood during the rainy season (Eboibi *et al.*, 2018). The geographical coordinates of the university are: 5.549° N and 5.570° N, 6.241°E and 6.249°E; and is made up of developed and undeveloped areas. The undeveloped area of the university is covered with natural vegetation, and the soil is mainly the alluvial type; while the built up area is covered by both alluvial deposits and imported laterite and sands.

The total experimental area used for this study was 1 km by 1 km (as shown in Figure 1) and was gridded at 200 m intervals (Figure 2). The central portion of the study area is occupied by administrative buildings and students' lecture halls; while the north and eastern regions are covered with dense natural vegetation.

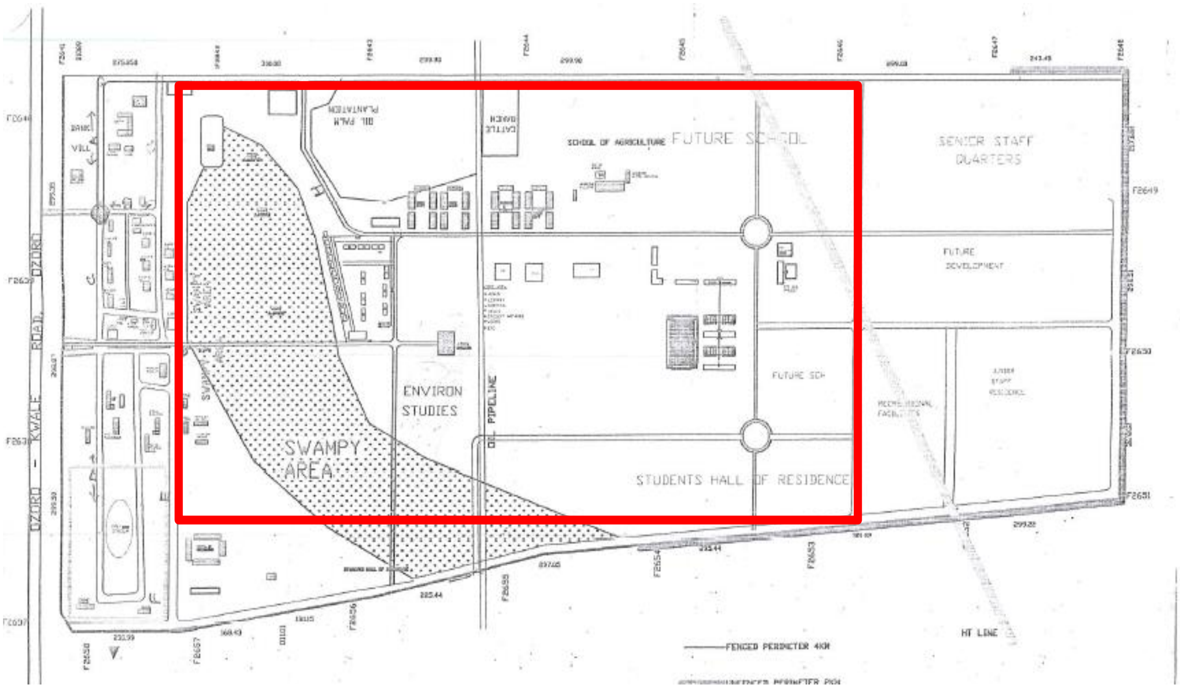

Figure 1. The layout map of the study area.

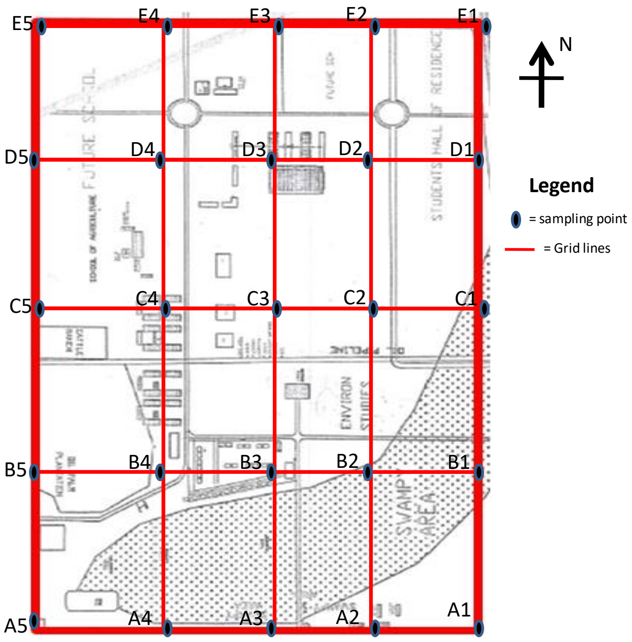

Figure 2. Grid Lines revealing the sampling locations at 200 m grids superimposed on layout map.

Soil sampling

At each grid point, the topsoil (0-30cm) was collected by using a soil auger. The co-ordinates of the spatial location were measured by using a global positioning system (GPS) device.

After collection, the soil samples were poured into a black plastic bag (Figure 3), and coded according to the sample location. The samples were collected during the peak of the dry season (March 2021); when the water table in the study area was very low. A total of 25 soil samples were collected for this study.

Figure 3. The collected soil samples.

Heavy metals concentrations and analysis

Each soil sample was air-dried, ground in a porcelain mortar, and then filtered with a 2 mm gauge nylon filter, as described by Agbi *et al.* (2021). The powdered soil sample (10 g) was measured with a digital balance and emptied into a heat resistance beaker. To this was then added a 15 mL mixture of concentrated inorganic acids (HNO_3, HCl, and H_2SO_4) in the ratio of 5:1:1, and heated in a water bath at a temperature of 100^{0}C until a transparent solution was obtained (Akpomrere and Uguru, 2020). The digested soil sample was cooled to room temperature under ambient environmental conditions, and filtered into a measuring cylinder using filter paper. Then distilled water was added to the filtrate to dilute it the 100 mL mark of the measuring cylinder. Lead and aluminum concentrations of the diluted digested solution were measured with the aid of the Atomic Absorption Spectrophotometer (AOAC, 2019; Turek *et al.*, 2019; Akpomrere and Uguru, 2020).

Data Analysis

The variability of lead and aluminum concentrations in the soil was carried out by using the ArcGIS geostatistical tool, and adopting the Kriging model.

RESULTS AND DISCUSSION

The mean concentrations of lead and aluminum in the soils collected from all the sampled locations are presented in Table 1. As shown in Table 1, the Pb and Al concentrations varied extensively across the area investigated in this study. Although the Pb concentration across the study area was fairly high, it was below the 85 mg/kg maximum allowable limit approved by the World Health Organization (WHO, 1996). Therefore, there is no clear Pb pollution risk on agricultural practices; although, it may have significant effects on the soil geotechnical properties.

Table 1. Metal concentration in soil samples.

Location	GPS co-ordinates	Metal concentration (mg kg^{-1})		Location	GPS co-ordinates	Metal concentration (mg kg^{-1})	
		Pb	Al			Pb	Al
A1	5.563 N, 6.249 E	16.3±0.4	998.44±23	**B1**	5.564 N, 6.249 E	16.1±0.9	844.49±8
A2	5.562 N, 6.248 E	12.8±0.3	641.22±14	**B2**	5.563 N, 6.248 E	12.8±1.1	3041.28±9
A3	5.562 N, 6.246 E	21.7±0.5	1120±32	**B3**	5.564 N, 6.246 E	18.9±0.8	1301.9±11
A4	5.560 N, 6.243 E	18.9±0.9	948.9±18	**B4**	5.562N, 6.243 E	15.2±0.5	1235.2±9
A5	5.560 N, 6.241 E	18.1±0.8	1018.1±13	**B5**	5.562N, 6.241 E	14.5±0.3	1514.5±15
C1	5.566 N, 6.248 E	26.2	1219±11	**D1**	5.568 N, 6.246 E	13.7±0.8	849.25±9
C2	5.566 N, 6.246 E	25.4	779.5±12	**D2**	5.568 N, 6.248 E	12.1±0.5	1266±14
C3	5.566 N, 6.244 E	17.3	499±8	**D3**	5.568 N, 6.245 E	13.3±0.4	1840±18
C4	5.566 N, 6.243 E	10.8	549±11	**D4**	5.568 N, 6.242 E	14.8±0.9	1393±11
C5	5.566 N, 6.240 E	15.8±0.5	515.8±8	**D5**	5.568 N, 6.241 E	16.5±2.2	1538±18
E1	5.570 N, 6.249 E	5.9±0.3	1840±10				
E2	5.570 N, 6.246 E	8.1±0.5	1245±13				
E3	5.568 N, 6.245 E	6.8±0.8	577.48±15				
E4	5.570 N, 6.243 E	10.6±0.4	1410±9				
E5	5.570 N, 6.241 E	12.5±1.2	1212±14				

Mean± standard deviation; n: 3

The results obtained in this study were plotted in variation maps shown in Figure 4 and Figure 5. The variation maps revealed that the lead concentration in the topsoil was lower when compared to the aluminum concentration in the topsoil. Based on the results outcome, the lead concentration in the topsoil within the study area ranged between 5.92 mg kg^{-1} and 26.2 mg kg^{-1}; while the aluminum concentration in the topsoil area ranged between 499 mg kg^{-1} and 1840 mg kg^{-1}. It can be observed from the soil predication maps that, the lead and aluminum concentrations were non-uniformly distributed across the study area.

As revealed in Figure 4, high lead concentration was recorded at the North-central part of the area studied; while low lead concentration was recorded at the North-eastern and Southern parts of the area studied. As depicted by the soil map, the lead concentration generally increased from the Eastern region to the Western region, with the peak lead concentration (26.2 mg kg^{-1}) recorded at the north-central region of the study area. In terms of the spatial distribution of aluminum in the topsoil, Figure 5 revealed that the highest aluminum concentration was recorded in the north-eastern and southern-eastern regions of the study area. However, the lowest aluminum concentration was recorded at the North-western region of the study area. Generally, the North-central part of the area studied had a fairly low aluminum concentration. As we moved from the north central part region to the Southern region of the study area, it was observed that aluminum concentration generally decreased, before it started to increase again, reaching a peak at the distant south-eastern region. These observations are similar to the previous report of Stirbescu *et al.* (2018), where the soil lead concentration was at the peak at the central region of the study area (Targoviste city). A similar trend of non- uniformity distribution of soil lead concentration was also observed by Atikpo and Ihimekpen (2018), in Amaonye forest of Ebonyi State, Nigeria. According to Naveen *et al.* (2018) the heavy metals concentrations often declined non-uniformly, as the spatial locations moved away from the main polluting source(s).

The high heavy metals concentration generally recorded in the north-central region may be attributed mainly to anthropogenic sources. According to Agbi *et al.* (2021) and Atikpo and Ihimekpen (2018), anthropogenic activities can cause a surge in heavy metals pollution in the soil. Similarly, the low soil lead concentration recorded at the far North-Eastern region of the study area could be attributed to the presence of dense natural vegetation; which acts as a phytoremediation agent. According to Akpokodje and Uguru (2019) and Palmroth *et al.* (2006), green plant helps to reduce the heavy metals and other toxic materials concentrations in the soil, by removing, containing and detoxifying the contaminants in the soil.

The findings of this research work will be helpful in planning frameworks for agricultural and constructional activities. Hani *et al.* (2014) reported that spatial locations and source capturing of soil heavy metals are essential for the identification of pollution hot-spot zones, and the assessment of potential pollutants generators in geotechnical related soil attributes.

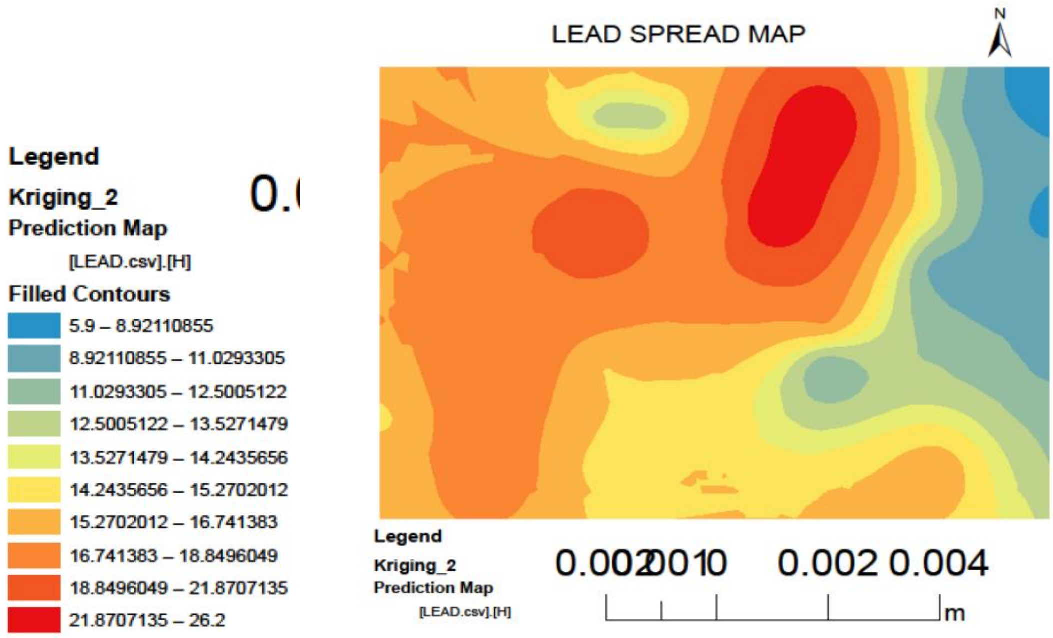

Figure 4. Prediction map of spatial variability of lead in the top soil.

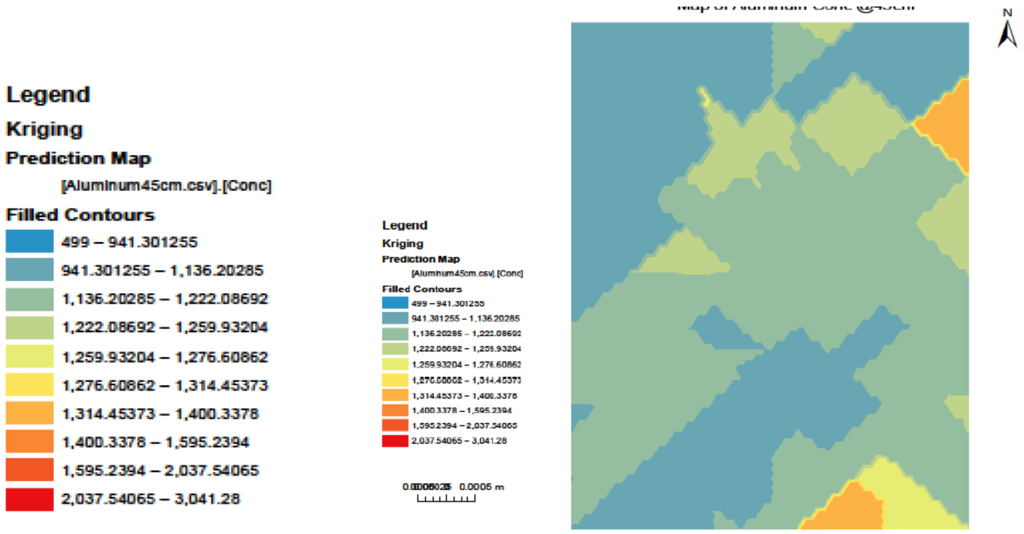

Figure 5. Prediction map of spatial variability of Aluminum in the top soil.

CONCLUSION

This study investigated the lead and aluminum concentrations in the topsoil, across a section of Ozoro community of Delta State, Nigeria. Twenty-five topsoil samples (0-30 cm depth) were collected at specified grid points. The lead and aluminum concentrations of the soil samples were determined in accordance to approved procedures. Generally, the study findings depicted that the lead concentration was lower than the aluminum concentration in the soil. Also, the findings of the study revealed that the lead and aluminum concentrations varied non-uniformly across the study area. Lead concentrations ranged from 5.92 mg kg^{-1} to 26.2 mg kg^{-1}; while the aluminum concentration ranged from 499 mg kg^{-1} to 1840 mg kg^{-1}. The study further revealed that the north-central region had the highest lead concentration; while the north-eastern and south-eastern parts were hot-spots of aluminum accumulation. Findings obtained from this study will be useful for agricultural and geotechnical purposes.

DECLARATION OF COMPETING INTEREST

The authors declare that they have no conflict of interest.

CREDIT AUTHORSHIP CONTRIBUTION STATEMENT

The authors declared that the following contributions are correct.
Hilary Uguru: Designed the research
Ovie Isaac Akpokodje: Edited the manuscript.
Goodnews Goodman Agbi: Write the original draft.

REFERENCES

Agbi GG, Akpokodje OI and Uguru H (2021). Evaluating the impact of traffic activities on the heavy metals concentrations along a major highway in Delta State, Nigeria. *Direct Research Journal of Public Health and Environmental Technology, 6: 45-51.*

Akpokodje OI and Uguru H (2019). Phytoremediation of petroleum products contaminated soil. *Archives of Current Research International, 18(1): 1-8.*

Akpomrere OR and Uguru H (2020). Uptake of heavy metals by native plants growing around an abandon crude oil refining site in southern Nigeria: A case study of African stargrass. *Direct Research Journal of Public Health and Environmental Technology. 5(2): 19-27.*

Akpokodje OI and Uguru H (2019). Bioremediation of hydrocarbon contaminated soil: assessment of compost manure and organic soap. *Transactions on Machine Learning and Artificial Intelligence, 7(5): 13-23.*

Alloway BJ (1990). Heavy Metals in soils. *Blackie Glasgow*, UK.

AOAC (2019). Official Methods of Analysis of AOAC INTERNATIONAL, 21st Edition. Association Official Analytical Chemists, Washington, DC., USA.

Atikpo E and Ihimekpen NI (2018). Spatial distribution of lead In Amaonye forest Soils of Ishiagu communities In Ebonyi State of Nigeria. *Nigerian Journal of Technology (NIJOTECH), 37(4): 1120-1127.*

Barceló J and Poschenrieder C (2002). Fast root growth responses, root exudates and internal detoxification as clues to the mechanisms of aluminum toxicity and resistance. *Environmental and Experimental Botany, 48:75–92.*

Begun A, Ramaiah M, Harikrishna O, Irfanulla K and Veena K (2009). Analysis of Heavy Metal Concentrations in Soil and Litchen from Various Localities of Hosur Road, Bangalore, India. *CODEN ECJHAO, E-A Journal of Chemistry, 6(1): 13-22.*

Burgos P, Madejon E, Perez-de-Mora A and Cabrera F (2006). Spatial variability of the chemical characteristics of a trace element contaminated soil before and after remediation. *Geoderma, 130: 157-175.*

Cemek B, Güler M, KiliÇ K, Demir Y, Arslan H (2007). Assessment of spatial variability in some soil properties as related to soil salinity and alkalinity in Bafra plain in northern Turkey. *Environmental Monitory and Assessment, 124: 223-234.*

Chibuike GU and Obiora SC (2014). Heavy metal polluted soils: Effect on plants and bioremediation methods. *Applied and Environmental Soil Science Volume 2014, Article ID 752708, 12 pages.*

Eboibi O, Akpokodje OI and Uguru H (2018). Growth performance of five bean (*Phaseolus* spp) varieties as influenced by organic amendment. *Journal of Applied Sciences & Environmental Management, 22: 759-763.*

EPA (2020). Lead in Soil. Available online at: https://www.epa.gov/sites/default/files/2020-10/documents/lead-in-soil-aug2020.pdf (June, 2021)

Friedlov´a M (2010). The influence of heavy metals on soil biological and chemical properties. *Soil and Water Research, 5(1): 21-27.*

Giller KE, Witter E and Mcgrath SP (1998). Toxicity of heavy metals to microorganisms and microbial processes in agricultural soils. *Soil Biology and Biochemistry, 30(10-11): 1389–1414.*

Hani A, Sinaei N and Gholami A (2014). Spatial variability of heavy metals in the soils of ahwaz using geostatistical methods. *International Journal of Environmental Science and Development, 5(3):294-298.*

Hua S, Juan L, Xiaojun M (2012). Heavy metals spatial distribution characteristics in a copper mining area of Zhejiang province. *Journal of Geographic Information System, 4: 46-54.*

Jafer HM, Mahdi BO, Majeed ZH and Jawad IT (2021). The Effect of local waste aluminium material on the geotechnical properties of soft soil. *International Journal Of Engineering Research & Technology (IJERT). 10(6): 437-441.*

Kidd PS and Proctor J (2001). Why plants grow poorly on very acid soils: are ecologists missing the obvious? *Journal of Experimental Botany, 52: 791-799.*

Marques APGC, Rangel AOSS and Castro PML (2009). Remediation of heavy metal contaminated soils: phytoremediation as a potentially promising clean-up technology. *Critical Reviews in Environmental Science and Technology, 39(8):622-654.*

Naveen BP, Sumalatha J and Malik RK (2018). A study on contamination of ground and surface water bodies by leachate leakage from a landfll in Bangalore, India. *International Journal of Geo-Engineering, 9(1):1-20.*

Nas FS and Ali M (2018). The effect of lead on plants in terms of growing and biochemical parameters: a review. *MOJ Ecology & Environmental Sciences, (4):265–268.*

Negahdar A, Shabanian M and NikGhalbPour M (2017). The effect of heavy metal contaminants on the shear strength parameters of sandy clay. *Amirkabir Journal of Civil Engineering, 50(5): 263-266.*

Ogbaran N and Uguru H (2021a). Assessment of Groundwater Quality Around an Active Dumpsite using Pollution Index. *Civil Enginering Research Journal 11(3): 1-8.*

Ogbaran AN and Uguru H (2021b). Evaluating the contamination degree and risk assessment of heavy metals around active dumpsite environment: A case study of Ozoro Community, Delta State, Nigeria. *Physical Science International Journal, 25(1): 39-51.*

Ohadi V, Amiri M and Ohadi M (2015). Micro-structural evaluation of lead heavy metal retention in stabilization and solidification with bentonite and cement. *The Journal of Engineering Geology, 9(1):2575–2592.*

Palmroth MRT, Koskinen PEP, Pichtel J, Vaajasaari K, Joutti A, Tuhkanen AT and Puhakka AJ (2006). Field-scale assessment of phytotreatment of soil contaminated with weathered hydrocarbons and heavy metals. *Journal of Soil and Sediments, 6(3): 128-136.*

Panda SK, Baluska F and Matsumoto H (2009). Aluminum stress signaling in plants. *Plant Signaling & Behavior, 4(7): 592–597.*

Rakesh Sharma MS and Raju NS (2013). Correlation of heavy metal contamination with soil properties of industrial areas of Mysore, Karnataka, India by cluster analysis. *International Research Journal of Environment Sciences, 2(10): 22–27.*

Sivaguru M and Horst WJ (1998). The distal part of the transition zone is the most aluminum-sensitive apical root zone of maize. *Plant Physiology, 116:155-163.*

Sobhanardakani S, Tayebi L and Farmany A (2011). Toxic metal (Pb, Hg, and As) contamination of muscle, gill and liver tissues of *Otolithes ruber*, *Pampus argenteus*, *Parastromateus niger*, *Scomberomorus commerson* and *Onchorynchus mykiss*. *World Applied Sciences Journal, 14(10): 1453-1456.*

Stirbescu RM, Radulescu C, Stihi C, Dulama ID, Chelarescu ED, Bucurica IA and Pehoiu G (2018). Spatial distribution of heavy metals in urban soils. *Romanian Reports in Physics, 1-15.*

Turek A, Wieczorek K and Wolf WM (2019). Digestion procedure and determination of heavy metals in sewage sludge— An analytical problem. *Sustainability, 11: 1-10.*

Wang WX and Rainbow PS (2008) Comparative approaches to understand metal bioaccumulation in aquatic animals. Comparative Biochemistry and Physiology. *Toxicology and Pharmacology, 148(4): 315-323.*

WHO (1996). Permissible limits of heavy metals in soil and plants (Geneva: World Health Organization), Switzerland.

Turkish Journal of Agricultural Engineering Research

https://dergipark.org.tr/en/pub/turkager
https://doi.org/10.46592/turkager.2021.v02i02.018

Turk J Agr Eng Res (TURKAGER)
ISSN: 2717-8420
2021, 2(2), 460-471

Research Article

Thermal Properties of New developed Nigerian Illa and Ekpoma Rice Flour Varieties as Effected with Moisture Content

Omenogor IKOKO[a] **Patrick Ejike IDE**[b*]

[a]Departmet of Agricultural and Bioenvironmental Engineering, Delta State Polytechnic Ogwashi Uku, Delta State, NIGERIA

*[b]*Department of Agricultural and Bioresource Engineering, Enugu State University of Science and Technology, Enugu State, NIGERIA*

(*): Corresponding author, Patrick.ide@esut.edu.ng

ABSTRACT

Thermal parameters of food flour moisture content and temperature give an insight in the development and prediction of models that meet the needs of process design models, it also determine the thermal load of a particular product during handling. The bulk density (ρ), thermal conductivity (k), specific-heat capacity (Cp) and diffusivity (α) of Illa and Ekpoma rice flour were studied at varied (MC) moisture content (%) level. The results showed significance in thermal properties values at the different MC levels. The MC increased from 10.56 to 18.50%, increased the specific heat capacity (Cp) from 5.72 to 48.61kJ kg^{-1} °C^{-1} and 6.84 to 29.41 kJ kg^{-1} °C^{-1} for Illa and Ekpoma rice variety respectively and thermal conductivity(k) from 0.03 to 1.56 W/m^0C and 0.03 to 0.38 W m^{-1} °C^{-1} for Illa and Ekpoma rice flour samples. Thermal diffusivity(α) and bulk density (ρ) of the processed Illa and Ekpoma rice flour samples decreased across the MC range of 10.56 to 18.50% (d.b). Thermal diffusivity(α) decreased from 4.38 to 1.25 x 10^{-4} m^2 s^{-1} and 3.42 to 1.30 x 10^{-4} m^2 s^{-1} for Illa and Ekpoma rice flour respectively while the values of bulk density (ρ) decreased from 697.72 to 676.34 kg m^{-3} and 687.49 to 664.26 kg m^{-3} for Illa and Ekpoma rice flour respectively.The developed model equations can be applied in estimation of thermal parameters of rice flour. Finally, Ekpoma and Illa rice flour sample displayed good thermal characteristics and it can be used as an alternative to imported wheat flour.
.

RESEARCH ARTICLE

Received: 04.09.2021
Accepted: 10.12.2021

Keywords:

- Thermal property,
- Moisture content,
- Rice varieties,
- Temperature,
- Rice flour

To cite: Ikoko O, Ide PE (2021). Thermal Properties of New Developed Nigerian Illa and Ekpoma Rice Flour Varieties as Effected with Moisture Content. Turkish Journal of Agricultural Engineering Research (TURKAGER), 2(2), 460-471.
https://doi.org/10.46592/turkager.2021.v02i02.018

INTRODUCTION

Rice is the most food crop in the world with higher demand that feeds almost more than half of the world population (Pokhrel *et al.*, 2020; Danbaba *et al.*, 2019; Singh *et al.*, 2005). It is the second most beneficial cereal crop after wheat mostly in Nigeria that is cultivated throughout the world (Oko *et al.*, 2012). It belongs to the family of Poaceae and its origin was traced via ancient civilization native in Southeast Asia (Pokhrel *et al.*, 2020). Pokhrel *et al.* (2020) and Bandumula, (2018), reported that ninety percent (90%) consumed rice in Asia and eleven Asian countries contributed globally, 87% rice production in the world, while Nigeria is the number one importer in African and third importer in the whole world (Sowunmi *et al.*, 2014). Rice after proper cooking is consumed and it contains about 40% to 80% of the calorie intake (Thomas *et al.*, 2013). The rice landrace has played important role in livelihood and food security of the populace as it serves as food (Pokhrel *et al.*, 2020; Bhat and Riar, 2017). The rice breed has diverse agro-morphological properties, and some of the breeds do very well in terms of yield (Sharma *et al.*, 2020). According to Pokhrel *et al.* (2020), the traditional landraces have been adopted as a result of their higher nutritional value than the hybrid and also have been used medically for treatments of some different diseases like diarrhoea, vocal clarity, vomiting, fever improve eyesight, haemorrhage, burns, infertility (Pokhrel *et al.*, 2020). With ever growing population in Nigeria, the demand and consumption of rice equally expected to increase.

The rice consumption rate in Nigeria have been estimated to 40kg rice per capita and it will continue to rise as long as the population rises (Adekoyeni *et al.*, 2018; Asiru *et al.*, 2018; Maji *et al.*, 2017; Nahemiah *et al.*, 2004). Among the 4.6million hectares of land readily available for cultivation, only 1.7 million hectares are utilized (GAIN, 2016 and Nwachukwu *et al.*, 2018). In 2016, globally, rice demand was approximately estimated to be 6.3 million metric tons while the short change in local supply was estimated to be 2.3 million metric tons (FMARD, 2016; Asiru *et al.*, 2018). The unsupplied 4 million metric tons were expected to be supplied by rice importation (Asuming-Brempong and Osei-Asare, 2007). The importation of rice (foreign) has caused a profuse effect on Nigeria's economy as it caused a severe danger in foreign exchange earnings and it also reduces nations' foreign reserve (Asiru *et al.*, 2018). As a result of all forgoing, there is a need to increase the landrace of rice with mind of improving quality and reducing the shortfall in rice and its based products supply.

This research work tends to in determination of the thermal properties of Illa and Ekpoma rice flour which will in due cause facilitate the thermal processing of the rice varieties. According to Mahapatra *et al.*, (2011) and Jica (2013) thermal treatments like drying, pasteurization, parboiling, cooling, sterilization, thawing, cooking are regularly in food handling and processing (Heldman, 2001). The information on thermal properties of agricultural materials like flour are vital for designing updated handling and storage systems (Lan *et al.*, 2000; Qi *et al.*, 2000; Kim *et al.*, 2003). The specific data of thermal properties of biomaterials are needed for both already existing food and newly developed products with their processes. In terms of processing and storage, thermal properties effects sensory and nutritional quality of food products. (Kamath *et al.*, 1994; Muramatsu *et al.*, 2005; Bozikova, 2003, Ide *et al.*, 2020). Despite that, thermal properties of rough rice have been reported in literatures, but the rice flour has limited literature to date. The growing demand for imported rice and high import demand have catalyzed the interest in the development of domestic rice varieties. Nigeria is the highest importer of rice in Africa, and the second highest in the World. Rice imports in Nigeria have represented a good proportion of total food imports overtime and there exists a threat to the Nigerian economy due to large volume of milled rice imports into Nigeria, with an import bill currently exceeding US$2 billion (Thomas *et al.*, 2013; Premium Time, 2017).

As a result of high demand for processed flour by food processors and industries. It is important to study their behavior of Illa and Ekpoma rice under different heat treatments. Therefore, the objectives of this research work was to investigate some thermal parameters of Illa and Ekpoma rice flour at different moisture content, and temperature using standard method.

MATERIALS and METHOD

Source of samples

Ekpoma rice was sourced from a local farm located Esan West, Local Government Area of Edo State while Illah rice was sourced from a local farm located in Oshimili North Local Government Area of Delta State both in Nigerian. Delta and Edo States are South-South part of Southern States in Nigeria. Delta State located within Latitude of 6.2059^{0}N and langitude of 6.6959^{0}E while Edo State is located 5.60^{0}N latitude and 6.32^{0}E longitude. Edo and Delta State are in tropical equatorial climate with mean annual temperature of 32.8^{0}C and annual rainfall ammount of 2673.8mm.

Preparation of the sample

The method reported by Jideani (2005) was used to prepare the rice sample into rice flour. The rice grains (1 kg) of Ekpoma and Illah rice species were selected and properly washed using warm distilled water at (65°C) water to remove unwanted materials attached on them from point of source capable of influencing the results. The partly processed samples were oven-dried (Multipurpose oven, with Model number OKH-HX-1A China) at 24 h for 50°C milled and sieved using locally fabricated attrition mill and sieved through 200 µm size respectively in order to obtain fine rice flour. The flour samples were further processed to three different moisture level 18.5, 12.50 and 10.56% (db), thereafter stored in a sealed plastic with appropriate labels and carried to the lab where the experiment was conducted.

Determination of the specific heat of rice flour

After the caloric values has been generated using bomb calorimeter, the specific heat capacity of rice flour was calculated using the method and equations reported by Association of Official Agricultural Chemists AOAC (2000) and Ide *et al.* (2020) on persimmon and horse-eye bean flour respectively.

$$Energy\ Content\ = \frac{E\Delta T - 2.3B - V}{g}\left(\frac{KJ}{kg}\right) \quad (1)$$

Where;

$E = Energy\ equivalent\ of\ the\ calorimeter = 13039$

$\Delta T = Temperature\ rise$

$B = Length\ of\ burnt\ wire$

$V = Titration\ volume$

$g = Weight\ of\ the\ sample$

Determination of the thermal conductivity of the rice flour

The thermal conductivity of rice flour was determined using the line heat source probe approach method on non-stable state heat conduction with equation reported by Ide *et al.* (2020); Bart-Plange *et al.* (2009); Mortaza *et al.* (2008); Sahin and Sumnu (2006).

$$K = \frac{Q}{4\pi\Delta T} \quad (2)$$

Where;

$K = Thermal\ conductivty$ ($Wm^{-1}\ {}^{0}C^{-1}$)

$Q = Power\ rating\ of\ the\ calorimeter\ (J)$

$\Delta T = Change\ in\ temperature\ (k)$

Determination of thermal diffussivity of the rice flour.

The thermal diffusivity (α) of the rice flour samples were determined by adopting bulk density, specific heat capacity and thermal conductivity values of the rice flour. The equation reported by Ide *et al.* (2020); Bart *et al.*, (2009) on determination of thermal parameters of Horse-eye bean and maize and cowpea flour respectively was used to calculate thermal diffusivity of rice flour.

$$\alpha = \frac{K}{\rho_b\, c_P} \quad (3)$$

Where;

$\propto = thermal\ diffusivity$ ($m^2\ s^{-1}$)

$k = thermal\ conductivity$ ($Wm^{-1}\ {}^{0}C^{-1}$)

$\rho b = bulk\ density$ ($kg\ m^{-3}$)

$Cp = specific\ heat\ capacvity\ (J/K(KG))$

Determination of the moisture content of rice flour

This is the quality of water contains in the sample. The experiment was conducted under the influence of three (3) different moisture contents 10.56%, 12.50%, and 18.5% under wet base. The method reported by Ide *et al.* (2019) on effect of moisture content on the thermal properties of Horse-Eye Bean was adopted in determining the moisture content of the samples. The hydrated samples and the moisture content of the samples were measured using determined weight of wet sample and weight of dried sample using the following equation reported by Ide *et al.* (2019).

$$Mc = \frac{Ww - WD}{WD}\ x\ 100\% \quad (4)$$

Where;

Mc = moisture content, %; Ww = wet samples; and WD = dried samples.

Determination of the bulk density of rice flour

The method described by Sadiku and Bamgboye (2014) was used to determine the bulk density of the rice flour at various conditions.

$$p_b = \frac{M_s}{V_s} \quad (5)$$

Where;
$\rho b = bulk\ density\ of\ the\ rice\ flour$ (kg m^{-3})
$Vs = volume\ of\ the\ rice\ flour$ (m^3)
$Ms = mass\ of\ the\ flour\ sample\ (kg)$

Analysis of Variance

The data generated from this research work were subjected to analysis of variance (ANOVA), with the means compared by Duncan's test at 5% of significance. All results were expressed as the mean value standard error (SE). Statistical analyses were performed using SPSS for Windows 8.0 SAS 1988 version. The best fit regression equations were generated using excel world application package

RESULTS and DISCUSSION

The summary of results of the determined thermal parameters of Illa and Ekpoma rice flour are presented in the Table 1.

Table 1. Effect of moisture content on the thermal properties of milled rice flour at temperature range of 50 to 350˚C.

Samples	Moisture content (%)	Bulk density (BD) kg m^{-3}	Specific heat Capacity (kJ kg^{-1} ^{0}C^{-1})	Thermal conductivity (W m^{-1} ^{0}C^{-1})	Thermal diffusivity (x10^{-4} m^2 s^{-1})
ILLA	18.50	676.34(1.05)	48.61(2.-5)	1.56(2.04)	1.25(3.08)
	12.50	692.67(3.05)	7.34(1.07)	0.069(3.23)	1.57(3.05)
	10.56	697.72(3.24)	5.72(3.06)	0.036(0.95)	4.38(2.03)
Mean value	***13.85***	***688.91***	***20.55***	***0.55***	***2.40***
EKPOMA	18.50	664.26(1.32)	29.41(0.45)	0.386(0.93)	1.305(3.05)
	12.50	681.29(3.90)	9.31(2.04)	0.068(2.04)	1.488(1.23)
	10.56	687.49(3.01)	6.84(2.06)	0.033(3.12)	3.428(0.33)
Mean value	***13.85***	***677.68***	***15.18***	***0.15***	***2.06***

The values in brackets are the standard deviation of the replicated data.

The bulk density of processed Illa and Ekpoma rice flour samples presented in Figure 1 showed that the bulk density of Illa and Ekpoma rice flour sample were 697.72, 692.67 and 676.34 kg m^{-3} for Illa rice flour and 687.49, 681.29, 664.26 kg m^{-3} for Ekpoma rice samples at MC range of 10.56, 12.50 and 18.50% respectively. It was observed that, the increase in MC from 10.56 to 18.50% of rice flour samples decreased the bulk densities of both Illa and Ekpoma rice flour from 697.72 to 676.43 kg m^{-3} and 687.49 to 664.26 kg m^{-3} respectively (Anita *et al.*, 2019; Mahapatra *et al.*, 2011).

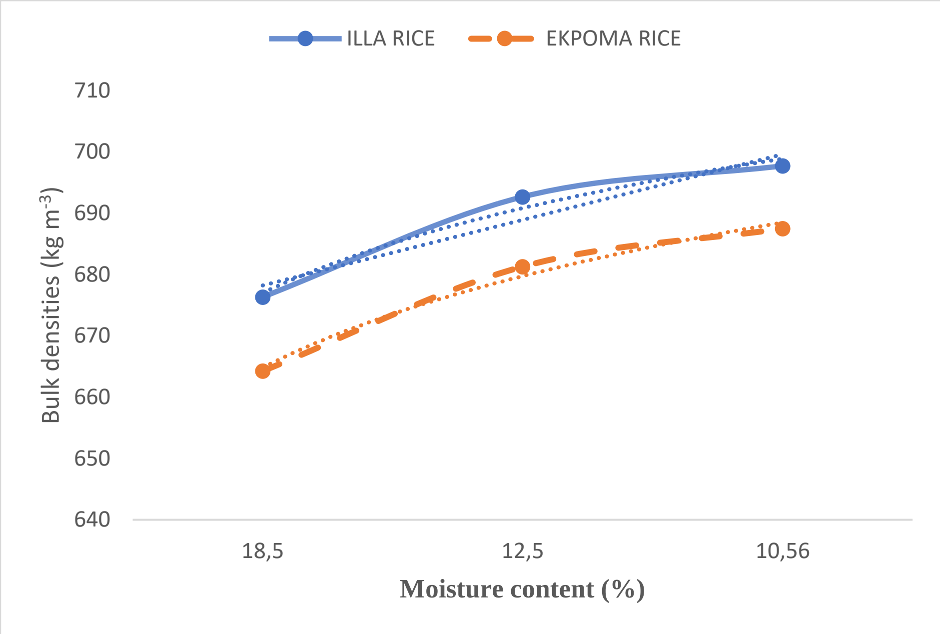

Figure 1. Moisture content effect on the bulk density of Milled ILLA and EKPOMA rice flour.

The observed different in bulk density and varieties were significant in MC ($p < 0.05$). This finding could be attributed to the fact that bulk density of the flour sample depends on thermal diffusivity. Bulk density effects both packing and transportation of food materials, the Illa rice flour sample with higher bulk density at 10.56% moisture content are known to exhibit better packaging factor and transportation advantages than those with low bulk density, based on this fact as the moisture content decreases the packing factor and transportation advantages increases *(*Arinola and Jeje, 2017*).* The relationship that existed between the bulk density and moisture content were best described in the following Equations (6) and (7).

$$BD = 19.902 \ln(MC) + 677.02T \quad R^2 = 0.9789 \tag{6}$$
$$BD = 21.514 \ln(MC) + 664.83T \quad R^2 = 0.9873 \tag{7}$$

for Illa and Ekpoma rice flour respectively. The trend of the bulk density graph of both sample exhibited logarithmic trend of best fit modelling equation on the effect of MC on the bulk density of processed rice flour samples (Table 2).

Table 2. Relationships of thermal properties with rice varieties, moisture content and temperature.

Thermal properties	Illa rice	R^2	Ekpoma rice	R^2
Bulk density (kg m^{-3})	$BD = 19.902\ln(MC) + 677.02T$	0.9789	$BD = 21.514\ln(MC) + 664.83T$	0.9873
Specific heat capacity (kJ kg^{-3} °C^{-1})	$Cp = 42.685(MC)^{-2.032T}$	0.9305	$Cp = 27.827(mc)^{-1.363T}$	0.9708
Thermal conductivity (W m^{-1}°C^{-1})	$K = 1.3421(MC)^{-3.694T}$	0.9706	$K = 0.3693(MC)^{-2.33T}$	0.9973
Thermal diffusivity (x10^{-4} m^2 s^{-1})	$\alpha = 4.1394(MC)^{-1.178T}$	0.9597	$\alpha = 3.2422(MC)^{-0.915T}$	0.9415

BD=Bulk density, *Cp*= specific heat capacity, *k*= thermal conductivity, *α*=thermal diffusivity, R^2 = R squared value.

The specific heat capacity of agricultural flour determines the quantity of thermal energy a unit of the food flour retains at every unite increase in temperature (Sandra and Bernarda 2015). It is basically important in thermal analysis of packaged food products. From the table and figure 1, it was observed that specific-heat capacity was measured with respect to changes in moisture content and temperature. It was noticed that specific-heat-capacity of the rice flour samples showed that Illa rice flour samples increased from 5.72, 7.34 and 48.61 kJ kg^{-3} ˚C^{-1} while Ekpoma rice flour samples increased from 6.84, 9.31 and 29.41 kJ kg^{-3} ˚C^{-1} as MC increased from 10.56, 12.50 and 18.50%, respectively.

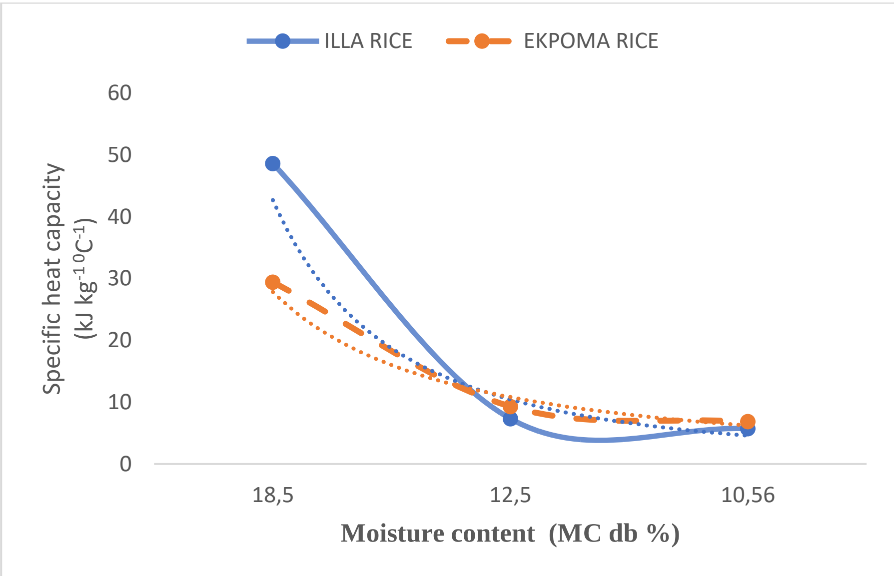

Figure 2. Moisture content effect on the specific heat capacity of Milled ILLA and EKPOMA rice flour.

The observed moisture content increase of the samples showed that, the moisture content and specific heat capacity varied significantly at ($p>0.005$) interval and this in line with the report of Anita *et al.* (2019) and Akbari and Chayjan (2017) reported on the effect of dry basis moisture content (MC) on African Walnut and persimmon for modelling of thermal properties of the samples. The relationship that existed between Cp (specific heat capacity) of the rice flour varieties as it was influenced by dry basis MC and heating temperature was stated via the quadratic regression equation with their *R* squared values as a drying constant as $Cp= 42.685(MC)^{-2.032T}$ R^2 = 0.9305 and $Cp = 27.827(mc)^{-1.363T}$ R^2 = 0.9708 (Table 2) for Illa and Ekpoma rice flour samples respectively. Almost in all cases, there was no relationship in the specific heat values of two rice varieties, the specific heat increased with increase in both moisture and temperature (Azadbakht *et al.*, 2013) and this is in line with Shrivastava and Datta (1999) and Singh and Goswami (2000) reported on thermal properties of mushrooms and cumin-seed revealed that the moisture content when correlate with the temperature it had a highly valid significant effect on Cp tested. The thermal conductivity of the processed rice flour samples was presented in the Figure 3.

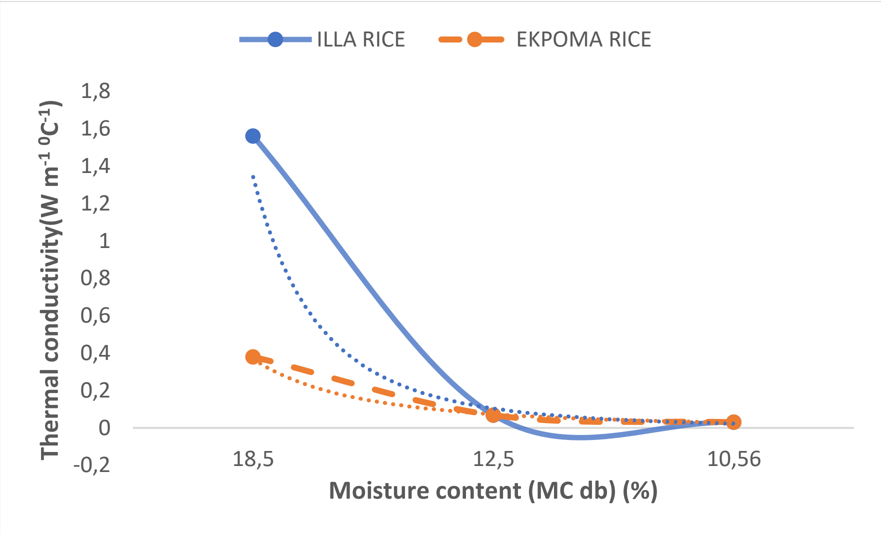

Figure 3. Moisture content and thermal conductivity relationship of Milled ILLA and EKPOMA rice flour.

The thermal conductivity of a food material measures the magnitude of thermal energy that transferred during thermal processing of the food material (Sandra and Bernarda, 2015). Thermal conductivity of both samples species was observed to be varied as moisture content (MC) increases. The corresponding increase in MC from 10.56 to 1.50% (db) caused the thermal conductivity (k) of the Illa and Ekpoma rice flour samples to be noticeably-increased from 0.036 to 1.56 W m^{-1} $^{0}C^{-1}$ and 0.03 to 0.38 W m^{-1} $^{\circ}C^{-1}$ at MC range of 10.56 to 18.50% respectively. It implies that thermal conductivity (k) determined at three (MC) level were differently significant at ($p < 0.05$). This increase in thermal conductivity of rice flour with increase in MC is due to magnitude of heat transferred in the flour and this is preferred when the sample is wet than when it is dried (Jibril *et al.*, 2016). The relationship of thermal conductivity of rice flour varieties and its moisture content is best expressed in the equations below, $K = 1.3421(MC)^{-3.694T}$ R^2 = 0.9706 and $K = 0.3693(MC)^{-2.33T}$ R^2 = 0.9973 for Illa and Ekpoma rice flour respectively (Table 2). This is very similar with what Aviara and Haque *(2001)* on thermal-properties of Guna seed and Mahapatra *et al.* (2013) on thermal-properties of Cowpea flour.

The thermal diffusivity of Illa and Ekpoma rice flour were presented Figure 4, showed that the thermal diffusivity of Ekpoma were 1.30, 1.48 and 3.42 x10^{-4} m^2 s^{-1} and for Illa were1.25, 1.57 and 4.38 x10^{-4} $m^2 s^{-1}$ at moisture content range of 18.50, 12.50 and 10.56%, respectively.

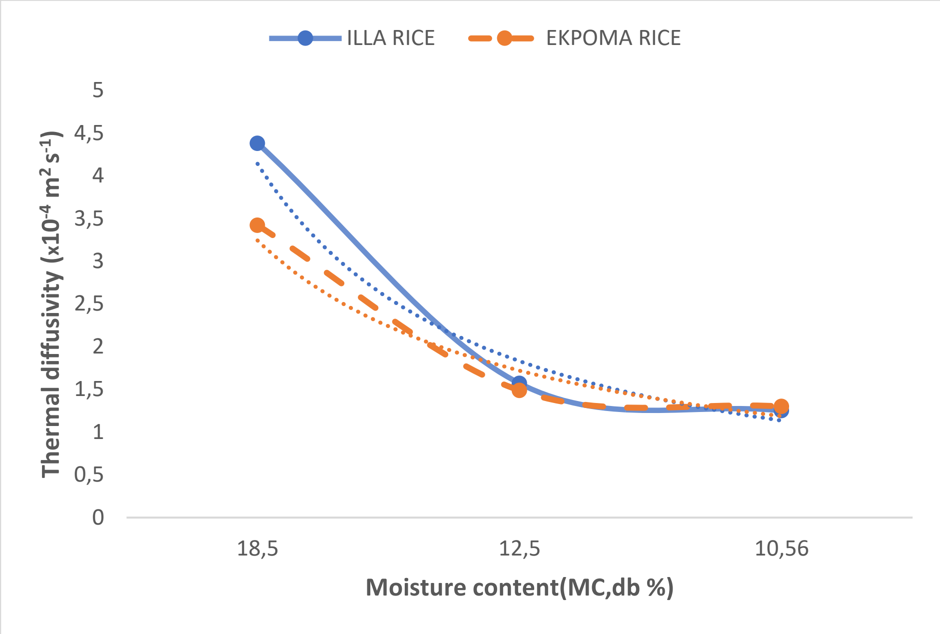

Figure 3. Moisture content effect on thermal diffusivity of Milled ILLA and EKPOMA rice flour.

It was observed that, the MC of rice flour- showed decreased in the thermal diffusivity of the processed samples. Thermal diffusivity reveals the extent at which food material retain heat either under storage or during thermal processing, it was therefore indicated that the Illa rice flour sample displayed higher rate of heat energy circulation among the particles of the flour than the Ekpoma rice flour. This is because the Illa rice flour recorded higher thermal diffusivity value of 4.38 x 10^{-4} $m^2 s^{-1}$ at 10.56% (db) moisture content and have the tendency of retaining much heat than Ekpoma rice sample. The findings were not similar with what Opoku *et al.* (2006) reported on hay timothy, where increase in moisture in the range of 7.7% to 17.1% will cause increase in their thermal properties (thermal conductivity and diffusivity) from 0.284 to 0.0605 W m^{-1} °C^{-1} and 1.024 to 3.031×10-7 m^2 s^{-1}. The observed different in MC and thermal diffusivity were validly significant ($p < 0.05$). This is attributed to the fact that thermal diffusivity of the flour sample depends on bulk density of food samples as they decreased with increase in moisture content. The relationship between the thermal diffusivity and MC was best described in the following equations below $\alpha = 4.1394(MC)^{-1.178T}$ $R^2 = 0.9597$ and $\alpha = 3.2422(MC)^{-0.915T}$ $R^2 = 0.9415$ for Illa and Ekpoma rice flour samples respectively (Table 2).

CONCLUSION

The thermal parameters of rice flour of Illa and Ekpoma rice varieties were determined at different moisture levels. The research results showed that the validly significant variation in thermal parameters values were varied per respect to different moisture content levels. The observed increase in MC from 10.56 to 18.50 %, had same correspond increased the specific heat capacity from 5.72 to 48.61 kJ kg^{-3} °C^{-1} and 6.84 to

29.41 kJ kg^{-3} $^{\circ}$C^{-1} for Illa and Ekpoma rice variety respectively and thermal conductivity from 0.03 to 1.56 W m^{-1} ^{0}C^{-1} and 0.03 to 0.38 W m^{-1} ^{0}C^{-1} for Illa and Ekpoma rice flour samples. Thermal diffusivity and bulk density of the processed Illa and Ekpoma rice flour samples decreased across the MC range of 10.56 to 18.50% (db). Thermal diffusivity decreased from 4.38 to 1.25 x10^{-4} m^{2} s^{-1} and 3.42 to 1.30 x10^{-4} m^{2} s^{-1} for Illa and Ekpoma rice flour respectively while the bulk density also decreased from 697.72 to 676.34 kg m^{-3} and 687.49 to 664.26 kg m^{-3} for Illa and Ekpoma rice flour, respectively. The developed model equations from the Figure 1 to Figure 4 can be applied in the estimation the thermal processing parameters of rice flour around the range treatments.

REFERENCES

Adekoyeni OO, Fagbemi SA and Ismaila AR (2018). Ofada rice identity, physical qualities and processing technology options for upgrading:A review. *Annual Research & Review in Biology 23(2): 1-9. Article no. ARRB.38938*

Akbari S and Chayjan RA (2017): Moisture content modelling of thermal properties of persimmon (cv. 'Kaki'). *Research Agricultural Engineering, 63: 71-78.*

Anita C, Ezeagba, Ike S. Oluka and Ejike PI (2019). Effect of moisture content and drying methods on the thermal properties of African walnut flour. *The Pacific Journal of Science and Technology,* 217.

AOAC (2000). Official Methods of Analysis 16 Ed. Association of Official Analysis Chemist. Washington DC.USA.

Arinola SO and Jeje OA (2017). Drying characteristics and thermalproperties of two local varieties of unripe plantain. *American Journal of Science and Technology, 4(5): 74-79.*

Asiru MA, Agada IG and Kolade O (2018). Impacts of rice importation on Nigeria's economy. *Journal of Scientific Agriculture, 2: 71-75..*

Asuming-Brempong S and Osei-Asare Y (2007). *Has imported rice crowded-out domestic rice production in Ghana? What has been the role of policy?* African Association of Agricultural Economists (AAAE) Conference Proceedings.

Aviara NA and Haque MA (2001). Moisture dependence of thermal properties of shea nut kernel. *Journal of Food Engineering, 47: 109-113.*

Azadbakht M, Khoshtaghaza MH, Ghobadian B and Minaei S (2013). Thermal properties of soybean pod as a function of moisture content and temperature. *American Journal of Food Science and Technology, 1(2): 9-13.*

Bandumula N (2018). Rice production in Asia: Key to global food security. *Proceedings of the National Academy of Sciences, India Section B: Biological Sciences*, *88(4): 1323-1328.*

Bart-Plange A, Asare V and Addo A (2009). Thermal conductivity of maize and cowpea. *Journal of Engineering and Technology, 2(3): 6-11.*

Bhat FM and Riar CS (2017). Physicochemical, cooking, and textural characteristics of grains of different rice (*Oryza sativa* L.) cultivars of temperate region of India and their interrelationships. *Journal of Texture Studies, 48(2): 160-170.*

Božiková M (2003). Thermophysical parameters of corn and wheat flour. *Research in Agricultural Engineering, 49(4): 157-160.*

Danbaba N, Idakwo PY, Kassum AL, Bristone C, Bakare SO, Aliyu U, Kolo IN, Abo ME, Mohammed A, Abdulkadir AN, Nkama I, Badau MH, Kabaraini MA, Shehu H, Abosede AO and Danbaba MK (2019). rice postharvest technology in Nigeria: An overview of current status, constraints and potentials for sustainable development. *Open Access Library Journal, 6: e5509.*
emefiele.html. 2015; accessed 17.04.2017

Federal Ministry of Agriculture and Rural Development (2016). The agriculture promotion policy (2016-2020). Federal Ministry of Agriculture and Rural Development, Abuja, Nigeria.

Global Agricultural Information Network (2016). Nigeria's grain and feed annual report. https://gain fas. usda.gov/Recent%20GAIN%20Publications/Grain%20and%20Feed%20Annual_Lagos_Nigeria_4-21-2016. pdf. 2016; Accessed 22.02.2021.

Heldman DR (2001). Prediction models for thermophysical properties of foods. In food processing operations modeling, design, and analysis; Irudayaraj, J., Ed.; Marcel Dekker, Inc.: *New York*, 2001; 1-24.

Ide PE, Eze PC and Offor BC (2019). Effect of moisture content on the physicomechanical properties of *Mucuna sloanei. International Journal of Scientific Engineering and Research (IJSER), 7(2): 91-96.*

Ide PE, Ike O and Eze PC (2020) Effect of moisture content on the thermal properties of horse-eye bean seeds relevant to its processing. University of Belgrade Faculty of Agriculture Institute of Agricultural Engineering. *Scientific* Journal *Agricultural Engineering, Year XLV No. 4, pp: 71 – 80.*

JICA (2013). Status of NRDS Implementation in Nigeria, Presentation at the Fifth General Meeting of CARD, 5-6 February 2013, Dakar, Senegal. JICA 2013 Status of NRDS Implementation in Nigeria, Presentation at the Fifth General Meeting of CARD, 5-6 February 2013, Dakar, Senegal.

Jibril N, Yadav KC, Binni MI and Kabir MH (2016). Study on effect of moisture content on thermal properties of bambara groundnut (*Vigna subterranea l.* Verdc.) seed. *Report and Opinion, 4(6): 52-58.*

Jideani VA (2005). Characteristics of local pearl millet *(Pennisetum glaucum)* grains. *Nigerian Food Journal, 23(1): 193-204.*

Kamath S, Puri VM and Manbeck HB (1994). Flow property measurement using the Jenike cell for wheat flour at various moisture contents and consolidation times. *Powder Technology, 81: 293-297.*

Kim YS, Flores RA, Chung OK and Bechtel DB (2003). Physical, chemical, and thermal characteristics of wheat flour milling coproducts. *Journal of Food Process Engineering, 26(5): 469-488.*

Lan Y, Fang Q, Kocher M and Hanna MA (2000). Thermal properties of tapioca starch. *International Journal of Food Properties, 3(1): 105-116.*

Mahapatra AK, Lan Y and Harris DL (2011). Influence of moisture content and temperature on thermal conductivity and thermal diffusivity of rice flours. *International Journal of Food Properties, 14(3): 675-683.*

Mahapatra AK, Melton SL and Isang EM (2013). Effect of moisture content on thermal properties of cowpea flours. *Agricultural Engineering International: The CIGR Journal. 15(2): 251-255.*

Maji AT, Ukwungwu MN, Danbaba N, Abo ME and Bakare SO (2017). Rice: History, Research and Development in Nigeria. In: Nahemiah, D., Nkama, I., Maji, A.T. and Ukwungwu, M.N., Eds., Rice in Nigeria, Traditional Recipes & Research Needs, *Ronab Graphix Print*, Bida, Nigeria, 65-84.

Mortaza A, Mohammad HK and Seyed RH (2008). Specific heat and thermal conductivity of berberis fruit (*Berberis vulgaris*). *American Journal of Agricultural and Biological Sciences, 3(1); 330-336.*

Muramatsu Y, Tagawa, A, Kasai, T. (2005). Effective thermal conductivity of rice flour and whole and skim milk powder. *Journal of Food Science*, *70(4): 279-287.*

Nahemiah D, Alabi MO, Nkama I and Abo ME (2004). Utilization of rice and rice by-products in Nigeria. In: Abo, M.E. and Abdullahi, A.S., Eds., Nigerian Rice Memorabilia, *Project Synergy Limited*, Abuja, Nigeria, 343-349.

Nwachukwu IM, Agwu NM and Ezeh CI (2008). *Comparative study of consumer purchase attitude of local and foreign rice in Abia State*. Proceedings of 42nd meeting of Agricultural Society of Nigeria held at Ebonyi State University, Abakaliki, 19-23 October 2008; pp.764-767.

Oko AO, Ubi BE and Dambaba N (2012). Rice cooking quality and physico-chemical characteristics: A comparative analysis of selected local and newly introduced rice varieties in Ebonyi State, Nigeria. *Food and Public Health, 2(1): 43-49.*

Opoku A, Tabil LG, Crerar B and Shaw MD (2006). Thermal conductivity and thermal diffusivity of timothy hay. *Canadian Biosystems Engineering. 48: 31-37.*

Pokhrel A, Dhakal A, Sharma S and Poudel A (2020) Evaluation of physicochemical and cooking characteristics of rice (Oryza sativa L.) landraces of Lamjung and Tanahun districts, Nepal. *Hindawi International Journal of Food Science, Volume 2020, Article ID 1589150, 11 pages.*

Premium Times (2017). Nigeria spends $2.41b on rice importation in 3 y–Emefiele.

Qi F, Lan Y, Kocher MF and Hanna MA (2000). Thermal conductivity of granular rice starches. *International Journal of Food Properties, 3(2): 283-293.*

Sadiku AO and Bamgboye I (2014). Moisture dependent mechanical and thermal properties of Locust bean (*Parkia biglobosa*). *Agricultural Engineering International: CIGR Journal 16(1): 99-106.*

Sahin S and Sumnu SG (2006). Physical properties of foods. *Springer Science Business Media*, LLC., 233 Spring Street, New York, NY 10013.

Sandra Budžaki and Bernarda Šeruga (2015) Specific heat and thermal conductivity of the croatian unleavened dough, *International Journal of Food Properties*, *18:10, 2300-2311.*

SAS (1988). SAS/STAT users guide, release 6.03, SAS institute Inc.,Carey NC.

Sharma S, Pokhrel A, Dhakal A and Poudel A (2020). Agro-morphological characterization of rice (*Oryza sativa* L.) landraces of Lamjung and Tanahun District, Nepal. *Annals of Plant Sciences, 9(2): 3731-3741.*

Shrivastava M and Datta AK (1999). Determination of specific heat and thermal conductivity of mushrooms (*Pleurotus- florida*). *Journal of Food Engineering, 39: 255-260.*

Singh KK and Goswami TK (2000) Thermal properties of cumin seed. *Journal of Food Engineering, 45: 181-187.*

Singh, N, Kaur L, Sodhi NS and Sekhon KS (2005). Physicochemical, cooking and textural properties of milled rice from different Indian rice cultivars. *Food Chemistry, 89(2): 253-259.*

Sowunmi FA, Omigie OC and Daniel DT (2014). Consumers' perception on Ofada rice in Ibadan North Local Government Area of Oyo State, Nigeria. *Journal of Economics and Sustainable Development, 5(16):78.*

Thomas R, Wan-Nadiah WA and Bhat R (2013). Physiochemical properties, proximate composition, and cooking qualities of locally grown and imported rice varieties marketed in Penang, Malaysia. *International Food Research Journal, 20(3): 1345-1351.*

Turkish Journal of Agricultural Engineering Research

https://dergipark.org.tr/en/pub/turkager
https://doi.org/10.46592/turkager.2021.v02i02.019

Turk J Agr Eng Res
(TURKAGER)
e-ISSN: 2717-8420
2021, 2(2): 472-492

Review Article

Mathematical Modeling of Food Processing Operations: A Basic Understanding and Overview

Manibhushan KUMAR[a] **Siddhartha VATSA**[b] **Mitali MADHUMITA**[c] **Pramod Kumar PRABHAKAR**[d*]

[a]*Department of Food Science and Technology, National Institute of Food Technology Entrepreneurship and Management, Kundli, Sonepat, HR, INDIA*

[b]*Department of Agriculture and Environmental Sciences, National Institute of Food Technology Entrepreneurship and Management, Kundli, Sonepat, HR, INDIA*

[c]*Department of Agricultural Engineering, School of Agriculture and Bio-Engineering, Centurion University of Technology and Management, Paralakhemundi, Odisha, INDIA*

[d]*Department of Food Science and Technology, National Institute of Food Technology Entrepreneurship and Management, Kundli, Sonepat, HR, INDIA*

(*): Corresponding author, pkprabhakariitkgp@gmail.com

ABSTRACT

Modeling is the core of food processing supported by many approaches and governed by heat, mass, and momentum transfer equations. The objective of this paper is to mainly discuss and introduce mathematical modeling of some food processes. Food processing is unique from other material processing, as it includes complex multiphase transport and change in material properties during processing. It poses a great challenge in food process engineering. Now a day's, consumers are taking more precautions before eating something. The way of food processing effectively impacts food quality. Most of the conventional industries use thermal processes like pasteurization, sterilization, and freezing. In recent years the main aim has been to improve these conventional processing technologies. Characterization of temperature distribution is done by mathematical modeling during processing, so this review paper aims to introduce mathematical modeling as a potential tool for the food processing industry. The mathematical models discussed in this article captures the essential features of a complex object or process based on a theoretical understanding of the phenomena and available measurements.

RESEARCH ARTICLE

Received: 12.04.2021
Accepted: 09.08.2021

Keywords:

- Simulation,
- Thermodynamic model,
- Retorting,
- Roasting,
- Microbial inactivation,
- Thermal processing

To cite: Kumar M, Vatsa S, Madhumita, Prabhakar P K (2021). Mathematical Modeling of Food Processing Operations: A Basic Understanding and Overview. Turkish Journal of Agricultural Engineering Research (TURKAGER), 2(2): 472-492. *https://doi.org/10.46592/turkager.2021.v02i02.019*

INTRODUCTION

Food processing is a transformation of the raw product into consumer-ready product by introducing several treatments like thermal (pasteurization, sterilization, drying, cooking etc.), mechanical (crushing, churning, or homogenization etc.) or combination (e.g., extrusion), and several other processes. Food materials are quite complex and non-homogeneous in nature. So, food processing is done to transfer raw ingredients into food or transfer food products into another form. Physico-structural properties and transport phenomenon is involved readily in food processing. Food constantly changes whether food is processed or not because it absorbs moisture (when kept in humidified conditions) or loses (when kept in dehumidified conditions or high temperatures). During processing like thermal treatment (pasteurization, sterilization, or cooling process), along with product temperature, other properties like biochemical (colour, flavour, nutrition etc.), physical (shrinkage, texture, bulk density etc.), chemical (denaturation, Maillard reaction, oxidation etc.) also change. Other dependent properties of food like thermal and electrical conductivity, specific heat, effective moisture diffusivity, permeability, and viscosity are a function of moisture content, temperature, and composition. So, during processing, all the properties mentioned above change, and the degree of changes depend on the extent of treatment. So, before processing food, optimization is done to have a more efficient process, with minimum losses. While optimizing any process, there needs to be detailed information about the characteristics and problems of food processing operations. Major food processing problems are covered in the following contexts: (a) While giving a thermal treatment or in a cooling process, the temperature change and biochemical changes like changes in nutrient profile, color, and texture have equal weightage to be understood. (b) When the food has continuous gain (from humid surroundings) or moisture loss (heating especially due to evaporation). (c) The basic properties like density, thermal conductivity, diffusivity, specific heat, permeability etc., are functions of composition, moisture content, and temperature, which keeps on changing, and thus their structure and changing behaviour needs to be understood thoroughly (d) The shrinkage (loss of moisture) or swelling (gain of moisture as a function of changing hygroscopicity can bring continuous changes in the food structure. (e) Irregular spaces are yet another problem. (f) Sometimes, multiple processes like temperature, moisture content, and phase change are often coupled with each other.

The prediction of different models has been developed based on the environmental conditions and the type of treatment offered to the corresponding primary food product. For example, suppose the prediction is done on the basis of microbial growth. In that case, it is extremely important to understand the responses of different microbes to the factors responsible for their growth. Thus, in the case of microbiological context, a model will be a mathematical expression that can integrate the survival, growth, and other biochemical processes under provided conditions (Prabbhakar *et al.*, 2019). Similarly, for other food processes, like evaporation of milk to form skimmed milk powder or let's say conversion of barley into beverage, all will include an expression which will describe the process, considering all parameters in the similar conditions at which the experiment is to be or has been done. As per Balsa-Canto *et al.* (2016), there are six major areas of division of drivers in innovations according to consumers survey, which can be classified as health value, pleasure, safety, ethics, convenience, and physical.

The competitiveness has thus increased many folds due to the increasing consumer demand which has added pressure on the companies to continuously modify with the market change. These goals can be efficiently and effectively achieved by optimization of models and computer-aided simulation. In recent years, several researchers have studied to understand the mechanism of food processing by conducting several experiments and using mathematical models.

Models have a vast scope. The relationships between the input and output processes make any model suitable to analyse the physical processes occurring in food. We term it as "research objective" in modeling. To say, if we consider the modeling of a sterilization process, the input parameter will be steam temperature, and output parameter will be bacterial death; thus, the impact of input on output parameters will be understood. After the revolution came in hardware and software parts and recent emerging computing techniques, the use of the model to design processes, and checking the "what if" situations arose. Hence, taking the above example, one can easily check the effect of the process variable (temperature) on the quality of sterilization undergoing. Future developments for a better change will introduce an optimization software that will bring the complete temperature profile in front of the researcher for best sterilization quality. This further increases the scope of modeling. Thus, the major drivers for advances in modeling are product processes and equipment design. There have been emerging technologies of food processing in today's date, including pulsed electric field, ultrasonic processing, non-ionizing radiations, etc. All these processes are characterized by some features. The research and development team generally have big challenges in front of them during competencies for developing an appropriate modeling approach due to (a) more and more complex food operations, (b) oversimplifying the food engineering phenomenon, and (c) generating compliance to food safety standards.

Along with process development, model modification and development are also taking place. Hence, making a selection of a proper model for a particular process is also important. For example, for understanding heat and mass transfer in drying, frying, baking, cooking, roasting, toasting, etc., selecting a model is important. Most researchers use a diffusion-based or single-phase model for heat and mass transfer for the above-mentioned process. These models are very simplified and do not consider the fundamentals of the physics of food processing (Khan *et al.*, 2018). In contrast to these models, the multiphase model is the best one, as it considers all phases' (liquid water, vapor, air) transport mechanisms separately. So, this model gives a better insight view of the transport mechanism. Mercier *et al.* (2014), Gulati *et al.* (2015), Kumar *et al.* (2016), Gulati *et al.* (2016) used the multiphase model to explain food processing in a more explicit way.

Models have numerous applications in food industries, whether it is logistic, quality, designing, or R&D, costing, energy consumption, processing. Friis *et al.* (2002) have shown CFD as a qualitative tool for designing hygienic process equipment using a 3-D flow model. Using this model, we can know a set of hydrodynamic parameters that play a crucial role in cleaning the closed process system; by using this, we can design complex equipment parts that will be very easy to clean. Current and novel applications of logistic optimization by industries are important and necessary because factors such as perishability, safety, variability, and flat payoff costs, because of its biological nature, the food supply chain is affected by increasing demand, pollution, water availability, and increasing costs and complexity. Modeling and simulation play an important role in scheduling operations, assessing sustainability, reducing waste, designing transportation networks, and planning the infrastructure of food supply chains. (García-Flores *et al.*, 2015), along with this modeling, also plays an important role in total quality management (TQM). Quality costing is the first step for preparing a case for the TQM initiative. Moreover, a realistic estimation of quality costs is an essential element of any TQM initiative. However, very few organizations use this method as it is very costly.

Baking is one of complex food processing where several phenomena occur simultaneously, which is chemical, biochemical, and physical phenomena such as gelatinization and formation of the porous structure. These changes affect the final quality of the product. These qualities also depend on flour type, fermentation time, protein content, and type of additives etc. Mohammadi *et al.*, (2020) has developed a mathematical model to predict crust temperature and weight loss of toast bread at different oven temperatures and time.

Zugarramurdi *et al.* (2007) have developed a mathematical model for the calculation of the costs associated with a specific quality level due to HACCP-based system implementation. The confidence development and validation of models is still a challenge even though there have been endless efforts in building rigorous models and simulation of numerical. In this paper, we will describe how model is formulated, with their actual application in food industries, and show up to what extent models wok like a physical prototype and how it is reconciled with experimental data.

MODELING APPROACH

Model is a mathematical analogue of a physical process. In modeling, different processes are expressed in the form of equations (mathematical) which are based on fundamental physics and have the general form of partial differential equations. Computational way of process simulation is achieved by the solution set of such partial differential equations. Model is generally used for understanding of physical process by using relationship between input and output parameters or used for designing or in checking the 'what if' scenarios, which helps in avoiding laborious and time-consuming experiments. Trystram (2012) has explained the main step necessary for modeling food or food processing. Modeling is widely used as a tool for optimum design, to understand process, prediction, used in different sector-wise innovation like automotive and aerospace industries, while this tool's contribution is unutilized in the food sector. The advantages of modeling as explained by Datta *et al.*, (2007) are many like providing insights into the process deeper as in the case of physics-based models which was not possible while experiments, then reducing the total number of experiments to few, which reduces time and expenses, optimization of processes, the prediction-based working (what if scenarios), automating complete process with control capability.

In modern science, all simple problems are solved easily. What remain problems are complex ones, which cannot be solved by simple experiments and deductions. To understand these problems, we have to decompose them into their constituting processes, and each of these processes has to be studied, analyzed, and modeled separately. In food processing, a mathematical model is used for the approximate representation of processes in mathematical terms. As processes are very complex and difficult to understand, it will be impossible for mathematical models to provide actual representation of a whole process. In formulating a mathematical model as shown in Figure 1, we only consider major input and output; negligible inputs and outputs are not considered. Still, mathematical modeling is an effective tool to evaluate the effect of process parameters on the outcome of certain processes as it is a rapid and expensive method. Mathematical modeling is only done after getting data in tabular or graphical form.

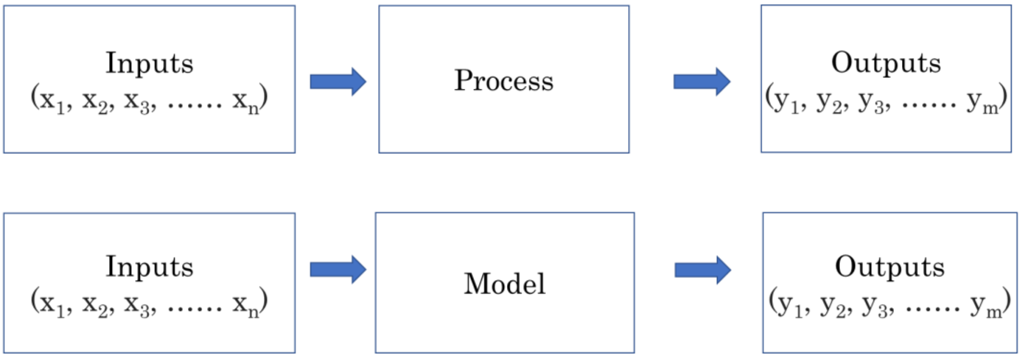

Figure 1. Comparison input/out for process and model.

The knowledge of fundamental physical mechanisms governing processes is a requirement in physical-based mathematical modeling. Integrated knowledge of engineering, chemistry, and microbiology is required to understand the multidisciplinary character of food processing. Erdogdu *et al.* (2017) have mentioned essential steps for mathematical modeling. Mathematical models may be classified into the In-observation model and physical-based models based on the selection of initial points while designing a model. In-observational models have the data from experiments which is the base for developing the model. This type of model is entirely empirical. The empirical model comes from introspection or observation (both). There is usually no theoretical background for them; these models are generally used to classify and characterize data, know generalized behaviour from the given measurements, and learn something from these observations. An empirical model is only applicable within the range of data during the experiment.

In contrast to observational models, the starting point for the physical-based models is universal laws of physics that determine the physics and the related equations. The very fundamental laws, such as Newton's laws of motion, define the models which are based on fundamental physics. These models have been validated against the data set generated during experiments, but the data doesn't exist before the existence of the model itself. Physics-based models are generally overweighed against others in the way that they are more trustable and calculations are more precise (since the initial point is universal conservation laws); also, the parameters can be easily measured with the help of available techniques. Among the various physical models, the most popular are continuum (macroscale) models (Datta, 2008). Many of the models based on observation and physical models are reported by Datta *et al.* (2007). Datta, 2008 has also mentioned that just like in other areas, analytical approaches were the foremost for the start of physics-based models, the first one being the work in sterilization and dehydration. Sterilization was also the base for the start of numerical modeling. Until the late 1980s, the analytical model was used for most of the problems. The mid-1990s became a revolution in the field of modeling of food processing as by then, there were so many improvements in numerical methods assisted with computer technology which was boomed by the introduction of Computational fluid dynamics (CFD) software making modeling very easy and user-friendly. Mathematical modeling may be categorized as per Figure 2.

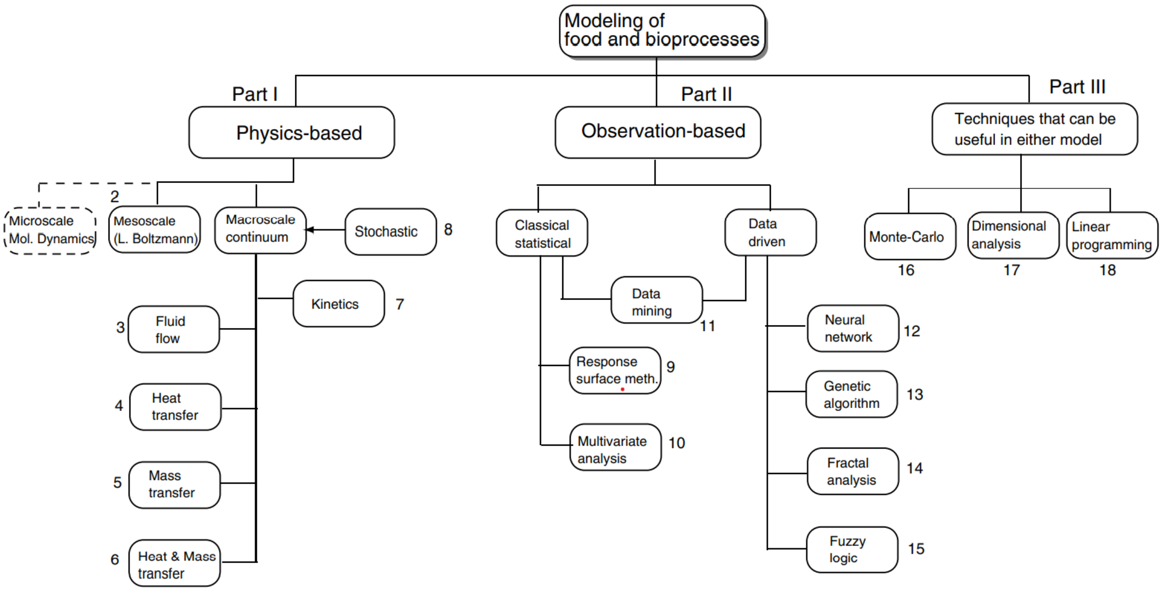

Figure 2. Different methods of modeling with some examples (Datta, 2008).

MODELING OF FOOD AND FOOD PROCESS

Keeping the base as existing theory and measurements, the main aim of modeling is to capture the essential mechanisms during the processing of food. The main steps are given below. Some of them being the structural design of the model: variable to be chosen, nature of the relationship, the ability of calculations are validated by test of identification of design of the structure.

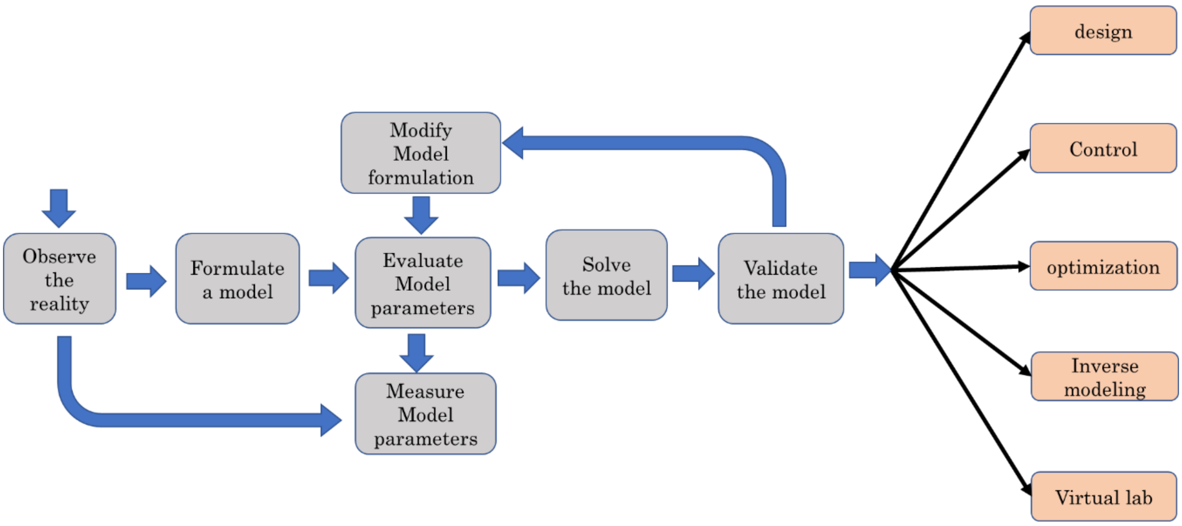

Figure 3. Framework of steps in modeling (design to validation) (Erdogdu *et al.*, 2017).

In the current generation, the physics-based models are becoming more realistic by including more detailed physics, which is possible due to advances in computer technology, making modeling more user-friendly, thus increasing its scope and application in product, process, and research and equipment design. Due to the unavailability of correlations between food quality, food safety and process parameters in physics-based models, physics-based models have not been made ready for food quality and safety yet. In observational models, physical processes are not required; hence these are highly preferred for modeling food safety and quality. In food industries, most of the problems of fluid mechanics are solved by modeling which use the application of laws of motion of Newton in fluids, such as dryer, cooler, designs for ovens, refrigerated vehicles, pasteurization systems, extrusion, heating and cooling systems. In the food sector, our focus is mainly upon quality or safety and, in many cases, both of them. Figure 4 represents that the modeling can be of two types: Safety model or Quality model. Product, process, and equipment designs are covered in the physical processes of a process model. The quality/safety model includes a quantitative description of quality and safety characteristics such as colour or microbes' concentration as a function of temperature.

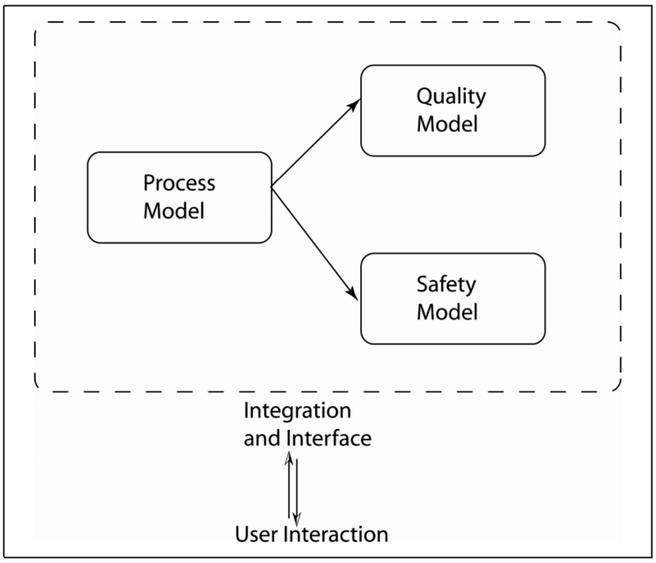

Figure 4. Modeling in food manufacturing as process model and quality/safety model.

Many qualities of food products during dryings like bulk density, porosity, stress cracking, shrinkage, crust formation, and case hardening are major concerns. Final texture during drying is relied upon the following factors: (1) different process parameters during drying and their histories like deformation, temperature, and moisture content, (2) the material's state: whether it is rubbery or glassy, and (3) the conditions of drying along with supporting external environment. Gulati *et al.* (2015) studied the phase transition between rubbery and glassy states of materials along which the deformation developed. Using these, a fundamental-based model for the coupled physics of transport was developed. The case hardening concept, along with various other quality attributes was known using this model. Due to the versatility of this modeling framework, the same can be applied in various other drying conditions to develop enhanced quality food products and highly efficient designed equipment based on food quality. Thus, food processing technologies' characterization, improvisation, and optimization can be easily achieved with the help of modeling. There are various fields where we can apply mathematical modeling like a model for HPP, canning, baking, roasting, grilling, frying, fouling, extrusion, brewing, microbial and enzymatic inactivation, heat & mass transfer (pasteurization, UHT etc.) models, which will be useful in the prediction of temperature profiles in a large solid-type of food, freezing, modeling of growth of ice crystal especially for ice-cream and lot more others. This paper contains modeling of conventional processing (freezing, retorting, pasteurization) which is mostly used in all food processing industries, and their effect on food (microbial inactivation) and equipment (Fouling). As food undergoes a complex transformation during processing, it makes the physics-based model less common in food processing (equipment design) compared to other sectors having major use like aerospace and automobile industry.

Scope of modeling

The standard methods used for food design, known as mathematical modeling, have not been effectively utilized in food process engineering; thus, enormous scope underlies there (Erdogdu *et al.,* 2017). A wide range of scales is covered in food processing based on physics-based models, which are,

(a) Molecular dynamics - micro-scale,
(b) Lattice-Boltzmann models - meso-scale, and s
(c) Macro-scale continuum models which are completely dependent on fluid flow, structural mechanics, heat and mass transfer and kinetics.

Empirical Methods were used where mutual relationships between variables are not unclear specially in a complex situation. MacFie (1994) theorized that new product development, a complex manufacturing process, can be developed using mathematical models, and it involved less work and more computing.

FOULING

Fouling is an unintended accumulation of food on a channel wall while processing which causes deposition. Fouling is a very common problem in food processing, majorly occurring in heat exchangers during thermal treatment due to the thermal instability of food ingredients. There are many structural and chemical changes during the heat treatment of food products. These changes result in making the constituents like proteins and minerals forming a film-like structure and being sticked upon the surface of food equipment. The layer which has been deposited is foulant, and the whole process is known as fouling. For example, milk fouling occurs in PHE, mainly due β-lactoglobulin (Georgiadis *et al.,* 2000). When milk temperature goes above 65^{o}C, β-lactoglobulin becomes thermal unstable and starts forming insoluble particles by irreversible polymerization.

It directly impacts operation performance by reducing heat exchanger efficiency, causing an increase in production loss, energy, and water losses because of repetitive cleaning operation and reduced system performance because of the pressure drop through the heat exchanger. Lots of authors have studied these deposits prevalent across different products. Optimization to the best-operating conditions can be achieved by using a specific model to minimize undesirable effects while heating in fouling. The prevalent models check upon the increasing heat transfer resistance and relate it with a rate of fouling. In the induction period, the thermal resistance doesn't increase with time; hence it is not considered except for boiling conditions. The basic mechanism of the film forming process is very much required for understanding the concept. There are two major thoughts regarding this fouling process: there is no role of mass transfer, a bulk controlled homogeneous reaction or the surface reaction process, and the mass transfer between the fluid containing protein and the thermal boundary layer. The deposition of protein is due to aggregated protein adhering to surface equipment which causes fouling, and this rate is directly proportional to the concentration of aggregation of proteins (Balsubramanian *et al.*, 2008). Few authors assumed that fouling is only due to protein aggregation, and few assuming that it is due to denaturation of protein. Few others believe that fouling is due to both protein denaturation and aggregation. So, based on different assumptions, there are various models. Manika *et al.* (2004) have mentioned that understanding heat exchanger fouling during pasteurization was still incomplete. So, he proposed a new model whose objective was to achieve profit per unit during one heating-cleaning cycle.

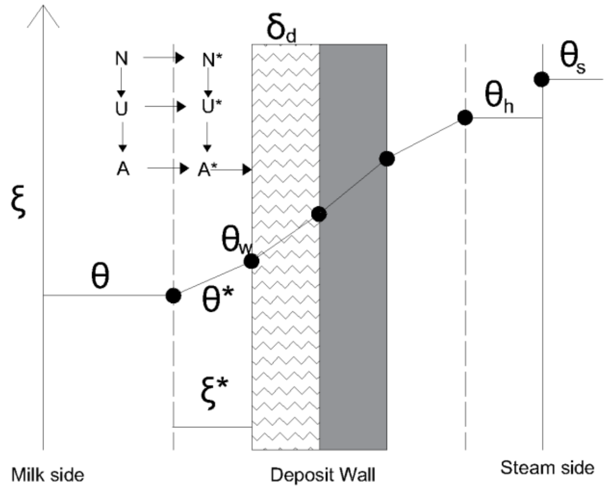

Figure 5. Fouling model.

The model considers two regions of fluid where fouling takes place: bulk and thermal layer. Deposit thickness at the end of the heating stage is

$$\delta_h(\xi) = \delta_0(\xi) + r(\xi) \cdot t_h \qquad (1)$$

Model of cleaning phase assumes two steps, namely swelling of deposit with the rate ω_y, and removal of swell deposit with the rate w_x.

$$\delta_c(\xi) = \frac{\omega_y}{\omega_x} \cdot \exp(-\omega_x t_c) \cdot [\, \exp\left(\frac{\omega_x}{\omega_y} \cdot \delta_h(\xi)\right) - 1\,] \qquad (2)$$

Where, t= time (c= cleaning time, h = heating time), ξ = Bulk layer condition ($0 \leq \xi \leq 1$), $\omega = deposit\ rate$ (y =for swelling, x= removal), δ = Deposit thickness (0 =initial condition, c = after cleaning, h= at the end of heating).

This model gives the dependence of deposit thickness after cleaning δ_c, versus initial (at the end of heating) thickness δ_h and cleaning time t_c. This model concludes that optimum pasteurization units consist of a long heating stage followed by short, infrequent cleaning.

Hydrodynamic and Thermodynamic Model

Jun *et al.* (2005b) have categorized fouling model into hydrodynamic and thermodynamic models, and integrated fouling dynamics models. In hydrodynamic and thermodynamic models, their patterns of flow streams made the mechanism of fouling clear in heat exchangers. Dynamic performance of plate heat exchangers was simulated by cinematic models; the time and space both are independent here. The main advantage here is the number of simulations is minimum which leads to an evaluation of performance in heat exchangers. A very simple approach to design problems is covered through one sweep of steady-state as well as dynamic profile view with the help of this model. Fouling behaviour in plate heat exchangers was studied with the help of 3-dimensional model in which the calculation gives virtual flow velocity fields, which further helped in forming new plate designs, and thus, the fouling on the surface was reduced, which was not possible in 2-dimensional configuration. In the 3-dimensional model, a region of turbulent backflow was also found, which emerged as a cause for elevated temperatures in specific regions and these regions were finally responsible for fouling. So, the CFD model has immense potential to help design a better plate that minimizes such occurrence of regions in a plate for reducing fouling. Continuity and momentum equations are used for describing flow equations in a 3-dimensional model. The continuity equation is defined below:

$$\frac{\partial u}{\partial x} + \frac{\partial v}{\partial y} + \frac{\partial w}{\partial z} = 0 \tag{3}$$

Momentum equations in all directions (x, y and z) are described below

$$\text{x-momentum: } \frac{\partial u}{\partial t} + u\frac{\partial u}{\partial x} + v\frac{\partial u}{\partial y} + w\frac{\partial u}{\partial z} = -\frac{1}{\rho}\frac{\partial p}{\partial x} + \vartheta\left[\frac{\partial^2 u}{\partial x^2} + \frac{\partial^2 u}{\partial y^2} + \frac{\partial^2 u}{\partial z^2}\right] \tag{4}$$

$$\text{y-momentum: } \frac{\partial v}{\partial t} + u\frac{\partial v}{\partial x} + v\frac{\partial v}{\partial y} + w\frac{\partial v}{\partial z} = -\frac{1}{\rho}\frac{\partial p}{\partial y} + \vartheta\left[\frac{\partial^2 v}{\partial x^2} + \frac{\partial^2 v}{\partial y^2} + \frac{\partial^2 v}{\partial z^2}\right] \tag{5}$$

$$\text{z-momentum: } \frac{\partial w}{\partial t} + u\frac{\partial w}{\partial x} + v\frac{\partial w}{\partial y} + w\frac{\partial w}{\partial z} = -\frac{1}{\rho}\frac{\partial p}{\partial z} + \vartheta\left[\frac{\partial^2 w}{\partial x^2} + \frac{\partial^2 w}{\partial y^2} + \frac{\partial^2 w}{\partial z^2}\right] \tag{6}$$

Transient energy equation for incompressible flow is given below

$$\frac{\partial T}{\partial t} + u\frac{\partial T}{\partial x} + v\frac{\partial T}{\partial y} + w\frac{\partial T}{\partial z} = \frac{k}{\rho C_p}\left[\frac{\partial^2 T}{\partial x^2} + \frac{\partial^2 T}{\partial y^2} + \frac{\partial^2 T}{\partial z^2}\right] \tag{7}$$

Where, u, v, w is velocity of component in x, y, and z direction respectively, t is time, ϑ is kinematic viscosity, ρ is density, P is pressure, k is thermal conductivity, C_p is the specific heat capacity of the substance. The above model can be used by coupling with CFD software, fouling behaviour in PHE system can be understood. Jun *et al.* (2005a) have studied 3-dimensional milk fouling using the computational fluid dynamics package FLUENT. Thus, the new surface configuration can be designed with the help of a 3-dimensional model, which would help in reducing the fouling.

Dynamic Fouling Model Incorporating Physico-Chemical Changes

The basis for developing the dynamic model is that the fouling is a transient process. The model was developed across various phases of fouling as it collects over the equipment with the time. The study of the denaturation of β- LG is conducted with the help of dynamic models, and the observations are recorded for the fouling. Delplace *et al.* (1996) conducted an experiment to calculate the dry mass of deposits with the help of a complex configuration of 13 plates. Native β- LG's amount at the outlet of the heat exchanger can be predicted with the help of the model. The numerical calculation of temperature profiles for each channel and steady-state conditions was used as a basis for simulating the amount of denatured protein and was used for testing the model. β- LG at the outlet of the exchanger was found with an experimental error of less than 10% (Balsubramanian *et al.*, 2008).

$$C(t) = \frac{C_0}{1+kC_0t} \tag{8}$$

For T less than 363.15 K, log k = 37.95 – 14.51 (10^3/T),

For T greater than 363.15 K, log k = 5.98 – 2.86 (10^3/T)

Where, C and C_0 = concentration of β- LG at time t and initial condition respectively.

k = second order constant rate, t = time, T = temperature.

Milk fouling in heat exchanger has been clearly understood, because of tremendous volume of milk and dairy product being processed worldwide, so intensive studies were done on it and most of the literature is limited to dairy products. Fouling problem has been a critical issue for other food products such as grape juice, tomato and orange juice. For cleaning and heat exchanging, understanding of interaction between foulants and contact surface is very critical. In food processing industries fouling may also be occurring across multiphase flowing foods through pipe. Kim *et al.* (2020) have developed a model by adopting the most common fouling model for a heat exchanger to predict deposition thickness of food channel.

DRYING

Drying involves coupled heat and mass transfer among the all-other food processing methods, making it a multi-physics model. However, food structure has many scales, but in food processing, specially drying, microstructural features play an important role. The quality of food materials and the structure have a good correlation. To design any food drying process, it is imperative to know the structure and behavior of the products & relationship between the structure and properties of food materials. However, the fundamental structure-property relationships are not very clearly understood till now; it may be due to the heterogeneous nature of food. Hence, food process engineers design the drying process by relying upon empirical data. The microstructure and product properties are completely different for different products. A recent trend approximates material's structure by using food drying models. A representative elementary volume exists that considers fluid phases as a fictitious continuum by adopting a larger description scale. Thus, models have a limited ability to capture the heterogeneity of the material (Welsh *et al.*, 2021).

The micro-level transport processes involved in multiscale modeling overcomes the above limitation. A simple macroscopic model will describe very less of drying phenomena. To describe all drying phenomena, multiscale modeling is required (Rahman *et al.*, 2018). Multiscale modeling is powerful technique that incorporate cellular homogeneity with micro-scale heat and mass transfer during drying. Multiscale model is combination of macro-scale model and micro-scale model (Figure 6). Thus, in the field of drying technology, multiscale modeling is a new yet very advanced approach. Welsh *et al.* (2018) has gave complete overview of multiscale modeling, there frameworks, and how factor affecting this model.

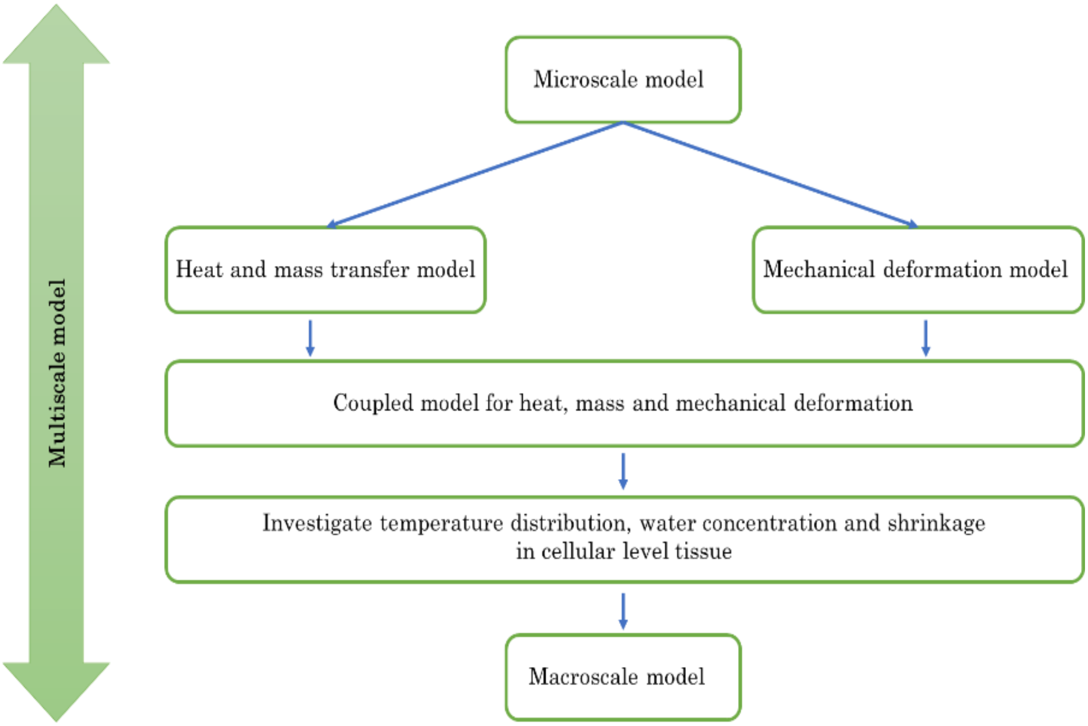

Figure 6. Multiscale approach in drying technology (Rahman *et al.*, 2018).

Effective Moisture Diffusion

Diffusion is a very complex phenomenon to understand during drying which includes majorly Knudsen flow, molecular diffusion, surface diffusion, and hydrodynamic flow. Welsh *et al.* (2021) have considered two spatial scales, which are microscale and macroscale. The macroscale model included applications of temperature and moisture-dependent diffusivity, while both microscale and macroscale included homogenized diffusivity. Effective homogenized diffusion was calculated by application of homogenization to the microscale domain. In macroscale mass transport phenomena, Fick's law of diffusion was used to derive the transport equation, given below:

$$\frac{\partial C}{\partial t} + \frac{1}{r}\frac{\partial}{\partial r}\left[-D_{i,\ eff}\, r\,\frac{\partial C}{\partial r}\right] + \frac{\partial}{\partial z}\left[-D_{i,\ eff}\frac{\partial C}{\partial z}\right] = 0 \quad (9)$$

A kind of Arrhenius relation is used to define the temperature-dependent effective diffusivity approach used for food drying in the macroscopic model, which is:

$$D_{T,\ eff} = D_0 e^{\frac{-E_a}{RT}} \quad (10)$$

Similarly, for products undergoing deformation, a shrinkage dependent effective diffusivity as a function of moisture content in relation to moisture dependent effective diffusivity in macroscopic model is defined as:

$$\frac{D_{ref}}{D_{M,\ eff}} = \left(\frac{b_0}{b}\right)^2 \tag{11}$$

The need of representation of heterogenous structure of food material was satisfied by introduction of microscale model. The previous macroscale mass transport equation has a coupled microscale mass transport equation defined as,

$$\frac{\partial}{\partial t} c(x, y, t) + \nabla \cdot \left(-D(x, y)\ \nabla \mathrm{c}(\mathrm{x}, \mathrm{y}, \mathrm{t})\right) = 0 \tag{12}$$

2-D homogenized effective tool called as tensor is used for calculation of microscopic effective diffusivity defined as,

$$D_{H,\ eff} = \begin{bmatrix} \frac{1}{\omega}\int_\omega D(x,y)\nabla(u_1(x,y) + e_1)d\omega & \frac{1}{\omega}\int_\omega D(x,y)\nabla(u_2(x,y) + e_2)d\omega \\ \frac{1}{\omega}\int_\omega D(x,y)\nabla(u_1(x,y) + e_1)d\omega & \frac{1}{\omega}\int_\omega D(x,y)\nabla(u_2(x,y) + e_2)d\omega \end{bmatrix} \tag{13}$$

$$e_1 = \begin{bmatrix} 1 \\ 0 \end{bmatrix},\ e_2 = \begin{bmatrix} 0 \\ 1 \end{bmatrix}$$

Where, C = instantaneous moisture concentration (mol m^{-3}), t = time (s), $D_{i,\ eff}$ = effective moisture diffusivity (m^2 s^{-1}) with I = *T, M, H.*

Where T = temperature dependent, M = moisture dependent, H = homogenized diffusivity respectively, D = cellular diffusivity (m^2 s^{-1}), D_0 = integration constant (m^2 s^{-1}), E_a = activation energy (J mol^{-1}), D_{ref} = reference diffusivity (m^2 s^{-1}), b_0 = initial product's thickness (m), b = product's thickness (m) at time t (s), ω = area of the macroscale domain, u_1 and u_2 = corrective factors and the solution of the periodic cell problem.

The knowledge of microstructure evolution is applied to provide new insights in consideration of the distribution of water molecules with the help of a homogenous diffusivity model. A more mechanistic approach is involved in determining diffusivity using the above model, which will further assist in the advanced food drying process. Welsh *et al.* (2021) have proven that there was greatly reduced error in convective drying of apples at 45°C and 60°C using this model, while at 70°C, the errors were increased due to more microstructure deformation resulting from an increase in temperature.

ROASTING PROCESS

Roasting is a process of cooking that uses dry heat where the hot air covers the food. To get optimum culinary from roasting process, setting of process parameters is done by experiencing judgment or skill of an individual. In such a case, it is really tough to upscale the oven roasting process, especially while transferring the technology to a new equipment or setting up a new process design. Numerous researchers have developed models of mass transfer during roasting based on different hypotheses, and most of them are based on diffusion. A pure diffusion-based model cannot fully describe the moisture transport phenomenon while the food is being roasted because of the shrinkage effect and capacity of water binding, both of which are not considered. During roasting of meat, protein denaturation occurs, which reduces the water holding capacity and the protein network has also induced shrinkage. This phenomenon greatly accelerates the gradient of pressure inside muscles, and modeling of such phenomena requires poro-elastic theory. Van der Sman, (2007) used this theory to explain water transport phenomena during meat cooking. As per his statement, there was a quite large increment in moisture content at the centre of whole meat and another author has disagreed on this. Feyissa *et al.* (2013) studied roasting of meat, developed a coupled heat and mass transfer model in a convection oven, and solved it using the COMSOL Multiphysics model. He concluded that there was no rise in water content at the centre, which contradicted the previous statement. Temperature and moisture distribution was understood as a function of moisture content and time in this model. The change in microstructure water-holding capacity and elastic modulus in meat could be easily incorporated with the help of this model. The physics of meat while roasting can be easily understood with the help of this process, and the temperature along with the moisture content can be predicted quickly. Aiming at correct and effective moisture loss maintaining the quality of food safety during roasting, this model will completely fit the purpose.

Microbial Biomass Modeling

Microbial modeling is used to predict microbial growth or decline under specific environmental conditions with the help of mathematical expression. The journey of microbial modeling started in 1920s with thermal death time, D and Z value calculation for canned food to ensure that food was free from *Clostridium botulinum* (food poisoning bacteria) (Whiting and Whiting, 2009). Microbial models are a function of mainly many extrinsic (Temperature, gaseous atmosphere) and intrinsic variables (pH, a_w) and are mainly the mathematical expressions that describe the number of microorganisms at a macroscopic scale in a given environment. There is a major role of probability of a microorganism while defining any microbial model since it lies in the context of population of microorganisms. Mathematical model of microbial growth estimation is most commonly used in the field of food safety research, but along with this, few alternative models like Monte Carlo simulation modeling, artificial neural network, individual based model etc., also used widely in the field of risk assessment studies (Esser *et al.*, 2015). Using this mathematical model, one can determine the mathematical growth curve; for this, we have to find a function relationship between the number of live cells and temperature. While collecting data of above mention parameters for understanding growth kinetics, it is necessary to maintain a controlled environment like temperature, pH, water activity (a_w), salt and sugar of medium. As per doing this, only principal factors play significant role in growth kinetics. Other factors like changes in solubility, gas diffusion, nutrients, and heat transfer were neglected. As of now, there are several models have been developed for microbial prediction. However, the model selection will depend on the quality and quantity of the generated data and the complete knowledge of the system. Currently, the data and knowledge are not adequate to form mechanistic or fundamental microbial models; hence there are only empirical, and some phenological models are currently available. There are mainly three classifications: primary, secondary, and tertiary.

The primary model is a mathematical expression which describes microbial growth as a function of time or survival curve (after heat treatment, i.e., sterilization). The primary model is either empirical, phenological, growth rate model, inactivation or survival model, or combination. This model does not explain the reason behind a particular pattern. Among empirical growth models, the Gompertz model is most widely used (McKellar *et al.*, 2003). This model can be written in the following equation.

$$log_e N\ (t) = A + C\ exp\ \{\ exp[-B\ (t - m)]\} \qquad (14)$$

Where *N(t)* is no of a cell at time t, *A* is the logarithmic value of initial population, *c* is asymptomatic logarithmic growth ratio, *B* is the relative growth rate, *t* is time, and *M* is time for maximum growth rate.

Major parameters that are considered in this are initial population size, or asymptotic population size, and relative growth rate. Because of flexibility in the Gompertz model, it has numerous applications in various sectors. As per Esser *et al.* (2015), Gompertz model, another model like the three-phase linearized growth or Buchanam model, and the logistic model are also widely used. These models do not describe all phase of microbial growth curve. Those models were used to predict density of population, but growth rate model is used to predict population growth rate as the name itself implies. As shown in equation no 14, the Gompertz model can be converted into a rate model (Peleg *et al.*, 2011). Verhulst (logistic) and Baranyi-Roberts model is the most commonly known rate growth model. Chick, (1908) has proposed a primary model to understand microbial inactivation kinetics and this model can be used if it is assumed that inactivation follows first-order kinetics. In the secondary model we apply the concept of D-value, though this concept may be insufficient. In secondary inactivation model, it describes k or D with respect to product T, pH and a_w.

$$D = D_{ref} \times 10^{\frac{T_{ref} - T}{z_T}} \times 10^{\frac{pH_{ref} - pH}{z_{pH}}} \times 10^{\frac{1 - a_w}{z_{a_w}}} \qquad (15)$$

Where, *D* = decimal reduction at *T* temperature, D_{ref} = required time at the reference temperature (T_{ref}) to decrease the bacterial concentration to 1/10, Z_T = required elevation in temperature to reduce the *D* value to 1/10, Z_{pH} = pH variation that enhances a reduction of 1/10th of the *D* value, z_{a_w} = difference of water activity (a_w) from 1 resulting in10-fold reduction of the *D* value.

Secondary mathematical model describe microorganism growth rate is affected by external factors such as pH and temperature, and water activity (a_w) (Peleg *et al.*, 2011). So, this model establishes a relationship between primary models and other intrinsic or extrinsic parameters. For quantitative study of microbial growth, Arrhenius model is still used as most prominently. McMeekin *et al.* (1993) have mentioned that applicability of Arrhenius model for microbial growth is because of inability to account for optimal growth temperature. Limitation of this model is that, it validated for restricted temperature range (i.e., growth rate of microorganism increases monotonically with temperature). Other mathematical models like Ratkowsky model (Ratkowsky *et al.*, 1983) or peleg-Corradini-Model (Peleg *et al.*, 2011) has explained how growth rate is dependent on temperature, pH and other factors. Primary and secondary models may be characterized as segregated or non-segregated, linear or non-linear, structured or non-structured (Whiting and Whiting, 2009). Tertiary models make the prediction tool complete by combining the other two models (primary and/or secondary model) with a computer interface. Computer program calculate microbial response with changing conditions, and do their comparison, or contrast the behaviour of several microorganisms. These models will help in various sectors like industries, extension, academia in food safety to understand, design or modify the outcome of several "what if" scenario.

In food sector, microbial growth plays important role in respect to food safety and quality, especially when we talk about perishable product like meat, milk etc. Contamination and growth are two major concerns for food industries. Traditionally, inspection and sampling used to maintain quality and safety of food products. Now using model one can predict microbial growth and their population, and how environmental factor (pH, storage temperature, packaging material) affect them. Cárdenas *et al.*, (2008) has shown the effect of a range of pH (6.1,5.8, and 5.6) at a variety of storage temperatures (0, 4, and 10°C) and was packed two films having different gas permeabilities (polyethylene and EVA SARAN EVA) on beef muscle extracted three bacteria (*Klebsiella* sp., E. *coli* and *Pseudomonas* sp.), which was inoculated on sample of ground meat and Gompertz model was used for microbial growth and linear equation and effect of temperature on specific microbial growth and lag phase duration value were modelled through Arrhenius type equation, to determining the corresponding activation energy. Swinnen *et al.* (2004) has covered well predictive modeling of microbial lag phase.

RETORT PROCESS

Packaged self-stable food products generally utilise thermal processing. An advanced form of food preservation is canning which includes retorting in semi-rigid flexible pouches. This process of thermal sterilization consists of heating food packed container in pressurized retort at specific temperature for particular length of time, depending upon nature of food. This time is calculated based on inactivation of bacteria in each container. If process fails in delivering sufficient lethality, causing risk of public health, probability of spoilage, further it will damage industries reputation. Loss of heat sensitive ingredient is always associated with any thermal process. So, both quality and safety require attention, while calculating process time and temperature, to avoid over or under-processing. Understanding temperature profile inside food container is very important, especially cold point, and it is majorly affected by heat transfer. The process time in canning is based on a specific degree of sterilization, while sensory properties and the texture present define the degradation of nutrients. Thermal processing has two opposing effects (desirable and undesirable), which are both time and temperature dependent. Thus, temperature change of any product is determined for a target sterilization value with the help of mathematical modeling of heat transfer focused on decreasing the rate of reduction of nutrients simultaneously assuring food safety. Some of author tried to understand retort process by experimentally, but due to high cost and time consumption in experiment did not find in-depth result (Mosna *et al.*, 2015). But in recent years, with the help numerical simulation these problems are understood deeply and allow us to set best thermal setting of particular process. Mosna *et al.* (2015) mentioned that among all other different numerical approach, CFD (computational fluid dynamics) is the most suitable for understanding the temperature profile inside the container during the retort process. Using this approach, most of the studies were done by considering the real configuration of the packaging; they all avoided the flow of steam-water movement inside a retort chamber. Mosna *et al.* (2015) have used three-dimensional geometric configuration to study internal temperature of cold spot in order to control time-temperature trend. Based on the results, they mention that chamber's internal configuration affects the heat exchange process. Cold point temperature is also affected by water content and total solids (plant origin); Gokhale *et al.* (2014) have suggested that must be a unified approach to mathematical modeling. They also have developed a semi-empirical unified model that is successfully extrapolated to predict product temperature over a range of process conditions for various products with a relative error is <10%.

BAKING PHENOMENA

There are a series of reactions taking place physically, chemically and biologically while baking which include volume expansion, formation of pores, starch gelatinization, protein denaturation, formation of crust and browning. Thus, there is simultaneously heat and water transport inside the chambers' environment as well as the product. Heat and water transport to product occur mainly through conduction from mold, radiation, natural and forced convection, condensing steam and evaporation of water. Baking is a high energy consuming process, so, overall energy consumption can be reduced with improving of product quality with the help of optimization of operating conditions (Sablani *et al.*, 1998). These transformations took place due to heat and mass transfer as well as mechanical deformation during baking of bread. The overall mechanism of baking not yet being clear makes it really difficult for predicting models under baking conditions. Any attempt to modify or alter the baking process requires an understanding of the physico-chemical changes involved in the process, so usually empirical and mathematical modeling approach is used. Model was solved by finite difference numerical method. Zhang *et al.*, (2016) has used spatial reaction engineering approach (S-REA) for modeling of browning kinetics while miniature bread baking using. Many equations of heat and mass transfer are used in S-REA which uses multiphase model approach where evaporation and condensation rates locally are described by the reaction engineering approach (REA). The models, as well as browning kinetics, are changed when the combination of S-REA approach with equations of moisture content and temperature with respect to colour change takes place. *Golchin et al.*, (2021) have developed mathematical models of weight loss and crust temperature of toast bread containing guar gum during baking process, and the predicted bread crust temperature and weight loss of bread (control and containing guar gum) were in a reasonable agreement with the experimental temperature with a coefficient of determination of 0.98 and 0.99, respectively. Zhang *et al*., (2006) have developed fully coupled model, it is developed for deformation and multiphase heat and mass transfer in bread baking. This model considers heat and moisture transport that is fully coupled with large volume change. Viscoelastic material property is used and is a function of temperature. The model displays the same transport and deformation characteristics as that observed from a baking experiment in terms of temperature, moisture loss, and surface browning. So, this model shows the interaction between transport and deformation and enables us to understand the baking process better.

INTEGRATION OF MODEL

Many processing steps are included in food processing which are all dependent. The models are present at all the stages of food processing, but they are built for specific purposes and the hypotheses are set accordingly having limitations to their applicability. The integration of all of these models is also complex (Figure 7). Considering these, three areas are only viable (1) Process engineering (mass transfer and heat transfer's characterization and modeling), (2) Microbiology, (production of metabolite along with characterization and modeling of bacterial load), and (3) Applied thermodynamics (modeling of physico-chemical characteristics in food). Physics-based models can be integrated with microbial growth or inactivation models. This type of model may be partially kept in the category of tertiary models under food microbiology literature (Perez-Rodriguez *et al.,* 2013). Amezquita *et al.* (2005) have modeled integrated heat transfer and dynamic growth of clostridium *Perfringens* in boneless ham and the results were validated for three cooling scenarios. There was one input to this growth model, which was predicted temperature history of the microbes; as a consequence, it was known that the observed and predicted readings were same, thus validating the model sufficiently where the largest value of deviation came out to be 0.37 $\log_{10}$ CFU/g in 6 out of 7 test scenarios. Pradhan *et al.,* (2007) have integrated kinetic and heat-mass transfer models to measure different properties like temperature, moisture content, survival of microbes, etc. under specific conditions in air stream impingement oven. There was difference between observed and predicted values. The absolute reason for this was that the water bath cooking for all products except chicken breasts used kinetic parameters along with the temperature histories which had been used for survival of bacteria. Marks, (2008) has given some limitations for integration models to be used with food processing models as: 1) The range of parameters are limited against collected data; 2) standard methodologies are absent; and 3) inadequate information regarding variability and uncertainty.

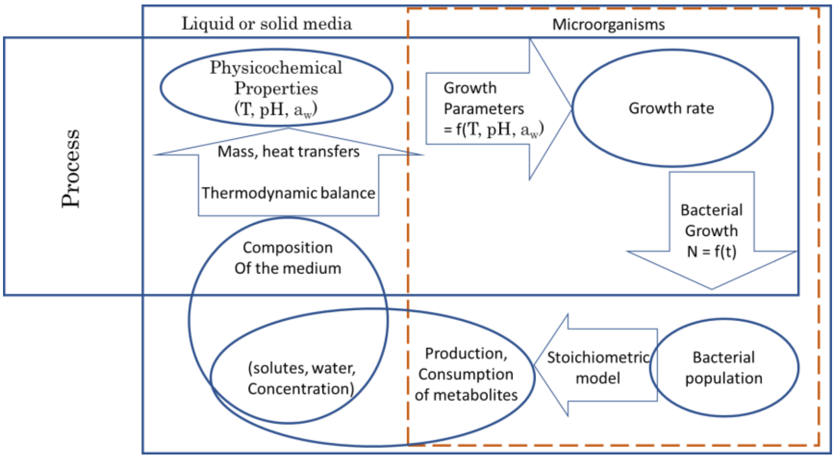

Figure 7. Variables and models involved in an integrated modeling approach, (Isabelle *et al.*, 2006).

CONCLUSION

This paper has appraised a fundamental understanding of mathematical models and how modeling has vast food and process design scope. The designing, optimizing, and innovation of the food processes underlie the very high potentials of modeling. Several parameters on quality and safety have enhanced effects because the number of overall experiments is reduced, which is conducted, being possible due to modeling. Hence, giving the consumer the exact food they want to eat with the help of reducing the microbial growth completely not affecting the quality and safety standards is the main aim of food processing, and how modeling could help to achieve such final quality has been explained in this paper. Implementing a mode in food processing will be a key feature for uncovering the actual micro-level physics involved in any process. So, modeling is undoubtedly one of the main areas for research in the food sector in the coming years.

ACKNOWLEDGEMENT

The authors are thankful to National Institute of Food Technology Entrepreneurship and Management, Kundli for providing the necessary support for this work.

DECLARATION OF COMPETING INTEREST

The authors declare that they have no conflict of interest.

CREDIT AUTHORSHIP CONTRIBUTION STATEMENT

Manibhushan Kumar: Conceptualization, writing -original draft, review, editing and visualization.
Siddhartha Vatsa: Writing -original draft, review, and editing.
Mitali Madhumita: Review, and editing.
Pramod K Prabhakar: Conceptualization, writing -original draft, review, editing and visualization.

REFERENCES

Amezquita A, Weller CL, Wang L, Thippareddi H and Burson DE (2005). Development of an integrated model for heat transfer and dynamic growth of *Clostridium perfringens* during the cooling of cooked boneless ham. *International journal of food microbiology, 101(2): 123-144.*

Balsa-Canto E, Alonso AA, Arias-Méndez A, García MR, López-Núñez A, Mosquera-Fernández M, Vázquez C and Vilas C (2016). Modeling and optimization techniques with applications in food processes, bio-processes and bio-systems. In Numerical Simulation in Physics and Engineering (pp.187-216). Springer, Cham.

Balsubramanian S, Puri VM and Jun S (2008). Fouling models for heat exchangers. *Food Process Operat Model, 107: 235.*

Cárdenas FC, Giannuzzi L and Zaritzky NE (2008). Mathematical modelling of microbial growth in ground beef from Argentina. Effect of lactic acid addition, temperature and packaging film. *Meat Science, 79(3): 509-520.*

Chick H (1908). An investigation of the laws of disinfection. *Epidemiology & Infection, 8(1): 92-158.*

Datta AK (2008). Status of physics-based models in the design of food products, processes, and equipment. *Comprehensive Reviews in Food Science and Food Safety, 7(1): 121-129.*

Datta AK (2016). Toward computer-aided food engineering: Mechanistic frameworks for evolution of product, quality and safety during processing. *Journal of Food Engineering, 176: 9-27.*

Datta AK and Sablani SS (2007). Mathematical modeling techniques in food and bioprocess: an overview (pp. 1-11). *CRC Press*, Boca Raton, FL, USA.

Delplace F, Leuliet JC and Tissier JP (1996). Fouling experiments of a plate heat exchanger by whey proteins solutions. *EUR (Luxembourg), 1-8.*

Erdogdu F, Sarghini F and Marra F (2017). Mathematical modeling for virtualization in food processing. *Food Engineering Reviews, 9(4): 295-313.*

Esser DS, Leveau JH and Meyer KM (2015). Modeling microbial growth and dynamics. *Applied microbiology and biotechnology, 99(21): 8831-8846.*

Feyissa AH, Gernaey KV and Adler-Nissen J (2013). 3D modelling of coupled mass and heat transfer of a convection-oven roasting process. *Meat science, 93(4): 810-820.*

Friis A and Jensen BBB (2002). Prediction of hygiene in food processing equipment using flow modelling. *Food and bioproducts processing, 80(4): 281-285.*

García-Flores R, de Souza Filho OV, Martins RS, Martins CVB and Juliano P (2015). Using logistic models to optimize the food supply chain. In Modeling Food Processing Operations (pp. 307-330). *Woodhead Publishing.*

Georgiadis MC and Macchietto S (2000). Dynamic modelling and simulation of plate heat exchangers under milk fouling. *Chemical Engineering Science, 55(9): 1605-1619.*

Gokhale SV and Lele SS (2014). Retort process modelling for Indian traditional foods. *Journal of Food Science and Technology, 51(11): 3134-3143.*

Golchin FM, Movahhed S, Eshaghi M and Chenarbon HA (2021). Mathematical modeling of weight loss and crust temperature of toast bread containing guar gum during baking process. *Food Science & Nutrition, 9(1): 272.*

Gulati T and Datta AK (2015). Mechanistic understanding of case-hardening and texture development during drying of food materials. *Journal of Food Engineering, 166: 119-138.*

Gulati T, Zhu H and Datta AK (2016). Coupled electromagnetics, multiphase transport and large deformation model for microwave drying. *Chemical Engineering Science, 156: 206-228.*

Isabelle L and Andre L (2006). Quantitative prediction of microbial behaviour during food processing using an integrated modelling approach: a review. *International Journal of Refrigeration, 29(6): 968-984.*

Jun S and Puri VM (2005a). 3D milk fouling model of plate heat exchangers using computational fluid dynamics. In *2005 ASAE Annual Meeting* (p.11). American Society of Agricultural and Biological Engineers.

Jun S and Puri VM (2005b). Fouling models for heat exchangers in dairy processing: a review. *Journal of Food Process Engineering, 28(1): 1-34.*

Kumar C, Joardder M U H, Farrell TW and Karim MA (2016). Multiphase porous media model for intermittent microwave convective drying (IMCD) of food. *International Journal of Thermal Sciences, 104: 304-314.*

Khan IH, Joardder MUH, Kumar C, Karim MA, Khan IH, Joardder MUH and Kumar C (2018). Multiphase porous media modelling : A novel approach to predicting food processing performance.8398.

Kim DH, Zohdi TI and Singh RP (2020). Modeling, simulation and machine learning for rapid process control of multiphase flowing foods. *Computer Methods in Applied Mechanics and Engineering*, *371: 113286.*

MacFie H (1994). Computer assisted product development. *World of Ingredients*, *10(11): 45-49.*

Manika MH, Bildeaa CS, Grievinka J and Marshmanb C (2004). Modelling and optimisation of milk pasteurisation processes. In *Computer Aided Chemical Engineering*, *18: 955-960.*

Marks BP (2008). Status of microbial modeling in food process models. *Comprehensive Reviews in Food Science and Food Safety*, *7(1): 137-143.*

McKellar RC and Lu X (2003). Modeling microbial responses in food. (Eds.). *CRC Press.*

McMeekin TA, Olley J, Ross T and Ratkowsky DA (1993). Predictive microbiology: theory and application. *Biotechnologia, 2(25): 94.*

Mercier S, Marcos B, Moresoli C, Mondor M and Villeneuve S (2014). Modeling of internal moisture transport during durum wheat pasta drying. *Journal of Food Engineering*, *124* : 19-27.

Mohammadi Golchin F, Movahhed S, Eshaghi M and Ahmadi Chenarbon H (2021). Mathematical modeling of weight loss and crust temperature of toast bread containing guar gum during baking process. *Food Science & Nutrition, 9(1): 272-281.*

Mosna D and Vignali G (2015). Three-dimensional CFD simulation of a "steam water spray" retort process for food vegetable products. *International Journal of Food Engineering*, *11(6): 715-729.*

Peleg M and Corradini MG (2011). Microbial growth curves: what the models tell us and what they cannot. *Critical Reviews in Food Science and Nutrition*, *51(10): 917-945.*

Perez-Rodriguez F and Valero A (2013). Predictive microbiology in foods. In Predictive Microbiology in Foods (pp. 1-10). *Springer*, New York, NY.

Prabhakar PK, Srivastav PP, and Pathak SS (2019). Kinetics of total volatile basic nitrogen and trimethylamine formation in stored rohu (*Labeo rohita*) fish. *Journal of Aquatic Food Product Technology*, *28(5): 452-464.*

Pradhan AK, Li Y, Marcy JA, Johnson MG and Tamplin ML (2007). Pathogen kinetics and heat and mass transfer–based predictive model for Listeria innocua in irregular-shaped poultry products during thermal processing. *Journal of Food Protection*, *70(3): 607-615.*

Rahman MM, Joardder MU, Khan MIH, Pham ND and Karim MA (2018). Multi-scale model of food drying: Current status and challenges. *Critical Reviews in Food Science and Nutrition*, *58(5): 858-876.*

Ratkowsky DA, Lowry RK, McMeekin TA, Stokes AN and Chandler R (1983). Model for bacterial culture growth rate throughout the entire biokinetic temperature range. *Journal of Bacteriology*, *154(3): 1222-1226.*

Sablani SS, Marcotte M, Baik OD and Castaigne F (1998). Modeling of simultaneous heat and water transport in the baking process. *LWT-Food Science and Technology*, *31(3): 201-209.*

Swinnen IAM, Bernaerts K, Dens EJ, Geeraerd AH and Van Impe JF (2004). Predictive modelling of the microbial lag phase: a review. *International journal of Food Microbiology*, *94(2): 137-159.*

Trystram G (2012). Modelling of food and food processes. *Journal of Food Eengineering*, *110(2): 269-277.*

Van der Sman RGM (2007). Moisture transport during cooking of meat: An analysis based on Flory–Rehner theory. *Meat Science*, *76(4): 730-738.*

Welsh ZG, Khan MIH and Karim MA (2021). Multiscale modeling for food drying: A homogenized diffusion approach. *Journal of Food Engineering*, *292:* 110252.

Welsh Z, Simpson MJ, Khan IH and Karim MA (2018). Multiscale Modeling for Food Drying. *State of the Art*. *17*, 1293-1308.

Whiting RC and Whiting RC (2009). *Critical Reviews in Food Science & Nutrition Microbial modeling in foods Microbial Modeling in Foods*. *8398 (1995).*

Zhang J and Datta AK (2006). Mathematical modeling of bread baking process. *Journal of Food Engineering*, *75(1): 78-89.*

Zhang L, Putranto A, Zhou W, Boom RM, Schutyser MA and Chen XD (2016). Miniature bread baking as a timesaving research approach and mathematical modeling of browning kinetics. *Food and Bioproducts Processing*, *100: 401-411.*

Zugarramurdi A, Parin MA, Gadaleta L and Lupin HM (2007). A quality cost model for food processing plants. *Journal of Food Engineering*, *83(3): 414-421.*

Turkish Journal of Agricultural Engineering Research

https://dergipark.org.tr/en/pub/turkager
https://doi.org/10.46592/turkager.2021.v02i02.020

Turk J Agr Eng Res (TURKAGER)
e-ISSN: 2717-8420
2021, 2(2): 493-507

Review Article (Derleme Makale)

Heavy Metal Pollution in Soil and Removal Methods

Osman SÖNMEZ[a]*, **Fatma Nur KILIÇ**[a]

[a] *Toprak Bilimi ve Bitki Besleme Bölümü, Ziraat Fakültesi, Erciyes Üniversitesi, 38039, Melikgazi Kayseri, TÜRKİYE*

(*): Corresponding author, osmansonmez@erciyes.edu.tr

ABSTRACT

Heavy metals decompose in the soil and cause pollution that is difficult to remove, due to their inability to turn into other compounds. Recently, the increase in population and increasing demand and industrialization and intensive agricultural practices in line with this cause environmental pollution. Heavy metal pollution can also occur from the parent material. Among the heavy metals in the soil, cadmium (Cd), copper (Cu), lead (Pb), cobalt (Co), arsenic (As), mercury (Hg) and zinc (Zn) have an important place. Heavy metal pollution can cause losses in agricultural areas, as well as adversely affect human health with the consumption of products grown in these areas. Heavy metal pollution in the soil can be controlled by physical, chemical or biological methods and/or processes, by isolation techniques, replacing contaminated soil, electrokinetic techniques, leaching and bioremediation techniques. In this review, heavy metal pollution and removal methods were evaluated.

REWIEV ARTICLE

Received: 06.09.2021
Accepted: 02.11.2021

Keywords:

- Soil pollution,
- Heavy metal,
- Remediation techniques

To cite: Sönmez O, Kılıç FN (2021). Toprakta Ağır Metal Kirliliği ve Giderim Yöntemleri Turkish Journal of Agricultural Engineering Research (TURKAGER), 2(2): 493-507. *https://doi.org/10.46592/turkager.2021.v02i02.020*

Toprakta Ağır Metal Kirliliği ve Giderim Yöntemleri

ÖZET

Ağır metaller toprakta ayrışarak kirliliğe yol açmaktadır ve bu kirliliğin giderilmesi metallerin başka bileşiklere dönüşememesinden dolayı zordur. Son zamanlarda nüfusun artış hızı ve artan ihtiyaç talebi ile bunun doğrultusunda sanayileşme, yoğun tarımsal uygulamalar çevre kirliliğine yol açmaktadır. Ağır metal kirliliği ana materyal kaynaklı da meydana gelebilmektedir. Toprakta yer alan ağır metaller arasında kadmiyum (Cd), bakır (Cu), kurşun (Pb), kobalt (Co), arsenik (As), civa (Hg) ve çinko (Zn) önemli bir yer tutmaktadır. Ağır metal kirliliği tarımsal alanlarda kayıplara neden olabildiği gibi, bu alanlarda yetiştirilen ürünlerin tüketimiyle birlikte insan sağlığını da olumsuz etkilemektedir. Toprakta ağır metal kirliliği fiziksel, kimyasal veya biyolojik yöntem ve/veya süreçlerle izolasyon teknikleri, kirlenmiş toprağın değiştirilmesi, elektrokinetik teknikler, yıkama, biyoremediasyon teknikleri ile kontrol altına alınabilmektedir. Bu derlemede ağır metal kirliliği ve giderim yöntemleri değerlendirilmiştir.

DERLEME MAKALESİ

Alınış tarihi: 06.09.2021
Kabul tarihi: 02.11.2021

Anahtar Kelimeler:

- Toprak kirliliği,
- Ağır metal,
- Islah teknikleri

Alıntı için: Sönmez O, Kılıç FN (2021). Heavy metal pollution in soil and removal methods. Turkish Journal of Agricultural Engineering Research (TURKAGER), 2(2): 493-507. *https://doi.org/10.46592/turkager.2021.v02i02.020*

GİRİŞ

Son yıllarda hızla artan dünya nüfusu, sanayileşme ve yoğunlaşan tarımsal uygulamalardan kaynaklı olarak, toprak ve çevrede ağır metal kirliliği hızlanmaktadır. Nüfus artışı ile gıda talebi, gıda tüketimi ve endüstriyel ürünlerdeki artış sonucu çevre kirliliği oluşmaktadır (Mikhailenko ve ark., 2020). Toprak kirliliği, temelde taşıma kapasitesini aşan ve toprak kalitesini değiştiren zehirli maddeler anlamına gelmektedir (Golui ve ark., 2019). Toprak kirliliğinin temel sebepleri ağır metaller, kanalizasyon ve mahsul tarlası gibi tarım alanlarına uygulanan büyük miktarlarda gübre ve pestisitler de dahil olmak üzere endüstriyel kentsel atıklardır (Chen ve ark., 2015). Endüstriyel üretim faaliyetlerinin sürekli emisyonu nedeniyle, metal toprak kirliliğinde sürekli bir artış söz konusudur (Weissmannová ve ark., 2019). Kirli topraklarda en çok bulunan ağır metaller sırasıyla Cr, Pb, Cu, Cd, Zn, Hg ve As'dır (Khalid ve ark., 2017). Ağır metaller yüksek bağıl yoğunluğa sahiptir ve düşük konsantrasyonda bile canlılar üzerinde toksik etkiler meydana getirmektedir (Ackova, 2018). İnsan sağlığı açısından kritik ağır metal limitleri Çizelge 1'de verilmiştir. Toprakta ağır metal kirliliği ekolojik çevre, gıda güvenliği, sürdürülebilir tarımın gelişimi için tehdit oluşturmaktadır (Yao ve ark., 2012). Gıda güvenliği ve sürdürülebilir tarım gelişimi için tehdit oluşturması, metallerin biyolojik olarak parçalanamaması ve yalnızca bir kimyasal durumdan diğerine aktarılabilir ve toprakta oldukça kalıcı olmasından ileri gelmektedir (Naila ve ark., 2019; Sun ve ark., 2020). Toprak, yer kürenin çoğunu örtü halinde kaplayan, iklim ve canlıların, topoğrafik koşullara bağlı olarak zamanla ana materyal üzerine yaptıkları ortak etkiler sonucu ortaya çıkmış, belirli karakteristiklere sahip, dinamik, açık, üç boyutlu, üç fazlı doğal bir bütündür. Toprak pH' sının değişmeye karşı gösterdiği dirence yani toprak tamponlama özelliğine bağlı olarak toprak kirleticileri toprak bünyesinde tutulmaktadır. Ağır metaller parçalanabilir olmadığından (Kirpichtchikova ve ark., 2006), biyolojik birikim yoluyla besin zincirinin tüm halkalarında ağır metal aktarımı meydana gelebilmektedir. Besin zincirinde oluşan ekolojik kirlilik farklı hastalıklara ve zehirlenmelere neden olabilmektedir (Adriano ve ark., 2004; Vareda ve ark., 2016; Almasi ve ark., 2016). Madencilik sektörü, farklı endüstri kolları, fosil yakıt kullanımı ve tarımsal ilaçların kullanımı gibi insan kaynaklı faaliyetler sonucunda ağır metallerin biyoyararlı ve hareketli formları çevreye yayılmaktadır (Kabata-Pendias, 2000; Bolan ve ark., 2003; Wuana ve Okieimen, 2011). Antropojenik etkiler ile ağır metal kirliliği toprağın mevcut biyotik özelliklerinin zamanla negatif yönde etkilenmesine yol açmaktadır (Çağlarırmak ve Hepçimen, 2010). Ağır metallerin toprakta birikmesi bitki bünyesindeki fizyolojik ve biyokimyasal faaliyetleri yüksek oranda etkilemektedir (Asri ve Sönmez, 2006). Ağır metal kirliliğinin olumsuz sonuçlarının zamanla artması ile çeşitli fiziksel, kimyasal ve biyolojik giderim teknikleri geliştirilmiştir örneğin üzerine çalışmalarda bulunulmuştur. Toprakta oluşan kirliliğin giderilmesinde belirlenen temel yaklaşımlar insan sağlığı ve ekolojik ortamın refahı için uygun ortam oluşturulması üzerinedir. Toprak kirliliği için uygun giderim yöntemlerinin seçilmesi toprakta bulunan ağır metalin tipine, doğasına, fizikokimyasal özelliklerine ve dağılımına bağlıdır (Schwalfenberg ve ark., 2018; Wuana ve Okieimen, 2011). Toprakta ağır metallerin giderimi için fiziksel, kimyasal, biyolojik teknikler olarak üç temel giderim tekniği bulunmaktadır. Toprakta ağır metal giderim tekniğinin belirlenmesinde uygulanan tekniğin az maliyetli, geniş alanlarda uygulanabilir, olumsuzluğun görüldüğü kirli alanda ağır metalin ciddi oranda mevcut ortamdan giderilebileceği bir teknik seçiminde bulunulması oluşan çevre kirliliğinin önlenmesinde veya kontrol altına alınabilmesinde önemli bir yer edinebilir.

Çizelge 1. Türkiye topraklarındaki insan sağlığı açısından ağır metal sınır değerleri (Başbakanlık Mevzuatı Geliştirme ve Yayın Genel Müdürlüğü, 2010).
Table 1. *Heavy metal limit values in terms of human health in Turkey (Prime Ministry Legislation Development and Publication General Directorate, 2010).*

Kirletici	Toprağın yutulması ve deri teması yoluyla emilim		Uçucu maddelerin dış ortamda solunması	Kaçak tozların dış ortamda solunması		Kirleticilerin yeraltı suyuna taşınması ve yeraltı suyunun içilmesi [1] (mg kg $^{-1}$ fırın kuru toprak)	
	(mg kg $^{-1}$ fırın kuru toprak)		(mg kg $^{-1}$ fırın kuru toprak)	(mg kg $^{-1}$ fırın kuru toprak)		SF = 10	SF=1
Arsenik	0.4	e	-	471	e	3	1
Bakır	3129	b,c	-	-	f	514	b,g
Kadmiyum	70	b,m	-	1124	e	27	b,g
Kobalt	23	b,c	-	225	e	5	b,g
Krom (toplam)	235	b,c	-	24	e	900000	1
Kurşun	400	n	-	-	f	135	b,g
Nikel	1564	b,c	-	-	f	13	1
Arsenik	0.4	e	-	471	e	3	1
Bakır	3129	b,c	-	-	f	514	b,g

[1] Akifere olan mesafenin 3m'den az olması, akiferin çatlaklı veya karstik olması ya da kirlilik kaynağı alanının 10 hektar veya daha büyük olması koşullarından herhangi birinin geçerli olması halinde seyrelme faktörü SF ^{DF}"1" ; diğer durumlarda SF "10" olarak kabul edilmelidir.

[a] Jenerik Kirletici Sınır Değerlerinin hesaplanmasında insan sağlığı üzerine riskler dikkate alınmıştır.

[b] Bu değerin hesaplanmasında tehlike endeksi "1" olarak kabul edilmiştir.

[c] Bu kirletici için deri emilim faktörü bulunmadığından sadece toprağın yutulması maruziyet yolu dikkate alınmıştır.

[d] Toprak doygunluk konsantrasyonu (C_{sat}).

[e] Bu değerin hesaplanmasında kanser riski "10^{-6}" olarak kabul edilmiştir.

[f] Bu maruziyet yolu için toksikolojik değer bulunmamaktadır.

[g] Bu değerin hesaplanmasında HBL değeri kullanılmıştır.

[h] Bu değerin hesaplanmasında Dünya Sağlık Örgütü'nün belirlediği içme suyu standardı kullanılmıştır.

[ı] Bu değerin hesaplanmasında TS-266 İnsani Tüketim Amaçlı Sular standardında içme ve kullanma suları için verilmiş olan sınır değer kullanılmıştır.

[i] Bu kirleticiye ait Di, ve Dw değerleri bulunmadığı için bu maruziyet yolu için sınır değer hesaplanamamıştır.

[j] Topraktaki kirletici konsantrasyonu ne olursa olsun, kimyasala özgü özellikler nedeniyle, bu maruziyet yolunun dikkate alınmasına gerek bulunmamaktadır.

[k] Bu sınır değer vinilklorür'e ömür boyunca sürekli olarak maruz kalındığı varsayılarak hesaplanmıştır.

[l] Bu sınır değer vinilklorür'e yetişkinlik döneminde sürekli olarak maruz kalındığı varsayılarak hesaplanmıştır.

[m] Bu sınır değerin hesaplanmasında kadmiyum'un besin yoluyla vücuda alınması için belirlenen RFD_a değeri kullanılmıştır.

[n]Bu değer ABD EPA, 1994'den alınmıştır (U.S. Environmental Protection Agency. 1994. RevisedInterimSoilLeadGuidancefor CERCLA Sitesand RCRA Corrective Action Facilities, EPA/540/F-94/043, Office of Solid WasteandEmergencyResponse, Washington, D.C. Directive 9355.4-12.).

[ö] Bu değer talyum sülfat (CAS No. 7446-18-6) için belirlenen RFD_a değeri kullanılarak hesaplanmıştır.

Ağır metallerin tanımı ve ağır metal kaynakları

Ağır metaller metalik özelliklere sahip, yoğunluğu 5 g cm^{-3}'den büyük ve atomik kütlesi 20'den büyük olan elementlerdir (Şekil 1). Ağır metal sözcüğü, literatüre çevre kirliliği ile dahil olmuştur. Çevrede yaygın olarak kadmiyum (Cd), bakır (Cu), kurşun (Pb), kobalt (Co), arsenik (As), cıva (Hg) ve çinko (Zn)ağır metalleri bulunmaktadır. Zn, Cd, Cu ve Pb'nin tahmini kalıcılık süreleri 70–510 yıl, 13–1100 yıl, 310–1500 yıl ve 740–5900 yıl iken, (Lindsay ve Doxtader, 1981) ılıman iklim koşullarında tahminen Cd için 75-380 yıl, Hg için 500-1000 yıl ve Cu, Ni, Pb ve Zn için 1000-3000 yıl olarak bildirilmiştir (He ve ark., 2005).

Şekil 1. Periyodik cetvel içerisinde mevcut ağır metaller (Ali ve Khan, 2018).
Figure 1. *Heavy metals present in the periodic table (Ali and Khan, 2018).*

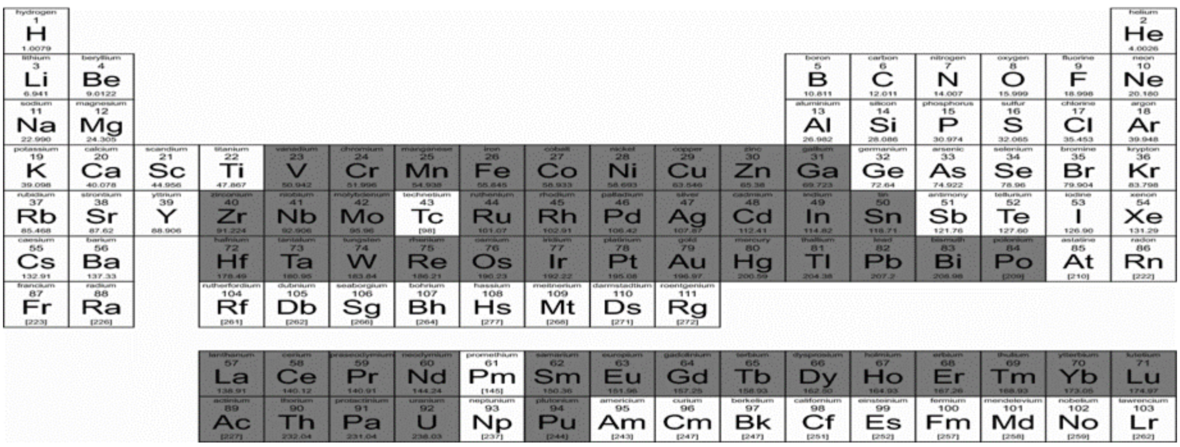

Ağır metaller genellikle toprak partiküllerine adsorbe halde bulunabildikleri gibi organik bileşikler meydana getirerek, minerallerin yapısına bağlı şekilde, şelatlı bileşiklerin bünyesinde çözünmüş halde, farklı hallerde bağlı iyon ya da katı halde çözeltiler formunda bulunabilmektedirler (Kafadar ve Saygıdeğer, 2010). Ağır metaller toprağın oluşumu esnasında ana materyalin bünyesinde silikat, sülfür ve karbonat halinde sabit bileşik şeklinde ya da doğal olarak silikatların bünyesinde adsorbe halde bulunabilmektedir (Okçu ve ark., 2009). Doğal olarak yer kürenin yapısında yer almasının yanında antropojenik faaliyetler ile sanayileşme, kentleşme ve yoğun tarımsal işlemler, toprakların ve çevrenin ağır metal yayılımının temel kaynaklarıdır (He ve ark., 2005).

Ağır metal kirliliği

Ağır metaller topraklarda uzun süre kalması, geri döndürülemez, az miktarda transfer miktarı, yüksek toksisite, karmaşık kimyasal özellikler ve ekolojik tepki gibi özelliklere sahip olmasından dolayı toprak kirliliğinde önemli bir terimdir. Ağır metaller inorganik kirleticiler arasında yer almaktadır. Toprağa doğal ve insan faaliyetleri ile ulaşan ağır metaller katyon değişim kapasitesi ve demir ve alüminyum oksitler, kil, toprak organik maddesi ile toprakta hareketsiz yani immobil olan ağır metallerin toprak içerisindeki birikimi indirgenebilmektedir. Bunların haricinde örneğin, organik karbon, toprak tekstürü, toprak sıcaklığı, toprağın su içeriği, kil tipi, fosfor, bikarbonatlar ve karbonat gibi farklı faktörlerde ağır metallerin toprak mevcudundaki aktif hareketlerini etkilemektedir (Yerli ve ark., 2020). Toprak çözeltisindeki katyonların değişebilir durumu fazla olan kil miktarı yüksek topraklar ve organik madde bakımından zengin topraklar, yüksek miktarda ağır metali tutabilmektedir. Bu tip topraklarda ağır metal kirliliği daha fazla etkili olmaktadır. Ağır metallerin kil ve organik maddeye bağlanmaları nedeniyle toprağın üst katmanında yoğun olarak bulunmaktadırlar (Kızıloğlu ve ark., 2008; Montiel ve ark., 2016). Ağır metallerin meydana getirdiği kirlilik bir ekosistemden diğer ekosistemlere besin zinciri yoluyla kolayca aktarılmaktadır. Ekosistem zincirinde oluşan kirlilik, canlıların bünyesine alınması ile büyük olumsuzluklara neden olmaktadır (Vareda ve ark., 2016). FAO tarafından sulama suyu, toprak ve bitkilerde toksik ağır metal konsantrasyonu için izin verilen sınır değerleri Çizelge 2'de gösterilmiştir. Bazı ülkelerin tarım topraklarındaki ağır metallerin kritik limitleri Çizelge 3' te gösterilmiştir. Ülkemiz topraklarında ağır metal konsantrasyonu gün geçtikçe artmaktadır. Ağır metal kirliliği için bazı çalışmalar yapılmıştır. Bu çalışmalardan bazıları aşağıda yer almaktadır.

Varol ve Erdem (2020), tarafından yapılan çalışmada; Özellikle sanayi faaliyetlerinin yoğun olduğu bölgelerden, toprak kirliliği seviyesini belirlemek için çalışma yapılmıştır. ICP MS cihazıyla yapılan ölçümlerde baryum (Ba) 135.5-389.7 mg kg^{-1} değerleri arasında bulunmuştur ve mevzuatta izin verilen limitlerin üzerinde bir değer olduğu saptanmıştır. Ni, Co ve Cr gibi elementler mevzuatta izin verilen limitlerin altında değerlerde ölçülmüştür.

Özkul (2019) tarafından yapılan çalışmada, Kütahya ilinde çocuk parklarındaki toprakların ağır metal içerikleri değerlendirilmiştir. Kütahya il merkezi yerleşim bölgesinde olan 19 çocuk parkından 0-10 cm derinliğinde toprak örnekleri alınmış ve Cd, As, Hg, Cu, Cr, Zn, Pb ve Ni ağır metallerinin analizleri ICP-MS yöntemi ölçülmüştür. Arsenik (As) için 9.60-260.90 mg kg^{-1}, kadmiyum (Cd) için 0.07-1.24 mg kg^{-1}, krom (Cr) için 16.10-55.50 mg kg^{-1}, bakır (Cu) için 9.13-65.23 mg kg^{-1}, civa (Hg) için 0.02-0.60 mg kg^{-1}, nikel (Ni) için 24.70-121.30 mg kg^{-1}, kurşun (Pb) için 13.06-113.60 mg kg^{-1} ve Zn için 28.70-252.90 mg kg^{-1} aralığında ağır metal konsantrasyonlarında olduğu tespit edilmiştir.

Özkan (2017) yaptığı çalışmada; Antakya-Cilvegözü karayolu çevresindeki tarım alanlarında ağır metal kirliliği ve karayolu uzaklığının toprakta ağır metal birikimi üzerine değişim durumu araştırılmıştır. ICP-OES cihazı kullanılarak ağır metaller, Pb 0.130-0.780 mg kg^{-1}, Cd 0-0.265 mg kg^{-1}, Ni 0.370-3.97 mg kg^{-1}, Cr 0-0.120 mg kg^{-1}, Co 0-1.83 mg kg^{-1}, Al 0-0.700 mg kg^{-1}, Fe 1.45-22.8 mg kg^{-1}, Cu 0.385-5.43 mg kg^{-1}, Mn 1.96-27 mg kg^{-1}, Zn 0-4.26 mg kg^{-1} değerleri arasında ölçülmüştür. Topraktaki demir (Fe) elementinin izin verilen sınır değerlerinin üzerinde olduğu saptanmıştır. Toprakta ağır metal konsantrasyonunun karayolu ile uzaklık arttıkça azaldığı tespit edilmiştir.

Topraktaki ağır metallerin toprak çözeltisi içerindeki hareketliliği toprak pH sına bağlı olarak değişmektedir. Toprakta ağır metal toksisitesi ile toprak pH'ı etkileşim içindedir (Cherfouh ve ark., 2018; Leuther ve ark., 2019). Toprakta hidrojen iyonlarının konsantrasyonlarının artışı sonucu toprakta asidik koşullar artmakta ve hidrojen iyonları ağır metallere göre yüksek çekimle toprağa bağlanmakta bu durum sonucunda da ağır metallerin serbest hale gelebilmektedir (Singh ve ark., 2016).

Yüksek seviyelerdeki ağır metaller bitki büyümesi için zararlıdır (Ghani, 2010). Bitkinin metabolik olaylarının olumsuz etkilenmesiyle bitkisel üretimde verim düşüklüğü meydana getirmektedir. Ağır metaller tohumların çimlenmesini birçok yönden etkilemektedir ve bundan dolayı potansiyel olarak mahsul verimini azaltmaktadır (Ahmad ve Ashraf, 2011). Özel yapıdaki bazı bitki türleri zarara uğramadan bünyelerinde ağır metalleri biriktirebilmektedirler (Wei ve Chen, 2006). Ağır metallerin olumsuz etkilerine rağmen tolerans göstererek bünyelerinde ağır metalleri muhafaza eden bitkilere akümülatör bitkiler denir. Örneğin; Mohsenzadeh ve Mohammadzadeh (2018) tarafından yapılan çalışmada fitoremediasyon testleri deneysel saksılar kullanılarak yapılmış, İran'ın Hamedan şehrinde bulunan çinko ve kurşun maden alanında yetiştirilen bitkilerin ağır metali bünyelerini alma kapasitelerini araştırmak için, *Conium maculatum*, *Stachys inflata* ve *Reseda lutea* üç baskın bitkinin vejatatif aksamında Cu, Pb, Zn, Cd ve Ni konsantrasyonlarına atomik absorpsiyon spektrometresi ile ölçülmüştür. *C. maculatum* Pb ve Zn'nin giderilmesinde, *S. inflata* Ni'nin azaltılmasında ve *R. lutea* Cu'nun azaltılmasında etkili olabileceği saptanmıştır.

Çizelge 2. Sulama suyu, toprak ve bitkilerde toksik ağır metal konsantrasyonu için izin verilen sınır değerleri (WHO/FAO, 2007).
Table 2. *Allowable limit values for toxic heavy metal concentration in irrigation water, soil and plants (WHO/FAO, 2007).*

Metal	Sulama suyu (µg ml^{-1})	Toprak (µg g^{-1})	Bitki (µg g^{-1})
Cd	0.01	3	0.2
Cu	0.20	140	40
Ni	1.40	50	67
Pb	0.015	300	0.30
Zn	2.0	300	60
Hg	0.01	30	0.03
Cr	0.10	150	5
As	0.01	20	0.1
Fe	0.50	50.000	450
Mn	0.20	80	500

Çizelge 3. Bazı ülkelerin tarım topraklarındaki bazı ağır metallerin kritik limitleri (Chokor ve Ekanem, 2016).
Table 3. *Critical limits of some heavy metals in agricultural soils of some countries (Chokor and Ekanem, 2016).*

Ülke	Bazı ağır metallerin tarım topraklarında kritik limitleri (mg kg $^{-1}$) (Chokor and Ekanem, 2016)				
	Cd	Cr	Cu	Pb	Zn
Kanada	0.5	20	30	25	50
Danimarka	0.3	50	30	40	100
Finlandiya	0.3	80	32	38	90
İsviçre	0.8	75	50	50	200
İrlanda	1.0	100	50	50	150
Rusya	0.2	90	55	32	100

Toprakta ağır metal giderim yöntemleri

Topraklarda meydana gelen ağır metal kirliliğinin iyileştirilmesi için birçok yöntem geliştirilmiştir. Temelde ikiye ayrılan bu yöntemler kirlenmiş toprağın yerinde iyileştirilmesi (in-situ) ve kirlenmiş toprağın alınarak başka yerde iyileştirilmesidir (ex-situ) (Gomes ve ark., 2013). Toprakta ağır metal kirliliğini iyileştirme yönteminin seçimi, sahanın özelliklerine, giderilecek kirleticilerin türlerine, kirleticinin konsantrasyonuna ve kirlenmiş ortamın son kullanıldığı duruma bağlı yapılmalıdır (Bhandari ve ark., 2007). İyileştirme yöntemleri fiziksel, kimyasal ve biyolojik işlemlerle gerçekleştirilmektedir.

Fiziksel iyileştirme yöntemleri: toprak değiştirme, izolasyon, çevreleme yöntemi ve ısıl işlem dahil olmak üzere fiziksel teknolojileri kullanarak toprağa verilen hasarı tersine çevirme veya durdurma süreci içeren işlemlerdir (Yao ve ark., 2012).

Toprak değiştirme teknolojilerinde, toprak yüzeyini kaplamak için fazla miktarda kirlenmemiş toprak kullanılmaktadır. Bu işlem ağır iş yükü ve yüksek maliyeti nedeniyle dar alanlar için daha uygundur.

Toprak izolasyonu teknolojileri, kirlenmiş alanların çevresine kirliliği taşımasını engellemek için bariyer duvarlarla etrafının kaplanması sağlanan sistemlerdir. Çelik, çimento, bentonit ve harç gibi geçirimsiz malzemelerden yapılmış fiziksel bariyerler, dikey ve yatay muhafaza için kullanılır. Toprak izolasyonu veya çevreleme yöntemleri doğrudan iyileştirme yöntemleri içerisinde yer almamaktadır (Jankaite ve Vasarevičius, 2005). Isıl işlemde toprağın ısıtılarak iyileştirilmesi için kirleticinin uçuculuğu ile gerçekleştirilir (Song ve ark., 2017).

Kimyasal iyileştirilme yöntemleri: kirlenmiş ortamdaki kirleticileri çıkarmak veya stabilize etmek için kimyasalların kullanımını içermektedir. Toprak yıkama ve immobilizasyon teknikleri (katılaştırma/stabilizasyon, vitrifikasyon ve elektrokinetik yöntem) dahil olmak üzere çeşitli kimyasal iyileştirme yöntemlerini içermektedir.

Toprakta yıkama yöntemleri, kirlenmiş toprağı temiz su, reaktifler ve diğer sıvılar ile topraktan kirleticileri süzmek amacıyla toprağın yıkanmasından meydana gelmektedir (Derakhshan Nejad *ve ark*, 2018). Ağır metal giderimi için su (Dermont ve ark., 2008), saponin (Maity ve ark., 2013), organik asit (Kim ve ark., 2013), şelatlayıcı maddeler (Jiang ve ark., 2011) yüzey aktif maddeler (Sun ve ark., 2011) ve düşük moleküler ağırlıklı organik asitler (Almaroai ve ark., 2012) gibi maddelerin topraklardaki kirleticilerin desorpsiyonunu etkilediği saptanmıştır.

Zhai ve ark. (2018) tarafından yapılan çalışmada, kireç, biochar ve siyah karbon kullanılarak toprak yıkama işlemi ve yerinde hareketsizleştirme çalışılmıştır. FeC kombinasyonu ile yıkama işleminden sonra Cd, Pb, Zn ve Cu metallerinde sırasıyla %62.9, %52.1, %30.0 ve %16.7 azalma saptanmıştır. Kireç ilavesi ile Cd, Cu, Pb ve Zn'nin biyoyararlanımında %36.5, %73.6, %70.9 ve %53.4 azalma belirlenmiştir. Aynı zamanda toprakta mikrobiyolojik iyileşmede olumlu etki gösterdiği tespit edilmiştir.

İmmobilizasyon teknikleri, çözünmeyen veya zor hareket eden, düşük toksik maddeler oluşturmak amacıyla kirlenmiş toprağa reaktifler veya materyaller eklenmesiyle ağır metallerin su, bitki ve diğer çevresel ortamlara geçişini azaltılmasının sağlanmasıyla yapılan tekniklerdir (Yao ve ark., 2012).

Ren ve ark. (2020) yaptıkları çalışmada, $Ca(H_2PO_4)_2$ domuz gübresi biyokömürü (PSMB) hazırlanmış ve toksik metallerin (Cd ve Pb) içeriği ve toprak besin elementi düzeyi üzerindeki etkilerini değerlendirmek için araştırılmıştır. PSMB'nin maksimum %3 oranında eklenmesi, Fengxian ve Kunming toprağında DTPA ile ekstrakte edilebilir Cd (%34.02 ve %47.73) ve Pb (%18.70 ve %24.58) konsantrasyonlarını önemli seviyede azalttığı saptanmıştır.

Vitrifikasyon teknikleri, aşırı yüksek sıcaklıkta çoğu inorganik kirleticiyi hareketsiz hale dönüştürülmesi ile oluşan tekniklerdir (USAEC, 2000).

Navarro ve ark. (2013) yaptığı çalışmada, İspanya'daki gümüş ve kurşun madenlerinden çıkan kirleticilerin güneş enerjisi teknolojisini kullanarak vitrifikasyon tekniği ile ıslahı çalışılmıştır. Vitrifikasyonun 1350°C'de Mn, Zn, Cu, Fe ve Ni' in immobilizasyonuna ile sonuçlandığını, 1050 °C' de ise Mn, Ni, Zn ve Cu'nun mobilize olduğunu saptamışlardır.

Elektrokinetik teknikler, kirletici yüklü türleri hareketli hale getirerek elektrotlarla doğru akım uygulamasıyla sağlanan tekniklerdir (Dindar ve ark., 2017).

Azhar ve ark. (2016) yılında yapılan çalışmada, elektrokinetik ve biyoremediasyon ıslah teknikleri birlikte kullanılmıştır. 50 V m^{-1} elektrik gradyanı kullanılarak 7 gün boyunca, anotta Lysinibacillus fusiformis bakterisi uygulanmıştır. Uygulama sonucu yaklaşık %78 civarında cıva konsantrasyonunda azalma olduğu tespit edilmiştir.

Kim ve ark. (2012) tarafından yapılan çalışmada, arsenik (As) ile kontamine olmuş toprağın ex-situ elektrokinetik ıslahı değerlendirilmiştir. As'ın desorpsiyonunu arttırmak için sırasıyla katolit ve anolit olarak etilendiamin tetraasetik asit (EDTA) ve sodyum hidroksit, siltli ve kumlu killi toprakta uygulanmıştır. Arsenik ortalama %78'i sekiz hafta sonra iki toprak tipinden uzaklaştırılmıştır. Toprak tiplerinde ortalama kaldırma oranları sırasıyla 1.06 ve 1.55 mg kg^{-1} $gün^{-1}$ olduğu saptanmıştır.

Biyolojik iyileştirme teknikleri: Biyoremediasyon işlemleri, kirlenmiş ortamın çevre dostu bir şekilde bitkilerin ve makro ve mikro organizmaların kullanılarak iyileştirilmesi temelinde yapılan işlemlerden oluşur (Dindar ve ark., 2017). Biyoremediasyon işlemlerinde, kirlenmiş ortamdan kirleticileri uzaklaştırmak, tümden gidermek veya hareketsiz duruma getirmek amacıyla bitkilerin ve mikroorganizmaların biyolojik mekanizmaları kullanılmaktadır (Ayangbenro ve Babalola, 2017). Biyoremediasyon teknikleri diğer fiziksel ve kimyasal tekniklerle kıyaslandığında büyük alanlar için daha az maliyetli ve çevre dostu bir tekniktir (Blaylock ve ark., 1997). Biyoremediasyon teknikleri sıcaklık, pH, nem, oksijen gibi faktörlerden etkilenebilmektedir (Dandan ve ark., 2007; Yao ve ark., 2012).

Kirlenmiş ortamların temizlenmesi için yararlanılan mikroorganizmalar toprak içerisinde bulunan ağır metalleri ayrıştıramaz/parçalayamaz ancak ağır metalleri çeşitli fiziksel ve kimyasal formlarına dönüştürerek bünyelerine alabilmektedirler (Bosecker, 1999). Kirlenmiş topraklarda genelde ağır metallerin uzaklaştırılmasında kullanılan mikroorganizmalar bakteri ve mantarlardır fakat maya ve algler de ağır metal uzaklaştırılmasında kullanılmaktadır (Coelho ve ark., 2015). Kirlenmiş ortamlarda ağır metallerin uzaklaştırılmasında bitki ve mikroorganizmaların birlikte kullanılması ile daha hızlı ve etkili sonuç alınmaktadır (Vangronsveld ve ark., 2009). Biyoremediasyon ile ağır metallerin uzaklaştırılması işlemlerinin iyi bir sonuç vermesi için ortam şartlarının biyoremediasyonu sağlayacak organizmalar için uygun olması ve uzaklaştırılması yapılacak ortamda yeterli organizma bulunması gerekmektedir. Biyobirikim, biyoliç (metallerin çözünebilir forma dönüşümü), biyosorpsiyon, biyotransformasyon ve biyomineralizasyon ve metal ile mikroorganizma etkileşimleri biyoremediasyonun bazı mekanizmaları olarak yer almaktadır (Sikkema ve ark., 1995). De ve ark. (2008) tarafından yapılan çalışmada, Kadmiyum ve kurşun detoksifiye etme potansiyellerini değerlendirmek için 25 ppm'de veya daha yüksek cıva konsantrasyonlarında büyüyebilen cıvaya karşı oldukça dirençli olan Alcaligenes faecalis, Bacillus pumilus, Pseudomonas aeruginosa, Brevibacterium iodinium bakterileri 100 ppm olan büyüme ortamından sırasıyla 72 ve 96 saat içinde Cd'nin %70'inden fazlasını ve Pb'nin %98'ini çıkardığı gözlemlenmiştir. Hg, Cd ve Pb için detoksifikasyon etkinlikleri, ağır metallerin biyoremediasyonunda önemli bir uygulama olabileceği saptanmıştır.

Özbucak ve ark. (2018) yaptığı çalışmada, Cu (bakır), Pb (kurşun), Zn (çinko) maden yatağı topraklarından izole edilen bazı bakterilerin, Biyoremediasyon potansiyelleri araştırılmıştır. *Pseudomonas luteola*, *Paenibacillus polymyxa* ve *Pseudomonas stutzeri* ağır metal absorbe potansiyeli yüksek olan bu türler, kültür ile çoğaltılmıştır. *P. polymyxa* ve *P. luteola* bakterilerinin birbirlerinden ayrı olarak bakır elementini, *P. luteola* ve *P. polymyxa* bakterilerinin kombinasyonlarında ise çinko elementini uzaklaştırmada etkili oldukları tespit edilmiştir. *P. polymyxa* ve *P. luteola* bakterinin ayrı ve birlikte olduğu uygulama ortamda kurşun miktarının saptanmıştır.

Fitoremediasyon teknolojileri: Fitoremediasyon, kirlenmiş toprakta kirleticiyi azaltarak temizlemek için kirleticileri sabitlemek veya adsorbe etmek amacıyla kullanılan tekniklerdir (Yao ve ark., 2012). Fitoremediasyon teknolojileri arasında fitoekstraksiyon, rizofiltrasyon, fitostabilizasyon, fitovolatilizasyon ve fitodegradasyon yer almaktadır (Kong ve Glick, 2017).

Toprakta metal kirleticilerin temizlenmesinde, rizofiltrasyon, fitostabilizasyon fitoekstraksiyon yöntemleri kullanılmaktadır. Toprakta organik kirleticilerin temizlenmesinde ise rizodegradasyon, fitovolatizasyon, fitodegradasyon yöntemleri kullanılmaktadır (Aybar ve ark., 2015). Akümülatör bitkiler, toprakta olan metal varlığına kıyasla toprak üstü aksamına daha fazla metal biriktirebilen ve toprak ağır metal ıslahında kullanılabilen bitkilerdir (Baker ve Walker, 1990). Hiperakümülatör bitkiler, topraktaki metal seviyesinden 50-500 kat daha fazla toprak üstü aksamlarında metal biriktirebilen bitkilerdir (Clemens, 2006). En çok bilinen hiperakümülatör bitkilerden, Thlaspi, Chenopodium, Urtica, Polygonum sachalase ve Allyssim bitkisel aksamlarında kadmiyum, nikel, bakır, çinko ve kurşun gibi metalleri biriktirme potansiyelleri yüksek bitkilerdir (Mulligan ve ark., 2001).

Fitostabilizasyon, çevredeki kirleticilerin hareketliliğini ve biyoyararlanımını azaltmayı amaçlamaktadır (Radziemska ve ark., 2018). Genelde erozyonun meydana geldiği alanlarda kirlilik görülen yerden kirleticinin toprakla temasını önlemek ve yer altı sularına sızmasının önüne geçilmesi amacıyla yapılmaktadır (Bert ve ark., 2009). Fitostabilizasyon tekniğinde bitkiler kökleri ile kirleticiyi fiziksel ve kimyasal olarak sabitlemektedirler (Jabeen ve ark., 2009).

Zeng ve ark. (2018) tarafından yapılan çalışmada, *Osmanthus fragrans* (OF), *Ligustrum vicaryi* L. (LV), *Loropetalum chinense var. rubrum* (LC), *Cinnamomum camphora* (CC) ve *Euonymus japonicas cv. aureomar* (EJ) beş farklı süs bitkisinde, sera koşullarında; Cd $(NO_3)_2.4H_2O$ formunda uygulanan kadmiyum (0, 6, 21 mg kg^{-1}) dozlarında bitkilere uygulanmıştır. Sonuçlara olarak, süs bitkilerinin toprak kadmiyum içeriği 24.6 mg kg^{-1} 'den az bulunmuştur. Gelişimlerinde herhangi bir sorun olmadığı ve kadmiyumun OF, LV, LC ve EJ bitkilerinin köklerinde biriktiği saptanmıştır. Süs bitkilerinin fitostabilizasyon da kullanılmasının önemli olabileceği düşünülmektedir.

Yang ve ark. (2014) yaptıkları çalışmada, *Alternanthera philoxeroides*, *Artemisia princeps*, *Bidens frondosa*, *Bidens pilosa*, *Cynodon dactylon*, *Digitaria sanguinalis*, *Erigeron canadensis* ve *Setaria plicata* bitki türlerinin Cd, Mn, Pb ve Zn ağır metallerinin biyokonsantrasyonları üzerine çalışılmıştır. Cd, Mn, Pb ve Zn için ilişkili topraklardan, biyokonsantrasyon faktörleri sürgünler ve köklerde 1'den az bulunmuştur. Özellikle mangan (Mn) fitostabilizasyonu için, sekiz bitki çeşidinin, ağır metallere karşı gösterdiği toleransın yüksek olduğu ve fitostabilizasyon tekniği için potansiyel bitki olabileceklerini saptamışlardır.

Fitoekstraksiyon, ortamdaki kirleticileri uzaklaştırmak ve toprağın uzun süreli temizliğini sağlamak amacıyla bitki kökleri tarafından topraktan kirleticilerin alınması, topraktan alınan kirleticilerin sürgüne veya diğer hasat edilebilir bitki aksamlarına taşınması anlamına gelmektedir (Bhargava ve ark., 2012). Hiperakümülatör bitkiler, kirleticileri bünyelerinde biriktirme potansiyelleri yüksek olabildiği için, fitoekstraksiyon da kullanılabilen bitki türleri arasında kullanılmalarının avantajlı olabileceği düşünülmektedir (Cristaldi ve ark., 2017).

Guo ve Miano (2010) tarafından yapılan bir çalışmada; çok yıllık otsu bitki Arundo donax'ın kadmiyum (Cd) ile kirlenmiş bir toprağa karşı fitoekstraksiyon kapasitesini değerlendirmişler sonucunda, yapraklarda ve rizomlarda sırasıyla 2.92-4.02 mg kg^{-1} ve 0.57-1.42 mg kg^{-1} arasında değerler elde etmişlerdir. Cd ile kirlenmiş toprağın fitoekstraksiyonda kullanılan Arundo donax'ın Cd'ı biriktirme kapasitesi açısından önemli olduğu saptanmıştır.

Salam ve ark. (2019) tarafından yapılan çalışmada, bakır (Cu) ve çinko (Zn) kirliliği görülen maden sahasında, dört Salix çeşidinin bitki gelişimi, bakır, çinko alımı ve fitoekstraksiyon kabiliyetleri değerlendirilmiştir. Çeşitlerde sürgünler, yapraklar ve köklerdeki toplam bakır konsantrasyonları 163-474 mg kg^{-1} ve çinko konsantrasyonları 776 -1823 mg kg^{-1} arasında bulunmuştur. Sonuç olarak, Salix çeşitlerinin önemli miktarda Cu ve Zn biriktirme potansiyelinin olduğu saptanmıştır.

Rizofiltrasyon, karasal veya sucul ekosisteme ait bitkilerin, köklerinden kirleticiyi emerek, konsantre etmek ve biriktirmek amacıyla kullanılmasıdır (Jadia ve Fulekar, 2009). Kara bitkileri kök alan miktarlarını arttırması ve potansiyel olarak toksik metalleri etkili bir şekilde ortadan kaldıran lifli ve uzun kök sistemlerine sahip olmaları nedeniyle sucul bitkilere göre daha çok tercih edilmektedirler (Ghori ve ark., 2015).

Ignatius *ve ark.* (2014) yapılan çalışmada, Pb içeren atık suyun *P. amboinicus* bitkisi tarafından rizofiltrasyonunun araştırılmıştır. 15 gün süresince hidroponik ortamda yetiştirilen aynı boyutlardaki *P. amboinicus* bitkileri, Pb (NO3)2 olarak sağlanan 5-200 mg l^{-1} Pb içeren 100 ml damıtılmış su içerinde uygulanmıştır. 20 günlük uygulamada bitki 100 mg l^{-1} Pb'ye kadar tolere etmiş ve (0, 5, 15, 25, 50, 100, 200) mg l^{-1} Pb konsantrasyonlarında sırasıyla (8.7, 9.26, 10.5, 11.11, 11.36, 11.76, 12.02) mg kg^{-1} ölçülmüştür. Pb'yi genelde köklerde biriktirerek toprak üstü aksamına taşınmasını kısıtladığı saptanmıştır.

Meyers ve ark. (2018) tarafından yapılan çalışmada, hidroponik ortamda yetiştirilen *Brassica juncea* (Hardal otu), 14 günlük büyüme periyodunda (3 günlük uygulama; kurşun (Pb) aktiviteleri 3.2, 32 ve 217) tarafından tutulan kurşun alımı ve dağılımı araştırılmıştır. X-ışını fotoelektron spektroskopisi ile yapılan ölçümde kurşun (Pb) birikimi kök uçlarında yoğun bir şekilde tespit edilmiştir. *B. juncea* fazla dallanan kökleri nedeniyle ağır metal rizofiltrasyonunda kullanılabileceği saptanmıştır.

Fitoremediasyon için bitki türleri hızlı büyümeli, bol vejetatif aksam, yüksek konsantrasyonlu metallere tolerans ve yüksek metal biriktirme yeteneği gibi özelliklere sahip olması gerekmektedir (Jabeen k 2009).

SONUÇ

Doğal ve insan faaliyetleri sonucu toprak kirliliği oluşmaktadır. Ağır metaller yüksek yoğunluklu toksik metallerdir. Başta toprakta ağır metal birikimiyle birlikte bitkinin bünyesine alınarak, özellikle insanların ve hayvanların tüketimi ile çok büyük riskler meydana getirmektedir. Ağır metallerin toprakta birikmesi toprakta kalite kaybı, bitkinin metabolik olaylarında gerileme meydana gelmesi ve devamında durması, insan ve hayvanlarda nörolojik ve kanserojenik olumsuzluklar doğurabilmektedir. Önemli bir sorun olan ağır metal kirliliğinin toprak bünyesinden giderilmesi veya en az düzeye indirilmesi büyük önem taşımaktadır. Bu açıdan yapılacak olan çalışmaların daha fazla kirliliğe sebep olmaması, ekosistemin korunması adına çevre dostu ve geniş alanlarda uygulanabilir olmalarına dikkat edilmesi gerekmektedir. Sonuç olarak, ıslah teknikleri göz önüne alınacak olunursa biyoremediasyon ve fitoremediasyon teknolojilerinin çevre dostu ve uygun maliyetli olmaları nedeniyle ağır metal kirliliğinin giderimi ve toprak sağlığının düzeltilmesi üzerine yapılan çalışmaların daha çok arttırılması gerekmektedir. Biyoremediasyon ve fitoremediasyon teknolojilerinde kullanılan tekniklerin kombinasyonlarının daha etkili ve hızlı sonuç verebileceği düşünülmektedir.

ÇIKAR ÇATIŞMASI

Yazar olarak herhangi bir çıkar çatışması olmadığını beyan ederiz.

YAZAR KATKISI

Yazarlar olarak makaleye aşağıdaki katkıların sunulduğunu beyan ederiz.

Osman Sönmez: Verilerin incelenmesi, makalenin son şeklinin verilmesi.
Fatma Nur Kılıç: Çalışmanın planlanması, literatür taraması, makalenin genel kontrolü.

KAYNAKLAR

Ackova DG (2018). Heavy metals and their general toxicity on plants, *Plant Science Today, 5: 15-19.*

Adriano DC, Wenzel WW, Vangronsveld J and Bolan NS (2004). Role of assisted natural remediation in environmental cleanup. *Geoderma, 122: 121-142.*

Ahmad MSA and Ashraf M (2011). Essential roles and hazardous effects of nickel in plants. *Reviews of Environmental Contamination and Toxicology*, *214: 125-167.*

Ali H and Khan E (2018). What are heavy metals? Long-standing controversy over the scientific use of the term 'heavy metals'–proposal of a comprehensive definition. *Toxicological & Environmental Chemistry*, *100: 6-19.*

Almaroai YA, Usman ARA, Ahmad M, Kim KR, Moon DH, Lee SS and Ok YS (2012). Effects of synthetic chelators and low-molecular-weight organic acids on chromium, copper, and arsenic uptake and translocation in Maize (*Zea mays* L.). *Soil Science*, *177: 655-663.*

Almasi A, Dargahi A, Ahagh MMH, Janjani H, Mohammadi M and Tabandeh L (2016). Efficiency of a constructed wetland in controlling organic pollutants, nitrogen, and heavy metals from sewage. *Journal of Chemical and Pharmaceutical Sciences*, *9: 2924-2928.*

Asri FÖ ve Sönmez S (2006). Ağır metal toksisitesini bitki metabolizması üzerine etkileri. *Derim 23: 36-45.*

Ayangbenro AS and Babalola OO (2017). A new strategy for heavy metal polluted environments: A review of microbial biosorbents. *International Journal of Environmental Research and Public Health*, *14(1): 94.*

Aybar M, Bilgin A ve Sağlam B (2015). Fitoremediasyon yöntemi ile topraktaki ağır metallerin giderimi, *Artvin Çoruh Üniversitesi Doğal Afetler Uygulama ve Araştırma Merkezi Doğal Afetler ve Çevre Dergisi*, *1(1-2): 59-65.*

Azhar ATS and Nabila ATA, Nurshuhaila MS, Zaidi E, Azim, MAM and Farhana SMS (2016). Assessment and comparison of electrokinetic and electrokinetic bioremediation techniques for mercury contaminated soil. *International engineering research and innovation symposium (IRIS) IOP Publishing IOP Conference Series. Materials Science Engineering, 160: 1-8.*

Başbakanlık Mevzuatı Geliştirme ve Yayın Genel Müdürlüğü (2010). https://www.resmigazete.gov.tr/eskiler/2010/06/20100608-3.htm (08/06/2010).

Baker AJM and Walker PL (1990). Ecophysiology of metal uptake by tolerant plants, in: Shaw A.J. (Ed.), Heavy metal tolerance in plants: *Evolutionary Aspects*, *CRC Press*, Boca Raton, 155-177.

Bert V, Seuntjens P, Dejonghe W, Lacherez S, Thuy HTT and Vandecasteele B (2009). Phytoremediation as a management option for contaminated sediments in tidal marshes, flood control areas and dredged sediment landfill sites. *Environmental Science and Pollution Research*, *16: 745-764.*

Bhandari A, Surampalli, RY, Champagne P, Ong SK, Tyagi RD and Lo IMC (2007). Remediation technologies for soils and groundwater. Remediat. *Remediation Technologies for Soils and Groundwater*, *60: 1-449.*

Bhargava A, Carmona FF, Bhargava M and Srivastava S (2012). Approaches for enhanced phytoextraction of heavy metals. *Journal of Environmental Management*, *105: 103-120.*

Blaylock MJ, Salt DE, Dushenkov S, Zakharova O, Gussman C, Kapulnik Y, Ensley BD and Raskin I (1997). Enhanced accumulation of Pb in Indian mustard by soil-applied chelating agents. *Environmental Science & Technology, 31: 860-865.*

Bolan NS, Adriano DC and Naidu R (2003). Role of phosphorus in (im)mobilization and bioavailability of heavy metals in the soil-plant system. *Reviews of Environmental Contamination and Toxicology, 177: 1-44.*

Bosecker K (1999). Microbial leaching in environmental clean-up programmes. *Process Metall, 9: 533-536.*

Chen M, Xu P, Zeng G, Yang, C, Huang D and Zhang J (2015). Bioremediation of soils contaminated with polycyclic aromatic hydrocarbons, petroleum, pesticides, chlorophenols and heavy metals by composting: Applications, microbes and future research needs. *Biotechnology Advances, 33: 745-755.*

Cherfouh R, Lucas Y, Derridj A and Merdy P (2018). Long-term, low technicality sewage sludge amendment and irrigation with treated wastewater under Mediterranean climate: impact on agronomical soil quality. *Environmental Science and Pollution Research, 25: 35571-35581.*

Chokor AA and Ekanem EO (2016). Heavy metals contamination profile in soil from automobile workshops in sapele, Nigeria. *World Journal of Analytical Chemistry, 4(2): 26-28.*

Clemens S (2006). Toxic metal accumulation, responses to exposure and mechanisms of tolerance in plants. *Biochimie*, *88(11): 1707-1719.*

Coelho M, Luciene M, Rezende HC, Coelho Luciana M, de Sousa PAR, Melo DFO and Coelho NMM (2015). Bioremediation of polluted waters using microorganisms. *Adv. Bioremediation Wastewater Polluted Soil, 1-22.*

Cristaldi A, Conti G, Jho EH, Zuccarello P, Grasso A, Copat C, and Ferrante M (2017). Phytoremediation of contaminated soils by heavy metals and PAHs. A brief review. *Environmental Technology & Innovation*, *8: 309-326.*

Çağlarırmak N ve Hepçimen Z (2010.) Ağır metal toprak kirliliğinin gıda zinciri ve insan sağlığına etkisi. *Akademik Gıda*, *8: 31-35.*

Dandan W, Huixin L, Feng H and Xia W (2007). Role of earthworm-straw interactions on phytoremediation of Cu contaminated soil by ryegrass. *Acta Ecologica Sinica*, *27: 1292-1298.*

De J, Ramaiah N and Vardanyan L (2008). Detoxification of toxic heavy metals by marine bacteria highly resistant to mercury. *Marine Biotechnology*, *10(4): 471-477.*

Derakhshan NZ, Jung MC and Kim KH (2018). Remediation of soils contaminated with heavy metals with an emphasis on immobilization technology. *Environmental Geochemistry and Health, 40: 927-953.*

Dermont G, Bergeron M, Mercier G and Richer-Laflèche M (2008). Soil washing for metal removal: a review of physical/chemical technologies and field applications. *Elsevier, 152(1): 1-31.*

Dindar E, Şen CN, Topaç ŞFO ve Başkaya HS (2017). Topraklarda organik azot fraksiyonlarının belirlenmesi. *Gazi Üniversitesi Mühendislik-Mimarlık Fakültesi Dergisi, 32: 767-775.*

Ghani A (2010). Toxic effects of heavy metals on plant growth and metal accumulation in maize (*Zea mays*). *Iranian Journal of Toxicology, 3: 325-334.*

Ghori Z, Iftikhar H, Bhatti MF, Nasar UM, Sharma I, Kazi AG and Ahmad P (2015). Phytoextraction: The use of plants to remove heavy metals from soil. *Plant Metal Interaction: Emerging Remediation Techniques*, *29: 361-384.*

Golui D, Datta SP, Dwivedi BS, Meena MC, Varghese E, Sanyal SK, Ray P, Shukla AK and Trivedi VK (2019). Assessing soil degradation in relation to metal pollution–a multivariate approach. *Soil and Sediment Contamination*, *28: 630-649.*

Gomes HI, Dias FC and Ribeiro AB (2013). Overview of in situ and ex situ remediation technologies for PCB-contaminated soils and sediments and obstacles for full-scale application. *Science of The Total Environment*, *237-260.*

Guo ZH and Miao XF (2010). Growth changes and tissues anatomical characteristics of giant reed (*Arundo donax* L.) in soil contaminated with arsenic, cadmium and lead. *Journal of Central South University of Technology, 17(4): 770-777.*

Hakeem KR (2015). Crop production and global environmental issues. *Crop Production* and *Global Environmental, Issues 1-598.*

He ZL, Yang XE and Stoffella PJ (2005). Trace elements in agroecosystems and impacts on the environment. *Journal of Trace Elements in Medicine and Biology, 19: 125-140.*

Ignatius A, Arunbabu V, Neethu J and Ramasamy EV (2014). Rhizofiltration of lead using an aromatic medicinal plant Plectranthus amboinicus cultured in a hydroponic nutrient film technique (NFT) system. *Environmental Science and Pollution Research*, *21(22): 13007-13016.*

Jabeen R, Ahmad A and Iqbal M (2009). Phytoremediation of heavy metals: Physiological and molecular mechanisms. *The Botanical Review, 75: 339-364.*

Jadia CD and Fulekar MH (2009). Phytoremediation of heavy metals: Recent techniques. *African Journal of Biotechnology, 8: 921-928.*

Jankaite A and Vasarevičius S (2005). Remediation technologies for soils contaminated with heavy metals. *Journal of Environmental Engineering and Landscape Management, 13: 109-113.*

Jiang W, Tao T and Liao ZM (2011). Removal of heavy metal from contaminated soil with chelating agents. *Open Journal of Soil Science, 01: 70-76.*

Kabata-Pendias A (2000). Trace elements in soils and plants. *CRC Press.*

Kafadar FN ve Saygıdeğer S (2010). Gaziantep ilinde organize sanayi bölgesi atik sulari ile sulanan bazı tarım bitkilerinde kurşun (pb) miktarlarinin belirlenmesi. *Ekoloji, 48: 41-48.*

Khalid S, Shahid M, Niazi NK, Murtaza B, Bibi I and Dumat C (2017). A comparison of technologies for remediation of heavy metal contaminated soils. *Journal of Geochemical Exploration*, *182: 247-268.*

Kızıloğlu FM, Turan M, Sahin U, Kuslu Y ve Dursun A (2008). Effects of untreated and treated wastewater irrigation on some chemical properties of cauliflower (*Brassica olerecea* L. var. *botrytis*) and red cabbage

(*Brassica olerecea* L. var. *rubra*) grown on calcareous soil in Turkey. *Agricultural Water Management, 95: 716-724.*

Kim JO, Lee YW and Chung J (2013). The role of organic acids in the mobilization of heavy metals from soil. *KSCE Journal of Civil and Environmental Engineering Research, 17: 1596-1602.*

Kirpichtchikova TA, Manceau A, Spadini L, Panfili F, Marcus MA and Jacquet T (2006). Speciation and solubility of heavy metals in contaminated soil using X-ray microfluorescence, EXAFS spectroscopy, chemical extraction, and thermodynamic modeling. *Geochimica et Cosmochimica Acta, 70: 2163-2190.*

Kim YH, Kim DH, Jung HB, Hwang BR, Ko SH and Baek K (2012). Pilot scale ex-situ electrokinetic remediation of arsenic-contaminated soil. *Separation Science and Technology*, *47(14-15): 2230-2234.*

Kong Z and Glick BR (2017). The role of plant growth-promoting bacteria in metal phytoremediation. *Advances in microbial physiology*, *71: 97-132.*

Leuther F, Schlüter S, Wallach R and Vogel HJ (2019). Structure and hydraulic properties in soils under long-term irrigation with treated wastewater. *Geoderma*, *333.*

Lindsay WL and Doxtader KG (1981). Environmental chemistry of the elements. *Journal of Environmental Quality, 10: 249-249.*

Maity JP, Huang YM, Fan CW, Chen CC, Li CY, Hsu CM, Chang YF, Wu CI, Chen CY and Jean JS (2013). Evaluation of remediation process with soapberry derived saponin for removal of heavy metals from contaminated soils in Hai-Pu, Taiwan. *Journal of Environmental Sciences*, *25: 1180-1185.*

Meyers DE Auchterlonie GJ, Webb RI and Wood B (2008). Uptake and localisation of lead in the root system of Brassica juncea*. Environmental Pollution*, *153(2): 323-332.*

Mikhailenko AV, Ruban DA Ermolaev VA and Loon AJ (2020). Cadmium pollution in the tourism environment: A literature review. *Geosciences, 10: 1-18.*

Mohsenzadeh F and Mohammadzadeh R (2018). Phytoremediation ability of the new heavy metal accumulator plants. *Environmental and Engineering Geoscience*, *24(4): 441-450.*

Montiel MM, Madejón E and Madejón P (2016). Effect of heavy metals and organic matter on root exudates (low molecular weight organic acids) of herbaceous species: An assessment in sand and soil conditions under different levels of contamination. *Environmental Pollution, 216: 273-281.*

Mulligan CN, Yong RN and Gibbs BF (2001). Remediation technologies for metalccontaminated soils and groundwater: an evaluation, *Engineering Geology*, *60: 193-207.*

Naila A, Meerdink G, Jayasena V, Sulaiman AZ, Ajit AB and Berta G (2019). A review on global metal accumulators mechanism, enhancement, commercial application, and research trend. *Environmental Science and Pollution Research*, *26: 26449-26471.*

Navarro A, Cardellach E, Cañadas I and Rodríguez J (2013). Solar thermal vitrification of mining contaminated soils. *International Journal of Mineral Processing*, *119: 65-74.*

Okçu M, Tozlu E, Kumlay A and Pehluvan M (2009). Ağır metallerin bitkiler üzerine etkileri. *Alınteri Journal of Agriculture Science*, *17(2): 14-26.*

Özbucak T, Ertürk Ö, Ergen AÖ, Polat G ve Özbucak S (2018). Maden yataklarında bulunan bazı bakterilerin ağır metallerin biyoremidasyonunda kullanılabilme potansiyellerinin belirlenmesi. *Ordu Üniversitesi Bilim ve Teknoloji Dergisi*, *8(1): 114-124.*

Özkan A (2017). Antakya-Cilvegözü karayolu etrafındaki tarım arazilerinde ve bitkilerdeki ağır metal kirliliği. *Çukurova Üniversitesi Mühendislik-Mimarlık Fakültesi Dergisi*, *32(3): 9-18.*

Özkul C (2019). Kütahya şehir merkezinde yer alan çocuk parklarındaki toprakların ağır metal kirliliğinin belirlenmesi. *Afyon Kocatepe Üniversitesi Fen ve Mühendislik Bilimleri Dergisi*, *19(1): 226-240.*

Radziemska M, Koda E, Bilgin A and Vaverková MD (2018). Concept of aided phytostabilization of contaminated soils in postindustrial areas. *International Journal of Environmental Research and Public Health, 15(24).*

Ren J, Zhao Z, Ali A, Guan W, Xiao R, Wang JJ and Li R (2020). Characterization of phosphorus engineered biochar and its impact on immobilization of Cd and Pb from smelting contaminated soils. *Journal of Soils and Sediments, 20(8): 3041-3052.*

Salam MMA, Mohsin M, Kaipiainen E, Villa A, Kuittinen S, Pulkkinen P and Pappinen A (2019). Biomass growth variation and phytoextraction potential of four Salix varieties grown in contaminated soil amended with lime and wood ash. *International journal of phytoremediation*, *21(13): 1329-1340.*

Schwalfenberg G, Rodushkin I and Genuis SJ (2018). Heavy metal contamination of prenatal vitamins, *Toxicology Reports*, *5: 390-395.*

Sikkema J, De Bont JAM and Poolman B (1995). Mechanisms of membrane toxicity of hydrocarbons. *Microbiological reviews, 59: 201-222.*

Singh S, Parihar P, Singh R, Singh VP and Prasad SM (2016). Heavy metal tolerance in plants: Role of transcriptomics, proteomics, metabolomics, and ionomics. *Frontiers in Plant Science, 6: 1-36.*

Song B, Zeng G, Gong J, Liang J, Xu P, Liu Z, Zhang Y, Zhang C, Cheng M, Liu Y, Ye S, Yi H and Ren X (2017). Evaluation methods for assessing effectiveness of in situ remediation of soil and sediment contaminated with organic pollutants and heavy metals. *Environment International, 105: 43-55.*

Sönmez S ve Asri F (2006). Ağir metal toksisitesini bitki metabolizması üzerine etkileri. *Derim, 23: 36-45.*

Sun H, Wang H, Qi J, Shen L and Lian X (2011). Study on surfactants remediation in heavy metals contaminated soils. ISWREP 2011- Proc. 2011 Int. Symp. *Water Resources Environmental Protection*, *3: 1862-1865.*

Sun R, Yang J, Xia P, Wu S, Lin T and Yi Y (2020). Contamination features and ecological risks of heavy metals in the farmland along shoreline of Caohai plateau wetland. *Chemosphere*, *254: 126828*.

U.S. Environmental Protection Agency (1994). Revised interim soil lead guidance for CERCLA sites and RCRA corrective action facilities. Report No.: OSWER Directive No. 9355.4-12. EPA/540/F-94/043. PB94-963282. Washington, DC: U.S. *Environmental Protection Agency, Office of Emergency and Remedial Response.*

USAEC (2000). In-situ electrokinetic remediation of metal contaminated soils technology status report US Army Environmental Center. https://cluin.org/download/toolkit/thirdednew/insituelectrokinetic.pdf (07.16.2020).

Vangronsveld J, Herzig R, Weyens N, Boulet J, Adriaensen K, Ruttens A, Thewys T, Vassilev A, Meers E, Nehnevajova E, Lelie D and Mench M (2009). Phytoremediation of contaminated soils and groundwater: Lessons from the field. *Environmental Science and Pollution Research*, *16: 765-794.*

Vareda JP, Valente AJM and Durães L (2016). Heavy metals in Iberian soils: Removal by current adsorbents/amendments and prospective for aerogels. *Advances in Colloid and Interface Science*, *237: 28-42.*

Varol Z ve Erdem DB (2020). Çorlu deresi ve yakın çevresi (Çerkezköy-Çorlu hattı) topraklarının ağır metal kirliliğinin değerlendirilmesi . *Toprak Bilimi ve Bitki Besleme Dergisi, 8(1): 26-35.*

Wei CY and Chen TB (2006). Arsenic accumulation by two brake ferns growing on an arsenic mine and their potential in phytoremediation. *Chemosphere, 63: 1048-1053*.

Weissmannová HD, Mihočová S, Chovanec P and Pavlovský J (2019). Potential ecological risk and human health risk assessment of heavy metal pollution in industrial affected soils by coal mining and metallurgy in Ostrava, Czech Republic. *International Journal of Environmental Research and Public Health, 16(22): 4495.*

WHO/FAO (2007). Joint FAO/WHO Food Standard Programme Codex Alimentarius Commission 13th Session. Report of the Thirty-Eight Session of the Codex Committee on Food Hygiene, Houston, United States of America (07/30/13).

Wuana RA and Okieimen FE (2011). Heavy Metals in Contaminated Soils: A Review of sources, chemistry, risks and best available strategies for remediation. *ISRN Ecology, 1-20.*

Yao Z, Li J, Xie H and Yu C (2012). Review on remediation technologies of soil contaminated by heavy metals. *Procedia Environmental Sciences, 16: 722-729.*

Yang S, Liang S, Yi L, Xu B, Cao J, Guo Y and Zhou Y (2014). Heavy metal accumulation and phytostabilization potential of dominant plant species growing on manganese mine tailings. *Frontiers of Environmental Science & Engineering*, *8(3): 394-404.*

Yerli C, Çakmakcı T, Şahin U ve Tüfenkçi Ş (2020). Ağır metallerin toprak, bitki, su ve insan sağlığına etkileri. *Türk Doğa ve Fen Dergisi, 9(Özel Sayı): 103-114.*

Zeng P, Guo Z, Cao X, Xiao X, Liu Y and Shi L (2018). Phytostabilization potential of ornamental plants grown in soil contaminated with cadmium, *International Journal of Phytoremediation*, *20 (4): 311-320.*

Zhai X, Li Z, Huang B, Luo N, Huang M, Zhang Q and Zeng G (2018). Remediation of multiple heavy metal-contaminated soil through the combination of soil washing and in situ immobilization. *Science of the Total Environment*, *635: 92-99.*

Turkish Journal of Agricultural Engineering Research

https://dergipark.org.tr/en/pub/turkager
https://doi.org/10.46592/turkager.2021.v02i02.021

Turk J Agr Eng Res (TURKAGER)
e-ISSN: 2717-8420
2021, 2(2): 508-516

Review Article

Chemical Coagulation: An Effective Treatment Technique for Industrial Wastewater

Aijaz PANHWAR[a*], **Aftab KANDHRO**[b], **Sofia QAISAR**[a]. **Mudasir GORAR**[c], **Eidal SARGANI**[d], **Humaira KHAN**[e]

[a] *PCSIR Laboratories Complex, Karachi, PAKISTAN*

[b] *M.A. Kazi Institute of Chemistry, University of Sindh Jamshoro, PAKISTAN*

[c] *Government Degree College Mehar District Dadu, Sindh, PAKISTAN*

[d] *Government Degree College Malir Cantonment, Karachi PAKISTAN*

[e] *M. A. Kazi Institute of Chemistry, University of Sindh, Jamshoro, PAKISTAN*

(*): Corresponding author, aijazap@yahoo.com

ABSTRACT

Industrial sector is a backbone of the economy throughout the world. Despite that there are a lot of benefits; such as development of urbanization, major contributor in economy's growth is sign of industrial development. There are a lot of adverse effects on environment including depletion and damage of our natural and precious resources. Textile, cement, paper and pulp, sugarcane, food, pharmaceuticals, chemical, paint and other industries are largest consumers of the freshwater; for meeting the requirements of industrial production requirement for the industrial sector for their production. As a result the discharged huge amount of water in form of highly polluted water, this is a great threat to our ecosystem. The unplanned industrialization is a prime responsible for degradation of environment. If industrial wastewater is not properly treated instantly, it may create foulest and septic conditions in adjacent parts of the industrial areas. The discharges acute poisonous wastewater by different industries is responsible for reduction of penetration in crops, and severely affects aquatic life. There are many treatment techniques such as coagulation, adsorption, membrane, biological etc. by different research studies disclosed that coagulation with different chemicals alum, ferric chloride, lime, PACl, PVA and ferrous sulphate are very effective for remove of pollution. The industrial wastewater creates several problems such as health problems, aquatic life including water pollution. In this paper reviews the chemical coagulation treatment technologies for industrial wastewater.

RESEARCH ARTICLE

Received: 20.10.2021
Accepted: 04.12.2021

Keywords:

- Alum,
- Chemical coagulation,
- Industrial wastewater,
- Polyaluminum,
- Chloride,
- Treatment techniques

To cite: Panhwar A, Kandhro A, Qaisar S, Gorar M, Sargani E, Khan H (2021). Chemical Coagulation: An Effective Treatment Technique for Industrial Wastewater. Turkish Journal of Agricultural Engineering Research (TURKAGER), 2(2): 508-516. https://doi.org/10.46592/turkager.2021.v02i02.021

INTRODUCTION

Water is a most vital and valuable source for all living organisms and also important role in environment. Decontaminated water is an important requirement for all living organisms including human beings. Wastewater may be considered as wealth, if we use it after treatment properly; due to utilization of treated wastewater we can increase agricultural production to tide over the hunger in world. otherside it seems a biggest problem of future not only in developing countries but it will affect in developed world by industrial development and rapid growth of population. Industrial wastewater has becomes environmental and health threat to urban populated areas as well it is assets if properly treated (Drechsel *et al.,* 2015; UN Water, 2015). Over the years, the industrial wastewater has been a cause of pollution due to rapid urbanization; industrial revolution and luxury life style are the main factors. Now a day, an estimated 80% of global industrial saline wastewater is discharging without proper treatment into the environment. Industrial wastewater is a gateway to environmental degradation and diseases by contaminated water. Industrial wastewater is defined as waste generated by manufacturing or industrial processes. Natural waters may be more contaminated by the discharge of industrial waste by different industries. Wastewater word is used for the mixture by industries, municipal and agriculture actions. It comprises biological, chemical and physical pollutants. Unregulated and indiscriminate discharge of industrial pollution is the greatest threat and is degrading the environment of the vicinity areas. Harmful compounds in wastewater may extremely interrupt marine ecosystems. The wastewater chunks the photosynthesis process which is basic need for plants. There is a major role of industrial wastewater for soil and water bodies polluting within the nearby areas; and also equally responsible for the contamination of canals, groundwater, other water resources as well as coastal line areas. Textile, sugarcane, leather, pulp and paper, cement, paint, tannery, chemical industries, food processing, packaging, ghee, fertilizer, pesticides, petroleum refineries, pharmaceuticals, rubber, thermal power houses (electricity generation), mainly plants by coal fire, are a main cause of industrial saline wastewater. Among these almost all industries are responsible for discharge of wastewater without any prior treatment, with significant levels of pollutants and metals such as chromium, mercury lead, and cadmium as well as selenium, arsenic, and nitrates and nitrites. Pollutants in industrial saline wastewater can be removed, converted or broken down during the treatment process. Industrial saline wastewater treatment is not an easy and affordable way to remove pollutants from wastewater especially in developing countries. It requires huge amount/budget for proper treatment to fulfill the mandatory requirements set by regulatory authorities. Around 80% of wastewater is released to the environment with none prior treatment, ultimately resulting in a rising worsening of overall water quality with harmful impacts on human similarly as ecosystems (UN WWAP, 2017). How does wastewater affect the environment; waterways are generally most at risk to the harmful effects of wastewater. Textile industry is one of the largest industrial sectors. It boosts the economic development worldwide (Ghaly *et al.,* 2014). The industry is responsible for generation of around one-fifth of industrial saline wastewater pollution throughout the world; using around twenty thousand chemicals which are highly toxic, used to make clothes and ultimately discharge without proper treatment, into environment. Textile sector is consumer of freshwater as compared to other industries.

The industry is also a biggest threat to the environment. Other side textile sector is a great contributor of economic development. Industrial saline wastewater is a main hurdle for growth of the textile industry. The wastewater is responsible for numerous complications such as health issues, and aquatic life in form of contamination of water (Isık and Sponza, 2006). Due to industrialization there is a prominently increasing pollution issues; a huge quantity of organic and industrial saline wastewater, the water and land is polluting gradually. It reduces sunlight, and disturbing photosynthesis process of aquatic plants (Zaharia *et al.*, 2009). The cement manufacturing industries are considered as one of the major environmental polluting industries in the world (Akeem, 2008). Sugarcane industry is also one of the biggest users of freshwater and responsible for addition of wastewater in environment. Wastewater generation by sugarcane industry is very hazard and threat to the environment, comprises of in high quantity of chemical oxygen demand (COD), biological oxygen demand (BOD), total dissolved solids (TDS), and Total suspended solids (TSS), which are mainly responsible for reduction of oxygen. If wastewater by industries is not treated at right time, it may create very worst conditions (foul smelling and septic condition) in vicinity of industrial areas. This toxic wastewater is also responsible for less penetration, and threat to crops and aquatic life (Zaharia *et al.*, 2009). The food and its allied packaging materials is around fifty percent of generated municipal solid waste (US EPA, 2014). The total generation of MSW in 2018 was 292.4 million tons, which was approximately 23.7 million tons more than the amount generated in 2017. This is an increase from the 268.7 million tons generated in 2017 and the 208.3 million tons in 1990 (US EPA, 2021). It is projected for millions ton of plastic made up of trillions of quantities swirling in oceans. Around 5% of the used plastic mass is noticeable on the surface; while the remaining is floating settled into the oceans (Winn, 2016; Thompson *et al.*, 2009; Khalil *et al.*, 2016; Nurul *et al.*, 2016).

CHEMICAL COAGULATION

Coagulation is used for the wastewater treatment around more than one century ago (Guven *et al.*, 2009). The chemical coagulation (conventional) is best method for removal of organic; if dose of the coagulant and adjustment of pH in optimal range. The increasing dose (more than use for turbidity removal) of the coagulant (alum) can achieve the best results for the removal of organic. Alum dose and pH are very important variables in industrial wastewater treatment process (Sahu and Chaudhary, 2013). Coagulation-flocculation is particularly employed for effective removal of colloidal sized particles. Aluminum salts are widely used as coagulants in water treatment process due to its effectiveness in removing a broad range of impurities, including colloidal particles and dissolved organic substances (Teh *et al.*, 2016; Zonoozi *et al.*, 2008). The alum as the coagulant is capable of achieving significant organic removal. The pH of the wastewater during coagulation has profound influences on the effectiveness of coagulation for organic removal. Organic removal is much better in slightly acidic condition. For water of higher organic content, the optimum pH is displaced to slightly more acidic values (Sahu, 2019); chemical coagulation (Sahu and Chaudhari, 2014), electrochemical treatment

(Sahu and Chaudhari, 2015). (Noppakhun and Thunyalux, 2016) used different coagulants ($Al_2(SO_4)_3.18H_2O$), Polyaluminum chloride (PACl), Ferric chloride hexahydrate; and ferric sulfate hepta hydrate for removal of pollutants such as color by $FeCl_3$, turbidity by Alum, $FeCl_3$ and $Fe_2(SO_4)_3$. Coagulation is considerably affected by pH changes and results in a significant removal of colored impurities (Tchamango *et al.,* 2010). Aluminum is easily available economically fit and highly efficient as compared to other metals for industrial effluent and drinking water treatment (Moussa *et al.,* 2017) reported that Alum shows decrease of COD and color reduction as compared to aluminum chloride which showed much reductions of ferrous sulfate. Coagulation and flocculation are usually followed by sedimentation, filtration and disinfection. The problems with this treatment process include poor % recovery, operational issues, arbitrary guidelines and dependency on various operational parameters (Holt *et al.,* 2002). Samsuddin *et al.* (2019) used alum, ferric chloride and Polyaluminum chloride (PACl) for selection of suitable coagulant. The optimum condition of the coagulant (pH, coagulant dosage, fast mixing speed) was determined by using Design Expert software. Results showed that alum can be used to effectively for removal of COD and TSS at high dosage. Polyaluminum chloride (PACl) allows formation of floc faster compared to other coagulant as it has high positive electrical charge so it can neutralize the charges of the colloidal easily and reduce the repellent between particles thus allows the particles to form larger flocs (Poddar and Sahu, 2017). By using PACl, percentage of COD that can be removed was much better and same for TSS removal (Aziz *et al.,* 2017). The most suitable coagulant was determined based on its efficiency to reduce COD and TSS in the wastewater at different dosages. By using alum and PACl as coagulant, the percentage of turbidity can be removed effectively (Ghafari *et al.,* 2010). $FeCl_3$ and alum has high percentage of turbidity removal at high dosage and achieved the reduction target. In contrast, PACl shows decreasing of percentage of turbidity removal at high dosage and did not achieve the target. This reduction may be due to charge reversal and re-stabilization of colloidal particles by reason of overdosing (Radhi and Borghei, 2017). By using PACl, the percentage of TSS removal was remarkable (Sahu, 2013; Aziz *et al.,* 2017). Similarly, 100% of TSS can be removed by using alum as coagulant. This removal is more than a percentage removal achieved by (Sahu, 2013; Alkaya and Demirer, 2011). In this case, PACl is the most efficient in removing TSS in the wastewater since it can reduce the same amount of TSS as alum at low dosage. In contrast, $FeCl_3$ gives less efficient result of TSS removal (Sahu, 2013). In chemical coagulation the alum, polyaluminum chloride, ferric chloride, polyvinyl alcohol and ferrous sulphate are effective for the reduction biochemical oxygen demand, chemical oxygen demand, suspended solids and oil & grease (Panhwar and Bhutto, 2020; Panhwar *et al.,* 2021).

Coagulants

Almost chemical coagulants are iron based or aluminum based chemicals, which can change the magnetic charge of particles in the water causing them to attract instead of repel each other. Arsenic, organic matter, chemical phosphorus, and pathogens are removed by chemical coagulants effectively.

pH Control

The control of pH adds acidic or basic chemicals to the wastewater, thereby allowing hydroxide ions to bond with heavy metals and precipitate out of the solution. In addition, greater acidity will kill bacteria and organic compounds by breaking them down at a cellular level.

Selection of Coagulant

Principally, there are four major categories of the coagulation as per application and nature; such as Aluminum salts (alum) Ferric and ferrous salts Lime Polymers Cationic Anionic and non-ionic polymers Natural (Kawamura, 1996; Sahu and Chaudhari, 2013). Before treatment of the industrial wastewater the selection of the coagulants is very crucial. There is a different work of coagulants in different quality parameter of wastewater. Many researchers have been reported on the effectiveness and optimal performance of different chemical coagulants (Table 1) for using in the treatment of industrial wastewater (Holt *et al.,* 2002).

Table 1. Use of different chemical coagulants for treatment of industrial wastewater.

S. No	Industries	Coagulant	Dosing	Optimum Alkalinity/ pH	Temp.	Max. Mixing/ rpm	Parameter	Remarks	Authors
1	Sugar Industries	($Al_2(SO_4)_3$+$FeSO_4$)and Aluminium salt $Al_2(SO4)$	5mg/l	7.1	nm	nm	COD	75% & 77% COD Reduction	Khan *et al.*, 2003
2	Pulp and paper	I- Calcium benoite + alum. II- polyaluminium chloride (PAC) as the chemical coagulant and bagasse fly ash (BFA). III- Poly-Aluminum Silicate-Chloride IV- aluminium chloride, poly aluminium chloride and copper sulphate	I-100 mg l^{-1}+ 200 mg l^{-1} II- 3 kg l^{-1} PAC, 2 kg for Fly. III- 40 mg l^{-1}. IV- PAC= 8 ml L^{-1} AlCl3=5ml l^{-1} CuSO4=5 ml l^{-1}	I-7 II-PAC= pH3 Fly ash =pH 4 III- pH-7 IV- PAC=pH5 AlCl3=pH4 CuSO4=pH6	I-nm II_nm III-nm IV- 18	I- 120. II-120. III-200. IV- flash-mixed	I- Color. II- Color and COD. III- Turbidity and COD IV- COD and Color	I-88% of color reduction found. II- COD 87%,and colour 95 %,. III- 93.13% and 91.12% . IV- PAC= COD to 84 % and 92 % $AlCl_3$= 74 % COD and 86 % colour $CuSO_4$= 76 % COD reduction and 78 %	I-Dilek and Bese, *2001* II- Srivastava *et al.*, 2005 III- Kadhum *et al.*, 2011 IV- Kumar *et al.*, 2011
3	Textile	PAC	25mg/l	7	nm	100	COD, TDS and turbidity	90.17, 74.09 and 93.47%, respectively	Sabur *et al.*, 2012
4	Pharmacy	$FeSO_4$, $FeCl_3$, and alum	$FeSO_4$ (500 mg l^{-1}), $FeCl_3$, (500 mg l^{-1}), and alum (250 mg l^{-1}),	pH9	Nm	nm	COD, SS	24–28% and 70%,	Gupta and Gupta, 2006
5	Pesticides waste water	$FeSO_4$ and Al_2SO_4 with H_2O_2	2 mg+20 ml	pH=5.5	nm	120	COD	FeSO4=57.77%	Upadhyay and Mistry, 2012
6	Petroleum wastewater	PACl, $FeCl_3$	10mg l^{-1}	pH=7.5	nm	150	Color, COD	PAC= 885 Color and 72% COD, $FeCl^3$=79 color and 67% COD	Farajnezhad, and Gharbani, 2012

CONCLUSION

Wastewater may be considered as wealth, if we use it after treatment properly; due to utilization of treated wastewater we can increase agricultural production to tide over the hunger in world. According to this study the recent developments elucidate that the physical treatment processes (primary treatment) has becomes an effective treatment technique and helpful before further treatment processes, which constitute the tertiary treatment. It would require the chemicals process only and time saving and treat huge quantity of water as compared to biological treatment which is time consuming. The same process used to produce water for re-use in industries and agriculture production. In chemical coagulation process the decontaminated process is very easy and time saving techniques and almost chemicals are easily available. It is an edge to this technique by adding or increasing dose of different chemical coagulants can improve the treatment efficiency for treatment of industrial wastewater. Due to this process the impressive results are achieved to reduce BOD, COD and suspended solids. It is feasible and affording treatment processes and well-known disposal procedure for discharge of industrial wastewater in freshwater bodies.

DECLARATION OF COMPETING INTEREST

The authors declare that they have no conflict of interest.

CREDIT AUTHORSHIP CONTRIBUTION STATEMENT

Aijaz Panhwar: Investigation, conceptualization, writing original draft.
Aftab Kandhro: Methodology, writing original draft.
Sofia Qaisar: Conceptualization
Mudasir Gorar: Review, and editing, references.
Eidal Sargani: Review, and editing, references.
Humaira Khan: Review, and editing, references.

REFERENCES

Akeem AO (2008). *Impact of Ewekoro cement factory on the surrounding water resources.* Bachelor of water resources and hydrology management research project, Federal University of Agriculture, Abeokuta, Nigeria, 2008.

Alkaya E, Demirer GN (2011) Anaerobic-fed and sequencing-batch treatment of sugar-beet processing wastes: a comparative study. *Water Environment Research, 83(3): 247-255.*

Aziz N, Effendy and Basuki KT (2017) Comparison of poly aluminium chloride (PAC) and aluminium sulphate coagulants efficiency in waste water treatment. *Plant, 2(1): 24-31.*

Dilek FB and Bese S (2001). Treatment of pulping effluents by using alum and clay-colour removal and sludge characteristics. *Water SA, 27(3): 361-366.*

Drechsel P, Wichelns D and Qadir M (2015). Wastewater: economic asset in an urbanizing world. In Drechsel, Pay; Qadir, Manzoor; Wichelns, D. (Eds.). Amsterdam, Netherlands: *Springer,* 3-14.

Farajnezhad H and Gharbani P (2012). Coagulation treatment of wastewater in petroleum ındustry using poly aluminum chloride and ferric chloride. *International Journal of Recent Research and Applied Studies, 131(1): 306-310.*

Ghafari S, Aziz HA, Bashir MJK. (2010). The use of poly-aluminum chloride and alum for the treatment of partially stabilized leachate: A comparative study. *Desalination, 257(1-3): 110-116.*

Ghaly A, Ananthashankar R, Alhattab M and Ramakrishnan V (2014) Production, characterization and treatment of textile effluents: a critical review. *Journal of Chemical Engineering Process Technology, 5(1): 1-19.*

Gupta SK and Gupta SK (2006). Treatment of Pharmaceutical Wastes, *Taylor & Francis Group.*

Guven G, Perendeci A and Tanyolac A (2009). Electrochemical treatment of simulated beet sugar factory wastewater. *Journal of Chemical Engineering*, *151(1-3): 149-159.*

Holt PK, Barton GW, Wark M and Mitchell CA (2002) A quantitative comparison between chemical dosing and electrocoagulation. Colloids and Surfaces A: *Physicochemical and Engineering Aspects, 211(2-3): 233-248.*

Isık M and Sponza DT (2006) Biological treatment of acid dyeing wastewater using a sequential anaerobic/aerobic reactor system. *Enzyme and Microbial Technology, 38(7):887-892.*

Kadhum MS, Abdulbari HA, Abbas AA (2011). Treatment of pulp and paper mill wastewater by poly-aluminum-silicate-chloride (pasic) through coagulation-flocculation process. *Al-Qadisiya Journal For Engineering Sciences 4(4): 546-555.*

Khan M, Kalsoom U, Mahmood T, Riaz M and Khan AR (2003). Characterization and treatment of industrial effluent from sugar industry. *Journal Chemical Society, 25(3): 242-247.*

Kumar P, Teng TT, Chand S and Kailas L (2011). Wastewater, treatment of paper and pulp mill effluent by coagulation. *International Journal of Civil and Environmental Engineering 3: 3.*

Kawamura S (1996). Optimization of Basic Water Treatment Processes, Design and Operation: Coagulation and Flocculation. *Journal Water Supply Research and Technology AQUA, 45(1): 35-47.*

Khalil HA, Davoudpour Y, Saurabh CK, Hossain MS, Adnan A, Dungani R, Paridah M, Sarker MZI, Fazita, MN and Syakir M (2016). A review on nanocellulosic fibres as new material for sustainable packaging: Process and applications. *Renewable and Sustainable Energy Reviews, 64: 823-836.*

Moussa DT, El-Naas MH, Nasser M and Al-Marri MJ (2017). A comprehensive review of electrocoagulation for water treatment: potentials and challenges. *Journal of Environmental Management, 186: 24-41.*

Noppakhun P and Thunyalux R (2016). Removal of color, turbidity, UV254 in treated wastewater of sugar factory by aluminum and iron based coagulants. *KKU Engineering Journal. 43(2): 364-366.*

Samsudin NS, Kabbashi NA and Jami MS (2019). Selection of Various Coagulants for sugar ındustry wastewater treatment. *Biological and Natural Resources Engineering Journal, 2(1): 1-9.*

Nurul MF, Jayaraman K, Bhattacharyya D, Mohamad MH, Saurabh CK, Hussin MH and HPS AK (2016). Green composites made of bamboo fabric and poly (lactic) acid for packaging applications. *A review. Materials*, *9: 435.*

Panhwar AA., Almani KF and Kandhro AA (2020). Environmental Degradation by Textile Industry; Performance of Chemical Coagulants and Activated Carbon for Removal of COD, BOD. *Technical Journal, 25(4): 16-20.*

Panhwar A and Bhutto S (2021). Improved Reduction of COD, BOD, TSS and Oil & Grease from Sugarcane Industry Effluent by Ferric Chloride and Polyaluminum Chloride Coupled with Polyvinyl Alcohol. *Ecological Engineering & Environmental Technology*, *22(2): 8-14.*

Poddar PK and Sahu O (2017). Quality and Management of Wastewater in Sugar Industry. *Applied Water Science*, *7(1): 461-468.*

Radhi AA and Borghei M (2017). Investigate the optimal dose for COD and TSS removal using chemical treatment, *The International Journal of Computation and Applied Sciences (IJOCAAS), 3(3): 271-277.*

Sabur MM, Khan AA and Safiullah S (2012). Treatment of textile wastewater by coagulation precipitation method. *Journal of Scientific Research 4(3): 623-633.*

Sahu OP (2019). Electro-oxidation and chemical oxidation treatment of sugar industry wastewater with ferrous material: An investigation of physicochemical characteristic of sludge. *South African Journal of Chemical Engineering, 28: 26-38.*

Sahu OP and Chaudhari PK (2014). Physicochemical treatment of sugar industry wastewater: Coagulation processes, Environment Quality Management, *23(4): 49-69.*

Sahu OP and Chaudhari PK (2015). Electrochemical treatment of sugar industry wastewater: COD and color removal. *Journal of Electroanalytical Chemistry, 739; 122-129.*

Sahu OP and Chaudhari PK (2013) Review on chemical treatment of industrial waste. *Journal of Applied Science and Environmental Management. 17(2): 241-257.*

Srivastava VC, Mall ID and Mishra IM (2005). Treatment of pulp and paper mill wastewaters with Polyaluminium chloride and bagasse fly ash. *Colloids and Surface A: Physiochemical Engineering Aspects 260: 17-28.*

Tchamango S, Njiki CPN, Ngameni E, Hadjiev D and Darchen A (2010). Treatment of dairy effluents by electrocoagulation using aluminium electrodes. *Science Total Environment, 408(4): 947-952.*

Teh CY, Budiman PM, Shak KPY and Wu TY (2016) Recent advancement of coagulation–flocculation and its application in wastewater treatment. *Industrial Engineering Chemical Research, 55(16): 4363-4389.*

Thompson RC, Moore CJ, vom Saal FS and Swan SH (2009b). Plastics, the environment and human health: current consensus and future trends. *Philosophical Transactions of the Royal Society B, 364: 2153-2166.*

UN Water (2015). Wastewater management-A UN-Water analytical brief. (2015). (World Meteorological Organization, Geneva, Switzerland), 1-52.

UN WWAP (2017). United Nations World Water Assessment Programme. The United Nations World Water Development Report. Wastewater: The Untapped Resource. Paris.

Upadhyay AP and Mistry NJ (2012). Feasibility of combined Fenton & coagulation method for the treatment of pesticides waste water. *International Journal of Engineering Research & Technology ,1(3): 1-7.*

US EPA (2014). US Environmental Protection Agency, Reducing Wasted Food & Packaging: A Guide for Food Services and Restaurants. *EPA*. Retrieved March 7, 2019, from [https://www.epa.gov/sites/production/files/201508/documents/reducing_wasted_food_pkg_tool.pdf].

US EPA (2021). US Environmental Protection Agency. https://www.epa.gov/facts-and-figures-about-materials-waste-and-recycling/national-overview-facts-and-figures-materials Wastes and Recycling. (01-09-2021).

Zaharia C, Suteu D, Muresan A, Muresan R and Popescu A (2009). Textile wastewater treatment by homogenous oxidation with hydrogen peroxide. *Environmental Engineering and Management Journal 8(6): 1359-1369.*

Zonoozi MH, Moghaddam MRA, Arami M (2008). Removal of acid red 398 dyes from aqueous solutions by coagulation/flocculation process. *Environment Engineering Management Journal, 7(6): 695-699.*

TURKISH JOURNAL OF AGRICULTURAL ENGINEERING RESEARCH

2020

TURKAGER